CHARLES UNIVERSITY

2nd FACULTY OF MEDICINE

POSTGRADUATE STUDY IN BIOMEDICINE:
NEUROSIENCE

SERHIY SOSNIYENKO

ENTRAINMENT OF THE CIRCADIAN SYSTEM IN RODENTS

PhD THESIS

PRAGUE
2010

Declaration:

I would like to certify that I completed my PhD thesis on my own and independently using below mentioned reference. In addition, I agree with my thesis to be archived at Department of Scientific Information of the 1st Medical Faculty, Charles University in Prague and to be used for learning purposes; assuming that everyone who would use my thesis for their presentations or publications would be obliged to cite it.

I agree with my thesis to be available in the electronic web at Digital repository of the Charles University in Prague (http://repozitar.cuni.cz). Thesis should be available only at Charles University in Prague.

Agree / ~~Disagree~~

Prague, 5.06.2010 Serhiy Sosniyenko

Identification record:

Sosniyenko Serhiy. *Entrainment of the circadian system in rodents*. Prague 2010. 82 pages, 5 attachments. PhD thesis. Charles University in Prague, 2nd medical faculty and Institute of Physiology, Academy of Sciences of the Czech Republic, v.v.i. Supervisor: PharmDr. Alena Sumova, DSc.

ABSTRACT:

The circadian clock located within the suprachiasmatic nuclei (SCN) of the hypothalamus responds to changes in the duration of day length, i.e. photoperiod, differently in the separate SCN parts. The aim of the study was i) to compare the effect of a long and a short photoperiod with twilight relative to that with rectangular light-to-dark transition on the daily profiles of clock gene expression and their protein levels within the rostral, middle and caudal regions of the mouse SCN; ii) to elucidate the dynamics of adjustment to a change of a long photoperiod to a short photoperiod of clock gene expression rhythms in the mouse SCN and in the peripheral clock in the liver, as well as of the locomotor activity rhythm; iii) to elucidate whether and how swiftly the immature rat fetal and neonatal molecular SCN clocks can be reset by maternal cues and iv) to reveal when and where within the rat SCN the photic sensitivity of clock gene expression develops during the early postnatal ontogenesis and to compare it with development of *c-fos* photoinduction. Mice and rats were used for experiments; their tissues were analyzed by in situ hynridization, immunohistochemistry, RT-PCR. The data indicated that i) the twilight photoperiod provides stronger synchronization among the individual SCN cell subpopulations than the rectangular one, and the effect is more pronounced under the short than under the long photoperiod; ii) different mechanisms of adjustment to a change of the photoperiod in the central SCN clock and the peripheral liver clock; iii) SCN clock is capable of significant phase shifts at fetal developmental stages when no or very faint molecular oscillations can be detected; iv) light sensitivity of the circadian clock develops gradually during postnatal ontogenesis before the circadian clock starts to control the response.

ACKNOLEDGMENTS

I want to take this opportunity to express my sincere appreciation to Dr. Alena Sumova. Due to her major efforts, enthusiasm and dedication this research was able to come true. Thanks to her daily support and careful supervision this project was able to be completed.

Separate acknowledgement is to Prof. Helena Illnerova as a “mother” of biological rhythm for her patronage and help in this project.

Also it wouldn’t have happened without assistance from Dr. Zdenka Bendova and Dr. Martin Sladek, as well as Mgr. Dana Parkanova, Dr. Kristyna Mateju and all EUCLOCK team mates.

Special appreciation to Mrs. Eva Suchanova for sincere help and support not only in the project.

Thank you dear all for the time spent together. This is unforgettable…

DECLARATION OF THE AUTHOR'S CONTRIBUTION TO PUBLICATIONS INCLUDED IN THE THESIS

Sosniyenko S., Hut R.A., Daan S., Sumová A. (2009): Influence of photoperiod duration and light-dark transitions on entrainment of *Per1* and *Per2* gene and protein expression in subdivisions of the mouse suprachiasmatic nucleus. *Eur. J. Neurosci*. 30, 1802-1814. **(IF 3.673)**

Serhiy Sosniyenko contributed substantially to this work (appropriate share 90%). He performed all experimental work by himself and significantly contributed to data evaluation.

Sosniyenko S., Parkanová D., Illnerová H., Sládek M., Sumová A. (2010) Different mechanisms of adjustment to a change of the photoperiod in the suprachiasmatic and liver clocks. *Am. J. Physiol. (Regul Integr Comp Physiol)*, 298, R959-R971. **(IF 3,272)**

Serhiy Sosniyenko and Daniela Parkanova contributed equally to this paper. S.S. performed experiment to reveal dynamics of adjustment of clock gene expression profiles to a change of the photoperiod in the SCN and D.P. performed the experiments in the liver. The appropriate share of S.S. was 50%.

El-Hennamy R., Matějů K., Bendová Z., **Sosniyenko S.,** Sumová A. (2008): Maternal control of the fetal and neonatal rat suprachiasmatic nucleus. *J. Biol. Rhythms*, 23, 435-444. **(IF 4,211)**

Serhyi Sosniyenko contributed to the study by his expertise and assistance with in situ hybridization technique to determine gene expression in the neonatal brain. The appropriate share of S.S. was 25%.

Matějů K., Bendová Z., El-Hennamy R., Sládek M., **Sosniyenko S.,** Sumová A. (2009) Development of the light sensitivity of clock genes *Period1*, *Period2* and immediate early gene *c-fos* within the rat suprachiasmatic nucleus. *Eur. J. Neurosci*. 29, 490-501. **(IF 3.673)**

Serhiy Sosniyenko contributed to the study by his expertise and assistance with in situ hybridization technique to determine gene expression in the neonatal brain. The appropriate share of S.S. was 15%.

Sumová A., Bendová Z., Sládek M., El-Hennamy R., Matějů K., Polidarová L., **Sosniyenko S.,** Illnerová H. (2008): Circadian molecular clocks ticking along ontogenesis. *Physiol. Research*, 57 (Suppl. 3): S139-S148. **(IF 1,505)**

Serhyi Sosniyenko contributed to the study by 10%.

LIST OF ABBREVIATIONS:

3V+ - third ventricle

AA-NAT – arylalkylamine N-acetyltransferase

AVP – arginine-vasopressin

Bmal1 – brain and muscle Arnt-like protein 1

bHLH – basic-helix-loop-helix

cAMP – adenosine 3',5'-monophosphate

c-fos –

CCGs – clock controlled genes

CKIε – casein kinase I epsilon

Clock - circadian locomotor output cycles kaput

CRE – Ca^{2+}/cAMP response element

CREB – Ca^{2+}/cAMP response element binding protein

Cry – Cryptochrome

C-SCN – caudal part of the SCN

CT – circadian time

Dbp – albumin gene D-site binding protein

DD – constant darkness

DMH – dorsomedial nucleus of the hypothalamus

E –day of embryonic development

ERK - extracellular signal-regulated kinase

FASPS – familial advanced sleep phase syndrome

FBXL3 – ubiquities E3 ligase of F-box family

GABA – γ–aminobutyric acid

GHT – geniculohypothalamic tract

hn – heteronuclear

IGL – intergeniculate leaflet

LD – light-dark period of the circadian cycle

LH – lateral hypothalamus

LL – constant light

MAPK – mitogen-activated protein kinase

MPO – medial preoptic region

M-SCN – middle part of the SCN

NMDA – N-methyl-D-aspartate

NPY – neuropeptide Y

OD – optical density

OX – optic chiasm

P – day of postnatal development

PAS –

Per – Period

PKCA – protein kinase C alpha

PRC – phase response curve

PVN – paraventricular nucleus

RA – rectangular

PBS – phosphate-buffered saline

REM – rapid eye movement

Rev-erbα – NR1D1 nuclear receptor

R-SCN – rostral part of the SCN

RHT – retinohypothalamic tract

Ror – retinoic acid-related orphan receptors

RT-PCR – real time polymerase chain reaction

SCN – suprachiasmatic nucleus

sPVz – subparaventricular zone

SO – supraoptic nucleus

Tim – Timeless

TW – twilight

UTP – uridinetriphosphate

VIP – vasoactive intestinal polypeptide

VLPO – ventrolateral preoptic nucleus

CONTENTS

1. INTRODUCTION

Living organisms are constantly exposed to changing environmental conditions. Changes of light and dark periods of the day as well as seasonal changes of the year are the most obvious and important examples of them. The content of this thesis primarily describes responses to light-dark changes which control daily rhythms on the Earth. In the past, changes that people observed in living organisms such as alternation of waking and sleeping periods or daily movements of plant leaves were explained as passive adjustment to the light-dark changes in the surroundings (light during the day and darkness during the night). Nowadays explanations differ. All organisms on the Earth from prokaryotic bacteria to human beings have developed abilities to adjust and react in advance to environmental changes, i.e., they can predict these changes. This enables them to react to them in advance. Mechanisms that drive these reactions are themselves driven by an endogenous oscillator, the so called biological clock, which generates biological rhythms in the organism. A branch of science that studies biological rhythms is named chronobiology from the Greek word *chronos* = time. Chronobiology started as a separate branch of science in 1960, but its progression, development and deeper understanding has occurred only in the last two decades with application of new molecular biology techniques. A number of clock genes involved in generating internal rhythms have been discovered as well as their interaction mechanisms based on transcriptional-translational feedback loops. Modern investigations in chronobiology are directed to better understanding of the entire time-keeping mechanism and inter- and intracellular interactions of single components of biological rhythms generation and their interconnections with changing environmental conditions. Effects of different day light periods, i.e., photoperiods, and generally, of light on the time-keeping system, belong to important chronobiological studies.

2. REVIEW

2.1 BIOLOGICAL RHYTHMS

2.1.1 GENERAL APPROACH

Biological systems are not static. Organisms inhabit environment that changes predictably over the course of the day and night. Hence variations of the timing and duration of individual biological activities in living organisms are necessary for many essential biological processes. For example, in animals these are eating, sleeping, mating, hibernation, migration, cellular regeneration, etc. and in plants, leaf movements, photosynthetic reactions, etc. Many of these changes are rhythmic as they recur at regular intervals, i.e., periods, and form thus biological rhythms.

According to duration of the periods, the biological rhythms are classified as follows:

Ultradian rhythms cycle with a period shorter than 24 hours. Those are e.g., the heart muscle activity, breathing frequency, or cycles of non-REM and REM sleep etc.

Circadian rhythms cycle with a period close to, but not equal to, 24 hours. Representative examples are e.g., sleep-wake cycle, rhythm in the locomotor activity, body temperature, daily hormonal changes.

Infradian rhythms cycle with a period longer than 24 hour. Those are annual cycles in migration or reproduction found in certain animals, estrus cycles or the human menstrual cycles.

When animals, plants or fungi live under constant environmental conditions, their daily rhythms usually do not stop or become disorganized. Most of them, i.e., the circadian ones, persist with a period that deviates only slightly from 24 hours; we say that they ‘free-run’. The free-running period has two remarkable properties: first, it is very accurate and its deviation may be only minutes in 24 hours and second, is temperature compensated, i.e.,

it is defended against changes in ambient temperature, in contrast to other metabolic functions (Hastings, 1997). Hence, circadian rhythms are apparently driven by an endogenous clock, i.e., a pacemaker that generates self-sustained oscillations. The endogenous period of this pacemaker (τ) is mostly measured by its rhythmic outputs, e.g., by monitoring rhythms in locomotor activity or body temperature under constant conditions not affected by any potential rhythmic stimulus in the environment, namely in constant darkness (Illnerova, 1994).

However, not all rhythmic processes in the organism are controlled by a biological clock. Only when cyclic processes persist under constant conditions, such as are steady temperature and permanent darkness, we can speak about a biological oscillator. Virtually all light-sensitive organisms from cyanobacteria to the man have circadian clocks. This indicates that at least in unicellular organisms such as cyanobacteria, protozoans and algae circadian oscillators may be built to work in a cell-autonomous fashion. Recent studies have shown this to be true also for fruit flies (Plautz *et al*, 1997), zebrafish (Whitmore *et al*, 1998) and mammals (Balsalobre *et al*, 1998; Yamazaki *et al*, 2000). Thus, many, if not most, body cells of these organisms have their own circadian clocks that continue to oscillate after they have been dissociated from the organism and grown in culture (Schibler, 2005).

2.1.2 CIRCADIAN RHYTHMS

Most of the studied daily biological rhythms are *circadian* rhythms. The term *circadian* comes from the Latin words *circa*, meaning "around" and *dies*, meaning " the day". The circadian period τ is approximately 24 hours, varying between 23 and 26 hours. The period is genetically determined and it is different in each species: e.g., in the mouse, it is 23.6 h, in the rat 24.2 h and in the man the average period is 24.2 h. This means that under constant conditions the locomotor activity of the mouse starts several min earlier each next day. However, under natural conditions the internal period τ is entrained or synchronized to the 24-hour day by an external entraining agent pr synchronizer. The most important entraining agents are day light-dark cycles, namely the light periods of the days. Other external synchronizers are feeding, environmental temperature or social factors (Hastings, 1997). The external synchronizers are named *zeitgebers*.

LD is an abbreviation for light (L) - dark (D) regimens to which animals are exposed. DD is an abbreviation for constant darkness, LL for constant light. When animals are maintained under a light-dark cycle with 12 hours of light and 12 h hours of darkness, LD12:12, and then released into DD, their subjective time under new non-periodic conditions is called the circadian time (CT): CT0-CT12 indicates a subjective day, i.e., the period of the original light interval, and CT13-CT24 indicates a subjective night, i.e., the period of the original dark interval. Light onset occurred originally at CT0, light offset at CT12.

2.2 THE CIRCADIAN SYSTEM

The circadian system consists of a central pacemaker that generates the above mentioned rhythms; efferent and afferent pathways that connect the central pacemaker with peripheral organs and peripheral oscillators that work concordantly with the central pacemaker as well as with each other and may generate their own oscillations.

2.2.1 THE CENTRAL OSCILLATOR OF CIRCADIAN RHYTHMICITY IN MAMMALS – THE SUPRACHIASMATIC NUCLEUS

2.2.1.1 Morphological characteristics of the suprachiasmatic nucleus

A pair of the suprachiasmatic nuclei (SCN) is located on both sides of the third ventricle, dorsally to the optic chiasm (Fig.1).

Individual SCN neurons contain an oscillation machinery, and it is possible that most of the approximately 20,000 neurons that comprise the bilateral rat SCN are “clock cells”. Based on retinal innervation patterns and on the observation that phenotypically distinct cell types define different regions (van den Pol, 1980), the SCN can be subdivided into a dorsomedial and a ventrolateral part. This general arrangement was observed in mice, rats, hamsters, and human. Phenotypically, the dorsomedial part or the shell is delineated by arginine-vasopressin (AVP)-containing cells, whereas the ventrolateral part or core contains a variety of cell phenotypes. The most ventral population is formed by a group of vasoactive intestinal polypeptide (VIP)-expressing neurons. Most of the SCN neurons also

produce γ–aminobutyric acid (GABA), which plays an important role in transmitting the phase information between the ventrolateral and dorsomedial SCN, as well as in coupling individual SCN neurons (Albus et al., 2005).

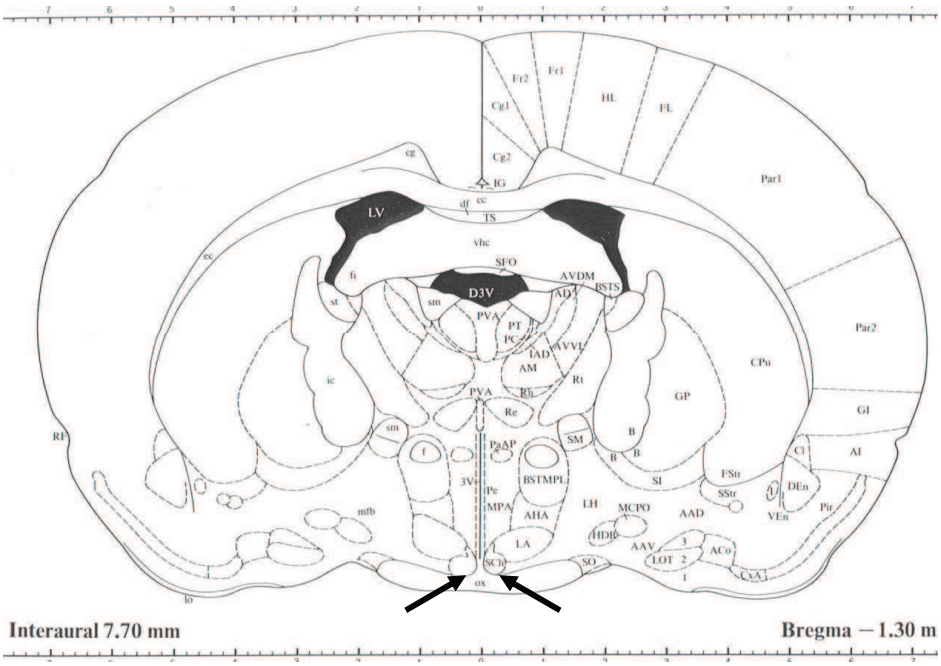

Fig.1. **Scheme of the coronal brain section depicting location of the suprachiasmatic nucleus in the rat brain.**

An arrow depicts location of the SCN on the basis of the brain. OX - optic chiasm, SO - supraoptic nucleus, 3V+ - third ventricle. *Adapted from Paxinos and Watson, 1986.*

2.2.1.2. Afferent and efferent pathways of the SCN

There are three main afferent pathways to the ventrolateral part of the SCN. The most important one is the retinohypothalamic tract (RHT), which transmits light signals from the retina directly to the SCN (Gooley *at el*., 2001, Albus *et al*., 2005) (Fig.2). It consists of dendritic processes of retinal ganglion cells and anatomically subdivides from the optic nerve above the optic chiasm. The RHT terminates in the ventrolateral part of the SCN. Its main neurotransmitter is glutamate, which binds to N-methyl-D-aspartate (NMDA) receptors of the SCN cells.

The other pathway from the retina to the SCN is indirect and leads first to the intergeniculate leaflet (IGL) of thalamus, and then as a part of geniculohypothalamic tract (GHT) to the ventrolateral SCN. Both light induced and mostly non-light induced signals are integrated in the intergeniculate leaflet on their way to the SCN. The main neurotransmitter is neuropeptide Y (NPY).

The third pathway, which is also indirect, starts in the raphe nuclei, part of the midbrain. Non-light induced signals reach the ventrolateral SCN by this pathway, usually being modulated by light-induced signals. The main neurotransmitter molecule in this pathway is serotonin (Sumova *et al.*, 1996).

The efferent pathways from the SCN lead through other parts of the brain and spinal cord to peripheral organs. In the brain, the pathways mostly lead to the midbrain, hypothalamus and thalamus (Abrahamson *et al.*, 2001). Signals in these pathways are transmitted by AVP and GABA neurotransmitters. Decreasing of the electrical activity of the SCN correlates with the decrease of GABA release. Via this mechanism, SCN regulates synthesis of melatonin in the pineal gland and informs the entire organism about environmental light conditions. Melatonin is synthesized and secreted due to norepinephrine release from nerve endings in the pineal during the nighttime, while during the daytime its level remains low.

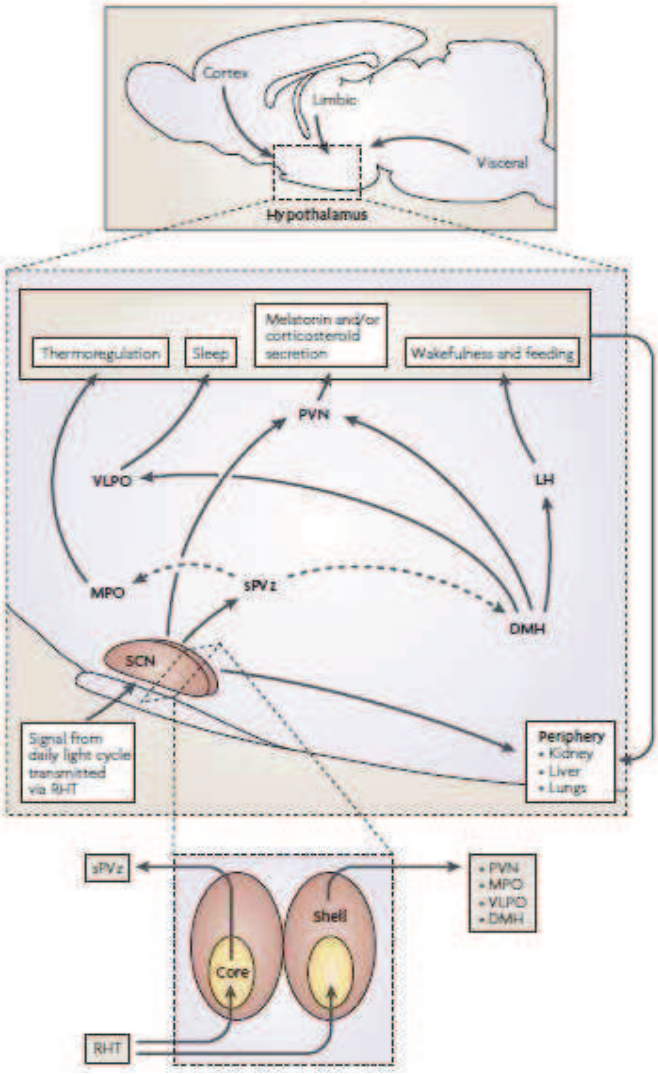

Fig.2 A schematic diagram of the suprachiasmatic nucleus and its input and output pathways. The mammalian circadian pacemaker in the hypothalamic suprachiasmatic nucleus (SCN) is organized into two major subdivisions, the core and the shell. The core region of the SCN receives information about the daily light cycle through the retinohypothalamic tract (RHT). Both neuronal and humoral signals function as output signals from the SCN to other regions of the brain and the periphery. The SCN output pathways are responsible for proper timing of diverse physiological functions, including hormone release, sleep–wake cycle, feeding behavior, and thermoregulation. The SCN output to the subparaventricular zone (sPVz) is relayed to the medial preoptic region (MPO) to control circadian rhythms of body temperature, and a separate projection through the dorsomedial nucleus of the hypothalamus (DMH) controls daily hormone secretion through the paraventricular nucleus (PVN) and sleep–wake cycles through the lateral hypothalamus (LH) and ventrolateral preoptic nucleus (VLPO). *Adapted from J. Takahashi 2008.*

2.2.1.3. Synchronization of cells within the SCN

Suprachiasmatic nucleus is vitally essential for generation of circadian rhythms which continue to run also in conditions without any external synchronizer. Experiments with *in vitro* cell dispersed cultures have showen that individual neurons exhibit differences in their intrinsic period. Even two neighboring neurons may oscillate with an opposite phase. Hence, each SCN neuron may be a single oscillator. In order that the entire SCN could generate an unambiguous rhythm, neurons are coupled together and synchronized with each other (Welsh *et al*., 1995; Yamaguchi *et al*., 2003). Most of the SCN neurons also produce GABA which plays an important role in transmitting the phase information between the ventrolateral and the dorsomedial SCN, as well as in coupling individual SCN neurons (Albus, 2005). Synchronization by VIP is also considered as it is synthesized by neurons of the ventrolateral SCN which accepts light induced impulses from the retina and synchronizes neurons in the dorsomedial SCN part. That explains dense projections from the ventrolateral to the dorsomedial SCN part, while projections in the opposite direction are minimal. Advantage of the SCN rhythmicity generated by a multiple-oscillator system based on interaction between individual cells is that variability of the rhythmicity during a long-term rhythm generation is decreased and its stability is maintained better than by a single neuron (Liu *et al.*, 1997; Aton *et* Herzog, 2005). An explicit phase generated by the SCN is a result of an internal synchronizer impingement via GABA and VIP and phase responses to light as well as to other external stimuli mediated by glutamate, NPY and serotonin. A proper functioning of the SCN is coordinated by generation of intracellular rhythmicity and intercellular synchronization processes (Liu *et* Reppert, 2000).

2.2.2 PERIPHERAL OSCILLATORS

In the past, the retina was thought to be the only organ along with the SCN where a circadian clock was considered. However, after the discovery of clock genes, this believe fell apart. A rhythmic expression of circadian clock genes was found not only in the SCN, but also in peripheral organs, such as the liver, lungs, heart, skeletal muscle, testes, and other. At the beginning, it was suggested that generation of rhythmicity in these organs was directly controlled by the suprachiasmatic nucleus and after its ablation the rhythms in

peripheral organs would (Reppert *et* Weaver, 2001). Later studies showed, however, that peripheral organs expressed tissue-specific differences in the circadian period and phase. Surprisingly, lesions of the SCN in mice did not abolish immediately circadian rhythms in peripheral tissues, but instead caused phase desynchrony among the tissues and individual oscillating cells. These results demonstrated that peripheral tissues expressed self-sustained circadian oscillations and suggested existence of organ-specific synchronizers of circadian rhythms at the cell and tissue level. However, the suprachiasmatic nucleus functions as a coordinator and synchronizer of all peripheral tissues and organs (Yoo *et al.*, 2004). Apparently, humoral and neuronal regulations are involved in this synchronization. Rhythmic expression of clock genes in peripheral organs is phase delayed by about 3 to 9 hours relative to their expression in the SCN. In addition to light entrainment via the SCN, peripheral oscillators can also be synchronized by food intake. In response to advances and delays of the environmental light cycle, the circadian rhythms in clock gene expression in the SCN phase shifted more rapidly than the rhythm of locomotor behavior or the rhythms in peripheral tissues (Yamazaki *et al*., 2000). Current studies also suggest that regulatory mechanisms of circadian clock genes expression in peripheral organs may in some aspects differ from those in the suprachiasmatic nucleus.

2.2.3 PINEAL GLAND AND MELATONIN

A remarkably constant feature of vertebrate physiology is a daily rhythm of melatonin in the circulation, which serves as the hormonal signal of the subjective night and day: melatonin levels are always elevated at night. Melatonin is secreted by the pineal gland and its rhythmic secretion is controlled by the SCN. Melatonin serves as conection between the neuronal and hormonal signaling (Illnerova *et* Vanecek, 1980). This low-molecular substance is synthesized from the amino acid tryptophan. The basis of the melatonin rhythm is the rhythm of one of the enzymes involved in its synthesis in the pineal gland – namely the rhythm of serotonin N-acetyltransferase (arylalkylamine N-acetyltransferase, AA-NAT, E.C. 2.3.1.87). In all vertebrates, the AA-NAT activity is high at night (Illnerová *et* Vaněček, 1988). The phase of the AA-NAT and melatonin rhythms reflects the phase of the SCN circadian clock. Dynamics of the AA-NAT enzyme is remarkable. Magnitude of the nocturnal increase in enzyme activity ranges from 7- to 150-

fold in dependence on a species. In all cases the nocturnal level of AA-NAT activity decreases very rapidly following exposure to light. The rhythmic synthesis of melatonin is one of the examples of the influence of the circadian clockwork in the SCN, which itself can be affected by melatonin on a feedback basis. Studies with ^{125}I-melatonin revealed melatonin binding sites in the suprachiasmatic nucleus (Vaněček *et al*., 1987). Many effects of melatonin on the animal organism were suggested, but only some of them were tested. The main function of melatonin is to inform the organism about the internal time of the biological clock: for example, a decrease of melatonin blood concentration in the morning in darkness denotes the end of the subjective night. Melatonin can also entrain and synchronize the endogenous clock: application of melatonin in the evening time phase-advances the biological clock while its application in the morning time delays the clock. The daily temporal pattern of synthesis and release of melatonin, mainly the length of the period of elevated melatonin levels, is involved in transferring the information on day length to the neuroendocrine-gonadal axis (Illnerová *et al*., 1984; Hastings *et al*., 1987). By this mechanism, animals get a signal for starting or ending the reproductive activity.

Administration of melatonin may also improve adaptation to a new time zone in people traveling across more time-zones. In elderly people with sleep impairments melatonin may improve sleep quality and it may also synchronize blind people with the 24hour day (Illnerova, 1996; Hastings, 1997).

2.3 MOLECULAR BASICS OF CIRCADIAN RHYTHMICITY

2.3.1. SEARCH FOR THE MOLECULAR BASIS

After the discovery of the suprachiasmatic nucleus as a central pacemaker in 1972 (Moore and Eichler, 1972; Stephan and Zucker, 1972), most studies were directed to understand how the circadian rhythmicity itself is generated. Previous studies showed that adding of protein synthesis inhibitor decreased oscillations, while administration of Na^+-channels inhibitor tetradoxin did not. Hence, generation of rhythmicity might not be related to the neuron synaptic activity, but rather it might depend on intracellular biochemical processes, namely o proteosynthesis. In the past decade, great progress in our understanding of the circadian rhythmicity has been made due to identification of a number

of clock genes responsible for generating molecular oscillations. A surprising finding that many circadian elements share structural and functional similarity between species as diverse, as *Drosophila* and the mouse came with identification of homologues of the fruit fly clock gene *Per* in mammals. This similarity was further confirmed when it was realized that in all studied circadian organisms the oscillatory mechanism was composed of autoregulatory feedback loops (Dunlap, 1999; Reppert et Weaver, 2001; Okamura *et al.*, 2002; Hastings et Herzog, 2004). These loops consist of positive and negative elements. Negative elements are proteins that inhibit transcription of their own genes, while positive factors stimulate clock genes transcription. This principle underlies the rhythmicity generation in animals, becoming more complex on the top of the evolutionary ladder. Most important circadian clock genes are as follows: *Clock* and *Bmal1* as positive elements, three *Period* (*Per1, Per2, Per3*) and two *Cryptochrome* (*Cry1* and *Cry2*) genes as negative elements, *Casein kinase Iε* affecting phophorylation of the clock gene products and some additional genes as are *Rev-erbα*, *Ror* group genes, *Dec1* and *Dec2*.

2.3.2 CLOCK GENES CHARACTERISTICS

2.3.2.1. Regulatory domains of proteins encoded by clock genes

Mutations in the Period gene and, consequently, changes in its protein product (PER) can shorten or lengthen the period τ of circadian rhythms. PER contains a motif of approximately 270 amino acids, the so-caled PAS domain, which is also present in three transcription factors of the basic-helix-loop-helix (bHLH) type in *Drosophila* single-minded gene product (SIM), and in both subunits of the mammalian dioxin receptor complex. The PAS domain may function as a dimerization domain in both SIM and the dioxin receptor complex, and PER may regulate circadian gene transcription partly by interacting with the PAS domain of bHLH--PAS-containing transcription factors (Huang *et al.*, 1993).The dimerization efficiency is decreased by several missense mutations in the PAS domain, including the original perL mutation, which lengthens circadian periods from 24 h to 29 h.

Positive elements of the molecular feedback loops contain similar bHLH domains. PAS-PAS dimers are able to recognize and bind to E-boxes (5′-CACGTG-3′), i.e., specific

sequences on gene promoters necessary for activation of mRNA expression (Hao *et al.*, 1997).

2.3.2.2. Circadian clock gene *Clock*

Name of Clock gene derives from the first letters of "circadian locomotor output cycles kaput" and reflects its function in the mouse with a mutated clock gene. The large transcription unit includes 24 exons spanning approximately 100,000 bp of DNA from which transcript classes of 7.5 and approximately 10 kb arise. *Clock* encodes a member of the bHLH-PAS family of transcription factors. It is a gene with a known circadian function and with features predicting DNA binding, protein dimerization, and activation domains. CLOCK represents one more example of a PAS domain-containing clock protein, which suggests that this motif may define, from a developmental point of view, a conserved feature of the circadian clock mechanism (King *et al*., 1997). In the SCN, *Clock* mRNA expression and protein production do not exhibit any rhythmicity or they are only slightly rhythmic under some LD regimens (Sumova et at., 2003). Therefore, it is obvious that the CLOCK protein has to interact with other transcriptional regulators in order to produce circadian rhythms. Homozygote *Clock* mutant mice became arrhythmic under constant darkness condition (Reppert *et* Weaver, 2001). Mutant CLOCK protein was apparently not able to activate fully transcription of other circadian clock genes, namely of *Per* and *Cry*.

Recent studies have, however, shown that CLOCK-deficient mice continue to express robust circadian rhythms in locomotor activity, though they have altered responses to light. In these CLOCK-deficient mice, clock gene mRNA and protein levels show alterations in both the master clock in the suprachiasmatic nuclei and in the peripheral clock in the liver, though molecular feedback loops continue to function (DeBruyne *et al.*, 2006). Probably, the transcription factor NPAS2 (Neuronal PAS domain protein 2) is able to functionally substitute for the CLOCK in the mouse clock in order to maintain circadian rhythmicity (DeBruyne *et al.*, 2007).

2.3.2.3. Circadian clock gene *Bmal1*

The name of the *Bmal1* gene derives from the first letters "brain and muscle Arnt-like protein". It is a super family gene, which encodes a bHLH/PAS transcription factor. The

BMAL1 protein with CLOCK protein composes a heterodimer. CLOCK-BMAL1 heterodimers activate transcription from E-box elements on the mouse *Per1* and *Cry1* genes. These heterodimers are the positive components of *Per* and *Cry* transcriptional oscillations (Gekakis *et al*., 1998). A robust circadian rhythm of *Bmal1* expression was detected in the suprachiasmatic nucleus with the highest level occurring during the subjective night (Abe *et al*., 1998). Loss of the BMAL1 protein in mice resulted in an immediate and complete loss of circadian rhythmicity in constant darkness. In light-dark cycles, their locomotor activity rhythm was impaired and activity levels were reduced. Thus, *Bmal1* is a non-redundant and essential component of the mammalian circadian pacemaker (Bunger et al., 2000).

2.3.2.4. Circadian clock gene *Period*

Three Period genes are identified in mammals, namely *Per1*, *Per2* and *Per3*. Each of the PER proteins possesses a protein dimerization PAS domain, suggesting that protein-protein interactions are important for their clock actions. A variety of PER-PER interactions have been demonstrated in vitro and in vivo (Kume et al., 1999); these interactions appear to be PAS mediated. In vitro studies in mammalian cell lines have also shown that PER1 and PER2 proteins can modestly inhibit the CLOCK:BMAL1-mediated transcription (Sangoram et al., 1998). Recent gene-targeting studies have shown that the PER proteins may have distinct functions. *Per1* expression is rapidly induced by a short duration exposure to light at night at levels sufficient to reset the clock (Shigeyoshi et al., 1997). Levels of *Per1* and *Per2* mRNA in the SCN exhibit significant circadian rhythm with maximal values during the light period of the day. In addition, both mRNAs are light sensitive and can be increased by light exposure during the subjective night but not during the subjective day (Shearman et al., 1997). *Per1* mutant animals exhibit shorter activity period in constant darkness, *Per2* mutants are arrhythmic, while *Per3* mutation does not affect the rhythmicity characteristics. Apparently, *Per3* gene is not necessary for circadian rhythms generation (Shearman *et al*., 2000).

Recent data have revealed that major biological pathways, including those critical to cell division, are under the circadian control. *Per1* provides an important link between the circadian system and the cell cycle system. Overexpression of *Per1* sensitizes human

cancer cells to DNA damage-induced apoptosis; in contrast, inhibition of *Per1* expression in similarly treated cells blunts apoptosis. Finally, PER1 levels were reduced in human cancer patient samples (Gery *et al*., 2006). Overexpression of either *Per1* or *Per2* in cancer cells inhibits their neoplastic growth. In vivo studies have shown that mice deficient in *Per2* exhibit a significantly higher incidence of tumor development after genotoxic stress. Loss and dysregulation of *Per1* and *Per2* gene expression have been found in many types of human cancers. Recent studies demonstrate that both PER1 and PER2 are involved in ATM-Chk1/Chk2 DNA damage response pathways and implicate a functional circadian system as a factor in tumor suppression (Chen-Goodspeed et al., 2007). These results highlight the importance of the circadian system for fundamental cellular functions and support the hypothesis that disruption of core clock genes may lead to cancer development.

2.3.2.4. Circadian clock gene *Cryptochrome*

There are two cryptochrome genes in mammals, *Cry1* and *Cry2*. Both act in the negative limb of the clock feedback loop. In cell lines, PER proteins inhibit only slightly the CLOCK:BMAL1 -mediated transcription. However, PER and CRY proteins dimers are efficient inhibitors of the transcription. This suggests the cryptochrome involvement in the negative limb of the feedback loop. CRY1 and CRY2 are rhythmically produced in the SCN. They interact with PER proteins, translocate them from cytoplasm to nucleus and block transcription of their own genes. Luciferase reporter gene assays however show that CRY1 or CRY2 alone are able to abrogate CLOCK:BMAL1-E box-mediated transcription. The PER and CRY proteins appear to inhibit the transcriptional complex differentially (Kume et al., 1999). In *Cry*-deficient mice, *Per1* and *Per2* mRNA levels are arrhythmic and expressed at mid to high levels in the SCN (Okamura et. al., 1999). Also, CRY1 and CRY2 proteins exhibit synchronous oscillations of nuclear localization in the SCN at the appropriate circadian time for negatively regulating their own transcription and transcription of *Per* genes (Reppert et Weaver, 2001).

2.3.2.5. Casein kinase Iε

The nuclear entry of circadian regulatory proteins that inhibit transcription of genes containing E-box in their promoters appears to be a critical component of the negative loop

in both Drosophila and mammals. The Drosophila double-time gene product, a casein kinase I epsilon (CKIε) homolog, has been reported to interact with PER and regulate the circadian cycle length. It seems that CKIε may regulate the mammalian circadian rhythmicity by controlling the rate at which PER1 protein enters into the nucleus (Vielhaber et al., 2000).

Tau mutant hamsters have a shortened circadian period of about 20 hours. *Tau* mutation weakens activity of CKIε and thus decreases phosphorylation of PER and CRY proteins. Consequently, their degradation is decreased as well. A quicker accumulation of these proteins occurs that leads to shortening of the circadian period. Similarly, a variantion in human sleep behavior called familial advanced sleep phase syndrome (FASPS) can be attributed to a missense mutation in a clock component, PER2. This variation shortens the circadian period *tau*. Affected individuals are "morning larks" with a 4-hour advance of the sleep, temperature, and melatonin rhythms. They have a serine to glycine mutation within the CKIepsilon binding region of PER2, which causes hypophosphorylation of the enzyme *in vitro* (Toh et al., 2001).

2.3.2.5. Circadian clock gene *Timeless*

Circadian rhythms in *Drosophila* depend on a molecular feedback loop generated by oscillating products of the *Per* and *Timeless* (*Tim*) genes. The relevance of mammalian *Tim* remains equivocal. It seems that most of its function was taken by CRY proteins. A rhythm of *Tim* mRNA level was only observed under LD conditions, but not under constant darkness (Tischkau *et al*., 1999). Conditional knockdown of TIM protein production in the rat suprachiasmatic nucleus disrupted its neuronal activity rhythms, and altered levels of known core clock elements. These data suggested that the mammalian TIM protein might be required for circadian rhythmicity and be a functional homolog of *Drosophila* TIM acting on the negative-feedback arm of the mammalian molecular clockwork (Barnes *et al.*, 2003). In addition, it was shown that the mouse *Tim* was essential for embryonic development, but did not have a substantial circadian function. Therefore, it is still difficult to say if and what role the mouse homolog of *Tim* plays in the circadian clock of mammals (Gotter *et al*., 2000).

2.3.2.5. Circadian clock gene *Rev-erbα*

Rev-erbα is an ubiquitously expressed orphan nuclear receptor which functions as a constitutive transcriptional repressor and is expressed in vertebrates with a robust circadian rhythm. Two *Rev-erbα* mRNA isoforms, namely *Rev-erbα1* and *Rev-erbα2* contain several E-box DNA sequences, which are activated by core circadian-clock components CLOCK and BMAL1. The CLOCK-BMAL1 heterodimer stimulates thus the activity of both *Rev-erbα1* and *Rev-erbα2* promoters. This activation is inhibited by overexpression of CRY1, a component of the negative limb of the circadian transcriptional loop (Triqueneaux et al., 2004). The protein product REV-ERBα binds to regulatory areas RevRE (Rev-erbα response elements) of other genes, namely Bmal1, and may thus cause their transcriptional inhibition (Harding *et* Lazar, 1993, Triqueneaux et al., 2004). The *Rev-erbα* gene expression exhibits a circadian rhythm with the maximal levels during the light period of the day.

2.3.2.6. Circadian clock gene *Ror*

Genes *Rorα, Rorβ, Rorγ* (retinoic acid-related orphan receptors) belong, similarly as *Rev-erbα* does to the orphan nuclear receptor group. In mammals, RORα along with REV-ERBα plays an important role in transcription of the clock gene *Bmal1*. Recent finding have demonstrated that all members of the REV-ERB (alpha and beta) and ROR (alpha, beta, and gamma) families repress and activate *Bmal1* transcription, respectively. In fact, transcription of Bmal1 depends on competition between REV-ERBs and RORs at their specific response elements (RORE) (Guillaumond *et al.*, 2005). *Rorα* mRNA reaches its maximum in the SCN during the subjective day; rhythm of *Rorβ* is not so prominent while *Rorγ* rhythmicity has not been recorded. *Rorα* mutants lose rhythms in *Bmal1* expression and their period is shortened. *Rorβ* mutant exhibit an impaired activity coordination and lengthening of the period of the circadian rhythm in activity (Sato *et al*., 2004). These results indicate that all members of the ROR family are important components of the molecular circadian clock.

2.3.2.7 Circadian clock gene *Dec*

Dec1 and *Dec2* are regulators of the mammalian molecular clock and form the fifth clock-gene family. *Dec1* and *Dec2* are basic helix-loop-helix transcription factors and repress CLOCK/BMAL1-induced activation of the mouse *Per1* promoter through direct protein-protein interactions with *Bmal1* and/or via competition for E-box elements. They are expressed in the suprachiasmatic nucleus in a circadian fashion, with a peak in the subjective day. A brief light pulse induces *Dec1* but not *Dec2* expression in the .suprachiasmatic nucleus in a phase-dependent manner (Honma *et al*., 2002). It is suggested that the CLOCK/BMAL heterodimer enhances *Dec2* transcription via E-boxes, but the induced transcription is then suppressed by DEC2. Hence, DEC2 affects its own rhythmic expression. In addition, CRY and PER may also modulate Dec2 transcription (Hamaguchi *et al.*, 2004). Alternations of the circadian systems are increasingly recognized as important risk factors for a disease initiation and progression and expression of *Dec* genes is rapidly induced by environmental stimuli and is highly increased in tumour tissues. Therefore, a de-regulated expression of *Dec* genes may probably alter normal circadian rhythms and contribut significantly to pathogenesis of many diseases including cancer (Li *et al*., 2004).

2.3.3. THE MOLECULAR OSCILLATOR MODEL

Researchers who have analyzed the circadian clock have worked day and night to uncover the mechanism that makes our biological clock tick. Their joint discoveries are remarkable. A molecular framework for the circadian rhythmicity has been suggested and roles and functions of clock genes and their protein products have been clarified (Reppert *et* Weaver, 2001). As mentioned previously, the intracellular molecular clockwork in the SCN consists of interacting positive and negative transcriptional-translational feedback loops (Fig.3). It takes approximately 24 hours before the entire cycle is completed. However, little is known about stechiometry and kinetics of this feedback loop. Recent data have shown that post-translational modification and degradation of circadian clock proteins are crucial steps for determining the length of the circadian period of the clock. One of the functions of the post-translational phosphorylation of clock proteins is to target

them for polyubiquitylation and degradation by the proteosomal pathway (Takahashi *et al*., 2008).

Among the positive components, *Bmal1* mRNA and protein cycle (Abe *et al*., 1998; Tamaru *et al*., 2000) in an opposite phase relative to the negative components, as is expression of *Per* and *Cry* whereas expression of *Clock* is not rhythmic. The transcriptional regulation appears to be fundamental to circadian oscillations. Expression of negative components PER and CRY is activated by the BMAL1-CLOCK heterodimer (Gekakis *et al*., 1998) and strongly repressed by CRY (Kume *et al*., 1999, Lowrey *et* Takahashi, 2000; Reppert *et* Weaver, 2001).

Both negative and positive components take part in three loops. The first of these is the negative autoregulatory PER/CRY feedback loop. Early in the day, the basic helix-loop-helix PAS-domain containing transcription factor CLOCK interacts with BMAL1 to activate transcription of the *Per* and *Cry* genes, resulting in high levels of these transcripts. In the evening, the PER and CRY proteins heterodimerize and translocate to the nucleus. During the night, the PER/CRY complex interact with the CLOCK/BMAL1 complex to inhibit transcription of their own genes. At the end of the night, the PER/CRY represor complex degrades, and CLOCK–BMAL1 can then start to activate a new cycle of transcription. The entire cycle takes approximately 24 hours to complete; however, little is known about stoichiometry and kinetics of this feedback loop (Lee *et al*., 2001)

The second loop is the negative autoregulatory BMAL1 feedback loop involving the gene *Rev-erba* which is activated directly by CLOCK/BMAL1 heterodimer. *Rev-erba* strongly represses *Bmal1* transcription. Although this secondary loop is not essential, it adds robustness to the molecular clock. There are other candidate clock components such as *Timeless*, *Dec1*, *Dec2*, which might contribute to the rhythmicity, but whose roles have not yet been clearly defined (Preitner *et al*., 2002; Sato *et al*., 2004).

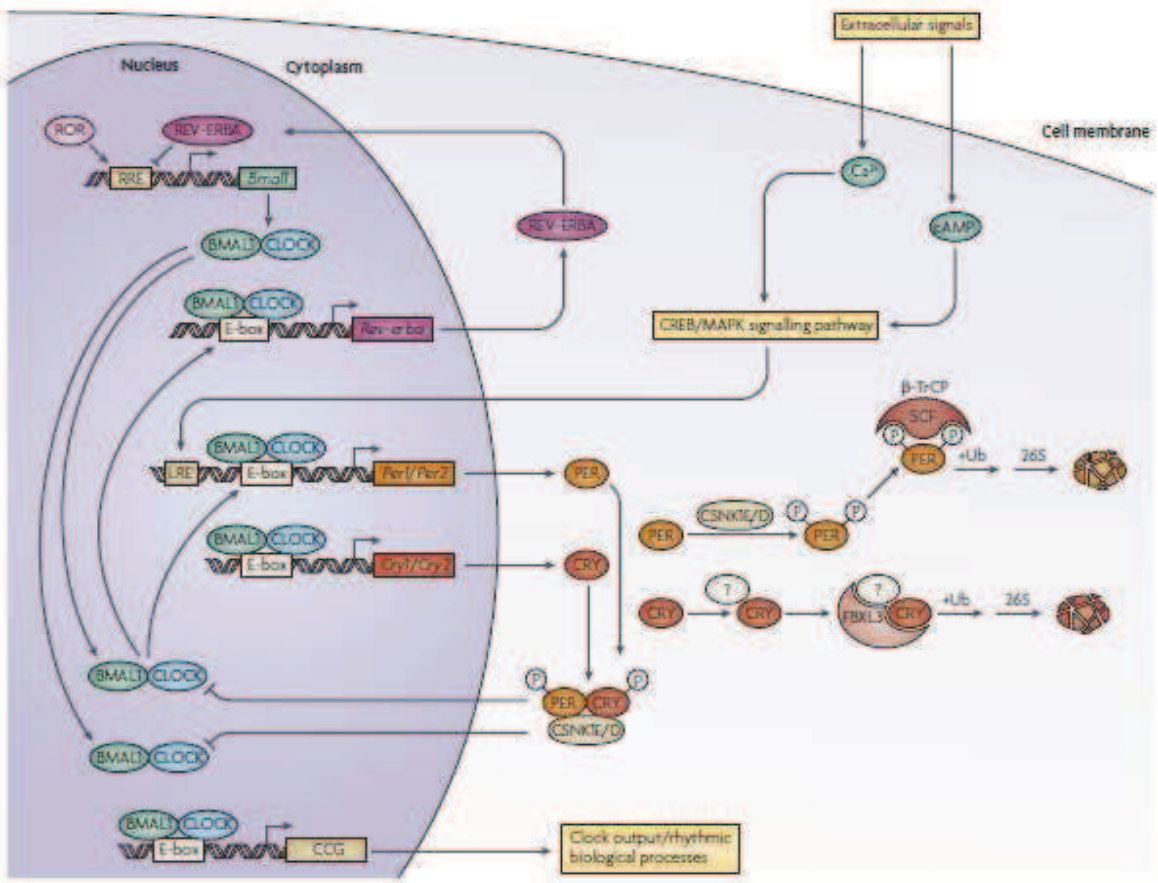

Fig.3 The mammalian circadian clock is composed of a transcriptional–translational feedback network. The circadian clock mechanism involves transcriptional–translational feedback loops comprised of a set of core clock genes. In mammals, the circadian clock is composed of a primary negative feedback loop involving the genes *Clock*, *Bmal1*, *Per1*, *Per2*, *Cry1* and *Cry2*. The secondary autoregulatory feedback loop is composed of *Rev-erba*, which is a direct target of the CLOCK/BMAL1 transcription activator complex. In addition to the transcriptional activators and repressors, post-translational modification and degradation of circadian clock proteins are crucial steps for generating circadian rhythms and determining their periods. Key kinases for PER and CRY phosphorylation are casein kinase 1 delta and epsilon. The β-TrCP1 and FBXL3 E3 ubiquitin ligase complexes have been implicated in targeting the PER and CRY proteins, respectively, for degradation. CCg, clock-controlled genes; CREB, cAMP response element-binding protein; E-box, CACgTg/T konsensus sequence; MAPK, mitogen-activated protein kinase; SCF, SCF E3 ubiquitin ligase; Ub, ubiquitin. *Adapted from J. Takahashi 2008.*

These two anti-phased loops combine to form the third positive forward loop through inter-activation: PER/CRY complexes activate *Bmal1* during the late day when their levels are high. Subsequently, BMAL1 accumulates, and when it reaches a high level around

midnight, BMAL1, together with CLOCK, activates *Cry* and *Per* genes expression. The different circadian time courses of oscillations of negative components and BMAL1 (Lowrey *et* Takahashi, 2000; Reppert *et* Weaver, 2001), may suggest a model for the transcriptional control of the mammalian clock that incorporates transcriptional switching on at late day and after midnight.

Circadian rhythms are remarkably stable and display a precise period in the absence of environmental cues, such as light. It is conceivable that multi-loops are more stable than a single loop in feedback regulatory systems. The PER/CRY loop appears to be critical to the regulatory process. The BMAL1 loop is interlocked with the main PER/CRY loop, and lends stability to the clock. Inter-activation between two loops may maintain the amplitude of mRNA oscillations of the clock and clock-controlled genes, thus providing a potential basis for the persistence of circadian clocks. The period precision may involve even more complicated mechanisms. Both PER/CRY and antiphased BMAL1, at high levels and at opposite circadian time points, provide feedback to repress their own gene transcription in nuclei. This event simultaneously sows the seed for the next circadian cycle through a positive forward loop, thereby setting up the timed suppression and promotion of self-oscillations, and forming a timing device.

It appears that the transcriptional potency of CRY is predominant within the mammalian clock. It is conceivable that, in the presence of CRY, the BMAL1-CLOCK dimers cannot function. This requires a mechanism whereby CRY and PER2 are removed from the nuclei around midnight, just when BMAL1-CLOCK turns on expression of the negative components and simultaneously turns off *Bmal1* transcription. Such clearance mechanisms, working in concert with CKI epsilon-PER2-related cytoplasmic delay of negative components (Toh *et al*., 2001), might contribute to period precision. PER1 does not appear to have a direct role in the clock gene transcription. However, the ability of PER1 to suppress PER2 at the post-transcriptional level (Zheng *et al*., 2001) may contribute to the clock period precision. Additional interactions between negative regulatory factors and their translocation mechanisms into the nucleus may be also involved in controlling the period of the clock.

In conclusion, all these data reveal that BMAL1 is activated by CRY1, CRY2, and PER2, but repressed by BMAL1-CLOCK. Both negative components (PER/CRY) and

positive components (BMAL1-CLOCK) play bi-directional transcription roles when at high levels during the late day and around midnight, respectively. The bi-directional transcription role at these two circadian times underlies the opposite phase of BMAL1 as compared to PER and CRY. The BMAL1 negative feedback loop interlocks with the PER/CRY negative feedback loop by inter-activation, forming a third positive forward loop in the mammalian clock. This transcriptional model suggests a molecular basis for maintenance of the stability, persistence, and period of circadian rhythms. The transcriptional potency of CRY is predominant within the mammalian clock, suggesting a clearance mechanism for PER/CRY which might be involved in the period maintenance (Yu et al., 2002).

Recently, along with the classic circadian core clockwork model, new elements responsible for regulation of clock genes interaction have been suggested: In the last decade, numerous studies have unveiled the pervasive role of microRNAs (miRNAs), a class of small, non-coding transcripts, in the post-transcriptional gene regulation in biological processes ranging from development to cancer. Until recently, the circadian clock has been modeled as simple, interlocking, transcriptional/translational feedback loops that drive a rhythmic gene expression of a few core 'clock' components. However, biological implications of miRNAs have been extended even to the circadian system by recent discovery that miRNAs are expressed in the suprachiasmatic nuclei, the master circadian clock in mammals, in a rhythmic and inducible fashion, and modulate the intrinsic pacemaker activity and resetting capacity of the SCN (Cheng et al, 2007).

Adenosine 3',5'-monophosphate (cAMP) signaling constitutes an additional, bona fide component of the oscillatory network. cAMP signaling is rhythmic and sustains the transcriptional loop of the suprachiasmatic nucleus, determining canonical pacemaker properties of amplitude, phase, and period. This role is general and is evident in peripheral mammalian tissues and cell lines, which reveals an unanticipated point of circadian regulation in mammals qualitatively different from the existing transcriptional feedback model. Thus, daily activation of cAMP signaling, driven by the transcriptional oscillator, in turn sustains progression of transcriptional rhythms. In this way, clock output constitutes an input to subsequent cycles (O'Neill *et al*., 2008).

Recent studies revealed a mutation in FBXL3 (ubiquities E3 ligase of F-box family) which interacts specifically with the CRY proteins. This mutation is caused by an isoleucine to threonine substitution and leads to a loss of FBXL3 function. In animals with this mutation, production of the PER1 and PER2 proteins is reduced; however, the CRY1 and CRY2 proteins are unchanged. The loss of FBXL3 function leads to a stabilization of the CRY proteins, which in turn leads to a global transcriptional repression of the *Per* and *Cry* genes. Thus, Fbxl3 defines a molecular link between CRY turnover and CLOCK/BMAL1-dependent circadian transcription in modulating the circadian period (Siepka *et al*., 2007; Godinho *et al*., 2007).

2.3.4. CLOCK CONTROLLED GENES

Recent studies have also shed light on the molecular mechanisms, by which the central clock may control circadian output genes. Some of these downstream genes appear to be regulated by the same DNA elements and transcription factors that govern the expression of the central clock genes themselves. Such genes are called clock-regulated genes (CCGs). The available evidence indicates that the central clock may regulate clock-controlled genes either directly by the same genes that drive central clock function or indirectly by cascades of circadian transcription factors. Evidence exists, however, that this regulation is not entirely unidirectional. Some output genes can feed back to influence certain parameters of the central clock itself (Brown *et* Schibler, 1999).

The arginine vasopressin gene (*Avp*), expressed in the SCN neurons, provides an excellent example of such a strategy. It is one of the principal transmitters in the SCN. Approximately 20% of neurons in the dorsomedial division of the SCN synthesize the peptide and a high proportion of SCN neurons (> 40%) are excited by AVP acting through the V1 receptor. This suggests that AVP may act as a feedback regulator of electrical activity within the nucleus. As the synthesis and release of AVP occurs in a circadian manner, this leads to a variable feedback excitation, which may contribute to the circadian pattern of activity of the neural clock. A role in amplifying the rhythmicity is supported by observations that animals deficient in AVP show reduced circadian amplitude of behavioral rhythms (e.g. of the locomotor and cortical electroencephalographic rhythms) (Ingram *et al*., 1998). The promoter region of this gene harbors an E-box motif similar to

the one which mediates transcriptional activation of the *Per* genes via heterodimers of the CLOCK and BMAL1 proteins. *Avp* transcription is drastically reduced in homozygous C*lock* mutant mice. Moreover, transient co-transfection studies show that expression of reporter genes carrying the *Avp* promoter are activated by CLOCK and BMAL1 and repressed by PER. Thus, *Avp* appears to be regulated exactly like the Per genes themselves (Jin *et al*., 1999).

Besides the clock genes constituting the core oscillatory loop, a transcription factor *Dbp* (named for albumin gene D-site binding protein), is expressed in the SCN with a clear rhythm in LD and DD conditions (Lopez-Molina *et al*., 1997). *Dbp* belongs to the PAR leucine zipper transcription factor family, which includes thyrotrophic embryonic factor and hepatic leukemia factor, and is known to increase transcription of several genes in the liver. DBP activates transcription of some genes in the liver such as the albumin, cholesterol 7a hydroxylase, and cytochrome P450 (CYP2C6) genes, by direct binding to their promoters. Expression of *Dbp* is endogenously highly rhythmic, with an amplitude comparable to that of *Per1* mRNA, and it is not influenced by an environmental light. Analysis of the *Per1* mRNA promoter region has revealed that the nucleotide sequence located between 228 and 237 of the *Per1* gene shows homology with the consensus DBP-binding sequence. This demonstrates that DBP directly binds to the *Per1* promoter and thereby increases its transcription. Furthermore, the DBP protein can be detected in the nuclei of pacemaker cells in the SCN concomitantly with a rise in *Per1* mRNA levels. It appears that *Dbp* transcription is regulated by CLOCK/BMAL1 and PER/CRY complexes similarly as *Per1* mRNA (Yamaguchi *et al*., 2000). The clock-controlled *Dbp* gene may thus play an important role in the central oscillatory mechanism.

A transcription factor E4BP4 is a mammalian homologue of the Drosophila *vrille* that functions as a key negative component of the circadian clock. It has been shown that the E4BP4-binding site (B-site) is required, in addition to a non-canonical E-box (E2 enhancer), for a robust circadian *Per2* expression in the cell-autonomous clock. While the E2 enhancer and the B-site are closely situated, correlations between the component bound to the E2 enhancer and that bound to the B-site remain obscure. E4BP4 interacts with the PER2 protein, which represses the transcriptional activity via the E-box enhancer. Interaction with the PER2 protein requires the carboxyl-terminal region that contains the

repression domain of E4BP4. In addition, it has been demonstrated that E4BP4 interacts with the CRY2 protein, a key negative regulator of the mammalian circadian clock. All these results suggest that E4BP4 is a component of the negative regulator of complex of the mammalian circadian clock (Ohno *et al.*, 2007).

The enzyme AA-NAT converts serotonin to N-acetylserotonin, the immediate precursor of melatonin. An increased synthesis of melatonin in the pineal gland caused by a norepinephrine treatment appears to result in stimulation of AA-NAT by an adenosine 3',5'-monophosphate mechanism. The activity of AA-NAT in the rat pineal gland may be more than 100 times higher at night than during the day. Its circadian rhythm persists in complete darkness or in blinded animals and is suppressed by light at night (Illnerova et al., 1982). The AA-NAT rhythm is 180 degrees out of phase with the serotonin rhythm and is similar to the norepinephrine and melatonin rhythms (Klein *et* Weller, 1970; Illnerova *et* Vanecek, 1980). The gene encoding AA-NAT contains an E-box DNA element. It has been shown that the human BMAL1/CLOCK heterodimers bind to the E box element on the AA-NAT gene and enhance its transcription. These findings suggest that binding of the clock gene products heterodimers to the E box is a critical element for expression of the AA-NAT gene (Chong *et al*., 2000).

2.4 SYNCHRONIZATION OF THE CIRCADIAN SYSTEM

2.4.1 SYNCHRONIZATION BY LIGHT

Every day, synchronization of the circadian system with environment is necessary for its proper functioning. The endogenously generated rhythms have to run with a precise 24-hour period of the solar day. The most important and strongest environmental synchronizer of the circadian system with the outside day is regular change of the light and dark period of the day, namely the light period. There are many experimental conditions designed for studying effects of light on the circadian system, e.g., releasing of animals into constant darkness and then exposing them to light pulses. In this way, the effect of light administrated at a certain phase of the circadian rhythm can be studied. A curve showing dependence of direction and magnitude of phase shifts of a light pulse application is called the phase response curve (PRC) (Fig. 4). Its course is usually similar in most of the studied

organisms. In general, the PRC shows that light stimuli during the subjective day do not evoke any phase shift of circadian rhythms; stimuli during the first half of the night cause phase delays of the circadian rhythms, while stimuli during the second half of the night cause phase advances of the rhythms (Pittendrigh *et* Daan, 1976). Under natural conditions, animals may be entrained to other factors besides light, e.g., to food intake. It is also important to consider the entraining effect not only of the entire light period of the day, i.e., photoperiod, but also of light around dusk and dawn, i.e., twilight.

Measuring of visual sensitivity to light suppression of pineal melatonin in golden hamsters using 300 s stimuli of monochromatic light (503 nm) in constant darkness showed that increasing stimulus irradiance caused a monotonic decrease in pineal-melatonin content. Irradiance greater than $3.5 \cdot 10^{10}$ photons / ($cm^2 \cdot s$) caused significant reductions of melatonin in the hamster pineal. Saturation of the response occurred above 10^{11} photons / ($cm^2 \cdot s$) and melatonin levels were suppressed to approximately 7% of levels measured in non-stimulated animals. The sensitivity of the photic-entrainment pathway for circadian rhythms has also been measured using identical stimulus parameters. Light suppression of pineal melatonin was 25 times (1.4 log units) more sensitive to irradiance than the phase-shifting response measured for the circadian rhythm of running-wheel activity. Both of these responses are, however, less sensitive to light than other visual responses measured behaviorally (Nelson *et* Takahashi, 1991). Thus, to cause a phase shift of a circadian rhythm, light intensity has to be significantly higher than that for light perception in the eye. This is probably necessary for preventing of phase shifts by a low intensity light, such as is a moon light at night.

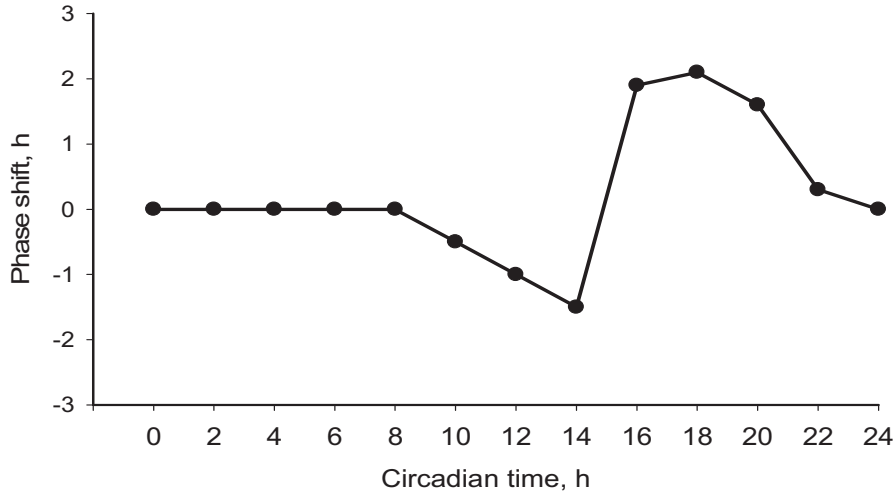

Fig.4 Example of a typical response curve.

The dependence of a phase shift direction and magnitude on the time of the light pulse application. Circadian time 0 indicates beginning of the day, circadian time 12 indicates beginning of the night, + phase advance, - phase delay. *Adapted and modified from Illnerova, 1986.*

2.4.2 LIGHT-INDUCED EXPRESSION OF CLOCK GENES

Using a wide variety of neurobiological and molecular genetic tools, key elements comprising the visual input pathway for SCN photoentrainment have been elucidated in rodents (Barinaga et al., 2002). Important questions remain concerning intracellular signals that reset the autoregulatory molecular loop within the photoresponsive cells in the SCN's retino-recipient subdivision, as well as concerning the intercellular coupling mechanisms that enable SCN tissue to generate phase shifts of overt behavioral and physiological circadian rhythms such as are the rhythm in locomotion or the rhythm in the SCN neuronal firing rate. Multiple neurotransmitters, protein kinases, and photoinducible genes add to the system complexity (Meijer *et* Schwarz, 2003).

The circadian clock integrates the temporal information on periods of the solar cycle and adjusts its phase to them in order to synchronize the organism's internal state to the local environmental day and night. Light in the late evening and early morning is the dominant entraining agent. In mammals, information about light during the subjective night is transmitted by glutamate released from the retinal projections to the circadian clock in the suprachiasmatic nucleus of the hypothalamus. The clock resetting requires

activation of ionotropic glutamate receptors which mediate Ca^{2+} influx. As it has been mentioned above, the response induced by such activation depends on the clock's temporal state: during the early night, light delays the clock phase, whereas in the late night it phase-advances the clock (Ding *et al*., 1998).

The process of synchronization by light involves induction of several genes. Brief exposure to light during the subjective night causes rapid induction of immediate-early genes, such as c-*fos* (Kornhauser *et al*., 1990). *c-fos* expression exhibits an endogenous circadian rhythm in the dorsomedial SCN, with the maximum during the subjective day and the minimum during the subjective night (Sumová et al., 1998). Following a light stimulus at night, *c-fos* is induced, but this time in the ventrolateral, i.e., retino-recipient part of the SCN (Jáč et al., 2000). This response to light in the ventrolateral SCN is gated, i.., it occurs only during the subjective night.

Light at night induces also two clock genes, namely *Per1* and *Per2*. In the mouse, a light pulse induces *Per1* mRNA within 15–30 min and *Per2* mRNA within 2 h (Albrecht *et al*., 1997; Shearman *et al*., 1997). Arousal and serotonin receptor activation induce acute down-regulation of *Per1* and *Per2* mRNAs expression in the SCN. Hence, these two genes may be involved in both photic and non-photic entrainment. Several lines of evidence indicate that *Per1* gene plays a central role in conveying the light-entraining information to the central clock. *Per1* is the only clock gene that has been convincingly shown to be induced very rapidly after light stimulation (Shigeyoshi *et al*., 1997). Studies on the promoter structure of *Per* genes and comparison of their regulation have shown that both *Per1* and *Per2* promoters contain E-boxes and respond to the CLOCK/BMAL1 heterodimer. In addition, both promoters contain also the cAMP-responsive elements (CREs) that bind the CRE-binding protein (CREB). The *Per1* promoter is responsive to synergistic activation of the cAMP and mitogen-activated protein kinase pathways, a physiological response that requires integrity of the CRE. In contrast, activation of Per promoters by CLOCK/BMAL1 occurs regardless of an intact CRE. Following a light stimulus at night, CREB is rapidly phosphorylated. Altogether, these results constitute strong evidence that CREB acts as a pivotal endpoint of signaling pathways for the regulation of *Per* genes and reveal that the signaling-dependent activation of *Per* genes is

distinct from the CLOCK/BMAL1-driven transcription required within the clock feedback loop (Travnickova-Bendova *et al*., 2002).

Recently, an additional photic input pathway to the mammalian circadian clock based on protein kinase C alpha (PKCA) was recently described. PKCA-deficient mice show an impairment of the light-mediated clock resetting. In the SCN of wild-type mice, light exposure at night evokes a transient interaction between PKCA and PER2 proteins that affects PER2 stability and its nuclear-cytoplasmic distribution. These posttranslational events, together with CREB-mediated transcriptional regulation, may be key factors in the molecular mechanism of the photic clock resetting (Jakubcakova *et al*., 2007).

In contrast to the above mentioned studies, which implicated PER1 and PER2 in transduction of photic information to the core circadian clockwork, another study with phase-shifting effects of light were applied in PER1-deficient and PER2-deficient mice. Surprisingly, they revealed that both phase delays and phase advances were observed in both *Per1* and *Per2* mutant mice. These results were not consistent with the hypothesis that PER1 and PER2 play necessary and non-overlapping roles in mediating the effects of light on the circadian clock (Bae *et* Weaver, 2003).

2.4.3 EFFECT OF PHOTOPERIOD ON CIRCADIAN SYSTEM

2.4.3.1 Synchronization with the photoperiod

As it has been mentioned above, the light period of the day, i.e., the photoperiod, is the most important synchronizer for circadian rhythms. In temperate geographic zones, the photoperiod changes during the course of the year. At the 50^{o} latitude (Prague is, e.g., situated at 50^{o} N latitude) the longest day is on the 21^{st} and 22^{nd} of June and lasts for about 16 hours, while the shortest one is on the 21^{st} and 22^{nd} of December and lasts for only about 8 hours. Animals can trace not only the duration of the day light, but rather whether the photoperiod increases or decreases within the course of the year (Hofmann et al., 1986). These changes affect the mammalian and marginally even the human behavior and physiology. Animals prepare for a forthcoming season by modulating their fur, feeding, reproductive, metabolic, and locomotor activity, etc. These responses to the photoperiod are called the photoperiodic reactions. In nocturnal rodents, the duration of the locomotor

activity responses to the photoperiod in such a way that it is shorter on long summer than on short winter days (Puchalski *et* Lynch, 1991; Elliott *et* Tamarkin, 1994).

The rhythmic production of the pineal hormone melatonin, which is a part of the timekeeping system, is also highly photoperiodic, both in nocturnal and in diurnal animals. Nor-epinephrine released at night from the nerve ending in the pineal increases level of cAMP, which then activates protein kinases. Consequently, CREB is phosphorylated. Its phosphorylated form enters into the nucleus and binds to the promoter of the AA-NAT gene, which contains CRE region. Transcription of the gene encoding AA-NAT, a crucial enzyme in melatonin synthesis, ensues (Baler *et al*., 1997). The period of the high night AA-NAT is by 5 -6 hours shorter in rats kept under a long, LD16:8, photoperiod than in those kept under a short, LD8:16, photoperiod. A short, 1-day adaptation to longer days, i.e., to transition from LD12:12 to LD16:8, involves an earlier morning decline of AA-NAT induced by an earlier 'light on'. Following a long-term adaptation to LD16:8, AA-NAT declines spontaneously 1 h before the morning 'light on'. A short, 1-day adaptation to shorter days, i.e., to transition of rats from LD12:12 to LD8:16, involves an earlier evening rise in AA-NAT and a spontaneous morning decline at approximately the same time as in LD12:12. Following a long-term adaptation to LD8:16, the period of high AA-NAT shifts towards the later part of the night and the activity declines about 1 - 2 hours before the 'light on'. In natural daylight, the period of the high night AA-NAT is the shortest in June and longest in December. The morning decline in AA-NAT might be induced by dawn on April 19th and June 20th, but is spontaneous on December 19th (Illnerova *et* Vanecek, 1980) (Fig.5, LEFT).

Seasonal changes of day length affect thus significantly the rhythm of melatonin synthesis (AA-NAT activity in the pineal gland), which is one of the output rhythms of the central circadian clock. In mammals such responses to the photoperiod might reflect photoperiodic changes in the circadian pace-making system within the suprachiasmatic nucleus that governs the circadian rhythms. It appears that this may be the case. Studies on daily profiles of the light-induced *c-fos* gene expression in the SCN of rats maintained either under a long or under a short photoperiod have revealed that the endogenous circadian rhythm of light responsiveness in the SCN is indeed altered by the photoperiod. The duration of the photosensitive subjective night under the short photoperiod lasts by 5 -

6 h longer than that under the long photoperiod. These results have provided the first evidence that a functional property of the SCN is altered by the photoperiod and they have suggested that the SCN itself is involved in the photoperiodic time measurement (Sumova *et al*., 1995a) (Fig.5 RIGHT).

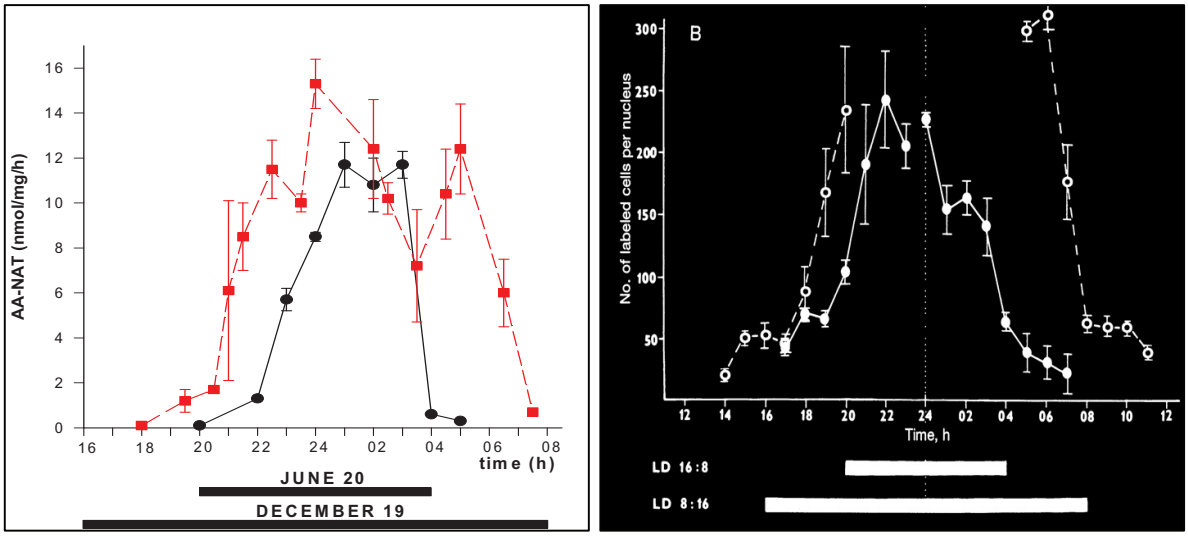

Fig.5 Two examples of circadian rhythms influenced by the photoperiod.
LEFT: Pineal N-acetyl transferase (AA-NAT) activity measured in rats maintained under a natural photoperiod and sacrificed on the June 20th (circles) and December 19th (squares). *Adapted from Illnerova and Vanecek, 1980.*
RIGHT: Light-induced c-FOS protein immunoreactivity measured in the SCN of rats maintained under an artificial long (LD 16:8) (closed circles) or short (LD 8:16) (open circle) photoperiod, then released into constant darkness and exposed to a single 30 min light pulse at various times, returned to darkness and killed 30 min following the end of the light pulse. Black bars under the graphs indicate duration of the dark phase on respective photoperiod. *Adapted from Sumova et al., 1995b.*

Furthermore, after a change from a long, LD16:8, photoperiod to a short, LD8:16, photoperiod, the interval enabling high *c-fos* photoinduction decompresses gradually and its full extension by 5-6 h is achieved only within 2 weeks. After a change from a short to a long photoperiod, the interval was compressed by 5-6 h within 3 days. The data indicate a

rapid adjustment of the photoperiod dependent-state of the SCN pacemaker to long days but only a slow one to short days (Sumova *et al*., 1995b).

More recent data show that the photoperiod affects i) the clock-driven rhythm in photoinduction of *c-fos* gene and of its protein product within the SCN, ii) the clock-driven spontaneous rhythms in clock-controlled, i.e. *Avp*, and in clock-related, i.e. *c-fos*, gene expression within the SCN, and iii) the core clockwork mechanism within the rat SCN. Hence, the entire central timekeeping mechanism within the circadian clock measures not only the daytime but also the time of the year, i.e. coming of the actual season (Sumova *et al*., 2004).

2.4.3.2 Effects of the photoperiod on the circadian clock genes expression

The mammalian *Per1* gene is expressed in the suprachiasmatic nucleus of the hypothalamus, where it is thought to play a critical role in generation of circadian rhythms. Information on the duration of a photoperiod is involved not only in duration of the melatonin signal or of the SCN interval in photosensitivity, but, most importantly, it is involved in the peak duration and amplitude of *Per* genes expression. Duration of the interval of elevated *Per1* (Messager *et al*., 1999; Steinlechner et al., 2002; Sumova *et al*., 2003) and *Per2* (Tournier *et al*., 2003) mRNA levels is significantly longer under a long photoperiod than under a short photoperiod. Circadian rhythms in PER1 and PER2 proteins in the SCN peaking approximately 12 h after lights-on, are modulated by the photoperiod as well (Nuesslein-Hildesheim *et al*., 2000; Sumova et al., 2002). The interval of elevated PER levels is longer under a long photoperiod than under a short one. These results indicate that core elements of the circadian clockwork respond to seasonal time and that encoding and decoding of the seasonal information may be mediated by actions of these transcriptional modulators.

A detailed analysis of the photoperiod effect on other clock genes has revealed that their expression may be also modulated by the photoperiod. The daytime increase of *Cry1* mRNA in the rat SCN is linked to the morning light onset: under a long photoperiod, it occurs earlier than under a short one. However, whereas *Per* mRNA declines from high daytime levels at about the same time under a long as well as under a short photoperiod, *Cry1* mRNA level declines earlier under a long photoperiod than under a short photoperiod.

Hence, the *Cry1* mRNA rhythm under a long photoperiod is merely phase-shifted towards earlier hours, but its waveform does not profoundly change. Similar to the *Per* mRNA rhythm amplitude, the *Cry1* rhythm amplitude also appears to be larger under a short than a long photoperiod (Sumova *et al*., 2003).

The morning *Bmal1* mRNA decline is also linked to the morning light onset: it occurs later under a short photoperiod than under a long one. Hence, the interval of elevated nocturnal *Bmal1* mRNA is longer under a short than a long photoperiod. The *Bmal1* mRNA rhythm amplitude appears also to be larger under a short than a long photoperiod, similar to the *Per1* mRNA and *Cry1* mRNA rhythm amplitudes. The longer duration of elevated *Bmal1* mRNA levels and the shorter duration of elevated *Per* mRNAs levels under a short photoperiod as compared to the duration under a long photoperiod corresponds well with the fact that *Bmal1* gene is expressed in an opposite phase to Per expression in the SCN (Tamaru *et al*., 2000; Sumova *et al*., 2003). *Bmal1* belongs to cycling genes in the SCN with putative Rev-erbα/Ror response elements in their promoter regions, whereas *Per* genes belong to cycling genes with putative cAMP response elements in their promoter regions (Preitner *et al*., 2002; Ueda *et al*., 2002). Whereas phases of the former genes consolidate to the subjective night, phases of the latter genes consolidate to the subjective day. The subjective night is characterized not just by the high *Bmal1* expression but by other parameters as well, among them by the elevated *c-fos* gene photoinduction in the SCN (Sumova *et al*., 1995a; Sumova *et al*., 1995b) or the high nocturnal pineal melatonin production. According to all the above listed parameters, the subjective night lasts longer on short than on long days. It remains to be elucidated how the photoperiod affected rhythms in *Bmal1* as well as in other clock genes expression control the photoperiod dependent rhythms in the SCN, pineal or elsewhere (Sumova *et al*., 2003).

Under a short photoperiod, *Clock* in the rat SCN is expressed in a rhythmic way, with a long interval of elevated *Clock* mRNA. Presence of the rhythm under the short photoperiod is in accordance with larger amplitudes of rhythms of other clock gene expression under the short photoperiod. Larger amplitudes of rhythms in clock gene expression on short days might be due mostly to lower minimal values under a short photoperiod as compared to those under a long photoperiod. It appears that the pacemaker

under the short photoperiod may resemble more than in constant darkness, when its state is not shaped by any photoperiod (Sumova *et al*., 2003).

The photoperiod modulates not just individual rhythms of clock gene expression but also a phase relationship between them. Under a short photoperiod, *Per1* mRNA starts to increase about 2 hours before the expected light onset, at the time of PER1 minimum; at the same time, *Clock* mRNA starts to decline. At the time of expected light onset, *Bmal1* mRNA starts to decrease. Two hours later, PER1 protein level starts to rise, and 4 hours later, at midday, *Clock* mRNA and *Cry1* mRNA starts to increase. *Bmal1* mRNA starts to rise around the expected light offset. After the offset, *Per1* mRNA starts to decline, well before its product PER1 attains its maximum (Sumova *et al*., 2003).

Under the long photoperiod, some of these phase relationships are roughly the same as under the short one. The morning *Per1* mRNA increase occurs close to the time of the PER1 protein minimum; PER1 rise is phase delayed by about 6 to 8 hours relative to the *Per1* mRNA rise and is roughly in phase with the *Cry1* mRNA rise (Maywood *et al*., 1999; Reppert *et* Weaver, 2001). Increase in PER1 protein, *Cry1* mRNA, and possibly CRY1 protein (Reppert *et* Weaver, 2001) precedes the *Bmal1* mRNA rise. Some phase relationships under a long photoperiod differ, however, from those under a short photoperiod: For example, whereas under a short photoperiod PER1 protein and *Cry* mRNA decline at about the same time, under a long photoperiod the *Cry1* mRNA decline precedes that of PER1 by more hours. In addition, the PER1 decline precedes the *Bmal1* mRNA decline by more hours under a short than a long photoperiod (Sumova *et al*., 2003). The data thus indicate that the entire complex molecular clockwork in the rat SCN is photoperiod dependent and hence may differ according to the season of the year.

2.4.3.3. Effects of the photoperiod on and within different SCN parts

The molecular clockwork is affected by the photoperiod and may thus serve as a basis not just for a daily clock but also for a seasonal clock. As it has been mentioned above, in rodents the interval of elevated *Per1* and *Per2* expression in the SCN is longer under a long than under a short photoperiod (Hastings, 2001; Steinlechner *et al.*, 2002; Sumová *et al.*, 2002; Sumová *et al.*, 2003). Recent data show that expression of some of the clock genes under various photoperiods is not necessarily synchronized throughout the

whole SCN. Marked regional differences in gene expression rhythms along the rostro-caudal axis of the hamster SCN have been reported. *Per2* expression is photoperiod-dependent in both the rostral and caudal SCN. Under a short photoperiod, the maximal expression occurs in synchrony in both parts, but under a long photoperiod the peak of expression in the caudal SCN precedes that in the rostral SCN (Hazlerigg *et al.*, 2005; Johnston *et al.*, 2005). A similar asymmetry has been reported for the electrical activity of horizontal SCN slices (Jagota *et al*., 2000). Another study using as markers of the SCN neuronal activity c-FOS and PER1 proteins shows that in hamsters maintained in short days, there is no detectable phase dispersion of the proteins daily profiles across the rostro-caudal extent of the nucleus whereas in animals maintained in long days, rhythms in the caudal SCN phase lead those in the mid- and rostral SCN by 4-8 h and 8-12 h, respectively (Yan *et* Silver, 2008).

A model of two separate, but mutually coupled, circadian oscillators has been proposed to explain photoperiodic responses of the locomotor activity rhythm and of the rhythm in melatonin production in nocturnal rodents: an evening oscillator, which drives the activity and melatonin production onset entrains to dusk, and a morning oscillator, which drives the end of activity and melatonin production entrains to dawn (Pittendrigh and Daan, 1976; Illnerova and Vanecek, 1982). Recently, more separately oscillating cell groups in the mouse SCN, which were at various circadian phases and responded to photoperiods in a different way, were described (Schaap et al., 2003; Rohling et al., 2006, Van der Leest et al., 2007). Continuous measurement of circadian rhythms in *Per1* expression by a bioluminescence reporter showed a bimodal pattern under a long photoperiod, when expression in the caudal part phase-advanced that in the rostral part. In contrast, under a short photoperiod *Per1* expression was unimodal (Inagaki *et al*., 2007; Naito *et al*., 2008). *Bmal1* expression rhythms exhibited antiphase oscillations to *Per1* rhythms under both long and short photoperiod. However, difference between *Bmal1* mRNA expression within different SCN regions was not as prominent as that of *Per1* expression. In long days, a significant difference was observed between the rhythms in the rostral and caudal SCN with the caudal rhythms exhibiting an early peak time relative to the rostral rhythms (Naito *et al*., 2008).

2.4.4 EFFECTS OF THE LIGHT TO DARK TRANSITION ON THE CIRCADIAN SYSTEM

The vast majority of laboratory studies have used animals maintained under a light-dark cycle with an abrupt, rectangular (RA), transition between light and darkness. However, in nature animals experience a gradual light-dark transition at dusk and dawn. Dynamics and duration of these transitions depend on season and latitude (Boulos *et al.*, 1996b; Boulos & Macchi, 2005). The spectral composition of artificial light cycles also differs from that of natural light, which varies during the twilight hours (McFarland & Munz, 1975). Light responsive SCN neurons exhibit sustained responses to light stimuli of long duration and respond to an increasing and decreasing light intensity (Meijer *et al.*, 1986). Under natural conditions, the circadian system may thus continuously monitor changes in environmental illuminance and utilize the information for entrainment (Usui, 2000). Inclusion of twilights (TW) into light-dark regimens affects several circadian locomotor parameters in a season- and latitude-dependent manner. In Syrian hamsters, the timing of activity onsets follows dusk in the presence of twilights but is more closely related to dawn in their absence. The activity offsets and midpoints occurred earlier under a TW than under a RA regime, with the difference most pronounced under a short photoperiod (Boulos *et al.*, 1996c). The presence of twilights results also in a lower day-to-day variability in activity onset times (Boulos & Macchi, 2005). Apart from the locomotor activity, also the pineal rhythm in AA-N-acetyltransferase activity was studied under natural photoperiods (Illnerova & Vanecek, 1980). So far, the effect of twilight on the molecular clockwork in the mammalian SCN has been only marginally studied. In our previous work, PER1 protein profiles in the SCN of rats maintained under natural photoperiods in summer and in winter resembled those of rats maintained under corresponding artificial photoperiods (Sumová *et al.*, 2002).

2.5. DEVELOPMENT OF THE CIRCADIA SYSTEM

2.5.1. DEVELOPMENT OF THE CENTRAL SCN CLOCK

Morphologically, the rodent SCN develops gradually (Moore, 1991). In the rat, in which the prenatal period lasts about 22 days, neurogenesis of the SCN begins on

embryonic day (E)14 and continues through E17. Neurons of the ventrolateral SCN are generated on E15-16 and neurons of the dorsomedial SCN on E16-17. Whereas the neurogenesis is completed on E18, the morphological maturation of the SCN neurons proceeds until the postnatal day (P)10. On E19, only sparse synapses may be observed. Synaptogenesis begins to progress only in the late prenatal and early postnatal periods, and then increases significantly from P4 to P10 (Weinert, 2005). It appears that the rat SCN is fully developed only on P10. A day-night variation in various functions, e.g., in metabolic activity, in the firing rate of the SCN neurons or in the *Avp* expression may appear, however, at a late embryonic stage (Weinert, 2005).

2.5.2. THE MOLECULAR CLOCKWORK DURING ONTOGENESIS

2.5.2.1. The SCN molecular clockwork

In the rat SCN at E19, *Per1*, *Per2*, *Cry1* and *Bmal1* are not yet expressed in a rhythmic way (Sladek et al., 2004). Levels of clock proteins PER1, PER2 and CRY1 not only do not exhibit any circadian variations, but, moreover, they are undetectable t E19. Therefore, at this stage of the development, the SCN circadian clock might not be able to generate synchronized oscillations. Rhythms in clock genes expression develop gradually. Their amplitude increases postnatally and adult-like stage amplitudes are attained around P10 (Sladek et al., 2004; Kovacikova et al., 2006). Hence it appears that the molecular clockwork in the SCN develops mainly postnatally. However, a possibility cannot be ruled out that during the late prenatal period, a small proportion of the SCN cells may be already rhythmic, but the methodological approach used in the above mentioned studies would not allow detecting a very low oscillating signal which might arise from a few SCN cells. Due to development of synaptic communication between these potentially rhythmic cells and non-rhythmic ones, the rhythms might gradually strengthen and their amplitude might increase.

2.5.2.2. The peripheral molecular clockwork

In the rat heart, circadian rhythms in the expression of clock genes *Per1, Bmal1* and clock-controlled gene *Dbp* could not be detected by Northern blot analysis on P2 (Sakamoto et al., 2002). Expression of *Per1, Bmal1* and *Dbp* began to be rhythmic between P2 and P5, but expression of *Per2* did not exhibit any rhythmicity until P14. Similarly, in the rat liver, clock gene expression determined by RT-PCR developed gradually during postnatal development (Sladek et al., 2007). At E20, only *Rev-erbα* mRNA exhibited a significant, high amplitude circadian oscillation, but the expression of *Per1*, *Per2* and *Cry1* was arrhythmic. Even at P2, *Rev-erbα* was still the only gene expressed rhythmically with high amplitude. At P10, *Per1* mRNA and at P20 *Per2* and *Bmal1* also began to be expressed in a circadian way but only as late as at P30, all of the studied clock genes were expressed rhythmically in the adult-like pattern (Sladek et al., 2007). The stable detection of the high-amplitude rhythm in *Rev-erbα* expression throughout ontogenesis ruled out the possibility that the lack of rhythmicity in the clock gene expression in the early development was due to desynchronization of oscillating cells in the liver. Rather, the cells might be synchronized by rhythmic humoral or neuronal cues impinging upon individual cells.

2.5.3. ENTRAINMENT OF THE CIRCADIAN SYSTEM DURING ONTOGENESIS

Majority of maternal signals that are delivered to the fetus transplacentally, exhibit circadian rhythms. Timing of maternal cues may provide fetuses with information about the external time. However, it is still not known whether and how maternal cues impinge on the fetal SCN clock. There is extensive evidence that primarily the maternal SCN sets the phase of the developing fetal clock (Sumova et al., 2006). The newly forming and appearing SCN rhythms in clock genes expression in the very late fetal and early neonatal stages are, from the beginning, in phase with the maternal clock (Sladek et al., 2004). Hormone melatonin or activation of dopaminergic pathways have been suggested as the entraining maternal cues for the fetal clock, but it remains to be elucidated whether and how the suggested cues may induce a rhythmic expression of clock genes (Sumova et al.,

2006). The exquisite maternal entrainment of the newborn rats rhythmicity becomes less important after the first week of their life when the photic entrainment starts to override the maternal entrainment. This holds true for laboratory rats. In nature, however, the switch from maternal to photic entrainment may correlate with the ability to pups to leave their underground burrows and get explored to the environmental light. The mechanism underlying the change in sensitivity of the clock to entraining signals is not fully understood. Though postnatally the SCN molecular clockwork gradually starts to be entrained by the environmental light-dark regime, the clockwork in the liver is first entrained by the rhythmic nursing of newborn rats by their mothers, i.e., by the cyclic food intake. Only later, during the weaning between the P15 and P30, rhythms in clock gene expression in liver attain the same phase as in adult rats (Sladek et al., 2007).

3. AIM OF THE WORK

3.1 To determine whether and how a short and a long photoperiod with artificial TW affect expression of the clock genes, namely of *Per1* and *Per2*, and their products PER1 and PER2, in the mouse SCN and to compare the effect of the TW photoperiods with those of the RA photoperiods.

Mice were entrained to a long photoperiod with 18 h of light and 6 h of darkness or a short photoperiod with 6 h of light and 18 h of darkness under abrupt RA or gradual TW light-to-dark transition. Thereafter, they were released into darkness and daily profiles of *Per1* and *Per2* expression as well as PER1 and PER2 levels were measured within the rostral, middle and caudal parts of the SCN.

3.2 To test a hypothesis that the mechanism of adjustment to the change of the photoperiod in the central clock differs from that in the peripheral clock. Therefore, the dynamics of changes in the rhythms of clock gene expression in different regions of the mouse SCN and in the liver during the transition from a long to a short photoperiod was studied.

Mice maintained under a regimen with 18 h of light and 6 h of darkness (LD18:6) were transferred to a regime with 6 h of light and 18 h of darkness (LD6:18). Three-, five- and thirteen-days after the change from the long to the short photoperiod, profiles of clock gene *Per1*, *Per2* and *Rev-erbα* expression were examined in the rostral, middle and caudal SCN and those of *Per2* and *Rev-erbα* also in the liver. Simultaneously, the locomotor activity of the mice before the transfer and up to the eleventh day after the transfer was monitored.

3.3. To determine i.) whether and how swiftly the immature fetal and neonatal molecular SCN clock can be reset by maternal cues and ii.) to elucidate when and where within the rat SCN the photic sensitivity of *Per1* and *Per2* develops during the early postnatal ontogenesis and to compare it with development of *c-fos* photoinduction. The specific aim was to uncover when the circadian clock begins to gate the sensitivity to light and, therefore, when it likely begins to be entrained by photic cues. For i.), pregnant rats

were exposed to a 6-h delay of one dark period, thereafter they were released into darkness and their pups were sampled postnatally for determination of the SCN rhythms in *c-fos* mRNA and heteronuclear (hn) *Avp*. For ii), rat pups with their mothers were released into constant darkness at various stages of their development, exposed to a light stimulus during their subjective day or in the first or second half of their subjective night and response of *Per1*, *Per2* and *c-fos* expression in their SCN was determined.

4. OVERVIEW OF THE USED METHODS

4.1. ANIMALS

For 3.1. and 3.2., two-month-old adult male C57Bl6/J mice were used. Mice maintained in animal facilities of the Institute of Physiology v.v.i., Academy of Sciences of the Czech Republic, Prague were delivered from Velaz s.r.o., Czech Republic. For experiments with the TW transition, mice were delivered from Harlan, Horst, the Netherlands and kept in animal facilities of the University of Groningen, Haren, the Netherlands. The gradual transition between darkness and light and vice versa was controlled by means of a computer-controlled shutter system. The animals were maintained for four weeks before sampling under a long, LD18:6, or under a short, LD6:18, photoperiod, or they were transferred from the long to the short photoperiod and sampled 3, 5, and 13 days following the transfer. The locomotor activity was monitored in mice maintained in LD18:6 or in those transferred from LD18:6 to LD6:18 till the 11^{th} day following the transfer. For 3.3., male and female Wistar (Bio Test s.r.o.; Konarovice, Czech Repulic) were maintained in LD12:12 for four weeks before mating. The day of delivery was designated as P0. The experiments were conducted under license no. A5228-01 with the U. S. National Institutes of Health and in accordance with Animal Protection Law of the Czech Republic (license no. 42084/2003-1020) and license no. DEC #4660A of the Animal Experimentation committee of the University of Groningen.

4.2 LOCOMOTOR ACTIVITY MONITORING

Throughout monitoring, the mice were maintained individually in cages equipped with infrared movement detectors attached above the centre of the cage top and enabling detection of the locomotor activity across the entire cage. A circadian activity monitoring system (Dr. H.M. Cooper, INSERM, France) was used to measure activity every minute and the resulting data was analyzed using Actiview Biological Rhythms Analysis software (Mini Mitter, Oregon, USA). Double-plotted actograms were generated for visualization of the data. The activity onset and offset was determined by two independent observers by fitting lines connecting at least five successive activity onsets or offsets by eye before and after the shift in the light-dark cycle.

4.3. TISSUE SAMPLING

For determination of *Per1* and *Per2* mRNA (3.1.), respectively, *Per1*, *Per2* and *Rev-erbα* mRNA (3.2.) in the mouse SCN, brains were removed, frozen immediately on dry ice and stored at -80^{0}C. Each brain was sectioned into five series of coronal 12-µm-thick slices in an alternating order throughout the entire rostro-caudal segment and processed for *in situ* hybridization. For determination of *Per2* and *Rev-erbα* mRNA in the liver (3.2.), dissected samples of the tissue were immersed immediately into an RNA later stabilization reagent (Quigen, Valencia, USA). Samples in RNA later were stored at 4^{0}C for no longer than one week prior to isolation of total RNA and subsequent real-time RT-PCR. For determination of PER1 and PER2 in the SCN (3.1.), deeply anesthetized mice were perfused through the ascending aorta with heparinized saline followed by phosphate-buffered saline (PBS) and then 4% paraformaldehyde in PBS. Brains were removed, post-fixed, cryoprotected in 20% sucrose in PBS, frozen on dry ice and stored at -80^{0}C. Each brain was sectioned into five series of 30 µm-thick coronal slices in alternating order throughout the whole rostro-caudal extent of the SCN and processed by free-floating immunohistochemistry. For the developmental study on *Per1*, *Per2, c-fos* and *Avp* gene expression (3.3.), the whole heads or brains were sectioned into series of 12-µm-thick coronal slices in an alternating order throughout the rostro-caudal extent of the SCN.

4.4. IN SITU HYBRIDIZATION

The cDNA fragments of rat *Per1,* rat *Per2*, rat *Rev-erbα*, rat *c-fos* and rat *Avp* were used as templates for *in vitro* transcription of complementary RNA probes. The probes were labeled using α[^{35}S]thio-UTP and the *in situ* hybridization was performed as described previously. Briefly, sections were hybridized for 20 h at 60^{0}C (*Per1, Rev-erbα*, *c-fos* and *Avp*) or at 61^{0}C (*Per2).* Following a post-hybridization wash, the sections were dehydrated in ethanol and dried. Finally, slides were exposed to a radiosensitive fils and developed. As a control, *in situ* hybridization was performed in parallel with sense probes on sections containing the SCN. The whole daily profiles of mRNA levels were determined using the same labeled probe and processed simultaneously under identical conditions.

Autoradiographs of sections were analyzed using an image analysis system to detect the relative optical density of the specific hybridization signal. For each animal, the mRNA was quantified bilaterally, for 3.1. and 3.2., at a representative rostral, middle and caudal SCN section and for 3.3. at the mid-caudal SCN section that contained the strongest hybridization signal. The OD for each animal was calculated as the mean of the values for the left and right SCN. To check the presence of the rostral, middle and caudal SCN (3.1. and 3.2.) and mid-caudal SCN (3.3.) in each section, the slides were counterstained with cresyl violet.

4.5. IMMUNOHISTOCHEMISTRY

For determination of PER1 and PER2 protein levels, the polyclocnal primary PER1 antiserum synthetized at the Massachusetts General Hospital Biopolymer Core Facility and the PER2 antiserum purchased from ADI, Greenwich, CT, USA, were used. Brain sections were processed by free-floating immunohistochemistry using the standard avidin-biotin method with diaminobenzidine as the chromogen (Vector Laboratories, Peterborough, UK). All sections were developed in diaminobenzidine for exactly the same time to achieve the same intensity of the background staining. Whole daily profiles of protein levels were determined within one assay under identical conditions. Labeled cell nuclei were counted in sections representing the R-, M- and C-SCN, by two independent observers using an image analysis system (ImagePro, Olympus, New Hyde Park, NY, USA). The intensity of background staining was set at the nearest area surrounding the SCN and every cell, with an intensity level above the background, was counted.

4.6. RNA ISOLATION AND REAL-TIME RT-PCR

Total RNA was isolated from the liver tissue stored in RNA later using RNeasy Mini kit according to the manufacturer's instructions. RNA concentrations were determined by spectrophotometry at 260 nm, and RNA quality was assessed by electrophoresis on a 1.5% agarose gel. The RT-PCR method was used to detect the clock gene mRNA as well as sequences of primers for *Rev-erbα, Per2* and *β2-microglobulin*. Briefly, 1μg of total RNA was reverse transcribed using an Improm II RT kit (Promega, Madison, USA) with random hexamer primers. Diluted cDNA was then amplified on a

LightCycler (Roche, Basel, Switzerland) using QuantiTect SYBR Green PCR kit (Qiagen, Valencia, USA) and corresponding primers. Relative quantification was achieved by using a standard curve and subsequently normalizing the clock gene expression to *β2-microglobulin*. The housekeeping gene *β2-microglobulin* was used for normalization. Its expression was stable throughout the day and did not vary markedly between the analyzed tissues. The data were expressed as mean ± S.E.M. as percent of maximal value for each expression profile.

4.7. DATA ANALYSIS

Data were analyzed by the one-way or the two-way ANOVA followed by the post-hoc analysis by the Student's –Newman-Keuls multiple range test with $P < 0.05$ being required for significance. When appropriate, also the cross-correlation analyses of t-test were used.

5. OVERVIEW OF THE RESULTS AND DISCUSSION

5.1 INFLUENCE OF PHOTOPERIOD DURATION AND LIGHT-DARK TRANSITIONS ON ENTRAINMENT OF *PER1* AND *PER2* GENE AND PROTEIN EXPRESSION IN SUBDIVISIONS OF THE MOUSE SUPRACHIASMATIC NUCLEUS

Sosniyenko S, Hut RA, Daan S, Sumová A. Eur J Neurosci. 2009 Nov;30(9):1802-14. Epub 2009 Oct 14.

5.1.1. EFFECT OF PHOTOPERIOD

Comparison of the *Per1* mRNA profiles of mice maintained under a long, LD18:6, photoperiod with those of mice maintained under a short, LD6:18, photoperiod revealed that the profiles under the long photoperiod differed significantly from those under the short photoperiod within the R-, M- and C-SCN, whether the LD transition was rectangular or with twilight hours. Similarly, *Per2* mRNA profiles in the R-. M- and C-SCN of mice experiencing the long RA photoperiod differed from those of mice experiencing the short photoperiod; in TW, the difference was strongly suggested. Also, PER1 protein profiles in the R-, M- and C-SCN under the long photoperiod differed from those under the short photoperiod, whether under RA or TW conditions. Although the effect of photoperiod was significant only for the M-SCN under RA, significant interactions effects were found in the R- and C-SCN. PER2 protein profiles under the long photoperiod were different when compared with those under the short photoperiod in the R- and M-SCN, but not within the C-SCN, whether under RA or TW.

Across the entire SCN, time of the evening decline and morning rise in *Per1* and *Per2* expression was affected by the photoperiod. When separate parts of the SCN under the long photoperiod with 18 h of daylight were compared with those under the short photoperiod with only 6 h of daylight, difference in duration of the interval between the morning *Per1* and *Per2* expression rise and the evening decline appeared to be present in the C- and M-, but not in the R-SCN under the photoperiod with RA or TW. Thus, duration of high *Per1* and *Per2* expression was longer under the long than under the short photoperiod only in the M- and C-SCN parts. Similarly, in previous studies when

representative sections from the mid-caudal position in the rat SCN were studied, the duration of *Per1* expression was also longer under the long than under the short photoperiod (Sumova et al., 2003). The PER1 protein profile in the M-SCN was also modulated by the photoperiod similar to that seen in rats (Sumova et al., 2002). Moreover, the PER2 protein profile in the M-SCN was modulated by the photoperiod as well.

5.1.2. EFFECT OF THE LIGHT-DARK TRANSITION

Comparison of the *Per1* mRNA profiles between the RA and TW photoperiod revealed that these profiles were significantly modulated by the type of LD transition. Under the short photoperiod, the *Per1* mRNA decline in the R-SCN was phase advanced by 2 h under TW as compared with that under RA. In the M-SCN, the *Per1* mRNA rise was phase-advanced by 2 h under TW than under RA and in the C-SCN both the morning *Per1* mRNA rise and the evening decline were phase-advanced by 2 h under TW than under RA. Under the long photoperiod, the *Per1* mRNA rise under RA was phase-advanced when compared with that under TW, both in the M- and C-SCN. Altogether, the profiles of *Per1* mRNA under the short TW photoperiod were phase-advanced relative to those under the short RA photoperiod, whereas under the long photoperiod, an earlier rise in *Per1* expression under RA as compared with that under TW was detected in the M- and C-SCN.

Per2 mRNA profiles were also modulated by the type of LD transition. Under the short TW photoperiod, the *Per2* mRNA decline in the R-SCN was phase-advanced by 2 h relative to that under the RA photoperiod. In the M- and C-SCN, the *Per2* mRNA rise in TW was advanced by 2 h as compared with that in RA. Thus, under the short photoperiod, the *Per2* mRNA decline in the R-SCN, or rise in the M- and C-SCN in TW appeared to be phase-advanced relative to those in RA. Under the long photoperiod, the *Per2* mRNA rise in the R-SCN occurred earlier in TW than in RA whereas in the M-SCN the *Per2* mRNA decline in TW was phase-advanced when compared that in RA. In the C-SCN, both the *Per2* mRNA rise and decline in TW and RA occurred at about the same time.

Considering the PER1 protein, the rise in PER1 levels in all parts of the SCN under the short TW photoperiod was phase advanced by 2 h as compared with that under the short RA photoperiod. Under the long photoperiod, the PER1 protein profiles in the R-, M-

and C-SCN under TW did not differ fro those under RA. The PER2 rise under the short TW photoperiod was phase-advanced relative to that under the short RA photoperiod in the M- and C-SCN. Similarly to PER1 protein, under the long photoperiod the PER2 profiles in the R-, M- and C-SCN under TW did not differ from those under RA.

The data demonstrate that under the short photoperiod, *Per1* and *Per2* mRNA profiles, as well as PER1 and PER2 rise, were phase-advanced in TW relative to those in RA. The earlier phase of the profiles of *Per* gene expression and protein levels under TW than under RA short photoperiods is in agreement with data on the locomotor activity rhythm in hamsters (Boulos et al., 1996a). In these studies, timing of the locomotor activity onset and offset also occurred earlier in the short photoperiods with TW that in those with RA. Moreover, the presence of TW resulted in a lower variability in the locomotor activity rhythm.

5.1.3. EFFECT OF THE TW LIGHT-DARK TRANSITION ON SYNCHRONY AMONG THE R-, M- AND C-SCN

Comparison of *Per1* mRNA profiles among R-, M- and C-SCN under the short photoperiod revealed a significant difference between the individual regions of the SCN under RA, but not under TW. Under RA, the *Per1* mRNA decline in the M- and C-SCN preceded that in the R-SCN. Under the long photoperiod, the profiles were desynchronized under both RA and TW conditions: the profile in the M- and C-SCN preceded that in the R-SCN. The better synchrony among the R-, M- and C-SCN parts found under TW as compared with that under RA in the short photoperiod was just suggested for profiles under the long TW photoperiod.

Comparison of *Per2* mRNA profiles among the R-, M- and C-SCN under the short photoperiod also revealed a significant difference between the individual parts of the SCN in RA, but not in TW. In RA, similar to the *Per1* mRNA profile, the *Per2* mRNA decline in the C-SCN was phase-advanced relative to that in the R-SCN. Under the long photoperiod, the individual parts of the SCN differed in RA as well as in TW: the *Per2* expression profile in the C-SCN was phase-advanced relative to that in the R-SCN under both conditions. However, under the long TW photoperiod, a higher degree of synchrony between the R-, M- and C-parts found under the short TW photoperiod was still suggested

as compared with the long RA photoperiod, namely due to the synchrony between the profiles in the R- and M-SCN. The PER1 protein profiles as well as the PER2 protein profiles in the C-SCN were phase-advanced relative to those in the R-SCN under the long, but not under the short photoperiod, be it with RA or TW.

The data showed that phases of *Per1* and *Per2* expression profiles as well as of PER1 and PER2 protein profiles in the R-, M- and C-SCN were more synchronized with each other under the short than under the long photoperiod. When RA and TW LD regimes were compared, *Per1* and *Per2* mRNA profiles in the R-, M- and C-SCN were completely synchronous under the short photoperiod with TW, but not with RA. Under the long photoperiod, the expression profiles within the R-, M- and C-SCN differed significantly in RA as well as in TW, however, a better synchronization among the individual parts in TW than in RA was indicated. Previous studies on the inter-phasing of the SCN cell subpopulations in rodents explored RA photoperiods only (Hazlerigg et al., 2005; Johnston et al., 2005; Yan and Silver, 2008, Naito et al., 2008). In all these studies, rhythms in gene expression or in proteins in the C-SCN preceded those in the R-SCN under the long photoperiod. These findings suggest that de-synchronization in clock genes expression among individual parts of the SCN might account for the photoperiodic modulation of the SCN function. In order to be "active" for an extended time under the long photoperiod, the SCN successively switches on its separate parts, the caudal part being the first and the rostral part the last. Consequently, under the very long photoperiod, the entire SCN may find itself in a daytime state for a longer time than its individual parts. The long photoperiod might affect intercellular synchrony among individual cell oscillators in the SCN (Van der Leest et al., 2007). Our results suggest that a TW photoperiod may provide better synchrony among populations of the SCN molecular oscillations than a RA one. The effect of twilight is stronger under conditions when animals are exposed to short photoperiods than when they are exposed to long ones.

5.2 DIFFERENT MECHANISMS OF ADJUSTMENT TO A CHANGE OF THE PHOTOPERIOD IN THE SUPRACHIASMATIC AND LIVER CIRCADIAN CLOCKS

Sosniyenko S, Parkanová D, Illnerová H, Sládek M, Sumová A. Am J Physiol Regul Integr Comp Physiol. 2010 Apr;298(4):R959-71. Epub 2010 Jan 13.

The aim of the study was to compare dynamics of responses of the rhythms in clock genes expression to transition from a long to a short photoperiod in the mouse central clock in the SCN with that in a peripheral clock, i.e, in the liver. Mice maintained in LD16:8 were transferred to LD6:18 and rhythms of *Per1*, *Per2* and *Rev-erbα* expression in R-, M- and C-SCN and of *Per2* and *Rev-erbα* expression in the liver were examined under the long photoperiod, three, five and thirteen days following transition of animals to the short photoperiod and in the short photoperiod. Moreover, the locomotor activity rhythm of the mice was monitored before the transfer and up to the eleventh day after the transfer. This approach allowed comparison between the dynamics and adjustment of the central and peripheral clocks and changes of the behavioral activity rhythm during the transition from the long to the short photoperiod.

5.2.1 ADJUSTMENT OF THE LOCOMOTOR ACTIVITY RHYTHM

Adjustment of the locomotor activity rhythm to the change from the long to the short photoperiod, i.e., extention of the interval of activity duration, occurred gradually only. The gradual increase in the activity duration was accomplished mostly by advancing the activity onset. Eleven days after the transition, the activity onset was fully adjusted to the change in the photoperiod as it did not differ from that under the short photoperiod, i.e., it occurred at about the time of the evening lights off. The difference between the shorter activity duration under the long photoperiod and the longer duration under the short photoperiod was consistent with the data of Inagaki et al. (2007).

5.2.2. ADJUSTMENT OF CLOCK GENE EXPRESSION RHYTHMS IN THE R-, M- AND C-SCN

The rise in *Per1* expression in individual SCN regions adjusted to the change from the long to the short photoperiod in different ways: it phase-advanced in the R-, slightly phase-delayed in the C- and did not change its phase in the M-SCN. In contrast, the *Per1* mRNA decline adjusted to the photoperiod change in a consistent manner, i.e., by a 4 – 6 h overall phase advance. The *Per1* mRNA profile adjusted first in the C-SCN, then in the M-SCN and in the R-SCN it adjusted as the last one. Under the long photoperiod, the *Per1* mRNA rhythm in the C-SCN was phase-advanced relative to that in the R-SCN. Following the transition to the short photoperiod, the R- and C-SCN *Per1* mRNA profile attained synchrony among each other gradually over the course of thirteen days.

The phase of the *Per2* mRNA rise changed only slightly after the change from the long to the short photoperiod: it phase-advanced in the R-SCN, delayed in the M-SCN and did not change in the C-SCN. In contrast to the *Per2* expression rise, the *Per2* expression decline, similar to *Per1* expression decline, adjusted in a consistent way to the change of the photoperiod. i.e., by a 4 h overall phase advances in all of the studied SCN regions. Comparing the dynamics of the change of the *Per2* mRNA profile among the SCN regions, the C- and M-SCN adjusted faster than the R-SCN. The *Per2* expression profiles in R- and C-SCN, desynchronized under the long photoperiod, became synchronized with each other only gradually following the photoperiod change. Even at thirteen days following the change they were not yet fully synchronized.

During the adjustment to the short photoperiod, the phase of the *Rev-erbα* expression rise advanced in the R- and M-SCN, but did not shift in the C-SCN. Similar to *Per1* and *Per2* mRNA profiles, also *Rev-erbα* mRNA decline adjusted to the photoperiod change only by advances, namely, by a 6 h, 8 h and 2 h overall advance in the R-, M- and C-SCN, respectively. Phase-shifts of the *Rev-erbα* rise, if any, were smaller than shifts in the decline. In contrast to *Per1* and *Per2* expression, the *Rev-erbα* expression profiles in

the R- and C-SCN may have been synchronized within five days following the photoperiod change.

Adjustment of the overt rhythm in the locomotor activity and of the SCN rhythms in expression of the clock genes *Per1*, *Per2* and *Rev-erbα* to transition of mice from long to short days proceeded mostly by phase advancing of the activity onset together with advancing of the *Per1*, *Per2* and *Rev-erbα* expression declines. It appears that the declines were locked more to the evening light offset than the rises were locked to the morning light onset. If this were the case, in mice the adjustment might proceed via phase-advancing markers joined to lights off, such as is the locomotor activity onset. In rats, the adjustment to short days proceeds mostly via phase-delaying of markers joined to the morning lights on (Illnerova 1986; Jac et al., 2000; Sumova et al., 1995a; 1995b, Sumova et al., 2003). The different strategy of adjustment to the transition from a long to a short photoperiod in the mouse compared to the rat is likely due to the fact that the endogenous circadian period of the mouse is shorter whereas that of the rat is longer than 24 h.

Under the long photoperiod, the *Per1*, *Per2* and *Rev-erbα* expression profiles in the C-SCN were phase-advanced relative to those in the R-SCN, in agreement with recently published data on desynchrony of rhythms in clock genes expression among different parts of the rodent SCN (Hazlerigg et al., 2005; Johnston et al., 2005; Inagaki et al., 2007; Naito et al., 2008; Yan and Silver, 2008; Sosniyenko et al., 2009). The profiles in *Per1*, *Per2* and *Rev-erbα* expression in individual SCN regions attained synchrony at various rates following the photoperiod transition: the *Rev-erbα* mRNA profile became synchronized faster than the *Per1* and *Per2* mRNA profiles. After the transition from the long to the short photoperiod, not only the clock gene expression profiles in individual SCN regions gradually became synchronized, but the interval of elevated clock gene expression also gradually shortened, at least in the M- and C-SCN. The shortening was due to large phase advances of the clock genes expression decline but only small, if any phase shifts of the rise. It appears that the photoperiod modulation of the SCN rhythms might be due to a changing phase-relationship among rhythms in the R-, M- and C-SCN regions as well as to different waveforms of the rhythms in population of cells within these individual SCN regions.

5.2.3. ADJUSTMENT OF CLOCK GENE EXPRESSION IN THE LIVER

The decline in *Rev-erbα* expression occurred at about the same time under the long and short photoperiod and also after three, five and thirteen days following the change from the long to the short photoperiod. In contrast, the rise adjusted to the change by an overall 4 h advance which was accomplished within thirteen days following the change. Due to the advance of the expression rise and no shift of the decline the duration of elevated *Rev-erbα* expression extended on short days. *Per2* expression adjusted to the change from the long to the short photoperiod by phase advancing of the expression rise as well as of the decline, however, the decline was advanced more than the rise. Within thirteen days after the photoperiod change, the rise was fully whereas the decline only partially adjusted to the change.

Our study confirmed that a peripheral clock might be modulated by the photoperiod, as it has been suggested by others (Andersson et al., 2005; Carr et al., 2003). It showed for the first time the effect of the photoperiod on *Per2* and *Rev-erbα* expression profile in the mouse liver. Whereas the interval of elevated *Per2* mRNA levels shortened under the short photoperiod relative to that under the long photoperiod due to a larger phase advance of the *Per2* decline than of the *Per2* rise, the *Rev-erbα* mRNA profile adjusted to the photoperiod change in a different way, i.e., by lengthening of the interval of elevated *Rev-erbα* mRNA levels.

These results indicate that photoperiodic modulation of the central SCN clock and of the peripheral clock in the liver may differ substantially. Whereas in the SCN the interval of elevated expression of all of the studied clock genes was longer under the long than under the short photoperiod, in the liver this finding held true for *Per2* but not for *Rev-erbα* expression; the interval of elevated *Rev-erbα* expression was shorter under long than under short days. This finding suggests different mechanisms for the photoperiodic modulation of the SCN and peripheral clocks. Following transition from the long to the short photoperiod, the subjective night might gradually extend due to the photoperiodic modulation of the SCN clock genes expression. Together with the extension of the

subjective night, the interval of *Rev-erbα* expression in the liver extended as well. This extension might be mediated either via direct signaling from the photoperiod-modulated SCN, or indirectly via the SCN modulation not only of the locomotor activity rhythm, but also the feeding rhythm. It might be the changed feeding rhythm which might also affect the peripheral *Rev-erbα* expression at the molecular level (Schibler et al., 2009).

5.3. RESETTING OF THE RAT CLOCK BY MATERNAL AND PHOTIC CUES DURING ONTOGENESIS

i) El-Hennamy, R., Matějů, K., Bendová, Z., **Sosniyenko, S**., Sumová, A. (2008): Maternal control of the fetal and neonatal rat suprachiasmatic nucleus. J. Biol. Rhythms 23 (5), 435-444.

ii) Matějů, K., Bendová, Z., El-Hennamy, R., Sládek, M., **Sosniyenko, S.,** Sumová, A. (2009): Development of the light sensitivity of the clock genes Period1 and Period2, and immediate-early gene c-fos within the rat suprachiasmatic nucleus. Eur. J. Neurosci. 29, 490-501.

iii) Sumová, A., Bendová, Y., Sládek, M., El-Hennamy, R., Matějů, K., Polidarová, L., **Sosniyenko, S.,** Illnerová, H. (2008): Circadian molecular clocks tick along ontogenesis. Physiol. Res. 57 (Suppl. 3), S139-S148.

5.3.1. MATERNAL CONTROL OF THE PHASE OF RHYTHMICITY WITHIN THE FETAL AND NEONATAL RAT SUPRACHIASMATIC NUCLEUS

In order to find out whether and how swiftly the immature fetal and neonatal SCN clock can be reset by maternal cues, pregnant rats maintained under the LD12:12 photoperiod were exposed to a 6 h delay of the dark period, i.e., to light till the middle of the night at various stages of the fetal development. Thereafter, they were released into constant darkness and their pups were sampled postnatally for determination of the SCN rhythms in *Per1*, *Per2* and *c-fos* mRNA and in *Avp* hnRNA. Adult rats maintained under the same LD photoperiod were exposed to the same shifting procedure in order to find out how quickly this shifting paradigm phase-delays the adult SCN clock, and thus, the maternal clock.

In adult rats, a significant delay of the locomotor activity was apparent three days after extension of the light period till the middle of the night. Also, three days after the delay of the dark period, the SCN rhythms in *c-fos* mRNA and in *Avp* hnRNA were phase delayed as compared with those in non-shifted rats, and five days after the delay, *Per1* and *Per2* mRNA rhythms in the SCN were phase delayed as well.

When pregnant rats were exposed to the delay of the onset of the dark period, i.e., to light till midnight, on gestational or embryonic day 20 (E20), at postnatal day 1 (P1) neither the profile of *c-fos* mRNA not the profile of *Avp* hnRNA was shifted. However, on P3 as well as P6, the daily SCN *Per1* and *Per2* mRNA profiles were phase-delayed relative to profiles of pups born to control mothers. The data indicated that the fetal SCN did not entrain in parallel with the maternal SCN, that is, within three days after the shifting procedure. As the prenatal period in rats lasts about 22 days, the rhythms of pups born to the shifted mothers should be phase delayed at P1, but they were not. They were phase delayed only at P3, i.e., within five days following the shifting procedure experienced by their mothers.

When pregnant rats were exposed to the delay of the dark onset already at E18, the daily profiles of *c-fos* mRNA and in *Avp* hnRNA in the neonatal rat SCN were phase delayed significantly at P1 relative to the profiles of pups born to control mothers. These data indicate that the fetal SCN entrained within five days after exposure of pregnant rats to the shifting procedure at E18. As pregnant rats were released into darkness immediately after the manipulation and pups were born in darkness, the observed phase shifts in the *c-fos* and *Avp* genes expression profiles were accomplished solely by non-photic maternal cues during the fetal development. It appears that the interval of five days elapsing between the maternal manipulation and detection of the phase shift within the pup's SCN was necessary. In contrast, only three days were needed to phase-shift the adult and hence also maternal SCN by photic cues. The results show for the first time a maternal entrainment of the SCN rhythms in gene expression at such early developmental stages. The ability of maternal cues to entrain the pup's molecular clockwork decreases during the postnatal development when maternal entrainment is gradually replaced by the photic one (Sumova et al., 2006).

5.3.2. THE POSTNATAL DEVELOPMENT OF RESPONSES TO LIGHT IN THE RAT SUPRACHIASMATIC NUCLEUS

The adult circadian clock in the SCN is reset by light administered during the subjective night, but not during the subjective day. The response to light is thus gated, i.e., restricted to the subjective night. Light administered in the first or second part of the night induces *Per1* and *c-fos* expression, whereas *Per2* expression is supposed to be induced by light administered only in the first half of the night (Meijer and Schwartz, 2003). The aim of our study was to find out when and where within the rat SCN the photic sensitivity of *Per1* and *Per2* develops during the early postnatal ontogenesis and to compare it with development of *c-fos* photoinduction. Especially, we wanted to know when the SCN sensitivity to light starts to be gated during ontogenesis. Mothers with their pups were released into darkness at P1, 3, 5 and 10 and *Per1*, *Per2* and *c-fos* mRNA levels were assessed 30 min, 1 h and 2 h following a 30 min light pulse administered either during the subjective day or in the first or in the second half of the subjective night.

Per1 and *c-fos* expression was induced already at P1 by a light pulse administered during the subjective night as well as during the subjective day. Hence, though both genes were photosensitive at such an early phase, their photoinduction was not gated to the subjective night. Since P3, *Per1* as well as *c-fos* mRNA increased significantly above the corresponding control levels following light pulses delivered during the subjective night, but not during the subjective day. For *Per2* mRNA levels at P1, no differences between the control groups and pups exposed to light pulses either during the subjective night or during subjective day were detected. At P3, *Per2* expression was induced slightly by a light pulse delivered in the second part of the subjective night and at P5 by light pulses administered in the first as well as in the second part of the night. However, at P5 a light pulse delivered during the subjective day still induced a slight response of *Per2*. Thus, it appears that photosensitivity of the three studied genes developed differently and the circadian clock started to gate its photosensitivity only gradually. The light-induced responses within the SCN at P1 were either not gated as it was in the case of *Per1* and *c-fos* photoinduction or were not yet significant as it was the case with *Per2*. At P3, the response to photic stimuli

seemed to be already gated by the circadian clock, however, expression of *Per2* was still marginally sensitive to light. Even at P5, the gating mechanism may not yet been completely precise and only at P10 the response to light appeared to be completely gated by the circadian clock.

Considering spatial distribution of the light induced *Per1*, *Per2* and *c-fos* mRNA within the SCN, it changed during the early ontogenesis. Light-induced *Per1* mRNA was located within a thin layer at the ventral border of the SCN at P1, and the area of the photoinduced signal expanded gradually with age. At P10, this area already resembled the adult ventrolateral SCN pattern. For *Per2*, a light pulse administered at P5 and P10 during the first half of the subjective night induced *Per2* expression within the entire area of the SCN whereas a pulse delivered in the second half of the night induced the expression mostly within the ventrolateral SCN. Following administration of light pulses during the subjective night, *c-fos* expression was induced mainly at the ventral border of the SCN at P1, and the ventrolateral area spread in the dorsal direction between P3 and P10.

At P1, light pulses induced *Per1* and *c-fos* expression, either during the day or during the nighttime. Apparently, photic information may reach the core clockwork components very early during the postnatal development (Weinert, 2005). The RHT, which connects the retina with the SCN, reaches the ventrolateral SCN by P1. However, the newborn pups lack the mechanism present in adult animals that restricts photic responses to the nighttime. The gating mechanism was present at P3, though it developed gradually further with the age till P10. The immature responses of the newborn rat SCN to photic stimulation during the daytime were rather due to undeveloped functional properties of the circadian clock itself (Sladek et al., 2004; Kovacikova et al., 2006) than to nonfunctioning photic pathways.

6. CONCLUSIONS

6.1 Across the entire SCN, the photoperiod modulated rhythms in *Per1* and *Per2* expression as well as in PER1 and PER2 protein levels, be it udner rectangular or twilight light-to-dark transition. In general, duration of elevated genes expression and their protein products was longer under the long than under the short photoperiod. Phases of *Per1* and *Per2* expression profiles as well as of PER1 and PER2 protein profiles in the R-, M- and C-SCN were more synchronized with each other under the short than under the long photoperiod. When RA and TW LD regimes were compared, *Per1* and *Per2* mRNA profiles in the R-, M- and C-SCN were completely synchronous under the short photoperiod with TW, but not with RA. Under the long photoperiod, the expression profiles within the R-, M- and C-SCN differed significantly in RA as well as in TW, however, a better synchronization among the individual parts in TW than in RA was indicated. The results suggest that a TW photoperiod may provide better synchrony among populations of the SCN molecular oscillations than a RA one. The effect of twilight is stronger under conditions when animals are exposed to short photoperiods than when they are exposed to long ones.

6.2 Following the change from the long to the short photoperiod, the locomotor activity rhythm adjusted to the change within eleven days by advancing the activity onset and hence by extension of the activity duration. Profiles of *Per1*, *Per2* and *Rev-erbα* expression in individual SCN regions, de-synchronized under a long photoperiod, attained synchrony at various rates following transition of mice from long to short days; synchronization of the *Rev-erbα* mRNA profile among individual SCN parts proceeded faster than that of the *Per1* and *Per2* mRNA profiles. After transition from the long to the short photoperiod, not only the clock gene expression profiles in individual SCN regions gradually became synchronized, but the interval of elevated clock gene expression also shortened gradually, at least in the M- and C-SCN. The shortening was due to large phase advances of the clock genes expression decline but only small, if any, phase shifts of the rise. Hence, the photoperiod modulation of the SCN rhythms might be due to a changing

phase-relationship among rhythms in the R-, M- and C-SCN regions as well as to different waveforms of the rhythms in population of cells within these individual SCN regions.

Moreover, the data demonstrated that mechanisms for the photoperiodic modulation of the SCN and peripheral clocks might be different. The *Rev-erbα* mRNA profile in the liver adjusted to the photoperiod change in a different way than in the SCN, i.e., by advancing the *Rev-erbα* expression rise and hence by lengthening of the interval of elevated *Rev-erbα* mRNA levels. However, the interval of elevated *Per2* mRNA levels shortened gradually under the short photoperiod relative to that under the long photoperiod due to a larger phase advance of the *Per2* decline than of the *Per2* rise,. It appears that the photoperiod modulated *Per2* expression profile similarly in the SCN and liver, while *Rev-erbα* expression profile was modulated differently. The *Rev-erbα* photoperiodic modulation paralleled that of the locomotor activity rhythm.

6.3. For maternal entrainment of the fetal SCN, the interval of five days after the maternal photic manipulation was necessary in order to detect phase shifts within the pup's SCN. In contrast, only three days were needed to phase-shift the adult and hence also maternal SCN by photic cues. These results show for the first time a maternal entrainment of the SCN rhythms in gene expression at such early developmental stages.

ii) Photosensitivity of *Per1, Per2* and *c-fos* gene expression developed differently during the early postnatal stage. The SCN clock started to gate its photosensitivity to the subjective night only gradually. The light-induced responses within the SCN at P1 were either not gated as it was in the case of *Per1* and *c-fos* photoinduction or were not yet significant as it was the case with *Per2*. At P3, the response of *Per1* and *c-fos* expression to photic stimuli began to be already gated by the circadian clock, however expression of *Per2* was still marginally sensitive to light. Even at P5, the gating mechanism might not yet been completely precise. Only at P10, the response to light appeared to be completely gated to the subjective night by the circadian clock. In conclusion, the study revealed that the newborn pups lack the mechanism present in adult animals that restricts photic responses to the nighttime. The gating mechanism began to be present at P3, though it developed gradually further till P10.

7. SUMMARY

This thesis aimed to contribute to our knowledge on mechanisms by which the mammalian circadian system responds to changes in the external environment, be it in adulthood or during ontogenesis. While for the adult animals changes in external light-dark conditions are the most important cues entraining the circadian clock, during the early developmental stage the clock is entrained mostly via maternal cues. Therefore, significant attention was devoted to mechanisms how changes in daylength, i.e., photoperiod, modulate the central and peripheral circadian clocks, and to mechanisms how sensitivity of the SCN clock to maternal and photic cues develops during ontogenesis. The results demonstrated that the SCN clock responded to changes in the external photoperiod by modulation of a phase relationship among different subpopulations of the SCN neurons and that this phase-relationship was affected by different ways of light-to-dark transition. Future studies should be directed to identify these cellular subpopulations more precisely. Also, exact mechanisms how the peripheral clocks adapt to a changing photoperiod need to be deciphered.

8. REFERENCES

Abe, H., Honma, S., Namihira, M., Tanahashi, Y., Ikeda, M., Honma, K. (1998): Circadian rhythm and light responsiveness of BMAL1 expression, a partner of mammalian clock gene Clock, in the suprachiasmatic nucleus of rats. *Neurosci Lett*,258(2),93-6

Abrahamson, E.E., Moore R.Y. (2001): Suprachiasmatic nucleus in the mouse: retinal innervation, intrinsic organization and efferent projections. Brain Research, 916, 172-191

Albrecht U, Sun ZS, Eichele G, Lee CC. (1997): A differential response of two putative mammalian circadian regulators, mper1 and mper2, to light. *Cell,* 91(7), 1055-64

Albus, H., Vansteensel, M.J., Michel, S., Block, G.D., Meijer, J.H. (2005): A GABAergic Mechanism Is Necessary for Coupling Dissociable Ventral and Dorsal Regional Oscillators within the Circadian Clock. *Current Biology*, 15, 886-893

Andersson, H., Johnston, J.D., Messager, S., Hazlerigg, D., Lincoln, D. (2005): Photoperiod regulates clock gene rhythms in the ovine liver. *Gen Comp Endocrinol*, 142(3), 357-63

Aton, S.J., Herzog, E.D. (2005): Come Together, Right ...Now: Synchronization of Rhythms in a Mammalian Circadian Clock, *Neuron*, 48, 531-534

Bae, K., Weaver, D.R. (2003): Light-induced phase shifts in mice lacking mPER1 or mPER2. *J Biol Rhythms*, 18(2), 123-33

Baler, R., Covington, S., Klein D.C (1997): The rat arylalkylamine N-acetyltransferase gene promoter. cAMP activation via a cAMP-responsive element –CCAAT complex. *J Biol Chem*, 272(11), 6979-85

Balsalobre A, Damiola F, Schibler U. (1998): A serum shock induces circadian gene expression in mammalian tissue culture cells. *Cell*, 93 (6), 929-37

Barinaga, M, (2002): How the brain's clock gets daily enlightement. *Science*, 295, 955-957.

Barnes, J.W., Tischkau, S.A., Barnes, J.A., Mitchell, J.W., Burgoon, P.W., Hickok, J.R., Gillette, M.U. (2003): Requirement of mammalian Timeless for circadian rhythmicity. *Science*, 302(5644), 439-42

Boulos, Z., Macchi, M., Houpt, T.A. & Terman, M. (1996a): Photic entrainment in hamsters: effects of simulated twilights and nest box availability. *J Biol Rhythms*, 11, 216-233.

Boulos, Z., Macchi, M. & Terman, M. (1996b): Twilight transitions promote circadian entrainment to lengthening light-dark cycles. *Am J Physiol*, 271, R813-818.

Boulos Z, Terman JS, Terman M. (1996c) Circadian phase-response curves for simulated dawn and dusk twilights in hamsters. *Physiol Behav*. 60(5), 1269-75.

Boulos, Z., Macchi, M.M. (2005): Season- and latitude- dependent effects of simulated twilights on circadian entrainment. *J Biol Rhythms*, 20(2), 132-44

Bunger, M.K., Wilsbacher, L.D., Moran, S.M., Clendenin, C., Radcliffe, L.A., Hogenesch, J.B., Simon, M.C., takahashi, J.S., Bradfield, C.A. (2000): Mop3 is an essential component of the master circadian pacemaker in mammals. *Cell*, 103(7), 1009-17

Brown SA, Schibler U. (1999): The ins and outs of circadian timekeeping. *Curr Opin Genet Dev.* 9(5) 588-94

Carr, A.J., Johnston, J.D., Semikhodskii, A.G., Nolan, T., Caqampanq, F.R., Stirland, J.A., Loudon, A.S. (2003): Photoperiod differentially regulates circadian oscillators in central and peripheral tissues of the Syrian hamster. *Curr Biol*, 13(17), 1543-8

Chen-Goodspeed, M., Lee, C.C. (2007): Tumor supression and circadian function. *J Biol Rhythms*, 22(4), 291-8

Cheng, H.Y.M., Papp, J.W., Varlamova, O., Dziema, H., Russell, B., Curfman, J.P., Nakazawa, T., Shimizu, K., Okamura, H., Impey, S., Obrietan, K. (2007): MicroRNA modulation of circadian-clock period and entrainment. *Neuron*, 54, 813-829

Chong NW, Bernard M, Klein DC. (2000): Characterization of the chicken serotonin N-acetyltransferase gene. Activation via clock gene heterodimer/E box interaction. *J Biol Chem.*, 275(42):32991-8.

DeBruyne, J.P., Noton, E., Lambert, C.M., Maywood, E.S., Weaver, D.R., Reppert, S.M. (2006): A clock shock: mouse CLOCK is not required for circadian oscillator function. *Neuron*, 50(3), 465-77

DeBruyne, J.P., Weaver, D.R., Reppert, S.M. (2007): CLOCK and NPAS2 have overlapping roles in the suprachiasmatic circadian clock. *Nat Neurosci*, 10(5),543-5

Ding, J.M., Buchanan, G.F., Tischkau, S.A., Chen, D., Kuriashkina, L., Faiman, L.E., Alster, J.M., McPherson, P.S., Campbell, K.P., Gillette, M.U. (1998): A neuronal ryanodine receptor mediates light-induced phase delays of the circadian clock. *Nature*, 394(6691), 381-4

Dunlap, J.C. (1999): Molecular Bases for Circadian Clocks. *Cell*, 96, 271-290

Elliott JA, Tamarkin L. (1994): Complex circadian regulation of pineal melatonin and wheel-running in Syrian hamsters. *J Comp Physiol*, 174(4): 469-84

Gekakis, N., Staknis, D., Nguyen, H.B., Davis, F.C., Wilsbacher, L.D., King, D.P., Takahashi, J.S., Weitz, C.J. (1998): Role of the CLOCK protein in the mammalian circadian mechanism. *Science*, 280(5369), 1548-9

Gery, S., Komatsu, N., Baldjyan, L., Yu, A., Koo, D., Koeffler, H.P. (2006): The circadian gene Per1 plays an important role in cell growth and DNA damage control in human cancer cells. *Mol Cell*, 22(3), 375-82

Godinho, S.I., Maywood, E.S., Shaw, L., Tucci, V., Barnard, A.R., Busino, L., Pagano, M., Kendall R., Quwailid, M.M., Romero, M.R., O´Neill, J., Chesham, J.E., Brooker, D., Lalanne, Z., Hastings, M.H., Nolan, P.M. (2007): The after-hours mutant reveals a role for Fbxl3 in determining mammalian circadian period. *Science*, 316, 897-900

Gooley, J.J., Lu, J., Chou, T.C., Scammell, T.E., Saper, C.B. (2001): Melanopsin in cells of origin of the retinohypothalamic tract. *Nature Neuroscience*, 4(12), 1165

Gotter, A.L., Manganaro, T., Weaver, D.R., Kolakowski, L.F. Jr., Possidente, B., Sriram, S., MacLaughlin, D.T., Reppert, S.M. (2000): A time-less function for mouse timeless, *Nat Neurosci*, 3(8), 755-6

Guillaumond, F., Dardente, H., Giguere, V., Cermakian, N. (2005): Differential control of Bmal1 circadian transcription by REV-ERB and ROR nuclear receptors. *J Biol Rhythms*, 20(5), 391-403

Hamaguchi, H., Fijimoto, K., Kawamoto, T., Noshiro, M., Maemura, K., Takeda, N., Nagai, R., Furukawa, M., Honma, S., Honma, K., Kurihara, H., Kato, Y. (2004):

Expression of the gene for Dec2, a basic helix-loop-helix transcription factor, is regulated by a molecular clock system. *Biochem J*, 382(Pt 1), 43-50

Hao, H., Allen, D.L., Hardin, P.E. (1997): A Circadian Enhancer Mediates PER-Dependent mRNA Cycling in *Drosophila melanogaster*. *Mol Cell Biol*, 17(7), 3687-93

Harding, H.P., Lazar, M.A. (1993): The orphan receptot Rev-ErbA alpha activates transcription via a novel response element. *Mol Cell Biol*, 13(5), 3113-21

Hastings, M.H., Walker, A.P., Herbert, J. (1987): Effect of asymmetrical reductions of photoperiod on melatonin, locomotor activity and gonadal condition of male Syrian hamsters. *J Endocrinol*, 114(2), 221-9

Hastings, M.H. (1997): Central clocking. *Trends Neurosci*, 20(10), 459-64

Hastings, M.H. (1997): Circadian clocks. *Current Biology*, 7(11), R607-2

Hastings, M.H. (2001): Modeling the Molecular Calendar. *J Biol Rhythms*, **16**, 117-123.

Hastings, M.H., Herzog, E.D. (2004): Clock genes, oscillators, and cellular networks in the suprachiasmatic nuclei. *J Biol Rhythms*, 19(5), 400-13

Hazlerigg, D.G., Ebling, F.J.P., Johnston, J.D. (2005): Photoperiod differentially regulates gene expression rhythms in the rostral and caudal SCN. *Curr Biol*, 15(12), R455-7

Hofmann, K., Illnerová, H., Vaněček, J (1986): Change in duration of the nighttime melatonin peak maz be a signal driving photoperiodic responses in the Djungarian hamster (Phodopus sungorus). *Neurosci. Lett.* 67, 68-72.

Honma, S., Kawamoto, T., Takagi, Y., Fujimoto, K., Sato, F., Noshiro, M., Kato, Y., Honma, K. (2002): Dec1 and Dec2 are regulators of the mammalian molecular clock. *Nature*, 419(6909), 841-4

Huang, Z.J., Edery, I., Rosbash, M. (1993): PAS is a dimerization domain common to drosophila period and several transcription factors, *Nature*, 364(6434), 259-62

Inagaki N, Honma S, Ono D, Tanahashi Y, Honma K. (2007): Separate oscillating cell groups in mouse suprachiasmatic nucleus couple photoperiodically to the onset and end of daily activity. *Proc Natl Acad Sci U S A.*, 104(18):7664-9

Illnerová, H. (1986): Circadian rhythms in the mammalian pineal gland, Academia, Praha, pp. 1-105.

Illnerová, H., Vaněček, J. (1980): Pineal rhythm in N-acetyltransferase activity in rats under different artificial photoperiods and in natural daylight in the course of year. *Neuroendocrinology*, 31(5), 321-6

Illnerová, H., Vaněček, J. (1982): Two-oscillator structure of the pacemaker controlling the circadian rhythm of N-acetyltransferase in the rat pineal gland. *J. Comp. Physiol.*, 15, 539-548.

Illnerová, H., Hoffmann, K., Vaněček, J. (1984): Adjustment of pineal melatonin and N-acetyltransferase rhythms to change from long to short photoperiod in the Djungarian hamster Phodopus sungorus. *Neuroendocrinology*, 38(3), 226-31

Illnerová, H., Vaněček, J. (1988): Entrainment of rat pineal rhythm in melatonin production by light. *Reprod Nutr Dev*, 28(2B), 515-26

Illnerová, H. (1994): Blížíme se k poznání podstaty biologických hodin?. *Vesmír 73*, 8, 425-426

Illnerová, H. (1996): Melatonin a jeho působení. *Vesmír 75*, 5, 266-269

Ingram, C.D., Ciobanu, R., Coculescu, I.L., Tanasescu, R., Coculescu, M., Mihai, R. (1998): Vasopressin neurotransmission and the control of circadian rhythms in the suprachiasmatic nucleus. *Prog Brain Res*, 119, 351-64

Jáč, M., Sumová, A., Illnerová, H. (2000): c-Fos rhythm in subdivisions of the rat suprachiasmatic nucleus under artifical and natural photoperiods. *Am J Physiol, Regul Integr Comp Physiol* 279, R2270-R2276.

Jagota A, de la Iglesia HO, Schwartz WJ. (2000): Morning and evening circadian oscillations in the suprachiasmatic nucleus in vitro. *Nat Neurosci.*, 3(4):372-6.

Jakubcakova, V., Oster, H., Tamanini, F., Cadenas, C., Leitges, M., van der Horst, G.T.J., Eichele, G. (2007): Light entrainment of the mammalian circadian clock by a PRKCA-dependent posttranslational mechanism. *Neuron*, 54, 831-843

Jin X, Shearman LP, Weaver DR, Zylka MJ, de Vries GJ, Reppert SM. (1999): A molecular mechanism regulating rhythmic output from the suprachiasmatic circadian clock. *Cell,* ;96(1):57-68.

Johnston, J.D. (2005): Measuring seasonal time within the circadian system: regulation of the suprachiasmatic nuclei by photoperiod. *J Neuroendocrinol*, 17(7), 459-65

King, D.P., Zhao, Y., Sangoram, A.M., Wilsbacher, L.D., Tanaka, M., Antoch, M.P., Steeves, T.D., Vitaterna, M.H., Kornhauser, J.M., Lowrey, P.L., Turek, F.W., Takahashi, J.S. (1997): Positional cloning of the mouse circadian clock gene. *Cell*, 89(4), 641-53

Klein , D.C., Berg, G.R., Weller, J. (1970): Melatonin synthesis: adenosine - 3′, 5′-monophosphate and norepinephrine stimulate N-acetyltransferase. *Science*, 168(934), 979-80

Kornhauser JM, Nelson DE, Mayo KE, Takahashi JS. (1990): Photic and circadian regulation of c-fos gene expression in the hamster suprachiasmatic nucleus. *Neuron*, 5(2): 127-34.

Kováčiková, Z., Sládek, M., Bendová, Z., Illnerová, H., Sumová, A. (2006): Expression of clock and clock-driven genes in the rat suprachiasmatic nucleus during late fetal and early postnatal development. *J. Biol. Rhythms* 21, 140-148.

Kume, K., Zylka, J.M., Sriram, S., Shearman, L.P., Weaver, D.R., Jin, X., Maywood, E.S., Hastings, M.H., Reppert, S.M. (1999): mCRY1 and mCRY2 are essential components of the negative limb of the circadian clock feedback loop. *Cell*, 98(2), 193-205

Lee C, Etchegaray JP, Cagampang FR, Loudon AS, Reppert SM. (2001): Posttranslational mechanisms regulate the mammalian circadian clock. *Cell*, 107(7):855-67.

Li, Y., Song, X., Ma, Y., Liu, J., Yang, D., Yan, B. (2004): DNA binding, but not interaction with Bmal1, is responsible for DEC1-mediated transcription regulation of the circadian gene mPer1. *Biochem J*, 382(Pt 3), 895-904

Liu, C., Weaver, D.R., Strogatz, S.H., Reppert, S.M. (1997): Cellular Construction of a Circadian Determination in the Suprachiasmatic Nuclei. *Cell*, 91, 855-860

Liu, C., Reppert, S.M. (2000): GABA Synchronizes Clock Cells within the Suprachiasmatic Circadian Clock. *Neuron*, 25, 125-128

Lopez-Molina L, Conquet F, Dubois-Dauphin M, Schibler U. (1997): The DBP gene is expressed according to a circadian rhythm in the suprachiasmatic nucleus and influences circadian behavior. *EMBO J*. 16(22):6762-71.

Lowrey PL, Takahashi JS. (2000): Genetics of the mammalian circadian system: Photic entrainment, circadian pacemaker mechanisms, and posttranslational regulation. *Annu Rev Genet*. 34:533-562. Review.

McFarland, W.N. & Munz, F.W. (1975): Part II: The photic environment of clear tropical seas during the day. *Vision Res*, **15**, 1063-1070.

Maywood ES, Mrosovsky N, Field MD, Hastings MH. (1999): Rapid down-regulation of mammalian period genes during behavioral resetting of the circadian clock. *Proc Natl Acad Sci U S A*., 96(26):15211-6.

Meijer JH, Groos GA, Rusak B. (1986): Luminance coding in a circadian pacemaker: the suprachiasmatic nucleus of the rat and the hamster. *Brain Res.*, 382(1):109-18.

Meijer, J.H., Schwartz, W.J. (2003): In search of the pathways for light-induced pacemaker resetting in the suprachiasmatic nucelus. *J Biol Rhythms*, 18(3), 235-49

Messager, S., Ross, A.W., Barrett, P., Morgan, P.J. (1999): Decoding photoperiodic time through Per1 and ICER gene amplitude. *Proc Natl Acad Sci U S A*, 96(17), 9938-43

Moore , R.Y., Eichler, V.B. (1972): Loss of a circadian adrenal corticosterone rhythm following suprachiasmatic lesions in the rat. *Brain Research* 42, 201-206.

Naito, E., Watanabe, T., Tei, H., Yoshimura, T., Ebihara, S. (2008): Reorganization of the suprachiasmatic nucleus coding for day length. *J Biol Rhythms*, 23(2), 140-9

Nelson, D.E., Takahashi, J.S. (1991): Sensitivity and integration in a visual pathway for circadian entrainment in the hamster (Mesocricetus auratus). *J Physiol*, 439, 115-45

Nuesslein-Hildesheim, B., O´Brien, J.A., Ebling, F.J., Maywood, E.S., Hastings, M.H. (2000): The circadian cycle of mPer clock gene products in the suprachiasmatic nucleus of the siberian hamster encodes both daily and seasonal time. *Eur J Neurosci*, 12(8), 2856-64

Ohno, T., Onishi, Y., Ishida, N. (2007): The negative transcription factor E4BP4 is associated with circadian clock protein PERIOD2. *Biochem Biophys Res Commun*, 354(4), 1010-1015

Okamura H, Miyake S, Sumi Y, Yamaguchi S, Yasui A, Muijtjens M, Hoeijmakers JH, van der Horst GT. (1999): Photic induction of mPer1 and mPer2 in cry-deficient mice lacking a biological clock. *Science*, 286(5449):2531-4.

Okamura, H., Yamaguchi, S., Yagita, K. (2002): Molecular machinery of the circadian clock in mammals. *Cell Tissue Res*, 309, 47-56

O'Neill, J.S., Maywood, E.S., Chesham, J.E., Takahashi, J.S., Hastings, M.H. (2008): cAMP-dependent signaling as a core component of the mammalian circadian pacemaker. *Science*, 320(5878), 879-80

Pittendrigh C., Daan S., (1976): Functional analysis of circadian pacemakers in nocturnal rodents. V. Pacemaker structure: A clock for all seasons. *J. Comp Physiol.*, 106 333-55

Plautz JD, Kaneko M, Hall JC, Kay SA. (1997): Independent photoreceptive circadian clocks throughout Drosophila. *Science*, 278(5343):1632-5.

Preitner, N., Damiola, F., Lopez-Molina, L., Zakany, J., Duboule, D., Albrecht, U., Schibler, U. (2002): The organ nuclear receptor REV-ERBalpha controls circadian transcription within the positive limb of the mammalian circadian oscillator. *Cell*, 110(2), 251-60

Puchalski W, Lynch GR. (1991): Circadian characteristics of Djungarian hamsters: effects of photoperiodic pretreatment and artificial selection. *Am J Physiol*, 261(3 Pt 2):R670-6.

Reppert, S.M., Weaver, D.R. (2001): Molecular Analysis of Mammalian Circadian Rhythms. *Annu. Rev. Physiol*, 63, 647-76

Rohling, J., Wolters, L., Meijer, JH (2006): Simulation of day-length encoding in the SCN: from single-cell to tissue-level organization. *J. Biol. Rhythms*, 21, 301-313.

Sakamoto, K., Oishi, K., Nagase, T., Miyazaki, K., Ishida, N. (2002): Circadian expression of clock genes during ontogeny in the heart. *Neuroreport* 13, 1239-1242.

Sangoram AM, Saez L, Antoch MP, Gekakis N, Staknis D, Whiteley A, Fruechte EM, Vitaterna MH, Shimomura K, King DP, Young MW, Weitz CJ, Takahashi JS. (1998): Mammalian circadian autoregulatory loop: a timeless ortholog and mPer1 interact and negatively regulate CLOCK-BMAL1-induced transcription. *Neuron*, (5):1101-13.

Sato, T.K., Panda, S., Miraglia, L.J., Reyes, T.M., Rudic, R.D., McNamamra, P., Naik, K.A., FitzGerald, G.A., Kay, S.A., Hogenesch, J.B. (2004): A funcional genomics

strategy reveals Rora as an component of the mammalian circadian clock, *Neuron*, 43(4), 443-6

Schaap, J., Albus, H., VanderLeast, H.T., Eilers, PH, Derari, L., Meijer, JH (2003): Heterogeneity of rhythmic suprachiasmatic nucleus neurons: implications for circadian waveform and photoperiodic encoding. *Proc. Natl. Acad. Sci. USA*, 100, 15994-15999.

Schibler, U. (2005): The daily rhythms of genes, cells and organs. *EMBO*, 6, S9-S13

Schibler, U. (2009): The 2008 Pittendrigh/Aschoff Lecture: Peripheral phase coordination in the mammalian circadian timing system. *J. Biol. Rhythms*, 24, 3-15.

Shearman, L.P., Zylka, M.J., Weaver, D.R., Kolakowski, L.F. Jr, Reppert, S.M. (1997): Two period homologs: circadian expression and photic regulation in the suprachiasmatic nuclei. *Neuron*, 19(6), 1261-9

Shearman, L.P., Jin, X., Lee, C., Reppert, S.M., Weaver, D.R. (2000): Targeted disruption of the mPer3 gene: subtle effects on circadian clock function. *Mol Cell Biol*, 20(17), 6269-75

Shigeyoshi, Y., Taguchi, K., Yamamoto, S., Takekida, S., Yan, L., Tei, H., Moriya, T., Shibata, S., Loros, J.J., Dunlap, J.C., Okamura, H. (1997): Light-induced resetting of mammalian circadian slock is associated with rapid induction of mPer1 transcript. *Cell,* 91, 1043-53

Siepka, S.M., Yoo, S.H., Park, J., Song, W., Kumar, V., Hu, Y., Lee, C., Takahashi, J.S. (2007): Circadian mutant Overtime reveals F-box protein FBXL3 regulation of cryptochrome and period gene expression. *Cell*, 129, 1011-1023

Sosniyenko, S., Hut, RA., Daan, S., Sumová, A. (2009): Influence of photoperiod duration and light-dark transition on entrainment of Per1 and Per2 gene and protein in subdivisions of the mouse suprachiasmatic ucleus. *Eur. J. Neurosci*., 30, 1802-1814.

Sosniyenko S, Parkanová D, Illnerová H, Sladek M, Sumová A. (2009): Different mechanisms of adjustment to the photoperiod in the suprachiasmatic nucleus and liver circadian clocks. *Am J Physiol Regul Integr Comp Physiol*. 2010 Jan 13.

Sládek, M., Sumová, A., Kováčiková, Z., Bendová, Z., Laurinová, K., Illnerová, H. (2004): Insight into molecular core clock mechanism of embryonic and early postnatal rat suprachiasmatic nucleus. *Proc Natl Acad Sci USA* 101, 6231-6236

Sládek, M., Jindráková, Z., Bendová, Z., Sumová, A. (2007): Postnatal ontogenesi of the circadian clock within the rat liver. *Am J Physiol Regul Integr Comp Physiol* 292, R1224-R1229

Steinlechner, S., Jacobmeier, B., Scherbarth, F., Dernbach, H., Kruse, F., Albrecht, U. (2002): Robust circadian rhytmicity of per1 and Per2 mutant mice in constant light, and dynamics of Per1 and Per2 gene expression under long and short photoperiods. *J Biol Rhythms*, 17(3), 202-9

Stephan, FK., Zucker, J. (1972): Circadian rhythms in drinking behavior and locomotor activity of rats are eliminated by hypothalamic lesions. *Proc Natl Acad Sci USA* 69, 1583-1586

Sumová, A., Trávníčková, Z., Peters, R., Schwartz, W.J., Illnerová, H. (1995a): The rat suprachiasmatic nucleus is a clock for all seasons. *Proc Natl Acad Sci U S A*, 92(17), 7754-8

Sumová, A., Trávníčková, Z., Illnerová, H. (1995b): Memory on long but not on short days is stored in the rat suprachiasmatic nucleus. *Neurosci Lett*, 200(3), 191-4

Sumová, A., Maywood, E.S., Selvage, D., Ebling, F.J., Hastings, M.H. (1996): Serotonergic antagonists impair arousal-induced phase shifts of the circadian system of the syrian hamster. *Brain Research*, 709(1), 88-96

Sumová, A., Trávníčková, Z., Mikkelsen, JD., Illverová, H. (1998): Spontaneous rhythm in c-Fos immunoreactivity in the dorsomedial part of the rat suprachiasmatic nucleus. Brain Research 801, 254-258

Sumová, A., Sládek, M., Jáč, M., Illnerová, H. (2002): The circadian rhythm of Per1 gene product in the rat suprachiasmatic nucleus and its modulation by seasonal changes in daylength. *Brain Res*, 947(2), 260-270

Sumová, A., Jáč, M., Sládek, M., Šauman, I., Illnerová, H. (2003): Clock gene daily profiles and their phase relationship in the rat suprachiasmatic nucleus are affected by photoperiod. *J Biol Rhythms*, 18(2), 134-44

Sumová, A., Bendová, Z., Sládek, M., Kovačiková, Z., Illnerová, H. (2004): Seasonal molecular timekeeping within the rat circadian clock. *Physiol Res*, 53(1), S167-76

Sumová A., Bendová Z., Sládek M., El-Hennamy R., Laurinová K., Jindráková Z., Illnerová H. (2006): The setting the biological time in central and peripheral clocks during ontogenesis. Minireview. *FEBS Letters* 580, 2836-2842

Takahashi JS, Hong HK, Ko CH, McDearmon EL. (2008): The genetics of mammalian circadian order and disorder: implications for physiology and disease. *Nat Rev Genet*., 764-75. Review.

Tamaru T, Isojima Y, Yamada T, Okada M, Nagai K, Takamatsu K. (2000): Light and glutamate-induced degradation of the circadian oscillating protein BMAL1 during the mammalian clock resetting. *J Neurosci*: 7525-30.

Tischkau, S.A., Barnes, J.A., Lin, F.J., Myers, E.M., Barnes, J.W., Meyer-Bernstein, E.L., Hurst, W.J., Burgoon, P.W., Chen, D., Sehgal, A., Gillette, M.U. (1999): Oscillation and light induction of timeless mRNA in the mammalian circadian clock. *J Neurosci*, 19(12), RC15

Toh, K.L., Jones, C.R., He, Y., Eide, E.J., Hinz, W.A., Virshup, D.M., Ptacek, L.J., Fu, Y.H. (2001): An hPer2 phosphorylation site mutation in familial advanced sleep phased syndrome. *Science*, 291(5506), 1040-43

Tournier, B.B., Menet, J.S., Dardente, H., Poirel, V.J., Malan, A., Masson-Pévet, M., Pévet, P., Vuillez, P. (2003): Photoperiod differentially regulates clock genes´ expression in the suprachiasmatic nucleus of Syrian hamster. *Neuroscience*, 118(2), 317-22

Trávníčková-Bendová, Z., Cermakian, N., Reppert, S.M., Sassone-Corsi, P. (2002): Bimodal regulation of mPeriod promoters by CREB-dependent signaling and CLOCK/BMAL1 activity. *Proc Natl Acad Sci U S A*, 99(11), 7728-33

Triqueneaux, G., Thenot, S., Kakizawa, T., Antoch, M.P., Safi, R., Takahashi, J.S., Delaunay, F., Laudet, V. (2004): The orphan receptor Rev-erbalpha is a target of the circadian clock pacemaker. *J Mol Endocrinol*, 33(3), 585-608

Ueda HR, Chen W, Adachi A, Wakamatsu H, Hayashi S, Takasugi T, Nagano M, Nakahama K, Suzuki Y, Sugano S, Iino M, Shigeyoshi Y, Hashimoto S. (2002): A transcription factor response element for gene expression during circadian night. *Nature*, 418(6897):534-9.

Usui (2000): Gradual changes in environmental light intensity and entrainment of circadian rhythms, *Brain Dev,* 22 Suppl 1:S61-4. Review.

van den Pol, A.N. (1980): The hypothalamic suprachiasmatic nucleus of rat: intrinsic anatomy. *J Comp Neurol*, 191(4), 661-702

Van der Leest, HT., Houben, T., Michel, S., Deboer, T., Albus, H., Vansteensel, MJ., Block, GD., Meijer, JH (2007): Seasonal encoding by the circadian pacemaker of the SCN. *Curr Biol*, 17, 468-473

Vielhaber, E., Eide, E., Rivers, A., Gao, Z.H., Virshup, D.M. (2000): Nuclear entry of the circadian regulator mPER1 is controlled by mammalian casein kinase I epsilon. *Mol Cell Biol*, 20(13), 4888-99

Weinert, D (2005): Ontogenetic development of the mammalian circadian system. *Chronobiol Int* 22, 179-205

Welsh, D.K., Logothetis, D.E., Meister, M., Reppert, S.M. (1995): Individual Neurons Dissociated from Rat Suprachiasmatic Nucleus Express Independently Phased Circadian Firing Rhytms. *Neuron*, 14(4), 697-706

Whitmore D, Foulkes NS, Strähle U, Sassone-Corsi P. (1998): Zebrafish Clock rhythmic expression reveals independent peripheral circadian oscillators. *Nat Neurosci*, 1(8):701-7.

Yamaguchi, S., Mitsui, S., Yan, L., Yagita, K., Miyake, S., Okamura, H. (2000): Role of DBP in the circadian oscillatory mechanism. *Mol Cell Biol*, 20(13), 4773-81

Yamaguchi, S., Isejima, H., Matsuo, T., Okura, R., Yagita, K., Kobayashi, M., Okamura, H. (2003): Synchronization of Cellular Clocks in the Suprachiasmatic Nucleus. *Science*, 302(5649), 1408-1412

Yamazaki, S., Numamo, R., Abe, M., Hida, A., Takahashi, R., Ueda, M., Block G.D., Sakaki, Y., Menaker, M., Tei, H. (2000): Resetting Central and Peripheral Circadian Oscillators in Transgenic Rats. *Science*, 288, 682-685

Yan L, Silver R. (2008): Day-length encoding through tonic photic effects in the retinorecipient SCN region. *Eur J Neurosci*: 2108-15.

Yoo, S.H., Yamazaki, S., Lowrey, P.L., Shimomura, K., Ko., C.H., Buhr, E.D., Siepka, S.M., Hong, H.K., Oh, W.J., Yoo, O.J., Menaker, M., Takahashi, J.S. (2004): PERIOD2::LUCIFERASE real-time reporting of circadian dynamics reveals

persistent circadian oscillation in mouse peripheral tissues. *Proc Natl Acad Sci U S A*, 101(15), 5339-46

Yu, W., Nomura, M., Ikeda, M. (2002): Interactivating feedback loops within the mammalian clock: BMAL1 is negatively autoregulated and upregulated by CRY1, CRY2, and PER2. *Biochem Biophys Res Commun*, 290(3), 933-41

Zheng B, Albrecht U, Kaasik K, Sage M, Lu W, Vaishnav S, Li Q, Sun ZS, Eichele G, Bradley A, Lee CC. (2001): Nonredundant roles of the mPer1 and mPer2 genes in the mammalian circadian clock. *Cell*, 105(5):683-94.

9. ATTACHMENTS

EJN fens European Journal of Neuroscience

European Journal of Neuroscience, Vol. 30, pp. 1802–1814, 2009 doi:10.1111/j.1460-9568.2009.06945.x

NEUROSYSTEMS

Influence of photoperiod duration and light–dark transitions on entrainment of *Per1* and *Per2* gene and protein expression in subdivisions of the mouse suprachiasmatic nucleus

Serhiy Sosniyenko,[1] Roelof A. Hut,[2] Serge Daan[2] and Alena Sumová[1]
[1]Department of Neurohumoral Regulations, Institute of Physiology, v.v.i., Academy of Sciences of the Czech Republic, Czech Republic
[2]Department of Chronobiology, University of Groningen, Haren, the Netherlands

Keywords: clock gene, clock protein, photoperiodic synchronization, SCN

Abstract

The circadian clock located within the suprachiasmatic nuclei (SCN) of the hypothalamus responds to changes in the duration of day length, i.e. photoperiod. Recently, changes in phase relationships among the SCN cell subpopulations, especially between the rostral and caudal region, were implicated in the SCN photoperiodic modulation. To date, the effect of abrupt, rectangular, light-to-dark transitions have been studied while in nature organisms experience gradual dawn and twilight transitions. The aim of this study was to compare the effect of a long (18 h of light) and a short (6 h of light) photoperiod with twilight relative to that with rectangular light-to-dark transition on the daily profiles of *Per1* and *Per2* mRNA (*in situ* hybridization) and PER1 and PER2 protein (immunohistochemistry) levels within the rostral, middle and caudal regions of the mouse SCN. Under the short but not under the long photoperiod, *Per1*, *Per2* and PER1, PER2 profiles were significantly phase-advanced under the twilight relative to rectangular light-to-dark transition in all SCN regions examined. Under the photoperiods with rectangular light-to-dark transition, *Per1* and *Per2* mRNA profiles in the caudal SCN were phase-advanced as compared with those in the rostral SCN. The phase differences between the SCN regions were reduced under the long, or completely abolished under the short, photoperiods with twilight. The data indicate that the twilight photoperiod provides stronger synchronization among the individual SCN cell subpopulations than the rectangular one, and the effect is more pronounced under the short than under the long photoperiod.

Introduction

Mammals exhibit an array of daily behavioral, physiological, hormonal, biochemical and molecular rhythms. Under natural conditions, the rhythms are entrained to the 24-h day by the light–dark (LD) cycle, mostly by the light period of the day (Pittendrigh, 1981). In temperate latitudes, the day length, i.e. photoperiod, changes during the year. In nocturnal rodents, duration of the locomotor activity and nocturnal melatonin signal are photoperiod-dependent, being shorter on long summer than on short winter days (Illnerová & Vaněček, 1980; Illnerová, 1988; Elliott & Tamarkin, 1994). The locomotor activity rhythm, the rhythm in melatonin production and other circadian rhythms are controlled by a central pacemaker located in the suprachiasmatic nucleus (SCN) of the hypothalamus (Klein & Moore, 1979; LeSauter *et al.*, 1996). The SCN is also affected by the photoperiod (Sumová *et al.*, 1995). Its rhythmicity is generated by the molecular clockwork (for review, see Takahashi *et al.*, 2008). Several mammalian genes, namely two Period genes (*Per1* and *Per2*), two Cryptochrome genes (*Cry1* and *Cry2*), *Clock*, *Bmal1*, *Rev-erbα, Rora* and casein kinase 1 epsilon (*CK1ε*), are thought to be mainly involved in the clockwork mechanism by forming interacting transcriptional–translational feedback loops. Most of these genes are expressed rhythmically; the expression of *Bmal1* is anti-phase to that of the *Per* and *Cry* genes. *Per* transcription is activated by the CLOCK-BMAL1 protein complex through its binding to E-box sequences located in the *Per* promoter region. The entire mechanism is not yet fully understood.

The functional state of the SCN itself is affected by the photoperiod and may thus serve as a basis not only for the daily clock, but also for the seasonal clock. In rodents, the interval of elevated *Per1* and *Per2* expression in the SCN is longer under a long photoperiod than under a short one (Hastings, 2001; Steinlechner *et al.*, 2002; Sumová *et al.*, 2002, 2003). Recent data showed that expression of some of the clock genes under various photoperiods is not necessarily synchronized throughout the entire SCN. Marked regional differences in gene expression rhythms along the rostro–caudal axis of the hamster SCN were reported. *Per2* expression was photoperiod-dependent in both the

Correspondence: Dr A. Sumová, as above.
E-mail: sumova@biomed.cas.cz

Received 25 February 2009, revised 11 August 2009, accepted 18 August 2009

rostral and caudal SCN; under a short photoperiod, the maximal expression occurred in synchrony in both parts, but under a long photoperiod the peak of expression in the caudal SCN preceded that in the rostral SCN (Hazlerigg *et al.*, 2005; Johnston *et al.*, 2005; Yan & Silver, 2008).

The vast majority of laboratory studies have used animals maintained under a LD cycle with abrupt, rectangular (RA), transitions between light and darkness. However, in nature, animals experience gradual LD transitions at dusk and dawn; the dynamics and duration of these transitions depend on season and latitude (Daan & Aschoff, 1975; Boulos *et al.*, 1996b; Boulos & Macchi, 2005). The spectral composition of artificial light cycles also differs from that of natural light, which varies during the twilight hours (McFarland & Munz, 1975; Hut *et al.*, 2000). Light-sensitive SCN neurons exhibit sustained responses to light stimuli of long duration and response to increasing and decreasing light intensity (Meijer *et al.*, 1986). Under natural conditions, the circadian system may thus continuously monitor changes in environmental illumination and utilize this information for entrainment (Usui, 2000). The inclusion of twilight LD transition (TW) in the regimens affected several circadian locomotor parameters in a season- and latitude-dependent manner. In Syrian hamsters, the timing of activity onset followed dusk in the presence of TW, but was more closely related to dawn in its absence. The offsets and midpoint of activity occurred earlier under a TW than under an RA regimen, with the difference most pronounced being observed under a short photoperiod. The presence of TW also resulted in lower day-to-day variability in activity onset times (Boulos & Macchi, 2005). In addition to the locomotor activity, also the pineal rhythm in arylalkyl-N-acetyltransferase activity was studied under natural photoperiods (Illnerová & Vaněček, 1980). So far, the effect of TW on the molecular clockwork in the mammalian SCN has been only marginally studied. In our previous work, PER1 protein profiles in the middle part of the SCN of rats maintained under natural photoperiods in summer and winter resembled those of rats maintained under the corresponding artificial photoperiods (Sumová *et al.*, 2002).

The aim of the present study was to determine in detail whether and how photoperiods with artificial TW affect expression of the clock genes, namely of *Per1* and *Per2*, and their products PER1 and PER2, in the mouse SCN and to compare the effect of the TW photoperiod with that of the RA photoperiod. Mice were entrained to a long photoperiod with 18 h of light and 6 h of darkness, or a short photoperiod with 6 h of light and 18 h of darkness under abrupt RA or gradual TW LD transition. Thereafter, they were released into darkness, and daily profiles of *Per1* and *Per2* expression and PER1 and PER2 levels were measured within the rostral (R), middle (M) and caudal (C) parts of the SCN.

Materials and methods

Animals

Two-month-old adult male C57Bl6/J mice (Velaz s.r.o., Czech Republic and Harlan, Horst, The Netherlands) were housed at a temperature of 23 ± 2°C with free access to food and water. For 4 weeks prior to the experiments, the animals were maintained under a long and short photoperiod with two different models of LD transition, namely the abrupt RA and gradual TW. For RA photoperiods, light was provided by overhead 40-W fluorescent tubes, and illumination during the light phase was between 50 and 200 lx, depending on cage position in the animal room. There was complete darkness during the dark period. Lights were on from 03.00 to 21.00 h for a long (LD18 : 6) photoperiod, and from 09.00 to 15.00 h for a short (LD6 : 18) photoperiod. For TW photoperiods, the light level during the dark phase was lower than 0.001 lx and the maximum light level during the light phase was 100 lx at the level of the cage. The gradual transition between darkness and light (and vice versa) took 1.5 h. It was controlled by the ACIS system (Spoelstra & Daan, 2008), which diminished light intensity without causing spectral changes by means of a computer-controlled shutter system.

Light intensity during twilight expressed logarithmically changed linear over time with a step size of 0.01 lx per 2 min. For the long photoperiod, the gradual decline of light intensity from 100 lx started at 20.15 h, and reached 0.01 lx at 21.45 h. The gradual increase in light intensity started from 0.01 lx at 02.15 h and reached 100 lx at 03.45 h. For the short photoperiod, the light intensity decline from 100 to 0.01 lx occurred between 14.15 and 15.45 h, and the light intensity rise from 0.01 to 100 lx occurred between 08.15 and 09.45 h. The log (intensity) mid-point of the TW increasing and decreasing slopes (at 1 lx) coincided with lights on and lights off in the RA light profiles for both photoperiods (Fig. 1A).

On the day of experiments, animals entrained to the short and long photoperiods with either RA or TW conditions were released into constant darkness, i.e. the morning light was not turned on. Every 2 h throughout the whole circadian cycle in complete darkness, four animals were sampled for *Per1* and *Per2* mRNA and three animals for PER1 and PER2 protein determination. For each photoperiod, the sampling was completed within 1 day. For experiments with RA transition, mice were maintained in animal facilities of the Institute of Physiology, v.v.i., Academy of Sciences of the Czech Republic, Prague. For experiments with TW transition, mice were kept in animal facilities of the University of Groningen, Haren, The Netherlands. The experiments were conducted under license no. A5228-01 with the US National Institutes of Health and in accordance with Animal Protection Law of the Czech Republic (license no. 42084/2003-1020) and license no. DEC #4660A of the Animal Experimentation committee of the University of Groningen.

In situ *hybridization*

For determination of *Per1* and *Per2* mRNA levels, mice were killed by decapitation immediately after cervical dislocation, brains were removed, immediately frozen on dry ice and stored at −80°C. Each brain was sectioned into five series of 12-μm coronal slices in alternating order throughout the entire rostro–caudal extent of the SCN and processed for *in situ* hybridization.

The cDNA fragments of rat rPer1 (980 bp; corresponds to nucleotides 581–1561 of the sequence in GenBank with accession no. AB002108) and rat rPer2 (1512 bp; corresponds to nucleotides 369–1881 of the sequence in Genbank with accession no. NM031678) were used as templates for *in vitro* transcription of complementary RNA probes. The r*Per1* and r*Per2* fragment-containing vectors were generously donated by Professor H. Okamura (Kobe University School of Medicine, Japan).

The probes were labeled using $\alpha[^{35}S]$thio-UTP (MP Biomedicals, Irvine, CA, USA), and the *in situ* hybridization was performed as described previously (Shearman *et al.*, 2000; Sládek *et al.*, 2004; Kováčiková *et al.*, 2006). Briefly, sections were hybridized for 20 h at 60°C (Per1) or 61°C (Per2). Following a post-hybridization wash, the sections were dehydrated in ethanol and dried. Finally, the slides were exposed to the BioMax MR film (Kodak) for 10 days and developed using the developer ADEFO-MIX-S and fixer ADEFO-FIX (ADEFO-CHEMIE Gmbh, Dietzenbach, Germany) in film processor Optimax (PROTEC GmBH, Oberstenfeld, Germany). As a

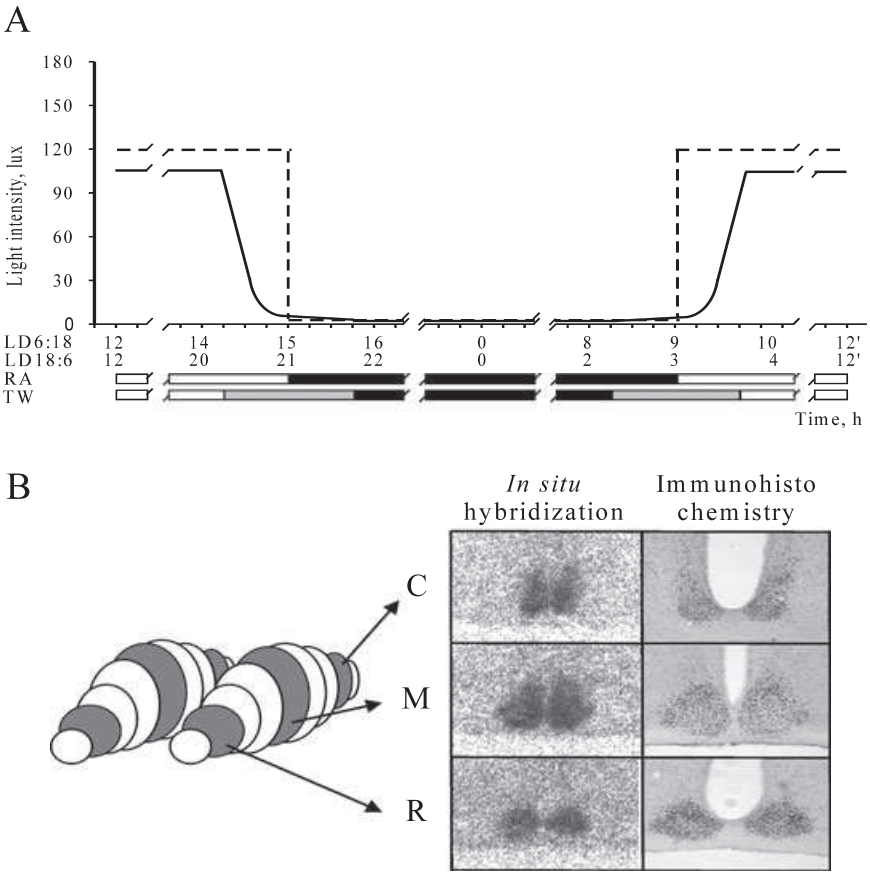

FIG. 1. Schematic cartoon of (A) experimental design of the light intensity changes during the rectangular (RA) and twilight (TW) photoperiod. Black bars depict intervals of the previous complete darkness, shaded bars depicts intervals of the TW. The *x*-axis is expressed in real time under the short (LD6 : 18 – upper line) and under the long (LD18 : 6 – lower line) photoperiod. (B) The SCN with marked rostral (R), middle (M) and caudal (C) sections (left), and representative *in situ* hybridization signals of *Per1* mRNA and of the immunohistochemistry staining of PER1 protein on sections from the corresponding parts of the SCN (right).

control, *in situ* hybridization was performed in parallel with sense probes on sections containing the SCN. For photoperiods with RA and TW transitions, the whole daily profiles of mRNA levels following the LD18 : 6 and LD6 : 18 were determined using the same labeled probe and processed simultaneously under identical conditions.

Autoradiographs of sections were analysed using an image analysis system (Image Pro, Olympus, New Hyde Park, NY, USA) to detect the relative optical density (OD) of the specific hybridization signal. In each animal, the mRNA was quantified bilaterally, at a representative R-, M- and C-SCN section (Fig. 1B). To define the position of the R-, M- and C-SCN on the film autoradiograph, the slides were counter-stained with Cresyl violet. The determination of the rostro–caudal position was based on typical shape of the nucleus at the coronal section (see Fig. 1B), as well as on distance from the utmost rostral section of the SCN; a section was considered to be rostral, middle and caudal when positioned within the 50–150-μm-, 250–350-μm- and 450–550-μm-thick compartment of the SCN, respectively. Each measurement was corrected for a non-specific background by subtracting OD values from the neighboring area in the hypothalamus that was free of specific signal. The background signal of the area, serving as an internal standard, was consistently low and did not exhibit marked changes with the time of day. In no case did *in situ* hybridization yield any specific signal using a sense probe. The OD for each animal was calculated as the mean of the values for the left and right SCN.

Immunohistochemistry

For determination of PER1 and PER2 protein levels, mice were deeply anesthetized with thiobarbital sodium (50 mg per kg, i.p.; Valeant Czech Pharma s.r.o., Praha, Czech Republic) and perfused through the ascending aorta with heparinized saline followed by phosphate-buffered saline (PBS; 0.01 M sodium phosphate, 0.15 M NaCl, pH 7.2) and then freshly prepared 4% paraformaldehyde in PBS. Brains were removed, post-fixed for 12 h at 4°C, and cryoprotected in 20% sucrose in PBS overnight at 4°C, frozen on dry ice and stored at −80°C. Each brain was sectioned into five series of 30-μm-thick coronal slices in alternating order throughout the whole rostro–caudal extent of the SCN and processed by free-floating immunohistochemistry using the standard avidin–biotin method with diaminobenzidine as the chromogen (Vector Laboratories, Peterborough, UK; Sumova *et al.*, 2002). The polyclonal primary PER1 antiserum was synthesized at the Massachusetts General Hospital Biopolymer Core Facility. It was raised in rabbits against amino acids 6–21 of the peptide sequence of mPER1 and characterized elsewhere (Sun *et al.*, 1997; Hastings *et al.*, 1999). The polyclonal primary PER2 antiserum was purchased from ADI (Greenwich, CT, USA). Specificity of the tissue staining was checked with and without blocking peptide (ADI, PER21-P; data not shown). All sections were developed in diaminobenzidine for exactly the same time to achieve the same intensity of the background staining. For photoperiods with RA and TW, the whole daily profiles of protein levels following the long and short photoperiod were

determined within one assay under identical conditions. Labeled cell nuclei were counted in sections representing the R-, M- and C-SCN (Fig. 1B) by two independent observers using an image analysis system (ImagePro, Olympus, New Hyde Park, NY, USA). The intensity of background staining was set at the nearest area surrounding the SCN, and every cell, with an intensity level above the background, was counted. For the C-SCN, some sections were damaged and, therefore, were excluded from counting. This decreased the number of samples at 12.00, 02.00 and 04.00 h under the short photoperiods from three to only two.

Statistical analysis

To ascertain whether daily profiles of *Per1* and *Per2* mRNA and PER1 and PER2 protein levels in the R-, M- and C-SCN under the long photoperiod differed from those under the short photoperiod, the profiles under these photoperiods both with RA and TW were compared by two-way analysis of variance (ANOVA, BMDP Statistical Software, University of California, Berkley, CA, USA). The two-way ANOVA was also used to reveal whether the profiles under the TW photoperiods differed from those under the RA photoperiods. Moreover, the two-way ANOVA was used to reveal whether the profiles in the R-, M- and C-SCN differ. In case of significant differences between the profiles and significant interaction effects as well as in case of significant differences between the profiles and non-significant interaction effect, the *post hoc* analysis by the Student's-Newman-Keuls multiple range test was performed with $P < 0.05$ being required for significance. The analysis was also used when a significant interaction effect suggested that the expression profiles might differ, even though the ANOVA did not reveal a significant difference.

The cross-correlation analysis was used to test phase differences between profiles when *post hoc* analysis revealed that the times of the rise and/or decline of gene expression and protein levels differed between the profiles. To asses non-parallel shifts of the rise and decline, the rising and declining parts of the profiles were analysed separately.

Results

Comparison of daily profiles of Per1 *mRNA and PER1 protein levels in mice entrained to the long and short photoperiod with RA and TW within the R-, M- and C- part of the SCN*

Per1 *mRNA*

Comparison of the *Per1* mRNA profiles between the long and short photoperiod revealed that the profiles under the long photoperiod differed significantly from those under the short photoperiod within the R-, M- and C-SCN, whether the LD transition was RA or TW (Table 1). Comparison of the *Per1* mRNA profiles between the RA and TW photoperiods revealed that these profiles were significantly modulated by the type of LD transition (Table 1). Subsequent analysis revealed the following differences between the photoperiods with RA and TW.

Under the short TW photoperiod, *Per1* mRNA levels within the R-SCN (Fig. 2A) first declined at 14.00 h (vs. 12.00 h, $P < 0.05$) and the decline continued until 16.00 h (vs. 14.00 h, $P < 0.05$). Under the short RA photoperiod, the first decline occurred at 16.00 h and continued until 18.00 h (vs. 14.00 and 16.00 h, respectively, $P < 0.01$). The first significant rise occurred at 04.00 h in TW as well as in RA (vs. 02.00 h, $P < 0.05$ under TW; vs. 22.00 h, $P < 0.05$ in RA), but under RA the rise continued further until 12.00 h. Cross-correlation analysis revealed a significant 2-h phase-advance in the decline of *Per1* mRNA levels under TW as compared with RA ($R = 0.986$, $P < 0.001$). In the M-SCN (Fig. 2B), the decline in *Per1* mRNA levels occurred at about the same time, i.e. at 16.00 h (vs. 14.00 h, $P < 0.01$) under RA and TW. However, the first significant rise occurred earlier under TW (at 04.00 vs. 02.00 h, $P < 0.01$) than under RA (at 06.00 vs. 04.00 h, $P < 0.01$). The cross-correlation test revealed a significant 2-h phase-advance in the rise of *Per1* mRNA levels under TW as compared with RA ($R = 0.989$, $P < 0.001$). In the C-SCN (Fig. 2C), *Per1* mRNA levels declined earlier under TW than RA; the decline occurred at 14.00 h (vs. 12.00 h, $P < 0.05$) in TW, but only at 16.00 h (vs. 14.00 h, $P < 0.01$) in RA. The rise was significant at 04.00 h (vs. 02.00 h, $P < 0.05$) under TW, but only at 06.00 h (vs. 04.00 h, $P < 0.01$) under RA. Cross-correlation analysis revealed a significant 2-h phase-advance in the rise of *Per1* mRNA levels under TW as compared with RA ($R = 0.973$, $P = 0.014$) as well as of the decline ($R = 0.948$, $P = 0.004$).

Under the long photoperiod, *Per1* mRNA levels in the R-SCN (Fig. 2D) began to decline earlier under TW (at 20.00 vs. 18.00 h, $P < 0.01$) than under RA (at 22.00 vs. 20.00 h, $P < 0.01$), but the minimum levels were achieved at the same time under RA and TW, i.e. at 22.00 h. The first significant rise in *Per1* mRNA levels occurred at 06.00 h (vs. 00.00 h, $P < 0.05$) under TW, but only at 14.00 h (vs. 12.00 h, $P < 0.05$) under RA. However, the cross-correlation analysis did not reveal a significant phase-advance, probably because of a non-parallel run of both profiles during the daytime hours: while under TW the profile exhibited a gradual rise; under RA intermediate levels were detected. In the M-SCN (Fig. 2E), the decline in *Per1* mRNA levels occurred at the same time under RA and TW, i.e. at 20.00 h (vs. 18.00 h, $P < 0.01$), and the rise was first significant at 06.00 h (vs. 22.00 h, $P < 0.05$) in RA and at 08.00 h (vs. 00.00 h, $P < 0.05$) in TW. The cross-correlation analysis revealed a significant phase-advance in the *Per1* mRNA rise under RA as compared with that under TW ($R = 0.961$, $P = 0.009$). In the C-SCN (Fig. 2F), the *Per1* mRNA levels declined at the same time under RA and TW, i.e. at 20.00 h (vs. 18.00 h, $P < 0.01$); the rise occurred significantly earlier under RA (at 04.00 vs. 22.00 h, $P < 0.05$) than under TW (06.00 vs. 04.00 h, $P < 0.01$). The cross-correlation analysis revealed a significant phase-advance in the *Per1* mRNA rise under the RA as compared with TW ($R = 0.974$, $P = 0.005$).

Comparison of *Per1* mRNA profiles among the R-, M- and C-SCN by the two-way ANOVA under the short photoperiod (Fig. 3A and C) revealed a significant difference between the individual regions of the SCN under RA, but not under TW (Table 1). The *post hoc* analysis revealed that under the short RA photoperiod, the *Per1* mRNA levels were significantly higher in the R-SCN than in M- and C-SCN at 14.00 h ($P < 0.01$) and 16.00 h ($P < 0.01$). The levels were also significantly higher in the R-SCN than in M-SCN at 04.00 h ($P < 0.05$) and 06.00 h ($P < 0.05$), and in the C-SCN than in M-SCN at 06.00 h ($P < 0.05$). The cross-correlation analysis did not reveal any significant phase-shift among the profiles in the R-, M- and C-SCN under the short RA. However, when the phase-shift in the decline was tested separately, the cross-correlation analysis revealed a 2-h phase-delay of the decline in the R-SCN as compared with the C- and M-SCN ($R = 0.978$ and 0.984, respectively; both $P < 0.001$). Under the long photoperiod (Fig. 3B and D), the two-way ANOVA revealed a significant difference among the R-, M- and C-SCN under RA, but not under TW, conditions. However, a significant interaction effect in TW still suggested differences between the profiles of the individual SCN regions (Table 1). In RA, the profiles between R- and C-SCN differed at 12.00, 18.00, 20.00, 00.00, 06.00, 08.00, 10.00 and

TABLE 1A. Short vs. long photo periods (two-way ANOVA comparing *Per1* and *Per2* mRNA and PER1 and PER2 protein levels)

	Per1						*Per2*					
	Photoperiod		Time		Interaction		Photoperiod		Time		Interaction	
	F_1-value	*P*-value	F_{12}-value	*P*-value	F_{12}-value	*P*-value	F_1-value	*P*-value	F_{12}-value	*P*-value	F_{12}-value	*P*-value
mRNA												
RA R	0.05	0.82	26.36	< 0.001	21.92	< 0.001	22.33	< 0.001	46.32	< 0.001	20.13	< 0.001
RA M	10.22	0.002	57.58	< 0.001	10.99	< 0.001	31.08	< 0.001	79.09	< 0.001	25.76	< 0.001
RA C	15.70	< 0.001	72.07	< 0.001	7.66	< 0.001	17.61	< 0.001	85.54	< 0.001	13.21	< 0.001
TW R	21.09	< 0.001	24.80	< 0.001	22.00	< 0.001	0.37	0.55	78.16	< 0.001	37.62	< 0.001
TW M	25.95	< 0.001	40.48	< 0.001	17.23	< 0.001	0.12	0.73	71.16	< 0.001	26.40	< 0.001
TW C	20.40	< 0.001	33.56	< 0.001	8.18	< 0.001	6.60	0.02	69.96	< 0.001	9.31	< 0.001
Protein												
RA R	2.41	0.13	10.05	< 0.001	3.10	0.01	0.00	0.99	11.35	< 0.001	4.57	< 0.001
RA M	21.83	< 0.001	61.46	< 0.001	17.49	< 0.001	6.19	0.02	31.84	< 0.001	7.67	< 0.001
RA C	0.55	0.46	5.80	< 0.001	2.00	0.05	1.66	0.21	9.42*	< 0.001	1.43*	0.23
TW R	0.54	0.47	14.10	< 0.001	8.83	< 0.001	3.57	0.07	9.14	< 0.001	3.57	< 0.001
TW M	2.40	0.13	33.03	< 0.001	18.25	< 0.001	10.71	0.002	39.84	< 0.001	11.62	< 0.001
TW C	0.12	0.73	7.061	< 0.001	2.50	0.02	0.91	0.35	6.84†	< 0.001	2.03†	0.06

TABLE 1B. Rectangular vs. twilight light-to-dark transitions (two-way ANOVA comparing *Per1* and *Per2* mRNA and PER1 and PER2 protein levels)

	Per1						*Per2*					
	LD transition		Time		Interaction		LD transition		Time		Interaction	
	F_1-value	*P*-value	F_{12}-value	*P*-value	F_{12}-value	*P*-value	F_1-value	*P*-value	F_{12}-value	*P*-value	F_{12}-value	*P*-value
mRNA												
S R	38.08	< 0.001	47.21	< 0.001	5.49	< 0.001	37.45	< 0.001	106.7	< 0.001	6.30	< 0.001
S M	13.66	< 0.001	86.38	< 0.001	7.92	< 0.001	16.30	< 0.001	147.9	< 0.001	9.47	< 0.001
S C	18.36	< 0.001	45.40	< 0.001	4.94	< 0.001	16.27	< 0.001	88.99	< 0.001	2.77	0.005
L R	8.28	0.01	38.58	< 0.001	2.54	0.008	125.7	< 0.001	49.87	< 0.001	1.33	0.22
L M	4.45	0.04	38.58	< 0.001	1.37	0.20	89.1	< 0.001	51.39	< 0.001	1.63	0.10
L C	19.29	< 0.001	70.03	< 0.001	1.43	0.18	57.31	< 0.001	78.41	< 0.001	3.68	< 0.001
Protein												
S R	10.81	0.002	22.45	< 0.001	2.43	0.02	6.52	0.014	15.62	< 0.001	2.08	0.04
S M	3.65	0.06	95.65	< 0.001	9.26	< 0.001	0.89	0.35	55.72	< 0.001	2.18	0.03
S C	1.55	0.22	9.93	< 0.001	1.47	0.18	7.37	0.02	9.96†	< 0.001	1.86†	0.09
L R	3.17	0.08	9.82	< 0.001	1.36	0.22	19.85	< 0.001	8.70	< 0.001	0.48	0.91
L M	1.06	0.31	32.75	< 0.001	1.45	0.18	1.72	0.20	27.63	< 0.001	1.74	0.09
L C	4.13	0.05	3.55	< 0.001	0.97	0.49	5.18	0.03	5.58*	< 0.001	1.35*	0.26

TABLE 1C. Rostral vs. middle vs. caudal SCN (two-way ANOVA comparing *Per1* and *Per2* mRNA and PER1 and PER2 protein levels)

	Per1						*Per2*					
	SCN part		Time		Interaction		SCN part		Time		Interaction	
	F_1-value	*P*-value	F_{12}-value	*P*-value	F_{12}-value	*P*-value	F_1-value	*P*-value	F_{12}-value	*P*-value	F_{12}-value	*P*-value
mRNA												
S RA	14.02	< 0.001	117.72	< 0.001	2.09	< 0.001	5.97	0.004	183.30	< 0.001	2.71	< 0.001
L RA	4.31	0.02	47.16	< 0.001	9.18	< 0.001	5.38	0.006	58.90	< 0.001	5.09	< 0.001
S TW	1.95	0.15	59.42	< 0.001	0.94	0.55	0.49	0.61	146.51	< 0.001	0.98	0.51
L TW	1.74	0.18	72.76	< 0.001	5.61	< 0.001	7.96	< 0.001	120.90	< 0.001	5.93	< 0.001
Protein												
S RA	41.20	< 0.001	43.58	< 0.001	3.77	< 0.001	101.83	< 0.001	20.34	< 0.001	4.69	< 0.001
L RA	98.41	< 0.001	13.79	< 0.001	2.92	< 0.001	33.39	< 0.001	22.37*	< 0.001	6.97	< 0.001
S TW	58.18	< 0.001	52.80	< 0.001	2.86	< 0.001	32.08	< 0.001	31.71†	< 0.001	3.26	< 0.001
L TW	59.15	< 0.001	19.09	< 0.001	2.59	< 0.001	66.01	< 0.001	17.29	< 0.001	3.33	< 0.001

*F_{10}-value; †F_{11}-value (applies to Tables 1A, 1B and 1C).

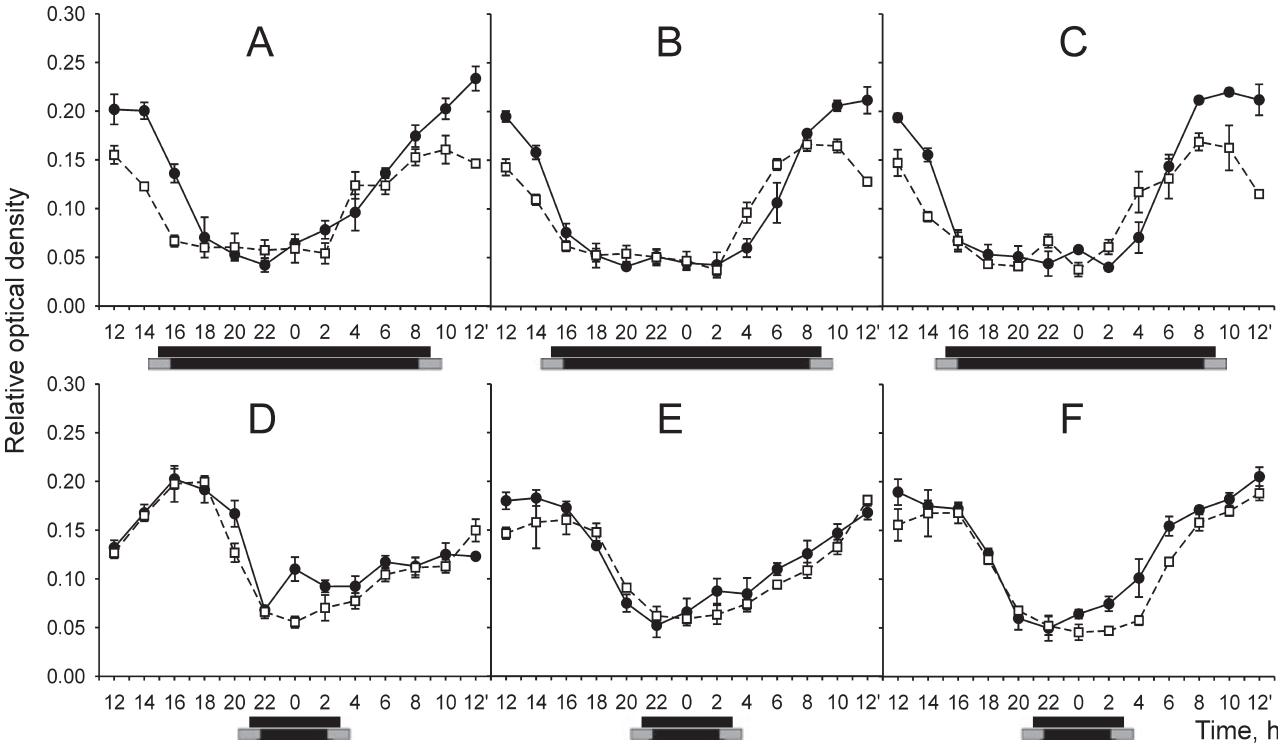

FIG. 2. Daily profiles of *Per1* mRNA levels within the rostral (A, D), middle (B, E) and caudal (C, F) part of the SCN of mice entrained to a short (A–C) or a long photoperiod (D–F) with a RA (solid line) or TW (dashed line) LD transition. Mice were released into darkness on the day of sampling. Data are expressed as relative optical density (OD). Each point represents mean ± SEM from four animals. Dark bars below the profiles depict intervals of the previous darkness; the upper bar indicates the photoperiod with RA and the lower bar with TW LD transition.

12.00 h ($P < 0.01$), between R- and M-SCN at 12.00, 18.00, 20.00, 00.00 and 12.00 h ($P < 0.01$), and between M- and C-SCN at 06.00, 08.00, 10.00 and 12.00 h ($P < 0.01$). In TW, the profiles between R- and C-SCN differed at 16.00 h ($P < 0.05$), 18.00, 20.00, 08.00, 10.00 and 12.00 h ($P < 0.01$), between R- and M-SCN at 16.00 h ($P < 0.02$), 18.00 and 20.00 h ($P < 0.01$), and between the M- and C-SCN at 18.00 h ($P < 0.05$), 08.00 and 10.00 h ($P < 0.01$). The cross-correlation analysis revealed a significant phase-delay in the profile in R- as compared with those in C- and M-SCN for RA ($R = 0.800$, $P < 0.002$ and $R = 0.723$, $P < 0.008$, respectively) as well as for TW ($R = 0.916$ and $R = 0.879$, respectively, both $P < 0.001$). No phase-shifts between the profiles in the M- and C-SCN were detected under the long RA and TW photoperiods.

Altogether, the profiles of *Per1* mRNA under the short TW photoperiod were phase-advanced relative to those under the short RA photoperiod within all parts of the SCN. Under the long photoperiod, *Per1* expression in TW declined in synchrony with that in RA within all parts of the SCN. In the R-SCN a significant rise occurred much later under RA than TW due to an extremely long interval of intermediate *Per1* mRNA levels that spanned half of the RA profile. However, an earlier rise of *Per1* expression under the long RA than TW photoperiod was detected in the M- and C-SCN. When the R-, M- and C-SCN *Per1* expression profiles were compared under the short photoperiod, the decline in the R-SCN was significantly phase-delayed as compared with that in the C- and M-SCN under RA, but all the SCN parts were in synchrony under the TW photoperiod. The better synchrony among the R-, M- and C- parts in the short photoperiod found under TW as compared with that under RA was just suggested for profiles under the long TW photoperiod: the significance of differences between the R-, M- and C-SCN profiles as well as the number of time points when the individual parts differed in *Per1* mRNA levels were lower under the long TW than RA photoperiod.

PER1 protein

The two-way ANOVA revealed that the PER1 protein profiles in the R-, M-, and C-SCN under the long photoperiod differed from those under the short photoperiod, whether under RA or TW conditions. Although the effect of photoperiod was significant only for the M-SCN under RA, significant interaction effects were found in the R- and C-SCN (Table 1). When PER1 protein profiles under the RA and TW photoperiods were compared under the short photoperiod, the two-way ANOVA revealed a significant difference between the profiles only in the R-SCN but not in the M- and C-SCN; however, a significant interaction effect was found in the M-SCN. Under the long photoperiod, the profiles differed significantly in the C-SCN only, but the interaction effect was not significant (Table 1).

A subsequent analysis revealed that under the short photoperiod, the decline in the PER1 level in the R-SCN (Fig. 4A) occurred simultaneously while under RA and TW (at 00.00 vs. 20.00 h, both $P < 0.05$). The rise, however, started earlier in TW (at 12.00 vs. 06.00 h, $P < 0.01$) than in RA (at 14.00 vs. 08.00 h, $P < 0.01$); the cross-correlation analysis revealed a significant 2-h phase-advance in PER1 rise under TW as compared with RA ($R = 0.926$, $P = 0.008$). In the M-SCN (Fig. 4B), the decline in the PER1 levels started earlier under TW (at 20.00 vs. 18.00 h, $P < 0.01$) than under RA (at 22.00 vs. 20.00 h, $P < 0.01$), but it was accomplished at about the same time under both RA and TW (at 00.00 vs. 20.00 h, $P < 0.01$ and vs. 22.00 h, $P < .01$, respectively). The rise also started earlier under TW (at 10.00 vs. 06.00 h, $P < 0.05$) than under RA (at 12.00 vs. 08.00 h,

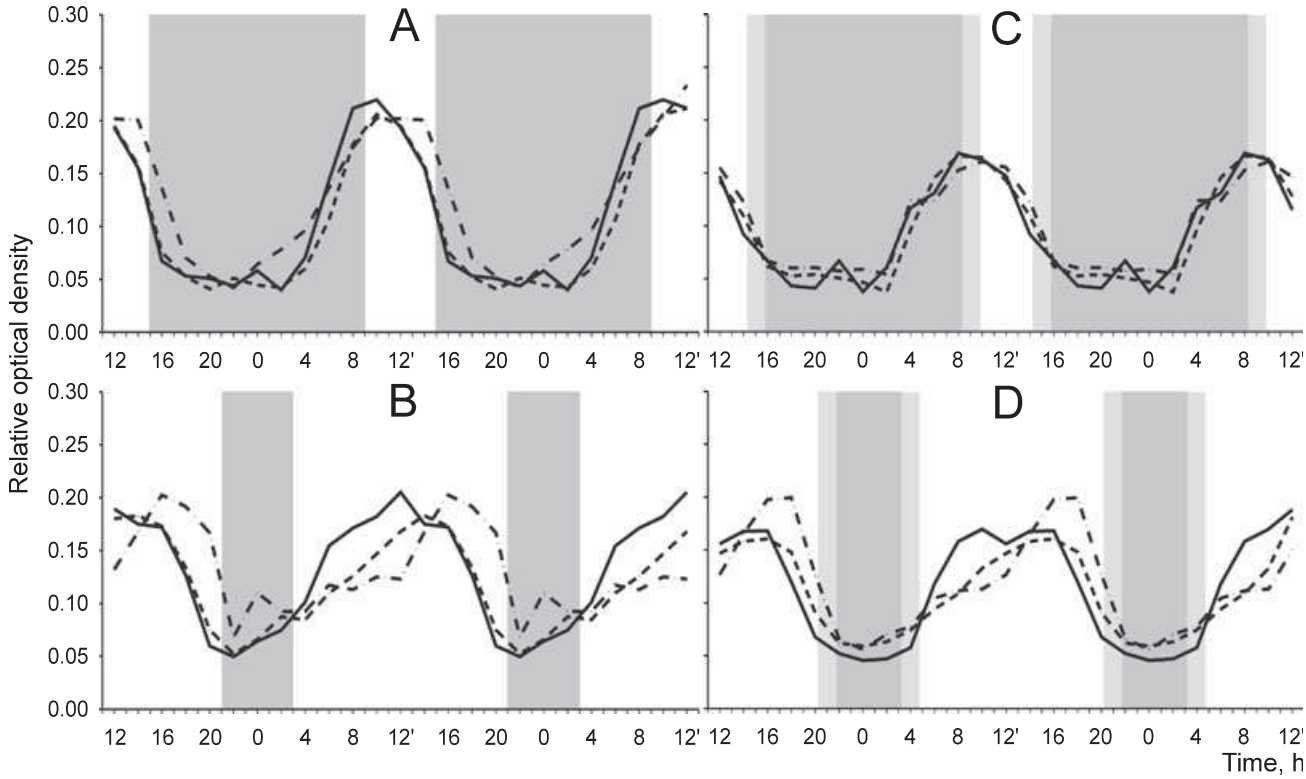

FIG. 3. Comparison of the *Per1* expression profiles within the R, M and C parts of the SCN in rats maintained under the long and short photoperiod with RA and TW LD transition. To visualize the phase relationship between the individual parts of the SCN under a particular photoperiod, the data from Fig. 2 were double-plotted, and the profiles of the R (dash dotted line), M (dashed line) and C (solid line) parts were depicted on the same graph. The gray columns represent the duration of the previous dark phase under the short (A, C) or long (B, D) photoperiods with RA (A, B) or TW (C, D) LD transition. For full data with means and SEM, see Fig. 2.

$P < 0.05$). Moreover, the cross-correlation analysis revealed a significant 2-h phase-advance in the rise in PER1 levels in the M-SCN under TW as compared with that under RA ($R = 0.971$, $P < 0.001$). In the C-SCN, though the effect of time was significant (Table 1), the subsequent analysis did not reveal any significant variations in PER1 levels between individual time points (Fig. 4C), probably due to the lower number of samples at three time points. Nevertheless, the cross-correlation analysis revealed a significant 2-h phase-advance in the PER1 rise under TW as compared with that under RA ($R = 0.967$, $P < 0.002$). Thus, under the short TW photoperiod the rise in PER1 levels in all parts of the SCN was advanced by about 2 h compared with that under the short RA photoperiod. Under the long photoperiod, the subsequent analysis did not reveal any significant variations in the C-SCN between individual time points under RA or TW (Fig. 4F; Table 1). Moreover, also the cross-correlation analysis did not reveal any significant shift between the profile under RA and that under TW photoperiod in the C-SCN. Therefore, the PER1 profiles under the long RA and TW photoperiods were in synchrony within the entire SCN.

Two-way ANOVA comparison of PER1 profiles among the R-, M- and C-SCN revealed that the profiles were significantly different (Table 1). When the R- and C-SCN were compared, the PER1 profiles differed only at few time points, namely at 20.00 h under the short TW photoperiod ($P = 0.044$), at 20.00 h ($P < 0.001$) and 04.00 h ($P = 0.018$) under the long RA, and at 22.00 h ($P = 0.007$) and 02.00 h ($P = 0.019$) under the long TW photoperiod. In contrast, the M-SCN profile was significantly different from those in the R- and C-SCN at most of the time points when PER1 levels were elevated, i.e. during the interval 16.00–20.00 h under the short RA and 10.00–22.00 h under the short TW photoperiod. Under the long RA photoperiod, levels in M-SCN were significantly elevated above those in the R-SCN during the interval 10.00–02.00 (with the exception at 14.00 h) and those in the C-SCN at all time points, with the exception at 14.00 and 12.00 h. Under the long TW photoperiod, levels in M-SCN were significantly higher than those in the R-SCN during the interval of 14.00–00.00 h and above those in the C-SCN during 14.00–04.00 h (with the exception at 16.00 h). The higher amplitude of the M-SCN rhythms reflects the fact that the area of the M-SCN where PER1-immunoreactive cells are counted is about double that of the R- or C-SCN. When phases of the R- and C-SCN profiles were compared, the cross-correlation analysis revealed a 2-h phase-advance in the PER1 profile in the C-SCN compared with R-SCN under the long RA ($R = 0.877$, $P < 0.001$) and TW ($R = 0.751$, $P = 0.005$) photoperiods, but not under the short photoperiods.

In conclusion, under the short photoperiod the PER1 rise in TW preceded that in RA within all SCN parts. The PER1 profile in the C-SCN was phase-advanced by 2 h relative to that in the R-SCN under the long, but not under the short, photoperiod with RA or TW.

Comparison of daily profiles of Per2 *mRNA and PER2 protein levels in mice entrained to the long or short photoperiod with RA and TW within the R-, M- and C- part of the SCN*

Per2 *mRNA*

In the R-, M- and C-SCN, *Per2* mRNA profiles with RA under the long photoperiod differed from those under the short photoperiod, and

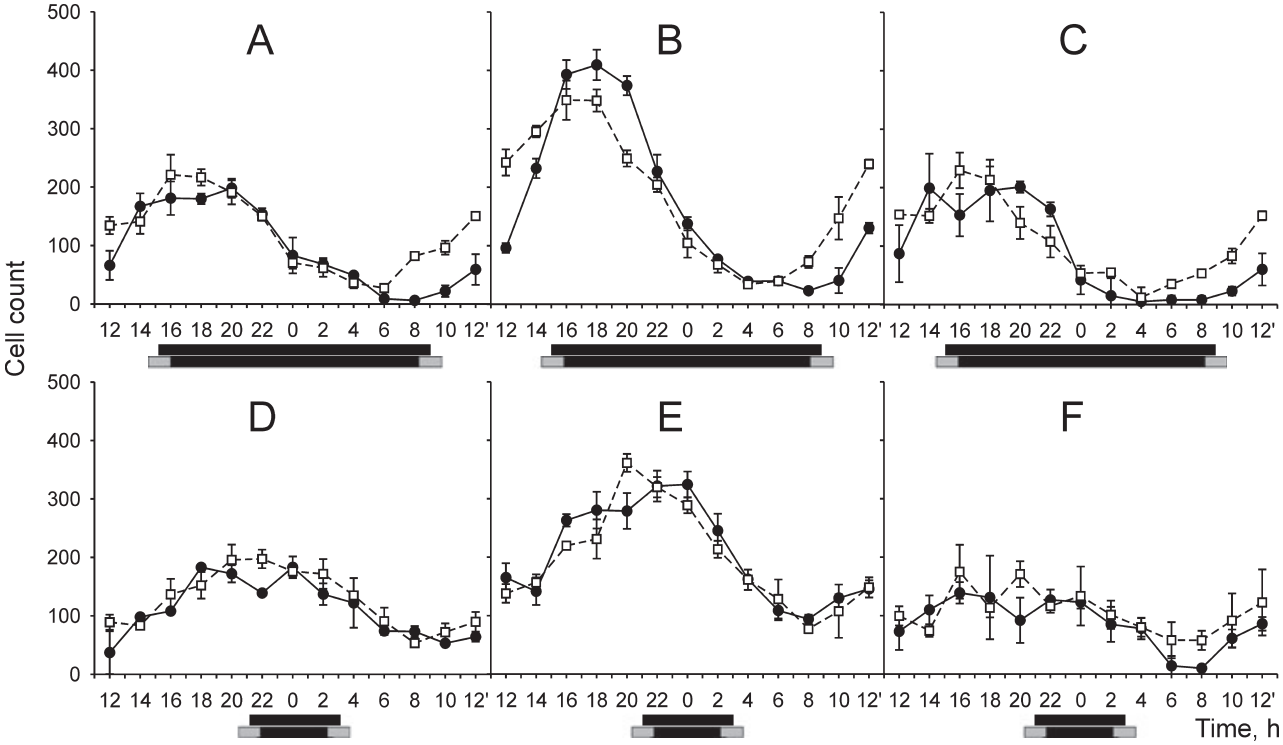

FIG. 4. Daily profiles of PER1 levels within the R (A, D), M (B, E) and C (C, F) part of the SCN of mice entrained to a short (A–C) or a long photoperiod (D–F) with a RA (solid line) or TW (dashed line) LD transition. The mice were released into darkness on the day of sampling. Data are expressed as relative OD. Each point represents mean ± SEM from three animals (only two at 12.00, 02.00 and 04.00 h). Dark bars below the profiles depict intervals of the previous darkness; the upper bar indicates the photoperiod with RA and the lower bar with TW LD transition.

in TW the difference was strongly suggested by highly significant interaction effects (Table 1). Further, these profiles were significantly modulated by the type of LD transition (Table 1).

Under the short photoperiod, the *Per2* mRNA level in the R-SCN (Fig. 5A) began to decline earlier in TW (18.00 vs. 16.00 h; $P < 0.01$) than in RA (20.00 vs. 18.00 h; $P < 0.01$), reaching its low level at 20.00 h in TW and 22.00 h in RA. The rise in *Per2* mRNA levels occurred at approximately the same time in RA and TW (08.00 vs. 06.00 h, $P < 0.01$). The cross-correlation analysis revealed a significant 2-h phase-advance in the decline of *Per2* mRNA levels in TW compared with RA ($R = 0.985$, $P < 0.001$). In the M-SCN (Fig. 5B), the decline in *Per2* mRNA levels occurred at approximately the same time in RA and TW; it started between 14.00 and 16.00 h in RA, and between 16.00 and 18.00 h in TW, and continued until 20.00 h under both conditions ($P < 0.01$). The rise occurred at 06.00 h (vs. 04.00 h, $P < 0.01$) in TW, but only at 08.00 h (vs. 06.00 h, $P < 0.01$) in RA. The cross-correlation analysis revealed a significant 2-h phase-advance in the *Per2* mRNA rise in TW as compared with RA ($R = 0.984$, $P < 0.001$). In the C-SCN (Fig. 5C), the *Per2* mRNA levels declined at 18.00 h (vs. 14.00 h, $P < 0.01$) in RA and TW, and the decline continued further until 20.00 h (vs. 18.00 h, $P < 0.01$). The significant rise occurred at 06.00 h (vs. 02.00 h, $P < 0.01$) under TW, but only at 08.00 h (vs. 06.00 h, $P < 0.01$) under RA. The cross-correlation revealed a significant 2-h phase-advance in the *Per2* mRNA rise in TW as compared with RA ($R = 0.983$, $P = 0.003$). Thus, under the short photoperiod, the *Per2* mRNA decline in the R-SCN, or rise in the M- and C-SCN in TW, appeared to be phase-advanced relative to that in RA.

Under the long photoperiod, the two-way ANOVA revealed significant differences between *Per2* mRNA profiles in RA and TW in all parts of the SCN (Table 1). However, in the R- and M-SCN, different mean values of the profiles under RA and TW resulted in non-significant interaction effects. *Per2* mRNA levels in the R-SCN (Fig. 5D) declined at the same time in RA and TW, i.e. at 00.00 h (as compared with 22.00 h, $P < 0.01$). The rise in *Per2* mRNA levels was slow and gradual under both TW and RA. It was significant at 08.00 h (vs. 06.00 h, $P < 0.01$) in TW and at 10.00 h (vs. 04.00 h, $P < 0.01$) in RA. The cross-correlation analysis revealed a significant 2-h phase-advance in the *Per2* mRNA rise in TW as compared with RA ($R = 0.985$, $P = 0.002$). Within the M-SCN (Fig. 5E), the *Per2* mRNA declined in RA and TW simultaneously, i.e. at 00.00 h (vs. 22.00 h, $P < 0.01$). A significant rise occurred at 06.00 and 08.00 h (as compared with 04.00 h, both $P < 0.01$) in RA and TW, respectively. The cross-correlation revealed a significant 2-h phase-advance in the *Per2* mRNA rise in RA as compared with TW ($R = 0.923$, $P = 0.025$). In the C-SCN (Fig. 4F), the decline in the *Per2* mRNA level occurred at about the same time in RA and TW, i.e. at 22.00 h (vs. 20.00 h in RA, $P < 0.01$; and vs. 14.00 h in TW, $P < 0.05$), though the decline was more gradual in TW than in RA. The rise also occurred simultaneously in RA and TW, and was significant for the first time at 08.00 h (vs. 06.00 h, $P < 0.01$).

Comparison of *Per2* mRNA profiles among the R-, M- and C-SCN under the short photoperiod (Fig. 7A and C) revealed that there was a significant difference between the individual parts of the SCN in RA, but not in TW (Table 1). The *post hoc* analysis revealed that under the short RA photoperiod, the *Per2* mRNA levels at 04.00 h were significantly higher in the C-SCN than in the M-SCN ($P < 0.05$), at 08.00 h they were higher in the C- and M-SCN than in the R-SCN ($P < 0.05$ and $P < 0.01$, respectively), at 16.00, 18.00 and 20.00 h

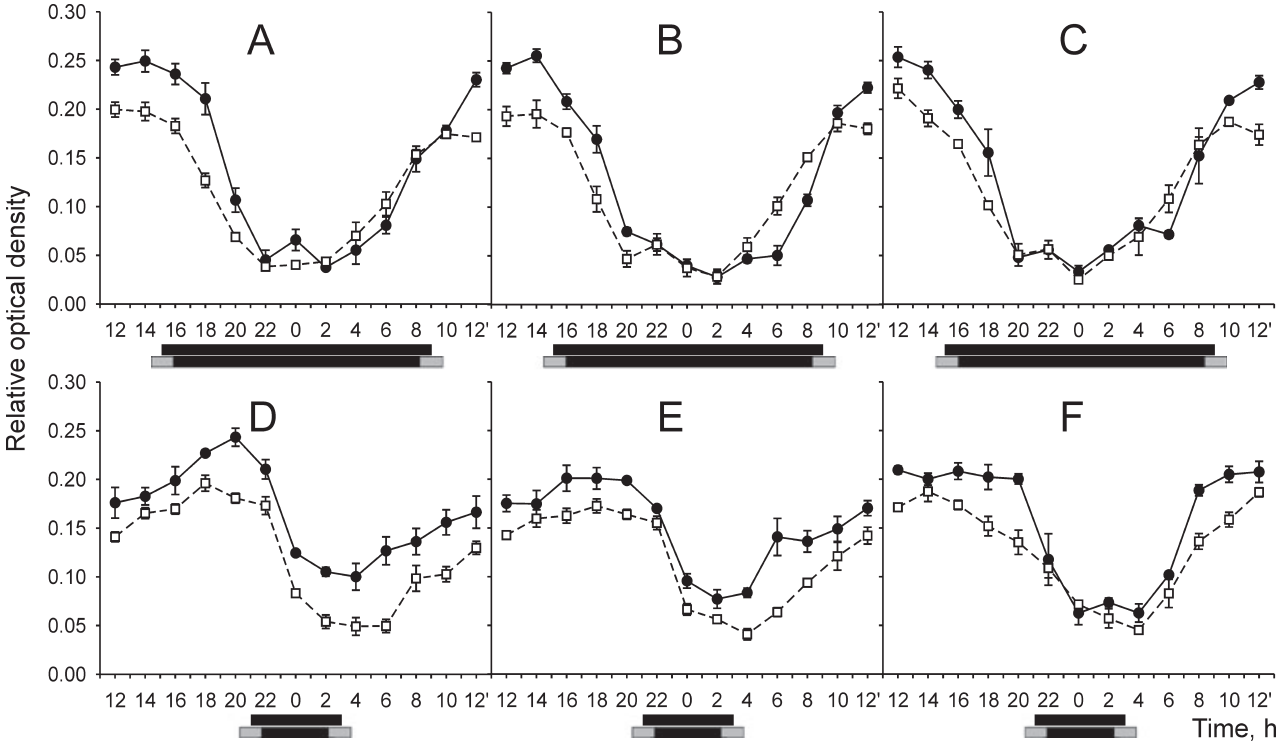

FIG. 5. Daily profiles of *Per2* mRNA levels within the R (A, D), M (B, E) and C (C, F) part of the SCN of mice entrained to a short (A–C) or a long photoperiod (D–F) with RA (solid line) or TW (dashed line) LD transition. For other details, see legend to Fig. 2.

they were higher in the R- than in the C-SCN ($P < 0.05$, $P < 0.01$ and $P < 0.01$, respectively), and at 18.00 and 20.00 h they were higher in the R- than in the M-SCN ($P < 0.01$). The cross-correlation analysis did not reveal any significant phase-shift among the *Per2* profiles in the R-, M- and C-SCN under the short RA. However, when a phase-shift in the decline was tested separately, the cross-correlation analysis revealed a 2-h phase-delay of the decline in the R-SCN as compared with the C-SCN ($R = 0.970$, $P < 0.001$). Under the long photoperiod (Fig. 6B and D), there was a significant difference between the individual parts of the SCN in RA and TW (Table 1). Under the long RA photoperiod, the *Per2* mRNA levels differed significantly between R- and C-SCN at 20.00, 22.00, 00.00, 08.00 and 10.00 h ($P < 0.01$), and at 04.00 and 12.00 h ($P < 0.05$), between R- and M-SCN at 20.00 h ($P < 0.01$) and 22.00 h ($P < 0.05$), and between M- and C-SCN at 22.00, 08.00, 10.00 ($P < 0.01$) and at 00.00, 06.00 and 12.00 h ($P < 0.05$). In TW, the levels between R- and C-SCN differed at 18.00, 20.00, 22.00, 06.00, 08.00, 10.00 and 12.00 h ($P < 0.01$) and at 12.00 h ($P < 0.05$), between R- and M-SCN only at 18.00 h ($P < 0.05$), and between M-and C-SCN at 12.00, 08.00, 10.00, 12.00 h ($P < 0.01$) and at 20.00 h ($P < 0.05$). The cross-correlation analysis demonstrated a significant phase-advance in the *Per2* expression profile in the C-SCN relative to that in the R-SCN in RA ($R = 0.863$, $P < 0.001$), as well as in TW ($R = 0.869$, $P < 0.001$).

Altogether, under the short photoperiod, the profiles of *Per2* mRNA in TW seemed to be phase-advanced, relative to those in RA, within all parts of the SCN. Under the long photoperiod, the *Per2* mRNA rise under TW occurred earlier than under RA in the R-SCN, later in the M-SCN and at the same time in the C-SCN; the decline was simultaneous in all the SCN parts. Hence under the long photoperiod, only the rise of *Per2* expression in the R-SCN was significantly affected by the type of LD transition. Under the short RA photoperiod the *Per2* mRNA decline in the R-SCN was significantly phase-delayed compared with that in the C-SCN, while under the short TW photoperiod all parts of the SCN were in synchrony. Under the long RA and TW photoperiods, the R-SCN profile was significantly delayed, relative to the C-SCN profile. However, under the long TW photoperiod, a higher degree of synchrony between the R-, M- and C-parts found under the short TW photoperiod was still suggested as compared with the long RA photoperiod, namely due to the synchrony between the profiles in the R- and M-SCN.

PER2 protein

The two-way ANOVA revealed that PER2 protein profiles were different under the long and short photoperiod in the R- and M-, but not within the C-SCN, whether under RA or TW (Table 1). When PER2 protein profiles under RA were compared with those under TW (Table 1), the two-way ANOVA revealed significant differences between the profiles in the R- and C-SCN both under the long and short photoperiod, but the interaction effect was significant only in the R-SCN under the short photoperiod. In the M-SCN, the difference between RA and TW was not significant under the short and long photoperiod, but under the short photoperiod there was a significant interaction effect (Table 1). Under the short photoperiod, the PER2 decline in RA in the R-SCN (Fig. 7A) was significant for the first time at 22.00 h (vs. 20.00 h, $P < 0.05$) and in TW at 02.00 h (vs. 20.00 h, $P < 0.05$), but the minimum levels were achieved at 02.00 h, i.e. at about the same time under both LD transitions. PER2 levels began to gradually rise earlier in TW than RA, but significantly elevated levels were achieved at the same time, i.e. at 18.00 vs. 12.00 h ($P < 0.01$) in RA and vs. 06.00 h ($P < 0.01$) in TW. In the M-SCN, PER2 levels declined simultaneously in RA and TW (Fig. 7B), i.e. at 22.00 h (vs. 20.00 h, $P < 0.01$), and the decline continued until 02.00 h (vs. 22.00 h, $P < 0.01$). Under RA, the first rise occurred at 14.00 h (vs. 12.00 h, $P < 0.01$) and continued until 18.00 h (vs. 14.00 h,

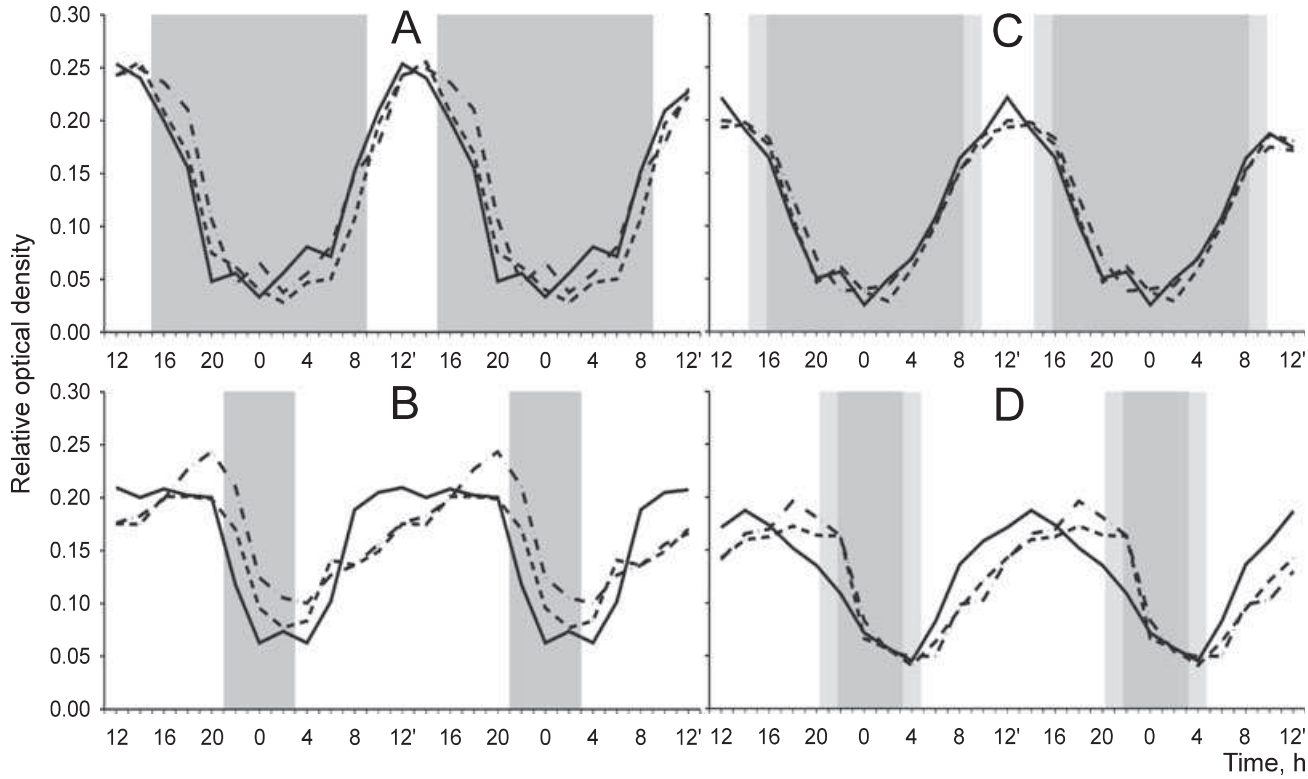

FIG. 6. Comparison of the *Per2* expression profiles in the R, M and C parts of the SCN of mice maintained under the long and short photoperiod with RA and TW LD transition. To visualize the phase relationship between the individual parts of the SCN under particular photoperiod, the data from Fig. 5 were double-plotted, and the profiles of the R (dash dotted line), M (dashed line) and C (solid line) parts were depicted in the same graph. The gray columns represent duration of the previous dark phase under the short (A, C) or long (B, D) photoperiods with RA (A, B) or TW (C, D) LD transition. For full data with means and SEM, see Fig. 5.

$P < 0.01$), whereas under TW the rise started at 12.00 h (vs. 10.00 h, $P < 0.05$) and continued until 16.00 h (vs. 14.00 h, $P < 0.01$). The cross-correlation analysis revealed a significant 2-h phase-advance in the PER2 rise in TW compared with short RA photoperiod ($R = 0.966$, $P < 0.002$). In the C-SCN (Fig. 7C), the decline in RA and TW appeared to be simultaneous, reaching its nadir level at 00.00 h (vs. 18.00 h in RA, $P < 0.05$, and 16.00 h in TW, $P < 0.05$). The rise was significant at 18.00 h (vs. 12.00 h, $P < 0.05$) in RA and at 16.00 h (vs. 10.00 h, $P < 0.05$) in TW. The cross-correlation analysis revealed a significant 2-h phase-advance in the PER2 rise in TW as compared with RA ($R = 0.925$, $P < 0.024$). Thus, under the short photoperiod the rise in PER2 levels in the M- and C-SCN parts under TW was advanced, compared with that under RA. Under the long photoperiod, PER2 levels within the R-SCN (Fig. 7D) decreased at 06.00 h (vs. 02.00 h, $P < 0.05$) under RA and at 08.00 h (vs. 22.00 h, $P < 0.05$) under TW. The levels increased significantly at 18.00 h (vs. 06.00 h, $P < 0.05$) in RA and at 22.00 h (vs. 12.00 h, $P < 0.05$) in TW. However, the cross-correlation analysis did not reveal any significant phase-shift between the RA and TW profiles. In the M-SCN (Fig. 7E), no significant difference between the profile under the long RA and that under the long TW photoperiod was revealed (Table 1) and, therefore, no *post hoc* comparisons were performed. In the C-SCN (Fig. 7F), neither the decline nor the rise in the PER2 protein under RA and TW was significant, and the cross-correlation analysis did not reveal any significant phase-shift between the RA and TW photoperiods. Therefore, under the long photoperiod, PER2 profiles in RA were in synchrony with those in TW in all SCN parts.

The two-way ANOVA revealed significant differences among PER2 profiles in the R-, M- and C-SCN (Table 1). Similar to PER1, the PER2 profiles in the R- and C-SCN differed only at a few time points, namely under the short RA photoperiod at 18.00 h ($P = 0.035$), 20.00 h ($P < 0.001$) and 00.00 h ($P = 0.038$), under the short TW photoperiod at 22.00 h ($P = 0.031$), and under the long TW photoperiod at 22.00 h ($P < 0.001$) and 00.00 h ($P = 0.020$). Under the long RA photoperiod, no difference between the R- and C-SCN was found. The M-SCN levels were significantly elevated above those in the R-SCN under the short RA photoperiod during the 12.00–04.00 h interval (with the exception of values at 14.00 and 18.00 h), under the short TW photoperiod at 12.00 h and between 16.00 and 20.00 h, under the long RA photoperiod during the 16.00–20.00 h interval, and under the long TW photoperiod between 14.00 and 00.00 h. Similarly, the M-SCN levels were significantly higher than those in the C-SCN under the short RA photoperiod between 12.00 and 02.00 h (with the exception of the value at 14.00 h), under the short TW photoperiod at 12.00 h and between 16.00 and 22.00 h, under the long RA photoperiod between 16.00 and 22.00 h, and under the long TW photoperiod between 14.00 and 02.00 h. Similar to PER1 profiles, the higher PER2 amplitude of the M-SCN rhythms reflects larger area of the M-SCN where PER2-immunopositive cells were counted as compared with the R- and C-SCN. When phases of the R- and C-SCN profiles were compared, the cross-correlation analysis revealed a 2-h phase-advance in the PER2 profile in the C-SCN, compared with that in the R-SCN under the long RA ($R = 0.857$, $P = 0.002$) and TW ($R = 0.676$, $P = 0.016$) photoperiods, but not under the short photoperiods.

In conclusion, under the short photoperiod the PER2 rise in TW was phase-advanced significantly relative to that in RA in the M- and C-SCN. Under the long photoperiod, the PER2 profile in RA was in synchrony with that in TW in all parts of the SCN. The PER2 profile

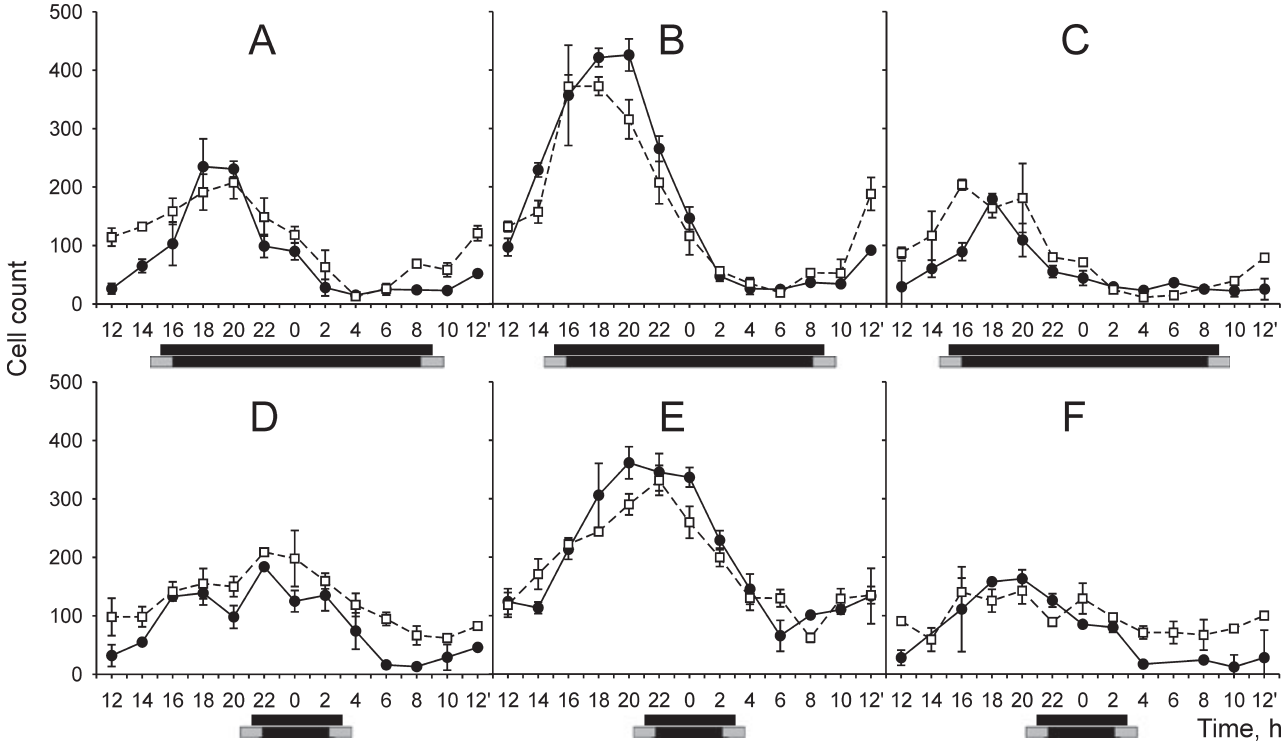

FIG. 7. Daily profiles of PER2 levels within the R (A, D), M (B, E) and C (C, F) part of the SCN of mice entrained to a short (A–C) or a long photoperiod (D–F) with RA (solid line) or TW (dashed line) LD transition. For other details, see legend to Fig. 4.

in the C-SCN was phase-advanced by 2 h relative to the profile in the R-SCN under the long RA and TW photoperiods, but not under the short RA and TW photoperiods.

Discussion

Our data demonstrate that the type of LD transition at dawn and dusk, i.e. RA or TW, affects photoperiodic modulation of the *Per1* and *Per2* expression and PER1 and PER2 protein profiles differently within separate parts of the mouse SCN.

Across the entire SCN, time of the evening decline and morning rise in *Per1* and *Per2* expression was affected by the photoperiod so that the duration of high *Per1* and *Per2* mRNA levels was shorter under the short photoperiod with only 6 h of daylight than under the long photoperiod with 18 h of daylight, whether under RA or TW conditions. This finding was in accordance with numerous previously published data (for review, see Daan *et al.*, 2001; Sumová *et al.*, 2004). When separate parts of the SCN were compared under the short and long photoperiod, the difference in duration of the interval between the rise and decline of *Per1* and *Per2* expression levels appeared to be present only in the C- and M-, but not in the R-SCN under the photoperiod with RA or TW. Thus, duration of high *Per1* and *Per2* expression was longer under the long than under the short photoperiod only in the M- and C-SCN parts, similar to previous studies when representative sections from the mid-caudal position in the rat SCN were studied (Sumová *et al.*, 2003, 2007). The PER1 protein profile in the M-SCN was also modulated by the photoperiod, similar to that seen in rats (Sumová *et al.*, 2002). Moreover, the present study in mice indicated photoperiodic modulation also of the PER2 protein profile within the M-SCN.

In addition, the data showed that phases of *Per1* and *Per2* expression profiles in the R-, M- and C-SCN were more synchronized with each other under the short than under the long photoperiods. When RA and TW LD regimes were compared, *Per1* and *Per2* profiles in the R-, M- and C-SCN were completely synchronous under the short photoperiod with TW, while in RA a 2-h delay in the *Per1* and *Per2* mRNA decline in the R-SCN, compared with other SCN parts, was detected. Under the long photoperiod, the expression profiles within the R-, M- and C-SCN parts differed significantly in RA as well as in TW. *Per1* mRNA profile in the C- and M-SCN was phase-advanced compared with that in the R-SCN both in RA and TW. Similarly, the *Per2* mRNA profile in the C-SCN was advanced to that in the R-SCN, again both in RA and TW. However, better synchronization among the individual parts in TW than in RA was indicated, similar to the situation under the short photoperiod, due namely to a lower number of time points when mRNA levels differed significantly among the individual SCN parts. At the protein level, PER1 and PER2 profiles were synchronized among the R-, M- and C-SCN under the short RA and TW photoperiods. Under the long RA and TW photoperiods, the C-SCN profiles phase-led by 2 h those in the R-SCN. Similarly to the mRNA profiles, differences between the R- and C-SCN protein profiles were more pronounced in the RA than in the TW photoperiod, due namely to higher statistical significance. The effect of the TW condition on synchrony among the individual SCN parts was thus significant under the short photoperiod and suggested under the long one.

Previous studies on the inter-phasing of the SCN cell subpopulations explored RA photoperiods only. In Siberian hamsters, exposure to a long photoperiod with 16 h of daylight induced desynchrony among *Per2*, *Rev-erbα* and *Dbp* expression rhythms the R- and those in the C-SCN, but not the *Avp* expression rhythms (Hazlerigg *et al.*, 2005; Johnston *et al.*, 2005). In Syrian hamsters, exposure to the same long photoperiod caused phase dispersion of the rhythms in c-FOS- and PER1-immunoreactivity, and the profiles in the C-SCN phase-led

those in the M- and R-SCN (Yan & Silver, 2008). In mice entrained to a long photoperiod with 16 h of daylight, not only *Per1* but also *Bmal1* expression profiles were advanced in the C-SCN, compared with the R-SCN (Naito *et al.*, 2008). In all of the above-mentioned studies, the rhythms in the C-SCN preceded those in the R-SCN under the long photoperiod. These data suggest that desynchrony and separation of phases in clock gene expression rhythms among individual parts of the SCN might account for the photoperiodic modulation of SCN function. In order to be 'active' for an extended time under the long photoperiod, the SCN successively 'switches on' its separate parts, the caudal part being first and the rostral part last. Consequently, under the very long photoperiod, the entire SCN may find itself in a daytime state for a much longer time than its individual parts.

Our findings on the impact of a long photoperiod on *Per1* and *Per2* expression profiles are supported by recent *in vitro* data on real-time expression recordings in SCN slices from mice entrained either to a long photoperiod with 18 h of daylight or to a short photoperiod with only 6 h of daylight. Robust circadian rhythms of *Per1-luc* activity were recorded in anterior and posterior SCN slices, with the exception for the anterior SCN slices from mice entrained to the long photoperiod. In these anterior slices, a bimodal pattern of *Per1-luc* activity was detected and the rhythm differed from that of the posterior part (Inagaki *et al.*, 2007). Concerning the protein data, no differences between the anterior and posterior SCN of mice entrained to a long photoperiod with 16 h of daylight were detected for PER2::luc activity *in vitro* (Mickman *et al.*, 2008), while in our *in vivo* study with 18 h of daylight, a 2-h phase-advance in the C-SCN PER2 profile was revealed compared with the R-SCN profile. For the mRNA profiles, similar to our study, higher variability in gene expression within the anterior part of the SCN under the long than under the short photoperiod was reported (Inagaki *et al.*, 2007; Mickman *et al.*, 2008). According to the current hypothesis, the photoperiod affects intercellular synchrony among individual cell oscillators in the SCN (Schaap *et al.*, 2003; Rohling *et al.*, 2006; VanderLeest *et al.*, 2007). Therefore, it seems plausible to speculate that the extremely long photoperiod with 18 h of daylight and an abrupt LD transition may cause desynchrony among individual cells in the R-SCN at dawn. Such desynchrony might be reflected by a long interval of intermediate levels of *Per1* mRNA sustaining across half of the daily expression profile (from CT0 to CT12) as observed in our study under the long RA photoperiod. Consequently, rhythms of the C-SCN might desynchronize from those of the R- and M-SCN. However, under the long TW photoperiod, the expression profiles within the R- and M-SCN were in synchrony with each other. Therefore, we can speculate that TW might attenuate the effect of a long photoperiod on synchrony among the SCN regions.

The data further demonstrate that under the short photoperiod, *Per1* and *Per2* mRNA profiles, as well as PER1 and PER2 rise, in TW were phase-advanced relative to those in RA. The *Per1* and *Per2* expression profiles in R-, M- and C-SCN were affected differently. The evening decline in *Per1* and *Per2* expression, but not the morning rise, was advanced in the R-SCN, while in the M- and C-SCN, mostly the morning rise was advanced. For the protein profiles, only the rise in PER1 and PER2 levels, but not the decline, was phase-advanced in all SCN parts, with the exception of PER2 in the R-SCN. The possibility that slight differences in the duration of the almost complete darkness between the RA and TW regimes might account for the phase differences cannot be ruled out. In our experimental arrangement, the light intensity under the TW conditions decreased gradually, and at the time of lights-off in RA there was still 1 lx in the TW photoperiod. The light intensity declined further, so that after 22 min there was 0.1 lx and after 45 min it reached 0.01 lx. Similarly, lights-on in the TW condition started from the level of 0.01 lx 45 min before the lights-on in RA, increased to 0.1 lx 22 min later and reached 1 lx at the time of the lights-on in RA. Nevertheless, the overall observed earlier phase of the profiles of *Per* gene expression and protein levels under TW than under RA short photoperiods is in agreement with previously published data on the locomotor activity rhythm in hamsters (Boulos *et al.*, 1996a, 2002; Boulos & Macchi, 2005). In these studies, timing of the locomotor activity onset and offset also occurred earlier in the short photoperiods with TW than with RA. Moreover, the presence of TW resulted in a lower variability in the locomotor activity rhythm. Based on these data, a hypothesis was formulated that LD transitions with TW might increase the strength of the LD cycle as an entraining cue.

Last, but not least, also under the long photoperiod the expression profiles of both *Per* genes were entrained with a slight difference depending on whether the LD transition was abrupt or gradual. Under the long TW photoperiod, the *Per1* and *Per2* mRNA rise was advanced, relative to that under RA in the R-SCN only, but delayed or not affected by the LD transition in other parts of the SCN. The data suggest that the extremely long 18-h photoperiod with an abrupt LD transition might cause desynchrony among cells in the R-SCN responding to dawn but not between those responding to dusk. Consequently, the significant rise in *Per1* expression in the whole population of the R-SCN cells in RA was postponed as compared with that in TW. If this were the case, TW might be more able to maintain synchrony among the SCN cells, compared with RA and, therefore, the rise in *Per1* and *Per2* expression in the population of the R-SCN cells may be achieved earlier. In contrast to the short photoperiod, no differences in PER1 and PER2 profiles between the long RA and the long TW photoperiod were detected in any part of the SCN.

Importantly, all the findings were obviously not due to a masking effect of the RA or TW transitions, because all profiles were examined after releasing mice into constant darkness. We are, however, aware of the fact that the TW simulation used did not have some aspects of the natural twilight. Although changes in spectral composition during the natural twilight periods are small (Hut *et al.*, 2000), they may play a role in circadian entrainment and photoperiodic responses. It is also important to note that the maximal light intensity of 100 lx used in this study might be three orders of magnitude lower than light intensities reached in nature. Therefore, more pronounced differences might be likely found if natural photoperiods with twilight were used. Also, while nocturnal animals living under natural conditions often only 'sample' light for a few minutes a day, spending most of the time underground (DeCoursey, 1986), our mice were maintained under LD conditions in standard cages without a den.

In conclusion, our results suggest that a TW photoperiod provides better synchrony among populations of the SCN molecular oscillators than a RA one. The effect of twilight is stronger under conditions when organisms are exposed to extremely short photoperiods, compared with long ones.

Acknowledgements

The authors gratefully acknowledge Professor Hitoshi Okamura (Kobe University School of Medicine, Japan) for Per1 and Per2 cDNA fragments used in the *in situ* hybridization, Professor Helena Illnerová for her helpful comments on the manuscript, Alena Dědičová for her help with statistical analysis, and Eva Suchanová for her excellent technical assistance. The study was supported by the 6th Framework Project EUCLOCK 018741, grant 309080503, and by Research Projects AV0Z 50110509 and LC554.

Abbreviations

C-SCN, caudal part of the suprachiasmatic nucleus; LD, light–dark regimen; LD18 : 6, light–dark regimen with 18 h of light and 6 h of darkness; LD6 : 18, light–dark regimen with 6 h of light and 18 h of darkness; M-SCN, middle part of the suprachiasmatic nucleus; OD, optical density; PBS, phosphate-buffered saline; RA, rectangular light-to-dark transition; R-SCN, rostral part of the suprachiasmatic nucleus; SCN, suprachiasmatic nuclei of the hypothalamus; TW, twilight light-to-dark transition.

References

Boulos, Z. & Macchi, M.M. (2005) Season- and latitude-dependent effects of simulated twilights on circadian entrainment. *J. Biol. Rhythms*, **20**, 132–144.

Boulos, Z., Macchi, M., Houpt, T.A. & Terman, M. (1996a) Photic entrainment in hamsters: effects of simulated twilights and nest box availability. *J. Biol. Rhythms*, **11**, 216–233.

Boulos, Z., Macchi, M. & Terman, M. (1996b) Twilight transitions promote circadian entrainment to lengthening light–dark cycles. *Am. J. Physiol. Regul. Integr. Comp. Physiol.*, **271**, R813–R818.

Boulos, Z., Macchi, M.M. & Terman, M. (2002) Twilights widen the range of photic entrainment in hamsters. *J. Biol. Rhythms*, **17**, 353–363.

Daan, S. & Aschoff, J. (1975) Circadian rhythms of locomotor activity in captive birds and mammals: their variations with season and latitude. *Oecologia*, **18**, 269–316.

Daan, S., Albrecht, U., van der Horst, G.T., Illnerova, H., Roenneberg, T., Wehr, T.A. & Schwartz, W.J. (2001) Assembling a clock for all seasons: are there M and E oscillators in the genes? *J. Biol. Rhythms*, **16**, 105–116.

DeCoursey, P.J. (1986) Light-sampling behavior in photoentrainment of a rodent circadian rhythm. *J. Comp. Physiol. [A]*, **159**, 161–169.

Elliott, J.A. & Tamarkin, L. (1994) Complex circadian regulation of pineal melatonin and wheel-running in Syrian hamsters. *J. Comp. Physiol. [A]*, **174**, 469–484.

Hastings, M.H. (2001) Modeling the Molecular Calendar. *J. Biol. Rhythms*, **16**, 117–123.

Hastings, M.H., Field, M.D., Maywood, E.S., Weaver, D.R. & Reppert, S.M. (1999) Differential regulation of mPER1 and mTIM proteins in the mouse suprachiasmatic nuclei: new insights into a core clock mechanism. *J. Neurosci.*, **19**, RC11.

Hazlerigg, D.G., Ebling, F.J. & Johnston, J.D. (2005) Photoperiod differentially regulates gene expression rhythms in the rostral and caudal SCN. *Curr. Biol.*, **15**, R449–R450.

Hut, R.A., Scheper, A. & Daan, S. (2000) Can the circadian system of a diurnal and a nocturnal rodent entrain to ultraviolet light? *J. Comp. Physiol. [A]*, **186**, 707–715.

Illnerová, H. (1988) Entrainment of mammalian circadian rhythms in melatonin production by light. *Pineal Res. Rev.*, **6**, 173–217.

Illnerová, H. & Vaněček, J. (1980) Pineal rhythm in N-acetyltransferase activity in rats under different artificial photoperiods and in natural daylight in the course of a year. *Neuroendocrinology*, **31**, 321–326.

Inagaki, N., Honma, S., Ono, D., Tanahashi, Y. & Honma, K. (2007) Separate oscillating cell groups in mouse suprachiasmatic nucleus couple photoperiodically to the onset and end of daily activity. *Proc. Natl. Acad. Sci. USA*, **104**, 7664–7669.

Johnston, J.D., Ebling, F.J. & Hazlerigg, D.G. (2005) Photoperiod regulates multiple gene expression in the suprachiasmatic nuclei and pars tuberalis of the Siberian hamster (Phodopus sungorus). *Eur. J. Neurosci.*, **21**, 2967–2974.

Klein, D.C. & Moore, R.Y. (1979) Pineal N-acetyltransferase and hydroxyindole-O-methyltransferase: control by the retinohypothalamic tract and the suprachiasmatic nucleus. *Brain Res.*, **174**, 245–262.

Kováčiková, Z., Sládek, M., Bendová, Z., Illnerová, H. & Sumová, A. (2006) Expression of clock and clock-driven genes in the rat suprachiasmatic nucleus during late fetal and early postnatal development. *J. Biol. Rhythms*, **21**, 140–148.

LeSauter, J., Lehman, M.N. & Silver, R. (1996) Restoration of circadian rhythmicity by transplants of the SCN ''micropunches''. *J. Biol. Rhythms*, **11**, 163–171.

McFarland, W.N. & Munz, F.W. (1975) Part II: The photic environment of clear tropical seas during the day. *Vision Res.*, **15**, 1063–1070.

Meijer, J.H., Groos, G.A. & Rusak, B. (1986) Luminance coding in a circadian pacemaker: the suprachiasmatic nucleus of the rat and the hamster. *Brain Res.*, **382**, 109–118.

Mickman, C.T., Stubblefield, J., Harrington, M. & Nelson, D.E. (2008) Photoperiod alters the phase difference between activity onset in vivo and mPer2:luc peak in vitro. *Am. J. Physiol. Regul. Integr. Comp. Physiol.*, **295**, R1688–R1694.

Naito, E., Watanabe, T., Tei, H., Yoshimura, T. & Ebihara, S. (2008) Reorganization of the suprachiasmatic nucleus coding for day length. *J. Biol. Rhythms*, **23**, 140–149.

Pittendrigh, C.L. (1981) Circadian systems: entrainment. In Aschoff, J. (ed), *Biological Rhythms. Handbook of Behavioral Neurology.* Plenum, New York, pp. 95–124.

Rohling, J., Wolters, L. & Meijer, J.H. (2006) Simulation of day-length encoding in the SCN: from single-cell to tissue-level organization. *J. Biol. Rhythms*, **21**, 301–313.

Schaap, J., Albus, H., VanderLeest, H.T., Eilers, P.H., Detari, L. & Meijer, J.H. (2003) Heterogeneity of rhythmic suprachiasmatic nucleus neurons: implications for circadian waveform and photoperiodic encoding. *Proc. Natl. Acad. Sci. USA*, **100**, 15994–15999.

Shearman, L.P., Sriram, S., Weaver, D.R., Maywood, E.S., Chaves, I., Zheng, B., Kume, K., Lee, C.C., van der Horst, G.T., Hastings, M.H. & Reppert, S.M. (2000) Interacting molecular loops in the mammalian circadian clock. *Science*, **288**, 1013–1019.

Sládek, M., Sumová, A., Kováčiková, Z., Bendová, Z., Laurinová, K. & Illnerová, H. (2004) Insight into molecular core clock mechanism of embryonic and early postnatal rat suprachiasmatic nucleus. *Proc. Natl. Acad. Sci. USA*, **101**, 6231–6236.

Spoelstra, K. & Daan, S. (2008) Effects of constant light on circadian rhythmicity in mice lacking functional cry genes: dissimilar from per mutants. *J. Comp. Physiol. [A] Neuroethol. Sens. Neural. Behav. Physiol.*, **194**, 235–242.

Steinlechner, S., Jacobmeier, B., Scherbarth, F., Dernbach, H., Kruse, F. & Albrecht, U. (2002) Robust circadian rhythmicity of Per1 and Per2 mutant mice in constant light, and dynamics of Per1 and Per2 gene expression under long and short photoperiods. *J. Biol. Rhythms*, **17**, 202–209.

Sumová, A., Trávníčková, Z., Peters, R., Schwartz, W.J. & Illnerová, H. (1995) The rat suprachiasmatic nucleus is a clock for all seasons. *Proc. Natl. Acad. Sci. USA*, **92**, 7754–7758.

Sumová, A., Sládek, M., Jáč, M. & Illnerová, H. (2002) The circadian rhythm of Per1 gene product in the rat suprachiasmatic nucleus and its modulation by seasonal changes in daylength. *Brain Res.*, **947**, 260–270.

Sumová, A., Jáč, M., Sládek, M., Šauman, I. & Illnerová, H. (2003) Clock gene daily profiles and their phase relationship in the rat suprachiasmatic nucleus are affected by photoperiod. *J. Biol. Rhythms*, **18**, 134–144.

Sumová, A., Bendová, Z., Sládek, M., Kováčiková, Z. & Illnerová, H. (2004) Seasonal molecular timekeeping within the rat circadian clock. *Physiol. Res.*, **53**(Suppl 1), S167–S176.

Sumová, A., Kováčiková, Z. & Illnerová, H. (2007) Dynamics of the adjustment of clock gene expression in the rat suprachiasmatic nucleus to an asymmetrical change from a long to a short photoperiod. *J. Biol. Rhythms*, **22**, 259–267.

Sun, Z.S., Albrecht, U., Zhuchenko, O., Bailey, J., Eichele, G. & Lee, C.C. (1997) RIGUI, a putative mammalian ortholog of the Drosophila period gene. *Cell*, **90**, 1003–1011.

Takahashi, J.S., Hong, H.K., Ko, C.H. & McDearmon, E.L. (2008) The genetics of mammalian circadian order and disorder: implications for physiology and disease. *Nat. Rev. Genet.*, **9**, 764–775.

Usui, S. (2000) Gradual changes in environmental light intensity and entrainment of circadian rhythms. *Brain Dev.*, **22**(Suppl 1), S61–S64.

VanderLeest, H.T., Houben, T., Michel, S., Deboer, T., Albus, H., Vansteensel, M.J., Block, G.D. & Meijer, J.H. (2007) Seasonal encoding by the circadian pacemaker of the SCN. *Curr. Biol.*, **17**, 468–473.

Yan, L. & Silver, R. (2008) Day-length encoding through tonic photic effects in the retinorecipient SCN region. *Eur. J. Neurosci.*, **28**, 2108–2115.

Am J Physiol Regul Integr Comp Physiol 298: R959–R971, 2010.
First published January 13, 2010; doi:10.1152/ajpregu.00561.2009.

Different mechanisms of adjustment to a change of the photoperiod in the suprachiasmatic and liver circadian clocks

Serhiy Sosniyenko,* Daniela Parkanová,* Helena Illnerová, Martin Sládek, and Alena Sumová
Institute of Physiology, Academy of Sciences of the Czech Republic, Prague, Czech Republic

Submitted 2 September 2009; accepted in final form 11 January 2010

Sosniyenko S, Parkanová D, Illnerová H, Sládek M, Sumová A. Different mechanisms of adjustment to a change of the photoperiod in the suprachiasmatic and liver circadian clocks. *Am J Physiol Regul Integr Comp Physiol* 298: R959–R971, 2010. First published January 13, 2010; doi:10.1152/ajpregu.00561.2009.—Changes in photoperiod modulate the circadian system, affecting the function of the central clock located in the suprachiasmatic nucleus (SCN) of the hypothalamus. The aim of the present study was to elucidate the dynamics of adjustment to a change of a long photoperiod with 18 h of light to a short photoperiod with 6 h of light of clock gene expression rhythms in the mouse SCN and in the peripheral clock in the liver, as well as of the locomotor activity rhythm. Three, five, and thirteen days after the photoperiod change, daily profiles of *Per1*, *Per2*, and *Rev-erbα* expression in the rostral, middle, and caudal parts of the SCN and of *Per2* and *Rev-erbα* in the liver were determined by in situ hybridization and real-time RT-PCR, respectively. The clock gene expression rhythms in the different SCN regions, desynchronized under the long photoperiod, attained synchrony gradually following the transition from long to short days, mostly via advancing the expression decline. The photoperiodic modulation of the SCN was due not only to the degree of synchrony among the SCN regions but also to different waveforms of the rhythms in the individual SCN parts. The locomotor activity rhythm adjusted gradually to short days by advancing the activity onset, and the liver rhythms adjusted by advancing the *Rev-erbα* expression rise and *Per2* decline. These data indicate different mechanisms of adjustment to a change of the photoperiod in the central SCN clock and the peripheral liver clock.

circadian clock; suprachiasmatic nucleus; liver; clock gene; photoperiodic entrainment

ORGANISMS LIVING IN TEMPERATE zones are exposed to seasonal changes in the day length, i.e., photoperiod. The mammalian circadian clock, located in the suprachiasmatic nucleus (SCN) of the hypothalamus (23), is affected by the photoperiod (50) and, therefore, overt rhythms driven by the clock, namely the rhythm in pineal melatonin production (16, 36) and the locomotor activity rhythm (5), are modulated by the photoperiod as well. The melatonin signal is short during a long summer photoperiod, whereas it is long during a short winter photoperiod (8, 13, 16). When animals are transferred from a long to a short photoperiod, the duration of elevated activity of arylalkylamine N-acetyltransferase (AA-NAT), the key enzyme in melatonin production, as well as that of high melatonin levels, gradually extend (11, 14, 15). The dynamics of the extension seems to be species dependent. In rats, it is completed within 2 wk (14), whereas in Djungarian hamsters, it is completed only after more than 6 wk (15). In most strains of laboratory mice, melatonin is not produced in the pineal gland, and therefore, the melatonin rhythm cannot be used as a measure of photoperiodic entrainment (9). However, locomotor activity in mice is modulated by the photoperiod, being longer under short than under long photoperiods (17).

The SCN rhythmicity is due to the SCN molecular clockwork (for reviews, see Refs. 7, 22, 34, 52). Mammalian clock genes are mostly expressed in a rhythmic way; the expression of *Bmal1* is anti-phase to that of the *Per, Cry,* and *Rev-erbα* genes. The clock genes and their protein products are involved in the core clockwork by forming negative and positive transcriptional-translational feedback loops: the clock proteins CLOCK and BMAL1 form heterodimers and drive the expression of the other genes, namely *Per1*, *Per2*, *Cry*, *Rev-erbα,* and *Rora*. PER and CRY proteins form complexes and interact with CLOCK:BMAL1 to inhibit their own expression. REV-ERBα represses transcription of *Bmal1*, and RORA, which competes with REV-ERBα, activates it. The important fine-tuning of the speed of the clock is achieved by regulating stability and/or subcellular localization of the clock proteins.

The daily profiles of clock gene mRNA and protein levels in the entire population of the SCN cells are affected by the photoperiod. In rodents, intervals of elevated *Per1* and *Per2* expression in the SCN are longer and that of *Bmal1* expression shorter under a long than under a short photoperiod (10, 27, 28, 32, 44, 46, 48). When rats are transferred from a long to a short photoperiod by an asymmetrical prolongation of the dark period into the morning hours, adjustment of the *Per1* and *Bmal1* mRNA rhythm to short days may not be accomplished within 13 days (47).

The SCN can be subdivided into two subdivisions that are morphologically and functionally distinct, i.e., into a ventrolateral part, called the core, and a dorsomedial part, called the shell (30). Cells of the core receive direct photic signals from the retina and respond by resetting the phase of the SCN rhythmicity. Cells of the shell exhibit spontaneous rhythmicity, and their resetting requires communication with the light-sensitive cells of the core SCN. Both SCN subdivisions are modulated by the photoperiod. In the rat, the endogenous interval of the ventrolateral SCN photosensitivity is ~5 to 6 h longer under a short photoperiod than under a long photoperiod (50). Following a symmetrical shortening of a long photoperiod, this interval gradually extends, and the adjustment to the change is complete within ~2 wk, similar to the AA-NAT rhythm (51). Rhythms typical of the dorsomedial SCN, such as that of endogenous expression of *c-fos* and arginine vasopressin genes, exhibit longer intervals of high expression on long days than on short days (18, 19, 49). Following a symmetrical shortening of the photoperiod, they adjust only gradually to the change (49). Recently, accumulated data suggest a functional divergence among subpopulations of SCN cells, not only along the ventro-dorsal but also along the rostro-caudal axis of the

Serhiy Sosniyenko and Daniela Parkanová contributed equally to this study.

Address for reprint requests and other correspondence: A. Sumová, Institute of Physiology, Academy of Sciences of the Czech Republic, Videnska 1083, 14220 Prague 4, Czech Republic (e-mail: sumova@biomed.cas.cz).

SCN. Rhythms in the rostral (R-), middle (M-), and caudal (C-) SCN regions differ in their phase, depending on the photoperiod. In the hamster, the maximal expression of *Per2* occurs synchronously in the R-SCN and C-SCN under a short photoperiod, but under a long photoperiod, the peak of expression in the C-SCN precedes that in the R-SCN (12, 20). Similarly in mice, *Per1* and *Per2* expression profiles in the R-SCN and C-SCN are synchronized under a short photoperiod but under a long photoperiod, the profiles in the C-SCN precede those in the R-SCN (17, 43). To date, no data on dynamics of synchronization among the individual SCN subpopulations after a change of the photoperiod have been reported.

Apart from the central pacemaker within the SCN, the circadian system consists of numerous peripheral clocks (2). The central clock is the only one that is entrained directly by photic cues via its connection with the retina. The peripheral clocks are entrained to the external world mostly via yet not fully identified neuronal and humoral SCN output pathways (21). So far, the effect of the photoperiod on peripheral clocks has been studied only marginally. In Syrian hamsters, a photoperiod-sensitive species, daily expression profiles of the clock gene *Per1* and the clock-controlled gene *Dbp* in the lung and heart (4), as well as clock genes in the liver (26), were modulated by the photoperiod. The *Per2* expression profile in the ovine liver is also affected by the photoperiod (1). In rats, the daily profiles in levels of the clock proteins PER1 and PER2 within the liver, lung, and heart under the long photoperiod differed from those under the short photoperiod (3). Although it seems that information on the external photoperiod may be processed by peripheral clocks, it is not known when and how these clocks adjust to a change in the photoperiod.

The aim of the present study was to test the hypothesis that the mechanism of adjustment to the change of the photoperiod in the central clock differs from that in the peripheral clock. Therefore, the dynamics of changes in the rhythms of clock gene expression in different regions of the mouse SCN and liver during the transition from a long to a short photoperiod were studied. Mice maintained under a regime with 18 h of light and 6 h of darkness (LD18:6) were transferred to a regime with 6 h of light and 18 h of darkness (LD6:18). Three, five, and thirteen days after the change from the long to the short photoperiod, expression profiles of the clock genes *Per1*, *Per2,* and *Rev-erbα* in the R-SCN, M-SCN, and C-SCN and of *Per2* and *Rev-erbα* in the liver were examined. Simultaneously, the locomotor activity of the mice was monitored before the transfer and up to the 11th day after the transfer. This approach allowed comparison between the dynamics of adjustment of the central and peripheral clocks and changes of the behavioral activity rhythm during the transition from a long to a short photoperiod.

MATERIALS AND METHODS

Animals

Two-month-old adult male C57BL6/J mice (Velaz s.r.o., Prague, Czech Republic) were housed at a temperature of 23 ± 2°C with free access to food and water. For 4 wk prior to the experiments, the animals were maintained under a long, LD18:6, photoperiod with lights on from 0300 to 2100. Thereafter, the long photoperiod was changed to a short, LD6:18, via a symmetrical shortening of the light interval by advancing the lights off from 2100 to 1500 and delaying the lights on from 0300 to 0900. Consequently, the lights were on from 0900 to 1500. Light was provided by overhead 40-W fluorescent tubes, and illumination during the light phase was between 50 and 200 lux, depending on cage position in the animal room. During the dark period, there was complete darkness. Five experimental groups were tested. *Group 1* were animals entrained to the long photoperiod for 4 wk and then sampled on the day before the change to the short photoperiod, *Group 2* animals were sampled on the third day after the change from the long to the short photoperiod. *Group 3* animals were sampled on the 5th day after the change from the long to the short photoperiod. *Group 4* animals were sampled 13 days after the change from the long to the short photoperiod, and *Group 5* animals were sampled 4 wk after the change from the long to the short photoperiod [data on the SCN *Per1* and *Per2* expression profiles in mice from *group 1* and *group 5* have been published elsewhere (43)]. On each sampling day, the animals were released into constant darkness at the time when the morning lights were switched on and killed rapidly by cervical dislocation under dim red light every 2 h throughout the whole circadian cycle.

The experiments were conducted under license no. A5228–01 with the U.S. National Institutes of Health and in accordance with Animal Protection Law of the Czech Republic (license no. 36215/2008–10001).

Locomotor Activity Monitoring

Throughout monitoring, the mice were maintained individually in cages equipped with infrared movement detectors attached above the center of the cage top, enabling detection of the locomotor activity throughout the entire cage. A circadian activity monitoring system (Dr. H. M. Cooper, Institut National de la Santé et de la Recherche Médicale, Lyon, France) was used to measure activity every minute, and the resulting data were analyzed using Actiview Biological Rhythms Analysis software (Mini Mitter, Bend, OR, USA). Double-plotted actograms were generated for visualization of the data. The activity onset and offset were determined by two independent observers by fitting lines connecting at least five successive activity onsets or offsets by eye before and after the shift in the light-dark cycle.

Tissue Sampling

For determination of *Per1, Per2,* and *Rev-erbα* mRNA in the SCN, brains were removed, frozen immediately on dry ice, and stored at −80°C. Each brain was sectioned into five series of coronal 12-μm-thick slices in an alternating order throughout the whole rostro-caudal extent of the SCN and processed for in situ hybridization. For each time point, four mice were killed; occasionally, one sample was lost.

For determination of *Per2* and *Rev-erbα* mRNA levels in the liver, dissected samples of the tissue were immersed immediately into an RNAlater stabilization reagent (Qiagen, Valencia, CA). Samples in RNAlater were stored at 4°C for no longer than 1 wk prior to isolation of total RNA and subsequent real-time RT-PCR.

In Situ Hybridization

The cDNA fragments of rat *rPer1* (980 bp; corresponds to nucleotides 581–1561 of the sequence in GenBank with accession no. AB002108), rat *rPer2* (1,512 bp; corresponds to nucleotides 369–1881 of the sequence in GenBank with accession no. NM031678) and *Rev-erbα* (1,109 bp; corresponds to nucleotides 558–1666 of the sequence in GenBank with accession no. BC062047) were used as templates for in vitro transcription of complementary RNA probes. The r*Per1* and r*Per2* fragment-containing vectors were generously donated by Professor H. Okamura (Kobe University School of Medicine, Kobe, Japan); the *Rev-erbα* was cloned in our laboratory (M. Sladek) using RT-PCR from rat liver RNA into pGEM-T vector (Promega, Madison, WI). The probes were labeled using α[^{35}S]thio-UTP (MP Biomedicals, Irvine, CA), and the in situ hybridization was performed as

described previously (25, 37, 42). Briefly, sections were hybridized for 20 h at 60°C (*Per1*, *Rev-erbα*) or 61°C (*Per2*). Following a posthybridization wash, the sections were dehydrated in ethanol and dried. Finally, the slides were exposed to BioMax MR film (Kodak, Rochester, NY) for 10 days and developed using ADEFOMIX-S developer and ADEFOFIX fixer (Adefo-Chemie, Dietzenbach, Germany) with an Optimax film processor (Protec, Oberstenfeld, Germany). As a control, in situ hybridization was performed in parallel with sense probes on sections containing the SCN. The daily profiles of the mRNA levels under the long and short photoperiods, as well as three, five and thirteen days after the change from the long to the short photoperiod were determined using the same labeled probe and processed simultaneously under identical conditions.

Autoradiographs of sections were analyzed using an image analysis system (Image Pro, Olympus, New Hyde Park, NY) to detect the relative optical density (OD) of the specific hybridization signal. For each animal, the mRNA was quantified bilaterally, at a representative R-SCN, M-SCN, and C-SCN section that contained the strongest hybridization signal. Each measurement was corrected for nonspecific background by subtracting OD values from the neighboring area in the hypothalamus that was devoid of the specific signal. The background signal of the area, serving as an internal standard, was consistently low and did not exhibit marked changes with the time of day. Specific signal was not found in any case in which the sense probe was used. Finally, to check the presence of the R-SCN, M-SCN, and C-SCN in each section, the slides were counterstained with cresyl violet. The OD for each animal was calculated as the mean of the values for the left and right SCN.

RNA Isolation

Total RNA was isolated from the liver tissue using the RNeasy Mini kit (Qiagen), according to the manufacturer's instructions. RNA concentrations were determined by spectrophotometry at 260 nm, and RNA quality was assessed by electrophoresis on a 1.5% agarose gel. Moreover, the integrity of randomly selected samples of total RNA was tested using an Agilent 2100 Bioanalyzer (Agilent Technologies, Santa Clara, CA).

Real-Time RT-PCR

The RT-PCR method used to detect the clock gene mRNA, as well as sequences of primers for *Rev-erbα, Per2,* and *β2-microglobulin* has been described previously (40). Briefly, 1 μg of total RNA was reverse transcribed using an Improm II RT kit (Promega) with random hexamer primers. Diluted cDNA was then amplified on a LightCycler (Roche, Basel, Switzerland) using the QuantiTect SYBR Green PCR kit (Qiagen) and corresponding primers. Relative quantification was achieved using a standard curve and subsequently normalizing the clock gene expression to *β2-microglobulin*. The housekeeping gene *β2-microglobulin* has been used for normalization previously (40, 41). Its expression was stable throughout the day and did not vary markedly between the analyzed tissues. The data were expressed as means ± SE. as percent of maximal value for each expression profile.

Statistical Analysis

One-way ANOVA was used to analyze differences in the duration of the locomotor activity and in the times of activity onset and offset during adjustment to the change in the photoperiod.

Gene expression profiles in the R-SCN, M-SCN, and C-SCN and in the liver were analyzed using a two-way ANOVA to analyze the effect of the time of day and the effect of the number of days following the change in photoperiod. To compare the dynamics of adjustment of the decrease and increase in expression of the genes in the SCN separately, the profiles were analyzed for two intervals: for *Per1,* from 1200 to 2200 and from 2400 to 1200′; for *Per2,* from 1200 to 2400 and from 0200 to 1200′; and for *Rev-erbα,* from 0800 to 2000 and from 2000 to 0600. Post hoc analysis assessed subsequent pairwise comparisons using the Student-Newman-Keuls multiple-range test, with $P < 0.05$ required for significance.

A two-way ANOVA was also used to assess differences among the expression profiles within the R-SCN, M-SCN, and C-SCN during adjustment to the change in the photoperiod (i.e., the effect of the time of day and the effect of the SCN regions were tested for each of the photoperiodic conditions).

For further analysis of the circadian rhythm characteristics, the expression profiles of *Per1, Per2,* and *Rev-erbα* in the R-SCN and C-SCN were fitted with single cosine curves, defined by the equation $Y = \text{mesor} + \{\text{amplitude} \cdot \cos[2 \cdot \pi \cdot (\text{X-acrophase})/\text{wavelength}]\}$ with a constant wavelength of 24 h. The least-squares regression method implemented with Prism 5 software (GraphPad, La Jolla, CA) was applied. Amplitude, acrophase, and coefficient of determination R^2 (i.e., goodness of fit) were calculated. The analysis allowed visualizing and modeling the dynamic expression of the clock genes in R-SCN and C-SCN during the changing photoperiodic conditions.

RESULTS

Adjustment of the Locomotor Activity Rhythms

Locomotor activity was monitored in 12 mice entrained to the long photoperiod, i.e., before the change in the photoperiod, and up to 11 days after the change in the photoperiod (see MATERIALS AND METHODS for details). A representative double-plotted actogram is shown in Fig. 1*A*. On the 13th day after the change, the mice released into darkness were sampled throughout the 24-h period for determination of gene expression (for data, see *Adjustment of Clock Gene Expression in the Liver*).

For each animal, the activity onset and offset, as well as the duration of activity, were calculated, and the data are summarized in Fig. 1*B*. A one-way ANOVA revealed significant differences between individual stages during the adjustment to the short photoperiod in the activity duration ($F_4 = 96.664$, $P < 0.001$), the activity onset ($F_4 = 52.730$, $P < 0.001$), and the activity offset ($F_4 = 11.300$, $P < 0.05$). Adjustment to the change from the long to the short photoperiod occurred gradually as the interval of activity duration increased significantly 3 days after the change when compared with that under the long photoperiod ($P < 0.001$), 5 days after the change when compared with that after 3 days ($P < 0.001$), and 11 days after the change when compared with that after 5 days ($P < 0.01$). The activity duration was not yet fully adjusted to short days, even on the 11th day after the change, as it was still significantly shorter than that under the short photoperiod ($P < 0.001$). The gradual increase in the activity duration was accomplished mostly by advancing the activity onset, which occurred significantly earlier on the 3rd, 5th, and 11th day ($P < 0.001$) when compared with the previous stage. On the 11th day, activity onset was fully adjusted to the change in the photoperiod, as it did not differ from that under the short photoperiod, i.e., it occurred at about the time of lights off. The activity offset did not change significantly during adjustment, only on *day 11* after the change, it advanced significantly compared with both the previous and subsequent stages ($P < 0.05$ and 0.01, respectively).

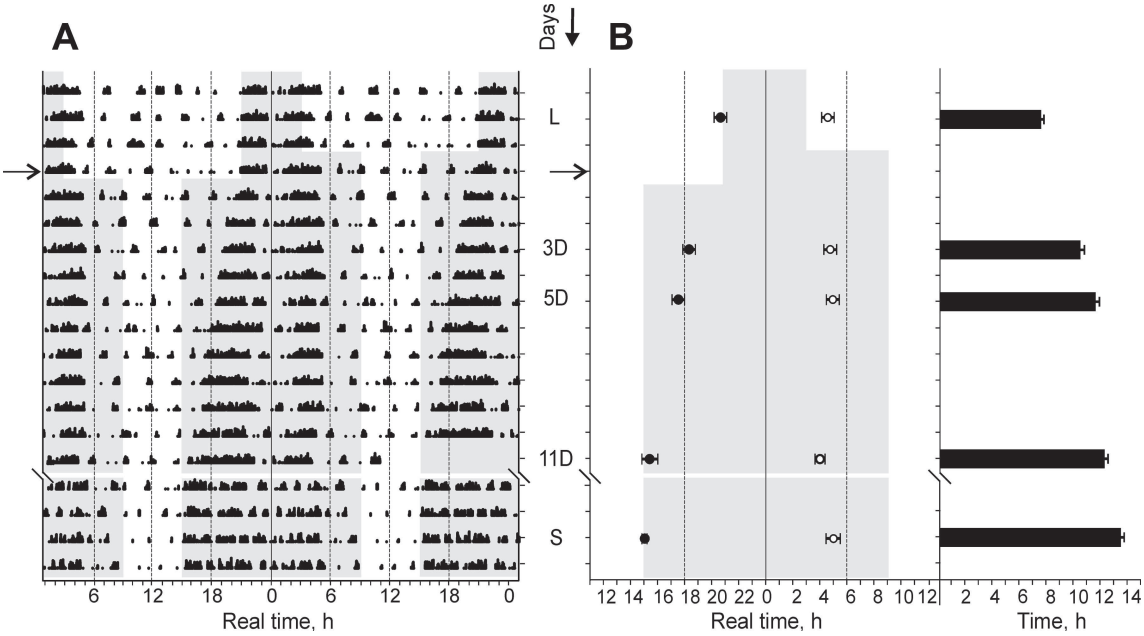

Fig. 1. *A*: representative double-plotted actogram of locomotor activity of a mouse subjected to the experimental procedure described in MATERIALS AND METHODS section. The shaded area marks the time when the mouse was maintained in darkness. The arrow (*A* and *B*) marks the day of transition from the long [18:6-h light-dark (LD18:6)] to the short [6:18-h light-dark (LD6:18)] photoperiod. *B, left*: activity onset (●) and offset (○) under the long photoperiod (L), three (3D), five (5D), and eleven (11D) days after the change to the short photoperiod and under the short photoperiod (S). *B, right*: duration of the locomotor activity (black columns) expressed in hours as detected on L, 3D, 5D, 11D, and S. The shaded area marks the time when the mice were maintained in darkness.

Adjustment of Clock Gene Expression Rhythms in the R-SCN, M-SCN, and C-SCN

Per1 mRNA profiles. Results demonstrated significant differences in the timings of the rise and decline of the *Per1* expression between LD18:6 (Fig. 2*A*), at 3 (Fig. 2*B*), 5 (Fig. 2*C*) and 13 (Fig. 2*D*) days after the transition from LD18:6 to LD6:18, and after 4 wk under the LD6:18 (Fig. 2*E*) in all SCN regions: For R-SCN, rise $F_4 = 17.07$ ($P < 0.001$) and decline $F_4 = 52.01$ ($P < 0.001$). For M-SCN, rise $F_4 = 19.20$ ($P < 0.001$) and decline $F_4 = 7.33$ ($P < 0.001$). For C-SCN, rise $F_4 = 20.20$ ($P < 0.001$) and decline $F_4 = 17.11$ ($P < 0.001$). The data from post hoc analyses are summarized in Table 1.

The rise in *Per1* expression in individual SCN regions adjusted to the change from the long to the short photoperiod in different ways. In the R-SCN, the *Per1* mRNA rise phase advanced by 10 h in total, and the advance was accomplished by a 6-h advance within the first 3 days and a 4-h advance between the 5th and 13th days following the transition to the short photoperiod. There was no overall shift in the *Per1* mRNA rise in the M-SCN during the adjustment to the short photoperiod; however, the rise first slightly delayed by 2 h within the first 3 days and then advanced to the previous phase between the 5th and 13th day after the change. The C-SCN rise adjusted to the short photoperiod by a 2-h overall delay accomplished by a 4-h phase delay within the first 3 days after the change followed by a 2-h advance between the 3rd and 5th day. Under the short photoperiod, the rise occurred at about the same time as on the 5th day after the change. Altogether, the phase of the *Per1* mRNA rise after the transition from LD18:6 to LD6:18 phase-advanced in the R-SCN, slightly phase-delayed in the C-SCN and did not change in the M-SCN.

The decline of the *Per1* mRNA adjusted to the photoperiod change in a relatively consistent manner in all SCN regions. In the R-SCN, the decline advanced by 6 h overall, first by 2 h within the 3 days after the change, by 2 h between the 3rd and 5th day and by another 2 h between the 5th and 13th day; on the 13th day, the decline occurred at the same time as under the short photoperiod. In the M-SCN, the decline advanced by 4 h overall, and the advance was accomplished gradually by a 2-h shift within the first 3 days and again between the 3rd and 5th day after the photoperiod change. On the 5th day, the decline was already entrained to the short photoperiod. In the C-SCN, the *Per1* mRNA decline adjusted to the change in the photoperiod by a 4-h advance within the first three days; thereafter, the phase of the decline did not change further. Hence, the *Per1* mRNA decline adjusted to the photoperiod change by phase-advancing in all SCN regions. Comparing the dynamics of the change in the *Per1* mRNA profile among the SCN regions, the C-SCN adjusted the first, followed by the M-SCN and the R-SCN adjusted as the last one.

As a consequence of the nonparallel adjustment of the rise and decline of the *Per1* expression in the individual SCN regions, the R-SCN and C-SCN attained synchrony among each other gradually over the course of the 13 days after the change from the long to the short photoperiod (Fig. 2). Thirteen days after the change, the timings of the rise and decline of the *Per1* expression in the R-SCN and C-SCN was the same (Table 1). Moreover, the cosinor fitted lines on the 13th day appeared to be in the same phase as under the short photoperiod (Fig. 5*D*). Therefore, synchrony of the *Per1* expression profiles between the R-SCN and C-SCN was attained on the 13th day after the change from the long to the short photoperiod.

Per2 mRNA profiles. Statistical analyses revealed significant differences in the timings of the rise and decline of the *Per2* expression between LD18:6 (Fig. 3*A*), at 3 (Fig. 3*B*), 5 (Fig. 3*C*), and 13 (Fig. 3*D*) days after the change from LD18:6 to

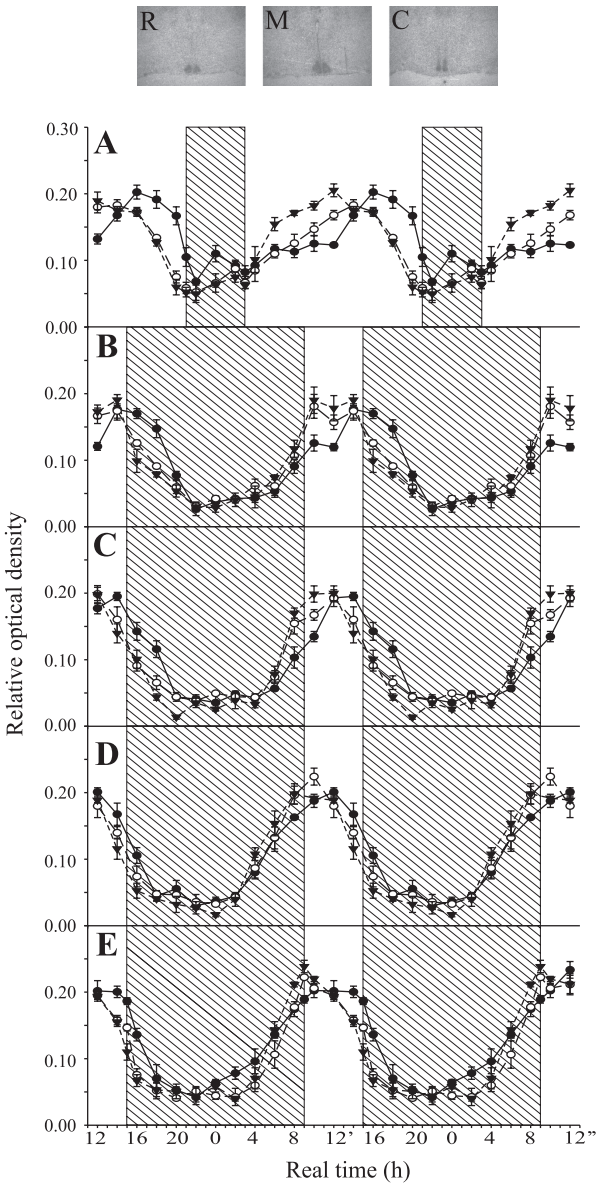

Fig. 2. *Top*: representative autoradiographs of the rostral (R), middle (M), and caudal (C) SCN sections examined by in situ hybridization for *Per1* expression. *Bottom*: daily profiles of *Per1* expression in the rostral (●), middle (○), and caudal (▼) SCN under the long photoperiod (*A*), 3 days (*B*), 5 days (*C*), and 13 days (*D*) after the change from the long to the short photoperiod, and under the short photoperiod (*E*). For better clarity of the phasing between the rostral, middle, and caudal SCN, the profiles were double-plotted (the second cycle was formed by repeating the data starting from 1400). The hatched areas depict intervals of darkness. A two-way ANOVA revealed that under the long photoperiod, the *Per1* expression profiles in the C-SCN and R-SCN differed at 1200, 1800, 2000, 0000, 0600, 0800, 1000, and 1200′ ($P < 0.01$). Three days after the photoperiod change, the mRNA levels between the R-SCN and C-SCN differed at 1200 ($P < 0.01$), 1600, 1800, 1000, and 1200′ ($P < 0.001$) and 5 days after the change, they differed at 1400 ($P < 0.001$), 1600 ($P < 0.01$), 1800, 0800, and 1000 ($P < 0.001$). Thirteen days after the change, the mRNA levels between the R-SCN and C-SCN differed only at two time points (at 1400 and 1600, $P < 0.01$), similar to under the short photoperiod.

LD6:18, and at 4 wk under LD6:18 (Fig. 3*E*) in all SCN parts. For R-SCN, rise $F_4 = 11.00$ ($P < 0.001$) and decline: $F_4 = 21.42$ ($P < 0.001$). For M-SCN, rise $F_4 = 6.48$ ($P < 0.001$) and decline $F_4 = 14.50$ ($P < 0.001$). For C-SCN, rise $F_4 = 6.87$ ($P < 0.001$) and decline $F_4 = 22.93$ ($P < 0.001$). The results from post hoc analyses are summarized in Table 1.

In the R-SCN, there was an overall advance in the *Per2* mRNA rise of 2 h following the change in photoperiod. The shift was accomplished first via a 4-h delay within 3 days after the change and then by three consecutive 2-h advances between the 3rd and 5th day, the 5th and 13th day, and after the 13th day. Therefore, the *Per2* mRNA rise was not fully adjusted to the short photoperiod even 13 days after the change. The M-SCN rise adjusted by an overall delay of 2 h, which comprised a phase-delay of 6 h within the first 3 days, and then advances of 2 h between the 3rd and 5th day and again between the 5th and 13th day following the change. In the C-SCN, there was no overall phase shift of the *Per2* mRNA rise following the transition from the long to the short photoperiod. The rise delayed by 2 h within the first 3 days after the transition, and then it advanced back by 2 h between the 5th and 13th day. Altogether, the phase of the *Per2* mRNA rise changed only slightly throughout the SCN, becoming advanced in the R-SCN, delayed in the M-SCN, or showing no change in the C-SCN.

In contrast to the rise, the *Per2* mRNA decline adjusted to the change in the photoperiod in a very consistent manner. In the R-SCN, it advanced by 4 h overall following the photoperiod change. This shift was accomplished by a 2-h advance that was initiated within the first 3 days and was completed on the 5th day, and further by a 2-h advance between the 5th and 13th day. The M-SCN decline also advanced by 4 h overall following the photoperiod change, i.e., by 2 h within the first 3 days and by another 2 h between the 5th and 13th day after the change. The *Per2* mRNA decline in the C-SCN also phase advanced by 4 h overall following the photoperiod transition, first by 2 h between the 3rd and 5th day and again by 2 h between the 5th and 13th day. Hence, the *Per2* mRNA decline adjusted to the change in photoperiod by advancing in all studied SCN regions. Comparing the dynamics of the change of the *Per2* mRNA profile among the SCN regions, the C-SCN and M-SCN adjusted faster than the R-SCN.

The *Per2* expression profiles in R-SCN and C-SCN became synchronized with each other only gradually (Fig. 3). However, at 13 days after the photoperiod change, they were not yet fully synchronized mainly due to phase-advanced *Per2* mRNA rise in the C-SCN compared with that in the R-SCN (Table 1 and Figs. 3*D* and 5*I*).

Rev-erbα mRNA profiles. Statistical analyses revealed significant differences in the timings of the rise and decline of the *Rev-erbα* expression between the long photoperiod (Fig. 4*A*), at 3 (Fig. 4*B*), 5 (Fig. 4*C*), and 13 (Fig. 4*D*) days after the photoperiod change, and after 4 wk under the short photoperiod (Fig. 4*E*) in all SCN regions. For R-SCN, rise $F_4 = 16.52$ ($P < 0.001$) and decline $F_4 = 13.88$ ($P < 0.001$). For M-SCN, rise $F_4 = 15.30$ ($P < 0.001$) and decline $F_4 = 9.51$ ($P < 0.001$). For C-SCN, rise $F_4 = 7.70$ ($P < 0.001$) and decline $F_4 = 8.61$ ($P < 0.001$). The results from post hoc analyses are summarized in Table 1.

The *Rev-erbα* mRNA rise in the R-SCN phase-advanced by 2 h overall after the change from the long to the short photoperiod. This adjustment proceeded via a 2-h phase delay during the first 3 days, followed by a 6-h advance between the 3rd and 5th day, and finally by a 2-h delay between the 5th and 13th day. The M-SCN rise adjusted to the change in the photoperiod

Table 1. *Time of the significant rise and decline in Per1, Per2, and Rev-erbα gene expression*

	Per1		*Per2*		*Rev-erbα*	
R	Rise	Decline	Rise	Decline	Rise	Decline
L	1400 (vs. 1200, $P < 0.05$)	2200 (vs. 2000, $P < 0.01$)	1000 (vs. 0400, $P < 0.01$)	0000 (vs. 2200, $P < 0.01$)	0600 (vs. 0000, $P < 0.05$)	2200 (vs. 1800, $P < 0.01$)
3D	0800 (vs. 0600, $P < 0.05$	2000 (vs. 1800, $P < 0.01$)	1400 (vs. 1200, $P < 0.05$)	2200 (vs. 2000, $P < 0.01$)	0800 (vs. 2000, $P < 0.001$)	2000 (vs. 1600, $P < 0.01$)
5D	0800 (vs. 0600, $P < 0.01$)	1800 (vs. 1400, $P < 0.01$)	1200 (vs. 0600, $P < 0.05$)	2200 (vs. 2000, $P < 0.001$)	0200 (vs. 2000, $P < 0.05$)	1600 (vs. 1200, $P < 0.001$)
13D	0400 (vs. 0200, $P < 0.05$)	1600 (vs. 1400, $P < 0.01$)	1000 (vs. 0800, $P < 0.05$)	2000 (vs. 1800, $P < 0.01$)	0400 (vs. 0000, $P < 0.001$)	1400 (vs. 1200, $P < 0.001$)
S	0400 (vs. 0200, $P < 0.05$)	1600 (vs. 1400, $P < 0.01$)	0800 (vs. 0600, $P < 0.01$)	2000 (vs. 1800, $P < 0.01$)	0400 (vs. 1800, $P < 0.001$)	1600 (vs. 1200, $P < 0.001$)
	Per1		*Per2*		*Rev-erbα*	
M	Rise	Decline	Rise	Decline	Rise	Decline
L	0600 (vs. 2200, $P < 0.05$)	2000 (vs. 1800, $P < 0.01$)	0600 (vs. 0400, $P < 0.01$)	0000 (vs. 2200, $P < 0.01$)	0600 (vs. 0000, $P < 0.001$)	2000 (vs. 1200, $P < 0.05$)
3D	0800 (vs. 0600, $P < 0.01$)	1800 (vs. 1600, $P < 0.001$)	1200 (vs. 0800, $P < 0.01$)	2200 (vs. 2000, $P < 0.01$)	0400 (vs. 2000, $P < 0.001$)	1400 (vs. 1200, $P < 0.05$)
5D	0800 (vs. 0600, $P < 0.001$)	1600 (vs. 1400, $P < 0.001$)	1000 (vs. 0600, $P < 0.001$)	2200 (vs. 2000, $P < 0.01$)	0200 (vs. 2000, $P < 0.001$)	1400 (vs. 1200, $P < 0.001$)
13D	0600 (vs. 0200, $P < 0.001$)	1600 (vs. 1400, $P < 0.001$)	0800 (vs. 0600, $P < 0.001$)	2000 (vs. 1800, $P < 0.01$)	0400 (vs. 0000, $P < 0.001$)	1200 (vs. 1000, $P < 0.001$)
S	0600 (vs. 0400, $P < 0.01$)	1600 (vs. 1400, $P < 0.001$)	0800 (vs. 0600, $P < 0.001$)	2000 (vs. 1800, $P < 0.01$)	0200 (vs. 1600, $P < 0.001$)	1200 (vs. 1000, $P < 0.001$)
	Per1		*Per2*		*Rev-erbα*	
C	Rise	Decline	Rise	Decline	Rise	Decline
L	0400 (vs. 2200, $P < 0.05$)	2000 (vs. 1800, $P < 0.01$)	0800 (vs. 0600, $P < 0.01$)	2200 (vs. 2000, $P < 0.01$)	0200 (vs. 0000, $P < 0.05$)	1400 (vs. 1200, $P < 0.05$)
3D	0800 (vs. 0000, $P < 0.05$)	1600 (vs. 1400, $P < 0.001$)	1000 (vs. 0800, $P < 0.001$)	2200 (vs. 2000, $P < 0.01$)	0200 (vs. 2200, $P < 0.001$)	1400 (vs. 0800, $P < 0.05$)
5D	0600 (vs. 0400, $P < 0.05$)	1600 (vs. 1400, $P < 0.001$)	1000 (vs. 0800, $P < 0.001$)	2000 (vs. 1800, $P < 0.01$)	0200 (vs. 0000, $P < 0.001$)	1400 (vs. 1000, $P < 0.05$)
13D	0400 (vs. 0200, $P < 0.05$)	1600 (vs. 1400, $P < 0.001$)	0800 (vs. 0600, $P < 0.001$)	1800 (vs. 1600, $P < 0.01$)	0200 (vs. 2000, $P < 0.001$)	1200 (vs. 1000, $P < 0.05$)
S	0600 (vs. 0400, $P < 0.01$)	1600 (vs. 1400, $P < 0.001$)	0800 (vs. 0600, $P < 0.001$)	1800 (vs. 1400, $P < 0.01$)	0200 (vs. 0000, $P < 0.05$)	1200 (vs. 0800, $P < 0.05$)

The expression profiles in the rostral (R-), middle (M-), and caudal (C-) SCN were analyzed using the two-way ANOVA for the effect of the time of day and the effect of the photoperiod, i.e., under a long (L) and a short (S) photoperiod, and three (3D), five (5D), and thirteen (13D) days after transition of animals from the long to the short photoperiod (see MATERIALS AND METHODS for details). Post hoc analyses revealed the times when the mRNA levels significantly increased above the minimal or decreased below the maximal levels.

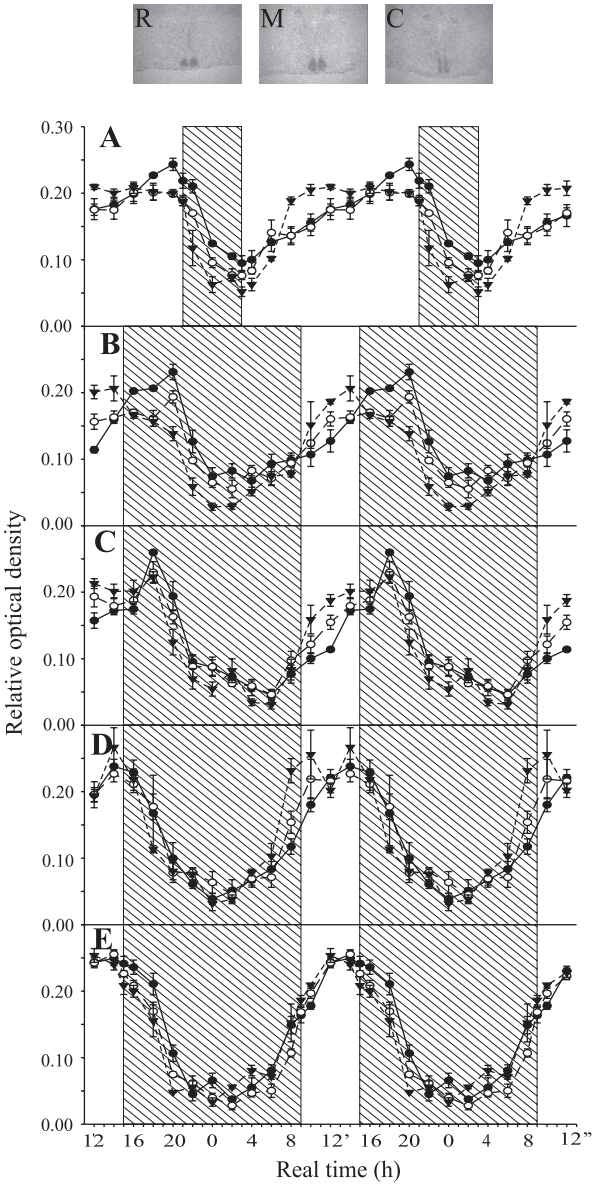

Fig. 3. *Top*: representative autoradiographs of the rostral (R), middle (M), and caudal (C) SCN sections examined by in situ hybridization for *Per2* expression. *Bottom*: daily profiles of *Per2* expression in the rostral (●), middle (○) and caudal (▼) SCN under the long photoperiod (*A*), 3 days (*B*), 5 days (*C*), and 13 days (*D*) after a change from the long to the short photoperiod, as well as under the short photoperiod (*E*). For further details, see Fig. 2 caption. A two-way ANOVA revealed that under the long photoperiod, the profiles in the C-SCN and R-SCN differed at 2000, 2200, 0000, 0800, 1000 ($P < 0.01$), 0400, and 1200′ ($P < 0.05$). Three days after the change of the photoperiod, they differed at 1200 ($P < 0.001$), 1400 ($P < 0.05$), 1800 ($P < 0.01$), 2000, 2200 ($P < 0.001$), 0000 ($P < 0.05$), 0200 ($P < 0.01$), and 1000 ($P < 0.05$). Five days after the change, the profiles in the C-SCN and R-SCN differed at 1200 ($P < 0.01$), 2000 ($P < 0.001$), 1000 ($P < 0.01$), and 1200′ ($P < 0.001$). Thirteen days after the change, the profiles differed only at two time points, i.e., at 0800 ($P < 0.001$) and 1000 ($P < 0.05$). Under the short photoperiod, the mRNA levels between the R-SCN and C-SCN differed at 1600 ($P < 0.05$), 1800, and 2000 ($P < 0.01$).

by an overall 4-h advance; this comprised a 2-h advance within the first 3 days and a further 2-h advance between the 3rd and 5th days after the change. The C-SCN rise did not phase-shift following the photoperiod change. Altogether, during the adjustment to the short photoperiod, the phase of the *Rev-erbα* rise advanced in the R-SCN and M-SCN and did not shift in the C-SCN.

The *Rev-erbα* mRNA decline in the R-SCN adjusted to the photoperiod change by an overall advance of 6 h; this involved a 2-h advance within the first 3 days and a 4-h advance between the 3rd and 5th day. The M-SCN decline advanced by 8 h

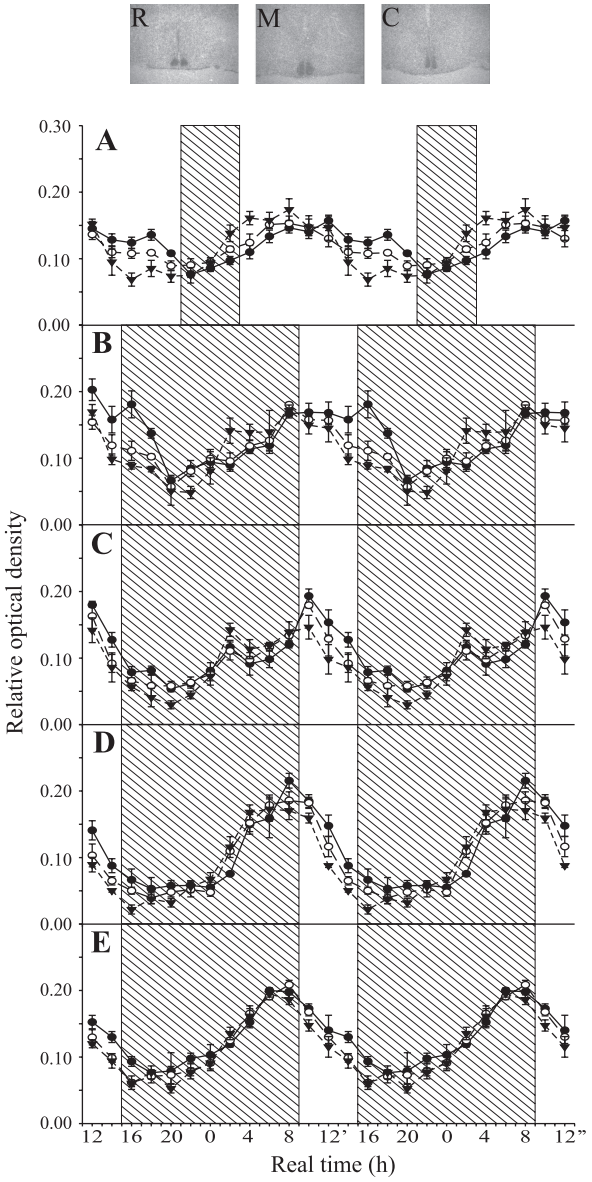

Fig. 4. *Top*: representative autoradiographs of the rostral (R), middle (M), and caudal (C) SCN sections examined by in situ hybridization for *Rev-erbα* expression. *Bottom*: daily profiles of *Rev-erbα* expression in the rostral (●), middle (○), and caudal (▼) SCN under the long photoperiod (*A*), 3 days (*B*), 5 days (*C*), and 13 days (*D*) after a change from the long to the short photoperiod, as well as under the short photoperiod (*E*). For further details, see Fig. 2 caption. A two-way ANOVA revealed that under the long photoperiod, the profiles in the C-SCN and R-SCN differed at 1600, 1800 ($P < 0.01$), 0200 ($P < 0.05$), and 0400 ($P < 0.01$). Three days after the change of the photoperiod, the mRNA levels in the R-SCN and C-SCN differed at 1400, 1600, 1800 ($P < 0.01$), and 0200 ($P < 0.05$). There were no differences among the R-SCN and C-SCN on the 5th and 13th days after the photoperiod change, as well as under the short photoperiod.

overall following the change from the long to the short photoperiod; this involved an advance of 6 h within the first 3 days and further advance of 2 h between the 5th and 13th day. The C-SCN decline advanced by 2 h between the 5th and 13th day after the photoperiodic change. Consistent with the *Per1* and *Per2* mRNA profiles, phase shifts of the *Rev-erbα* mRNA rise, if any, were smaller than shifts in the decline.

During adjustment to the short photoperiod, *Rev-erbα* expression profiles in the R-SCN and C-SCN synchronized to each other also gradually (Fig. 4 and Fig. 5, *K–O*). The *Rev-erbα* mRNA rise occurred at the same time in the R-SCN and C-SCN on the 5th day and the decline on the 13th day after the change in the photoperiod (Table 1). There were no differences among the R-SCN and C-SCN profiles on the 5th and 13th days after the photoperiod change, as well as under the short photoperiod (Fig. 4). Also, the cosinor fits of the R-SCN and C-SCN profiles on the 5th day after the photoperiod change (Fig. 5*M*) attained similar phase relationship as under the short photoperiod (Fig. 5*O*). Therefore, in contrast to *Per1* and *Per2* expression, the *Rev-erbα* expression profiles in the individual parts of the SCN may have been synchronized on the 5th day after the photoperiod change.

Adjustment of Clock Gene Expression in the Liver

Rev-erbα mRNA profiles. A two-way ANOVA among the *Rev-erbα* mRNA profiles under the long (Fig. 6*A*) and short (Fig. 6*E*) photoperiod, as well as after 3 (Fig. 6*B*), 5 (Fig. 6*C*), and 13 (Fig. 6*D*) days following the change from a long to a short photoperiod revealed a significant effect of time (F_{12} = 37.183, $P < 0.001$). Although the effect of group was not significant, a highly significant interaction effect (F_{48} = 3.239, $P < 0.001$) suggested differences among individual profiles. The *Rev-erbα* mRNA decline occurred at the same time, i.e., at 1600 (vs. 1400, $P < 0.01$), under the long and the short photoperiod and also after 3, 5, and 13 days following the photoperiod change. In contrast, the rise adjusted to the change by phase-advancing: it occurred at 1200′ under the long photoperiod (vs. 1000, $P < 0.001$), at 1000, 3, and 5 days after the change (vs. 0800, $P < 0.01$ and $P < 0.001$, respectively) and at 0800 13 days after the change and under the short photoperiod (vs. 0600, $P < 0.01$ and $P < 0.05$, respectively). From the 3rd day onward, the *Rev-erbα* mRNA level at 1000 was significantly elevated above that under the long photoperiod ($P < 0.001$). Also, the *Rev-erbα* mRNA levels at 0800 on the 13th day after the change and that of under the short photoperiod were significantly elevated above those under the long photoperiod ($P < 0.001$) and 3 and 5 ($P < 0.01$) days after the change. The data show that the *Rev-erbα* expression profile in the liver adjusted to the photoperiod change within 13 days by advancing the expression rise by 4 h.

Per2 mRNA profiles. A two-way ANOVA of *Per2* mRNA profiles under the long (Fig. 6*F*) and short (Fig. 6*J*) photoperiod and after 3 (Fig. 6*G*), 5 (Fig. 6*H*), and 13 (Fig. 6*I*) days following the photoperiod change revealed a significant effect of time (F_{12} = 40.344, $P < 0.001$), group (F_4 = 13.092, $P < 0.001$), and an interaction effect (F_{48} = 4.526, $P < 0.001$). The *Per2* mRNA rise occurred at 1800 (vs. 1400, $P < 0.01$) under the long photoperiod, at 2000 (vs. 1200, $P < 0.001$) on the 3rd day and again at 1800 on the 5th day. On the 13th day after the change and under the short photoperiod, the *Per2* mRNA rise was significant already at 1400 (vs. 0600, $P < 0.001$ and vs. 0800, $P < 0.01$, respectively). However, under the short photoperiod, the mRNA levels rose further significantly until 1800 (vs. 1400, $P < 0.01$). The decline occurred at 0200 under the long photoperiod (vs. 0000, $P < 0.01$) and advanced on the 5th day (0000 vs. 2200, $P < 0.001$) following the photoperiod change. On the 13th day, the decline was not yet fully adjusted to the short days because under the short photoperiod, it occurred at 2000 (vs. 1800) and continued further (2200 vs. 2000, $P < 0.05$). The *Per2* mRNA levels at 1400 on the 13th day after the photoperiod change and under the short photoperiod were significantly elevated above those of the long photoperiod ($P < 0.001$). Also, the mRNA level at 2200 under the short photoperiod was significantly lower than under the long photoperiod and on the 3rd, 5th, and 13th day after the photoperiod change ($P < 0.01$). The data show that over a period of 13 days, the *Per2* expression profile in the liver adjusted only partially to the change in the photoperiod, i.e., by fully advancing the *Per2* mRNA rise but only partly the decline.

DISCUSSION

Following transition of mice from a long to a short photoperiod, the duration of locomotor activity increased gradually and fully adjusted to the short photoperiod within 11 days. Importantly, the extension of activity proceeded almost entirely into the evening hours, as the evening activity onset, but not the morning activity offset, advanced significantly. The difference between the activity duration under the long photoperiod and that under the short photoperiod is consistent with previously published data (17). In the *Per1*, *Per2,* and *Rev-erbα* expression rhythms, the mRNA decline in all SCN regions adjusted to the photoperiod change by strong advances and the rise adjusted by only slight, if any, phase shifts (with the exception of *Per1* mRNA rise in the R-SCN). Thus, adjustments of the overt rhythm in the locomotor activity and of the SCN rhythms in expression of the clock genes *Per1*, *Per2,* and *Rev-erbα* to transition mice from long to short days proceeded mostly by phase advancing of the activity onset together with advancing of the *Per1*, *Per2* and *Rev-erbα* expression declines. It appears that the declines were locked more to the evening light offset than the rises were locked to the morning light onset. If this were the case, in mice, the adjustment might proceed via phase-advancing markers joined to lights off, such as with the locomotor activity onset. In rats, the adjustment to short days proceeds mostly via phase-delay-

Fig. 5. Model of dynamics of adjustment of *Per1* (*A–E*), *Per2* (*F–J*), and *Rev-erbα* (*K–O*) expression profiles to a change from a long to a short photoperiod within the rostral (solid line) and caudal (dashed line) SCN. The data in Figs. 2–4 were fitted with a cosine curve by the cosinor analysis method to visualize the phase differences between the R-SCN and C-SCN. The R-SCN and C-SCN profiles were compared under the long (*A, F, K*) and short (*E, J, O*) photoperiod and 3 (*B, G, L*), 5 (*C, H, M*), and 13 (*D, I, N*) days after a change from the long to the short photoperiod. Amplitude (amp), acrophase (acro) and R2 (goodness of the fit) of the profiles in the rostral and caudal SCN are depicted in the insets of each graph.

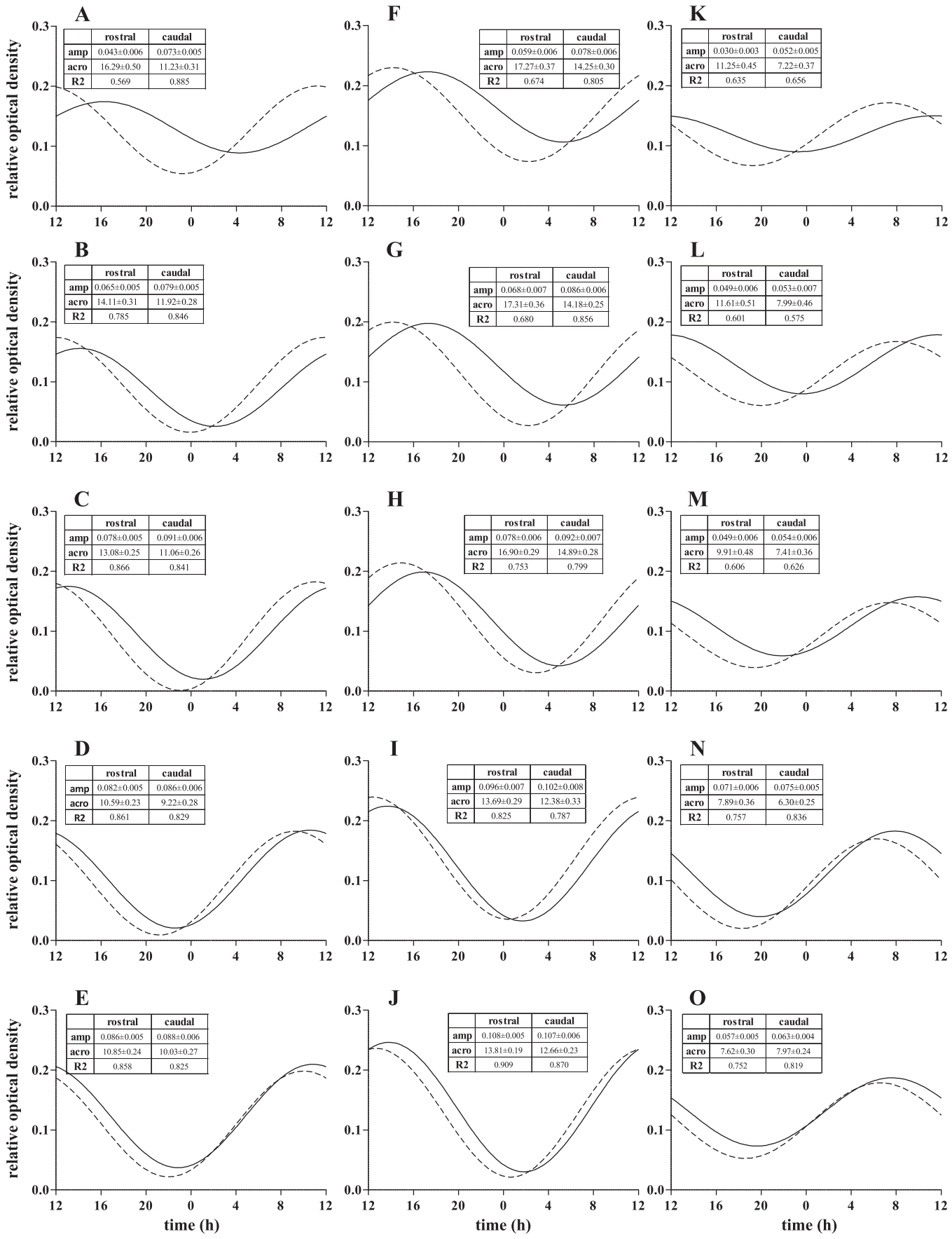

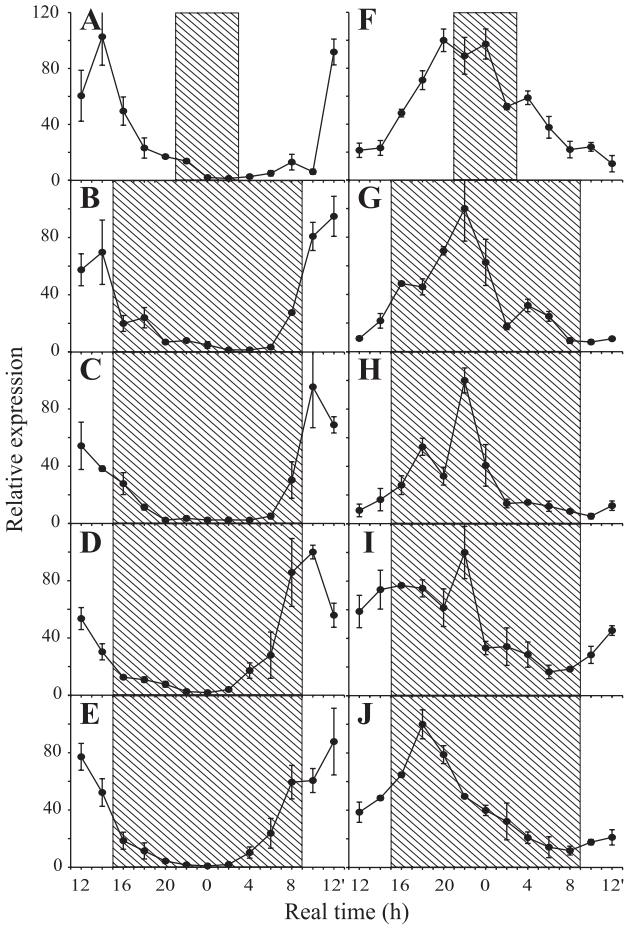

Fig. 6. Daily profiles of *Rev-erbα* (*A–E*) and *Per2* (*F–J*) expression in the liver. The profiles were determined under the long photoperiod (*A*, *F*), 3 days (*B*, *G*), 5 days (*C*, *H*), and 13 days (*D*, *I*) after the change from the long to the short photoperiod, as well as under the short photoperiod (*E*, *J*). The hatched areas depict intervals of darkness.

ing of markers joined to lights on, e.g., the decline of the pineal AA-NAT activity (14) and of the SCN c-Fos photoinduction (50), as well as the rise of the spontaneous c-Fos and PER1 proteins levels and arginine vasopressin mRNA in the SCN (18, 19, 46, 49). The different strategy of adjustment to the transition from a long to a short photoperiod in the mouse compared with rat is likely due to the fact that the endogenous circadian period of the mouse is shorter, whereas that of the rat is longer than 24 h.

The dynamics and mode of the rise and decline in the clock gene expression adjustment to the short photoperiod differed among individual SCN regions and among the clock genes. In the R-SCN, the rise adjusted to the photoperiod change by a large and rapid advance in the case of *Per1*, whereas for *Per2* and *Rev-erbα* a slight shift was attained via gradual delays and advances. In contrast, the decline of *Per1*, *Per2,* and *Rev-erbα* mRNA advanced gradually and consistently in response to the photoperiod change. The adjustment of the R-SCN expression profiles to the change in photoperiod was accomplished within 13 days, with the exception of the *Per2* mRNA rise, which took even longer. In the M-SCN and C-SCN, the adjustment was achieved by gradual delays, advances, or no shifts of the rise, but by consistent phase advances of the declines of all three gene mRNAs. The adjustment of the M-SCN and C-SCN expression profiles to short days was accomplished within 13 days. It appears that the adjustment to the photoperiod change was likely driven by advancing the decline of clock gene expression. In the C-SCN, it might be initiated by advancement of the *Per1* mRNA decline.

Under the long photoperiod, the *Per1, Per2,* and *Rev-erbα* expression profiles in the C-SCN were phase-advanced relative to those in the R-SCN, in agreement with recently published data on desynchrony among rhythms in clock gene expression and PER1 protein in individual regions of the rodent SCN (12, 17, 20, 31, 43, 55). The desynchrony among clock gene expression profiles in individual SCN regions might partly account for the longer interval of elevated clock gene expression in the entire SCN under the long photoperiod: separate SCN regions might switch on expression one after another, with the C-SCN coming first and the R-SCN last. Consequently, the entire SCN might find itself in a day-time state for a longer time than individual SCN regions (43). From comparison of the waveform of the expression profiles in individual SCN regions, it appears that the rises in the *Per1, Per2,* and *Rev-erbα* expression occurred not only later but also notably slower in the R-SCN than that in the C-SCN. This finding is in accordance with in vitro studies that demonstrated higher variability in the *Per1-luc* and PER2::luc single cell rhythmicity in the anterior vs. posterior SCN under a long photoperiod (17, 29). The outcome of the present study showed the dynamics of how the desynchronized SCN regions under a long photoperiod attained synchrony after changing to the short photoperiod. Three and five days following transition from a long to a short photoperiod, the phases of the *Per1* and *Per2* expression profiles in the R-SCN and C-SCN still differed. *Per1* mRNA profiles attained synchrony in the R-SCN and C-SCN within 13 days following the transition, but *Per2* mRNA profiles required more time to become completely synchronized. The *Rev-erbα* mRNA profile in the R-SCN differed from that in the C-SCN on the third day following the photoperiod change, but 5 days after the change, the profiles were already synchronized. Thus, the profiles of *Per1, Per2,* and *Rev-erbα* expression in individual SCN regions attained synchrony at different rates following the photoperiod transition; the *Rev-erbα* mRNA profile became synchronized faster than the *Per1* and *Per2* mRNA profiles.

Following transition from a long to a short photoperiod, not only did the clock gene expression profiles in individual SCN regions gradually become synchronized, but the interval of elevated clock gene expression also gradually shortened, at least in the M-SCN and C-SCN. The shortening was due to large-phase advances of the clock gene expression decline but only small, if any, phase shifts of the rise. It appears that the photoperiodic modulation of the SCN rhythms might be due to a changing phase-relationship among rhythms in the R-SCN, M-SCN, and C-SCN regions, as well as different waveforms of the rhythms in populations of cells within these individual SCN regions. It remains to be elucidated whether this photoperiodic response is mediated by affecting synchrony among individual oscillating cells in the M-SCN and C-SCN (35, 38, 54) and/or by affecting the single cell oscillators within the SCN regions.

In addition to the central SCN clock, the peripheral clocks are also supposed to be modulated by the photoperiod (1, 3, 4, 26). The present study demonstrates for the first time the effect

of the photoperiod on *Per2* and *Rev-erbα* expression profiles in the mouse liver. Following transition from a long to a short photoperiod, the *Per2* mRNA rise, as well as the decline, gradually phase advanced relative to those under the long photoperiod. The adjustment of the entire rhythm took longer than 13 days. Because the *Per2* mRNA decline phase-advanced more than the rise, the interval of elevated *Per2* mRNA levels under the short photoperiod was shorter than that under the long photoperiod. Interestingly, the *Rev-erbα* mRNA profile adjusted in a different way. The *Rev-erbα* expression rise phase-advanced gradually and was completely advanced within 13 days after the photoperiod change, whereas the decline did not phase shift at all. Consequently, duration of the elevated *Rev-erbα* expression in the liver extended within 13 days after shortening of the photoperiod.

These results indicate that photoperiodic modulation of the central SCN clock and of the peripheral clock in the liver may differ substantially. Whereas in the SCN, the interval of elevated expression of all of the studied clock genes was longer under the long than under the short photoperiod, in the liver, this finding held true for *Per2* but not for *Rev-erbα* expression; the interval of elevated *Rev-erbα* expression was shorter under long than short days. This finding suggests different mechanisms for the photoperiodic modulation of the SCN and peripheral clocks. It is plausible that following transition from a long to a short photoperiod, the subjective night gradually extended because of the photoperiodic modulation of the SCN clock gene expression (see above), and the interval of behavioral activity increased. Together with the subjective night, the interval of *Rev-erbα* expression in the liver extended as well. This extension might be mediated either via direct signaling from the photoperiodically modulated SCN and/or indirectly via the SCN, presumably via SCN modulation of the behavioral/feeding rhythms. *Rev-erbα* promoter also contains, apart from an E-box responsible for its control by the CLOCK:BMAL1 heterodimer, other response elements that might be responsible for switching on/off the gene transcription. One of these response elements, Rev-DR2/RORE, is a target for both Rev-Erbα and RORα, i.e., the clockwork feedback factors (33), as well as for peroxisome proliferator-activated receptor-γ (PPARγ) and PPARα nuclear receptors (6), which undergo circadian oscillation (56) and are activated by fasting. Interestingly, PPARα was also suggested to play a role in *Per2* resetting via FGF21-mediated effects on cAMP response element binding signaling and NAD^+ levels (39). Another potential candidate for *Rev-erbα* modulation might be glucocorticoid signaling (53). Thus, *Rev-erbα* gene expression might be directly regulated by feeding rhythm, which is closely related to the behavioral state of the organism. Indeed, in agreement with the above proposition, adjustment of the *Rev-erbα* mRNA rhythm, but not the *Per2* mRNA rhythm, to a short photoperiod reflected that of the locomotor activity: the onset of the activity, as well as of the *Rev-erbα* expression phase-advanced, whereas the offset did not change and, thus, duration of the elevated *Rev-erbα* expression and locomotor activity lengthened. The longer interval of elevated *Rev-erbα* mRNA levels might result in a longer interval of *Bmal1* suppression and, consequently, shortening of the interval when BMAL1 induces *Per2* gene expression. This outcome might explain why the liver *Rev-erbα* rise and *Per2* decline phase advanced together during adjustment to transition from a long to a short photoperiod. At the same time, *Per2* expression is likely under the control of systemic cues emanating from the SCN because dynamics of the liver *Per2* expression profiles adjustment and the change of the *Per2* mRNA rhythm waveform by shortening the peak duration corresponded with an adjustment of the SCN *Per2* expression profiles. This speculation is supported by findings from Schibler's group who demonstrated that mice with a conditionally inactivated hepatocyte clock still show rhythmic *Per2* expression in the liver. Thus, *Per2* expression is driven not only by the local clockwork in the liver, but also directly by the SCN clock (24).

Perspectives and Significance

A strong circadian time-keeping system appears to be involved in prevention against sleeping, metabolic, and cancer disorders. However, the circadian system may be weakened by desynchronization among its parts, such as among the central SCN and peripheral clocks. Previous data have demonstrated that the SCN and peripheral clocks may adjust to shifts of a light-dark cycle with different rates (45). Our study on rhythms in clock gene expression in mice showed that individual SCN parts, desynchronized under a light-dark cycle with a long photoperiod, resynchronized with different rates after a transition to a short photoperiod, with the rate depending on the particular clock gene. Adjustment to short days was achieved mostly by phase-advancing the clock gene expression decline. In parallel with the adjustment in the SCN, also the locomotor activity rhythm adjusted gradually to the photoperiod change. In the liver, one of the clock genes, *Per2*, adjusted to the transition in a similar manner as in the SCN, i.e., by shortening of its daily expression, whereas another clock gene, *Rev-erbα*, as well as the locomotor activity rhythm adjusted to the transition by lengthening of the expression and activity. In summary, the findings revealed that dynamics of adjustment of the circadian system to an environmental change is complex. Studies of the mechanisms are necessary to gain insights into consequences of such environmental changes on the strength and integrity of the circadian system and, consequently, human health.

ACKNOWLEDGMENTS

The authors gratefully acknowledge Prof. Hitoshi Okamura (Kobe University School of Medicine, Kobe, Japan) for *Per1* and *Per2* cDNA fragments for in situ hybridization, Alena Dědičová for statistical analysis, and Eva Suchanová for her excellent technical assistance.

GRANTS

The study was supported by the 6th Framework Project EUCLOCK 018741; Grant 305090321 and by Research Projects AV0Z 50110509 and LC554.

DISCLOSURES

No conflicts of interest are declared by the authors.

REFERENCES

1. **Andersson H, Johnston JD, Messager S, Hazlerigg D, Lincoln G.** Photoperiod regulates clock gene rhythms in the ovine liver. *Gen Comp Endocrinol* 142: 357–363, 2005.
2. **Balsalobre A, Damiola F, Schibler U.** A serum shock induces circadian gene expression in mammalian tissue culture cells. *Cell* 93: 929–937, 1998.

3. **Bendová Z, Sumová A.** Photoperiodic regulation of PER1 and PER2 protein expression in rat peripheral tissues. *Physiol Res* 55: 623–632, 2006.
4. **Carr AJ, Johnston JD, Semikhodskii AG, Nolan T, Cagampang FR, Stirland JA, Loudon AS.** Photoperiod differentially regulates circadian oscillators in central and peripheral tissues of the Syrian hamster. *Curr Biol* 13: 1543–1548, 2003.
5. **Elliott JA, Tamarkin L.** Complex circadian regulation of pineal melatonin and wheel-running in Syrian hamsters. *J Comp Physiol [A]* 174: 469–484, 1994.
6. **Fontaine C, Dubois G, Duguay Y, Helledie T, Vu-Dac N, Gervois P, Soncin F, Mandrup S, Fruchart JC, Fruchart-Najib J, Staels B.** The orphan nuclear receptor *Rev-Erbα* is a peroxisome proliferator-activated receptor (PPAR) γ target gene and promotes PPARγ-induced adipocyte differentiation. *J Biol Chem* 278: 37672–37680, 2003.
7. **Fu L, Lee CC.** The circadain clock: pacemaker and tumour suppressor. *Nat Rev Cancer* 3: 350–361, 2003.
8. **Goldman BD.** Mammalian photoperiodic system: formal properties and neuroendocrine mechanisms of photoperiodic time measurement. *J Biol Rhythms* 16: 283–301, 2001.
9. **Goto M, Oshima I, Tomita T, Ebihara S.** Melatonin content of the pineal gland in different mouse strains. *J Pineal Res* 7: 195–204, 1989.
10. **Hastings MH.** Modeling the molecular calendar. *J Biol Rhythms* 16: 117–123, 2001.
11. **Hastings MH, Walker AP, Herbert J.** Effect of asymmetrical reductions of photoperiod on pineal melatonin, locomotor activity and gonadal condition of male Syrian hamsters. *J Endocrinol* 114: 221–229, 1987.
12. **Hazlerigg DG, Ebling FJ, Johnston JD.** Photoperiod differentially regulates gene expression rhythms in the rostral and caudal SCN. *Curr Biol* 15: R449–R450, 2005.
13. **Illnerová H.** The suprachiasmatic nucleus and rhythmic pineal melatonin production. In: *Suprachiasmatic Nucleus: The Mind's Clock*, edited by Klein DC, Moore RJ, and Reppert SM. New York: Oxford University, 1991, p. 197–216.
14. **Illnerová H, Hoffman K, Vaněček J.** Adjustment of the rat pineal N-acetyltransferase rhythm to change from long to short photoperiod depends on the direction of the extension of the dark period. *Brain Res* 362: 403–408, 1986.
15. **Illnerová H, Hoffmann K, Vaněček J.** Adjustment of pineal melatonin and N-acetyltransferase rhythms to change from long to short photoperiod in the Djungarian hamster *Phodopus sungorus*. *Neuroendocrinology* 38: 226–231, 1984.
16. **Illnerová H, Vaněček J.** Pineal rhythm in N-acetyltransferase activity in rats under different artificial photoperiods and in natural daylight in the course of a year. *Neuroendocrinology* 31: 321–326, 1980.
17. **Inagaki N, Honma S, Ono D, Tanahashi Y, Honma K.** Separate oscillating cell groups in mouse suprachiasmatic nucleus couple photoperiodically to the onset and end of daily activity. *Proc Natl Acad Sci USA* 104: 7664–7669, 2007.
18. **Jáč M, Kiss A, Sumová A, Illnerová H, Ježová D.** Daily profiles of arginine vasopressin mRNA in the suprachiasmatic, supraoptic and paraventricular nuclei of the rat hypothalamus under various photoperiods. *Brain Res* 887: 472–476, 2000.
19. **Jáč M, Sumová A, Illnerová H.** c-Fos rhythm in subdivisions of the rat suprachiasmatic nucleus under artificial and natural photoperiods. *Am J Physiol Regul Integr Comp Physiol* 279: R2270–R2276, 2000.
20. **Johnston JD, Ebling FJ, Hazlerigg DG.** Photoperiod regulates multiple gene expression in the suprachiasmatic nuclei and pars tuberalis of the Siberian hamster (*Phodopus sungorus*). *Eur J Neurosci* 21: 2967–2974, 2005.
21. **Kalsbeek A, Palm IF, La Fleur SE, Scheer FA, Perreau-Lenz S, Ruiter M, Kreier F, Cailotto C, Buijs RM.** SCN outputs and the hypothalamic balance of life. *J Biol Rhythms* 21: 458–469, 2006.
22. **King DP, Takahashi JS.** Molecular genetics of circadian rhythms in mammals. *Annu Rev Neurosci* 23: 713–742, 2000.
23. **Klein DC, Moore RJ, Reppert SM (Eds.).** *Suprachiasmatic nucleus: The Mind's Clock*. New York: Oxford University, 1991.
24. **Kornmann B, Schaad O, Bujard H, Takahashi JS, Schibler U.** System-driven and oscillator-dependent circadian transcription in mice with a conditionally active liver clock. *PLoS Biol* 5: e34, 2007.
25. **Kováčiková Z, Sládek M, Bendová Z, Illnerová H, Sumová A.** Expression of clock and clock-driven genes in the rat suprachiasmatic nucleus during late fetal and early postnatal development. *J Biol Rhythms* 21: 140–148, 2006.
26. **Maronde E, Pfeffer M, Glass Y, Stehle JH.** Transcription factor dynamics in pineal gland and liver of the Syrian hamster (*Mesocricetus auratus*) adapts to prevailing photoperiod. *J Pineal Res* 43: 16–24, 2007.
27. **Messager S, Hazlerigg DG, Mercer JG, Morgan PJ.** Photoperiod differentially regulates the expression of *Per1* and ICER in the pars tuberalis and the suprachiasmatic nucleus of the Siberian hamster. *Eur J Neurosci* 12: 2865–2870, 2000.
28. **Messager S, Ross AW, Barrett P, Morgan PJ.** Decoding photoperiodic time through Per1 and ICER gene amplitude. *Proc Natl Acad Sci USA* 96: 9938–9943, 1999.
29. **Mickman CT, Stubblefield J, Harrington M, Nelson DE.** Photoperiod alters the phase difference between activity onset in vivo and *mPer2*::*luc* peak in vitro. *Am J Physiol Regul Integr Comp Physiol* 295: R1688–R1694, 2008.
30. **Moore RY, Speh JC, Leak RK.** Suprachiasmatic nucleus organization. *Cell Tissue Res* 309: 89–98, 2002.
31. **Naito E, Watanabe T, Tei H, Yoshimura T, Ebihara S.** Reorganization of the suprachiasmatic nucleus coding for day length. *J Biol Rhythms* 23: 140–149, 2008.
32. **Nuesslein-Hildesheim B, O'Brien JA, Ebling FJ, Maywood ES, Hastings MH.** The circadian cycle of *mPER* clock gene products in the suprachiasmatic nucleus of the siberian hamster encodes both daily and seasonal time. *Eur J Neurosci* 12: 2856–2864, 2000.
33. **Raspe E, Mautino G, Duval C, Fontaine C, Duez H, Barbier O, Monte D, Fruchart J, Fruchart JC, Staels B.** Transcriptional regulation of human *Rev-erbα* gene expression by the orphan nuclear receptor retinoic acid-related orphan receptor alpha. *J Biol Chem* 277: 49275–49281, 2002.
34. **Reppert SM, Weaver DR.** Molecular analysis of mammalian circadian rhythms. *Annu Rev Physiol* 63: 647–676, 2001.
35. **Rohling J, Wolters L, Meijer JH.** Simulation of day-length encoding in the SCN: from single-cell to tissue-level organization. *J Biol Rhythms* 21: 301–313, 2006.
36. **Rollag MD, Niswender GD.** Radioimmunoassay of serum concentrations of melatonin in sheep exposed to different lighting regimens. *Endocrinology* 98: 482–489, 1976.
37. **Shearman LP, Sriram S, Weaver DR, Maywood ES, Chaves I, Zheng B, Kume K, Lee CC, van der Horst GT, Hastings MH, Reppert SM.** Interacting molecular loops in the mammalian circadian clock. *Science* 288: 1013–1019, 2000.
38. **Schaap J, Albus H, VanderLeest HT, Eilers PH, Detari L, Meijer JH.** Heterogeneity of rhythmic suprachiasmatic nucleus neurons: Implications for circadian waveform and photoperiodic encoding. *Proc Natl Acad Sci USA* 100: 15994–15999, 2003.
39. **Schibler U.** The 2008 Pittendrigh/Aschoff lecture: peripheral phase coordination in the mammalian circadian timing system. *J Biol Rhythms* 24: 3–15, 2009.
40. **Sládek M, Jindráková Z, Bendová Z, Sumová A.** Postnatal ontogenesis of the circadian clock within the rat liver. *Am J Physiol Regul Integr Comp Physiol* 292: R1224–R1229, 2007.
41. **Sládek M, Rybová M, Jindráková Z, Zemanová Z, Polidarová L, Mrnka L, O'Neill J, Pácha J, Sumová A.** Insight into the circadian clock within rat colonic epithelial cells. *Gastroenterology* 133: 1240–1249, 2007.
42. **Sládek M, Sumová A, Kováčiková Z, Bendová Z, Laurinová K, Illnerová H.** Insight into molecular core clock mechanism of embryonic and early postnatal rat suprachiasmatic nucleus. *Proc Natl Acad Sci USA* 101: 6231–6236, 2004.
43. **Sosniyenko S, Hut RA, Daan S, Sumová A.** Influence of photoperiod duration and light-dark transitions on entrainment of *Per1* and *Per2* gene and protein expression in subdivisions of the mouse suprachiasmatic nucleus. *Eur J Neurosci* 30: 1802–1814, 2009.
44. **Steinlechner S, Jacobmeier B, Scherbarth F, Dernbach H, Kruse F, Albrecht U.** Robust circadian rhythmicity of *Per1* and *Per2* mutant mice in constant light, and dynamics of *Per1* and *Per2* gene expression under long and short photoperiods. *J Biol Rhythms* 17: 202–209, 2002.
45. **Stokkan KA, Yamazaki S, Tei H, Sakaki Y, Menaker M.** Entrainment of the circadian clock in the liver by feeding. *Science* 291: 490–493, 2001.
46. **Sumová A, Jáč M, Sládek M, Šauman I, Illnerová H.** Clock gene daily profiles and their phase relationship in the rat suprachiasmatic nucleus are affected by photoperiod. *J Biol Rhythms* 18: 134–144, 2003.
47. **Sumová A, Kováčiková Z, Illnerová H.** Dynamics of the adjustment of clock gene expression in the rat suprachiasmatic nucleus to an asymmet-

rical change from a long to a short photoperiod. *J Biol Rhythms* 22: 259–267, 2007.
48. **Sumová A, Sládek M, Jáč M, Illnerová H.** The circadian rhythm of Per1 gene product in the rat suprachiasmatic nucleus and its modulation by seasonal changes in daylength. *Brain Res* 947: 260–270, 2002.
49. **Sumová A, Trávníčková Z, Illnerová H.** Spontaneous c-Fos rhythm in the rat suprachiasmatic nucleus: location and effect of photoperiod. *Am J Physiol Regul Integr Comp Physiol* 279: R2262–R2269, 2000.
50. **Sumová A, Trávníčková Z, Peters R, Schwartz WJ, Illnerová H.** The rat suprachiasmatic nucleus is a clock for all seasons. *Proc Natl Acad Sci USA* 92: 7754–7758, 1995.
51. **Sumová A, Trávníčková Z, Illnerová H.** Memory on long but not on short days is stored in the rat suprachiasmatic nucleus. *Neurosci Lett* 200: 191–194, 1995.
52. **Takahashi JS, Hong HK, Ko CH, McDearmon EL.** The genetics of mammalian circadian order and disorder: implications for physiology and disease. *Nat Rev Genet* 9: 764–775, 2008.
53. **Torra IP, Tsibulsky V, Delaunay F, Saladin R, Laudet V, Fruchart JC, Kosykh V, Staels B.** Circadian and glucocorticoid regulation of *Rev-erbα* expression in liver. *Endocrinology* 141: 3799–3806, 2000.
54. **VanderLeest HT, Houben T, Michel S, Deboer T, Albus H, Vansteensel MJ, Block GD, Meijer JH.** Seasonal encoding by the circadian pacemaker of the SCN. *Curr Biol* 17: 468–473, 2007.
55. **Yan L, Silver R.** Day-length encoding through tonic photic effects in the retinorecipient SCN region. *Eur J Neurosci* 28: 2108–2115, 2008.
56. **Yang X, Downes M, Yu RT, Bookout AL, He W, Straume M, Mangelsdorf DJ, Evans RM.** Nuclear receptor expression links the circadian clock to metabolism. *Cell* 126: 801–810, 2006.

Maternal Control of the Fetal and Neonatal Rat Suprachiasmatic Nucleus

Rehab El-Hennamy, Kristýna Matějů, Zdena Bendová, Serhiy Sosniyenko, and Alena Sumová[1]
Institute of Physiology, Academy of Sciences of the Czech Republic, Prague, Czech Republic

Abstract The molecular clockwork underlying the generation of circadian rhythmicity within the suprachiasmatic nucleus (SCN) develops gradually during ontogenesis. The authors' previous work has shown that rhythms in clock gene expression in the rat SCN are not detectable at embryonic day (E) 19, start to form at E20 and develop further via increasing amplitude until postnatal day (P) 10. The aim of the present work was to elucidate whether and how swiftly the immature fetal and neonatal molecular SCN clocks can be reset by maternal cues. Pregnant rats maintained under a light-dark (LD) regimen with 12 h of light and 12 h of darkness were exposed to a 6-h delay of the dark period and released into constant darkness at different stages of the fetal SCN development. Adult rats maintained under the same LD regimen were exposed to an identical shifting procedure. Daily rhythms in spontaneous *c-fos*, *Avp*, *Per1*, and *Per2* expression were examined within the adult and newborn SCN by *in situ* hybridization. Exposure of adult rats to the shifting procedure induced a significant phase delay of locomotor activity within 3 days after the phase shift as well as a delay in the rhythms of *c-fos* and *Avp* expression within 3 days and *Per1* and *Per2* expression within 5 days. Exposure of pregnant rats to the shifting procedure at E18, but not at E20, delayed the rhythm in *c-fos* and *Avp* expression in the SCN of newborn pups at P0-1. The shifting procedure at E20 did, however, induce a phase delay of *Per1* and *Per2* expression rhythms at P3 and P6. Hence, 5 days were necessary for phase-shifting the pups' SCN clock by maternal cues, be it the interval between E18 and P0-1 or the interval between E20 and P3, while only 3 days were necessary for phase-shifting the maternal SCN by photic cues. These results demonstrate that the SCN clock is capable of significant phase shifts at fetal developmental stages when no or very faint molecular oscillations can be detected.

Key words circadian system, suprachiasmatic nucleus, ontogenesis, maternal entrainment, rat

The intrauterine period is important for postnatal development of mammals. During this period, a developing organism is mostly protected from the influence of the external environment, but it is continuously exposed to the internal maternal milieu. The majority of maternal signals that are delivered to the fetus transplacentally exhibit circadian rhythms. Maternal circadian rhythms are driven by an endogenous clock located within the suprachiasmatic nuclei (SCN) of the hypothalamus (Klein et al., 1991). The

1. To whom all correspondence should be addressed: Alena Sumová, Institute of Physiology, v.v.i., Academy of Sciences of the Czech Republic, Vídeňská 1083, 142 20 Praha 4, Czech Republic; e-mail: sumova@biomed.cas.cz.

JOURNAL OF BIOLOGICAL RHYTHMS, Vol. 23 No. 5, October 2008 435-444
DOI: 10.1177/0748730408322635

clock is dominantly entrained by the light-dark regimen of the solar day, mainly by its light period (Pittendrigh, 1981). Therefore, timing of maternal cues may provide fetuses with information about the external time. However, it is still not known whether and how maternal cues impinge on the fetal SCN clock.

In the rat, the prenatal period lasts for about 22 days. Neurogenesis of the SCN begins on embryonic day (E) 14 and is completed at E18, but the morphological maturation of the SCN neurons proceeds gradually until postnatal day (P) 10 (Moore, 1991). Synaptogenesis within the SCN appears to be a slower process: at E19, only sparse synapses can be observed. The process begins to progress only in the late prenatal and early postnatal periods, and then increases noticeably between P4 and P10 (Weinert, 2005). Thus, during the prenatal period, although SCN neurons are present, the multilevel intercellular coupling may not yet be functional. The coupling strengthens during the 1st postnatal week, and the rat SCN is developed to its full complexity only at P10. Therefore, morphological development of the SCN extends well into the postnatal period. The development is genetically determined and occurs without input from the external environment (Jud and Albrecht, 2006). A question remains as to whether the morphologically immature SCN clock serves as a self-sustaining clock or whether it functions first as an hourglass oscillator and only later becomes an autonomous clock (Sumová et al., 2008). During the late prenatal period, the SCN exhibits day-night variation in metabolic activity (Reppert and Schwartz, 1984), in *Avp* mRNA levels (Reppert and Uhl, 1987), and in the firing rate of its neurons (Shibata and Moore, 1987). In adults, all of these rhythms are supposed to be driven by the SCN clock. However, within the fetal SCN, the rhythms might arise also from cyclically appearing maternal cues that impinge on fetal SCN neurons. Such maternal "zeitgebers" might trigger rhythms in neuronal and metabolic activity as well as in *Avp* mRNA levels. Indeed, it has been demonstrated that transcription of *Avp* might be regulated by a non-clock-related mechanism (Iwasaki et al., 1997; Burbach et al., 2001). Recent data using a more reliable marker of transcription rate than detection of mRNA, that is, detection of heteronuclear RNA as a nascent transcript, revealed circadian rhythmicity in transcription of the *Avp* gene in the rat SCN only at P1, but not at E20 (Kováčiková et al., 2006).

A self-sustained clock generates circadian rhythmicity through molecular clockwork composed of interactive transcriptional-translational feedback loops. A contemporary model of the molecular core clockwork presumes that rhythmic expression of clock genes, namely, *Per1*, *Per2*, *Cry1*, *Cry2*, *Rev-erba*, *Bmal1*, as well as their proteins, drives the circadian clock in a cell-autonomous fashion (for review, see Fu and Lee, 2003; Ko and Takahashi, 2006; Reppert and Weaver, 2001). The molecular core clockwork develops gradually during ontogenesis. Ohta et al. reported clear daily rhythms of *Per1* and *Per2* mRNA in the rat SCN at E20 (Ohta et al., 2002, 2003). However, other authors did not detect significant rhythms in *Per1*, *Per2*, *Cry1*, and *Bmal1* mRNA in the rat SCN at E19 (Sládek et al., 2004), when the fetal rat SCN is already formed (Moore, 1991) and the rhythm in metabolic activity has become apparent (Reppert and Schwartz, 1984). Moreover, at that stage, clock gene proteins PER1, PER2, and CRY1 not only did not exhibit any circadian variation, but were in fact undetectable (Sládek et al., 2004). At E20, the rhythm in *Per1* expression began to form, but the amplitude was very low (Kováčiková et al., 2006). Rhythms in clock gene expression developed gradually during the postnatal period, and adult-level amplitudes were achieved only at P10 (Kováčiková et al., 2006). Similarly, molecular oscillations equivalent to those observed in adults were not detected in the fetal hamster SCN (Li and Davis, 2005). In mice, Shimomura et al. reported a significant oscillation in *Per1* but not in *Per2* mRNA in the SCN at E17, and that the amplitude of the oscillations increased progressively with postnatal age (Shimomura et al., 2001). The aforementioned data suggest that during fetal development, the SCN circadian clock is not able to generate high-amplitude synchronized oscillations in clock gene expression and, therefore, may not be able to function as a self-sustained clock.

In the present study, we aimed to determine whether and how swiftly the immature fetal and neonatal molecular SCN clock can be reset by maternal cues. The maternal SCN clock was shifted by a 6-h delay of the dark period at different stages of fetal SCN development. The impact of the shift on the prenatal SCN clock was assessed by determining profiles of spontaneous oscillations in *c-fos* and *Avp* expression on the 1st postnatal day. *c-fos* and *Avp* expression profiles were chosen as phase markers because clock gene expression exhibits only very low amplitude oscillations in the rat SCN at this developmental stage (Kováčiková et al., 2006). To investigate an impact of the shift on the molecular core clockwork in the SCN on the postnatal day 3 and 6, *Per1*

and *Per2* mRNA profiles were monitored because at these developmental stages amplitudes of both rhythms already allow determination of phase shifts. We assumed that a circadian clock that is not capable of generating synchronized molecular oscillations, as is the case for the fetal rat SCN, would not be entrained by maternal cues. However, we found a significant phase shift of the SCN clock at fetal developmental stages when no or only faint molecular oscillations were detected. This finding might suggest that maternal cues drive rather than entrain the immature fetal rat SCN clock.

MATERIALS AND METHODS

Animals

Male and female Wistar rats (Bio Test s.r.o., Konárovice, Czech Republic) were maintained for at least 4 weeks at a temperature of 23 ± 2 °C and under a light-dark cycle with 12 h of light and 12 h of darkness (LD 12:12) per day, with lights on from 0700 to 1900 h. The rats had free access to food and water throughout the whole experiment. Light was provided by overhead 40-W fluorescent tubes, and illumination was between 50 and 200 l× depending on cage position in the animal room. Vaginal smears were taken from females to determine the day of estrus; on the same day, females were mated with males. The day when female rats were found to be sperm-positive was designated embryonic day 0 (E0); the day of delivery, which occurred at about E22, was designated postnatal day 0 (P0).

All experiments were conducted under license No. A5228-01 with the U.S. National Institutes of Health and in accordance with Animal Protection Law of the Czech Republic (license No. 42084/2003-1020).

Experimental Protocol

On gestational days 18 and 20, pregnant rats were divided into 2 groups. A control group remained untreated under the previous LD regimen. The other group was exposed to a 6-h delay of 1 dark period, so that the light was switched off and on by 6 h later than before, that is, at 0100 and 1300 h, respectively (Fig. 1). At the next cycle, rats of both groups were released into constant darkness (DD) at 1900 h and were kept in darkness until pups were born and sampled at 2-h intervals at P0-1, P3, and P6. The time of the original light onset experienced by pregnant rats was designated as circadian time (CT) 0 and the time of the original light offset was designated as CT12. Simultaneously, adult male rats were subjected to treatment identical with that experienced by control and phase-shifted groups of pregnant rats, to provide evidence for the efficiency of the procedure for phase-delaying circadian rhythmicity within the adult SCN. Adult rats were monitored for locomotor activity and/or killed under anesthesia at 2-h intervals throughout the 24-h cycle, 3 or 5 days after the 6-h delay of the dark period. Pups were killed by rapid decapitation at 2-h intervals of the 24-h cycle at P0-1, P3, and P6. Brains were removed, immediately frozen on dry ice, and stored at –80 °C. They were sectioned into 5 series of 12-µm-thick slices in alternating order throughout the whole rostrocaudal extent of the SCN. Sections were further processed for *in situ* hybridization to determine profiles of *c-fos* mRNA and *Avp* hnRNA at P0-1 and in adults, and of *Per1* and *Per2* mRNA at P3, P6, and in adults.

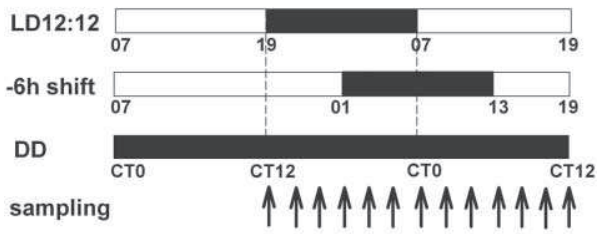

Figure 1. Experimental protocol for the shifting procedure. Pregnant rats were maintained in a light-dark cycle with 12 h of light and 12 h of darkness per day (LD 12:12) with lights on at 0700 h and lights off at 1900 h. On gestational day 18 or 20, rats were divided into 2 groups. For the group exposed to the shifting procedure, the light period was extended so that lights-off and lights-on were delayed by 6 h and occurred at 0100 h and 1300 h, respectively. Rats in the control group remained under the previous LD regimen. Thereafter, the lights were turned off at 1900 h. The next morning, the lights were not turned on and rats of both groups were maintained in constant darkness (DD) until sampling of their pups. Time of the original light onset was designated as CT0 and the time of the original offset as CT12. Pups were sampled at 2-h intervals at postnatal day P0-1, P3, and P6 starting at CT12. Simultaneously, adult male rats were subjected to treatments identical to those of the control and phase-shifted groups of pregnant rats and sampled 3 and 5 days after the treatment.

Locomotor Activity Monitoring

Adult male and female rats were maintained individually in cages equipped with infrared movement detectors attached above the center of the cage top, enabling detection of locomotor activity across the

whole cage. Activity was measured every minute using a circadian activity monitoring system (Dr. H.M. Cooper, INSERM, France) and was analyzed by Actiview Biological Rhythms Analysis software (Mini Mitter, Bend, OR). Double-plotted actograms were generated for visualization of data. The activity onset and offset was determined by 2 independent observers by fitting lines connecting at least 5 successive activity onsets or offsets by eye before and after the shift of the light-dark cycle.

In Situ Hybridization

The cDNA fragments of rat *c-fos* (1160 bp; corresponds to nucleotides 141-1300 of the sequence in GenBank accession number X06769), *Avp* (506 bp; identical to nucleotides 796-1302 of the intronic sequence in GenBank accession number X01637), *Per1* (980 bp; corresponds to nucleotides 581-1561 of the sequence in GenBank accession number AB002108), and *Per2* (1512 bp; corresponds to nucleotides 369-1881 of the sequence in GenBank with accession number NM031678) were used as templates for in vitro transcription of complementary RNA probes. The *Per1* and *Per2* fragment-containing vectors were generously donated by Professor H. Okamura (Kobe University School of Medicine, Kobe, Japan) and the *c-fos* fragment-containing vector was generously donated by Dr. Tom Curran (Children's Hospital of Philadelphia, Philadelphia, PA). The *Avp* cDNA was cloned in our laboratory (Kováčiková et al., 2006). Probes were labeled using ^{35}S-UTP, and the in situ hybridizations were performed as described previously (Kováčiková et al., 2006; Shearman et al., 2000; Sládek et al., 2004). The sections were hybridized for 20 h at 60 °C. Following a posthybridization wash, the sections were dehydrated in ethanol and dried. Finally, the slides were exposed to the film BIOMAX MR (Kodak) for 10 to 14 days and developed using the ADEFO-MIX-S developer and ADEFOFIX fixer (Adefo-Chemie Gmbh, Dietzenbach, Germany). Brain sections from control and phase-shifted animals were processed simultaneously under identical conditions.

Autoradiographs of sections were analyzed using an image analysis system (Image Pro, Olympus, New Hyde Park, NY) to detect relative optical density (OD) of the specific hybridization signal. In each animal, mRNA or hnRNA was quantified bilaterally, always at the midcaudal SCN section containing the strongest hybridization signal. Each measurement was corrected for nonspecific background by subtracting OD values from the same adjacent area in the hypothalamus. The background signal of that area served as an internal standard and it was consistently low and did not exhibit marked changes with time of the day. Finally, slides were counterstained with cresyl violet to check the presence and the midcaudal position of the SCN in each section. For each time point, 3 or 4 rats were killed. The OD for each animal was calculated as a mean of values for the left and right SCN.

Data Analysis

Data were analyzed by 2-way analysis of variance (ANOVA) for the group and time differences. Subsequently, the Student-Newman-Keuls multiple range test was used, with a significance level of $p < 0.05$. Cross-correlation analysis was used to test phase differences between the profiles of gene expression.

RESULTS

Effect of a 6-h Phase Delay of the Dark Period on the Locomotor Activity and Profiles of *c-fos*, *Avp*, *Per1*, and *Per2* Expression in the SCN of Adult Rats

We first aimed to determine how the shifting procedure affects the maternal SCN. Dynamics of the SCN entrainment in adult rats were assessed from the locomotor activity recordings before and after the 6-h shift of the dark period. A representative locomotor activity actogram is depicted in Figure 2. The phase delay of locomotor activity was apparent by the 3rd day after the shift of the dark phase.

To provide further evidence that the adult SCN had phase shifted, we determined daily profiles of *c-fos* and *Avp* expression on the 3rd day and of *Per1* and *Per2* expression on the 5th day after the delay of the dark period in the SCN of control rats and those exposed to the shifting procedure (shifted group).

For *c-fos* mRNA levels (Fig. 3A), the 2-way ANOVA revealed a significant effect of time ($F = 35.9$, $p < 0.001$). Although the effect of group was not significant, the highly significant interaction effect ($F = 10.2$, $p < 0.001$) suggested the presence of differences at specific time points between the *c-fos* mRNA profiles for the control and shifted groups. *c-fos* mRNA levels at CT24 and CT2 were significantly higher ($p < 0.001$) and levels at CT12 and CT6 were significantly lower ($p < 0.001$) in controls than in

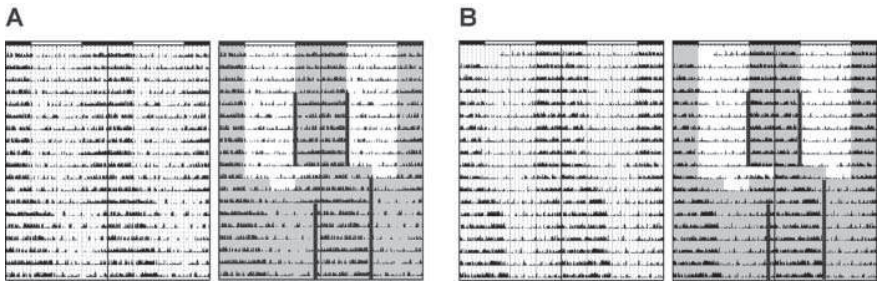

Figure 2. Representative double-plotted actogram of locomotor activity of 1 female (A) and 1 male (B) rat subjected to the experimental procedure described in Figure 1. The white and black bars on the top of the actogram represent the light and dark periods of the LD cycle prior to exposure to the shifting procedure. On the left side, the actogram shows raw data without labeling. On the right side, the actogram is depicted with a shaded area that marks time when the rat was maintained in darkness. Activity onset and offset before and after the phase shift was determined by 2 independent observers by fitting lines connecting at least 5 successive activity onsets or offsets by eye (the vertical lines on the right side actogram).

the shifted group. The entire daily profile of *c-fos* expression was phase delayed by about 2 h in animals exposed to the shifting procedure compared with the profile of control animals (correlation coefficient $R = 0.967$, $p < 0.001$).

For *Avp* hnRNA levels (Fig. 3B), the 2-way ANOVA revealed a significant effect of time ($F = 189.5$, $p < 0.001$) and of group ($F = 30.8$, $p < 0.001$) as well as a significant interaction effect ($F = 14.2$, $p < 0.001$). *Avp* hnRNA levels were significantly higher at CT22, CT24, and CT2 ($p < 0.001$) and significantly lower at CT12 ($p < 0.05$) in controls compared with the shifted group. Apparently, the rise but not the decline in *Avp* expression was phase delayed by about 2 h in animals exposed to the shifting procedure compared with the control animals (correlation coefficient $R = 0.977$, $p < 0.001$).

For *Per1* mRNA levels (Fig. 3C), the 2-way ANOVA revealed significant effects of time ($F = 167.4$, $p < 0.001$), group ($F = 6.2$, $p < 0.05$), and interaction ($F = 33.3$, $p < 0.001$). The levels were significantly higher at CT2 and CT4 ($p < 0.001$) and lower at CT12, CT14 ($p < 0.001$), and CT16 ($p < 0.05$) in the control than in the shifted group. The entire daily profile of *Per1* expression was phase delayed by about 2 h in animals exposed to the shifting procedure compared with the controls (correlation coefficient $R = 0.978$, $p < 0.001$).

For *Per2* mRNA levels (Fig. 3D), the 2-way ANOVA revealed a significant effect of time ($F = 58.7$, $p < 0.01$). Although the effect of group was not significant, the highly significant interaction effect ($F = 7.7$, $p < 0.001$) suggested the presence of differences at specific time points between the *Per2* expression profiles for the control and the shifted groups. *Per2* mRNA levels were significantly higher at CT2 and CT4 ($p < 0.001$) and significantly lower at CT18 ($p < 0.001$) in controls than in the shifted group. The entire daily profile of *Per2* expression was phase delayed by about 2 h in animals exposed to the shifting procedure compared with that of the control animals (correlation coefficient $R = 0.947$, $p < 0.001$).

Effect of the Maternal Phase Shift at E20 on Profiles of *c-fos* and *Avp* Expression in the SCN at P0-1 and of *Per1* and *Per2* Expression at P3 and P6

Our second aim was to investigate whether exposure of pregnant rats to the shifting procedure on gestational day 20 (E20) entrains the fetal SCN. To determine whether the shift could be accomplished during prenatal period within 3 days, the profiles of *c-fos* and *Avp* expression were assessed in newborn pups at P0-1. To determine whether the shift is detectable during the postnatal period, the profiles of *Per1* and *Per2* expression were determined at P3 and P6.

For levels of *c-fos* mRNA at P0-1 (Fig. 4A), the 2-way ANOVA revealed a significant effect of time ($F = 28.2$, $p < 0.001$) and of group ($F = 10.6$, $p < 0.01$) as well as a significant interaction effect ($F = 3.6$, $p < 0.001$). Although there were significant differences in *c-fos* mRNA levels between the control and the shifted group at specific time points, a significant rise in *c-fos* mRNA levels occurred at the same time, that is, at CT2, in controls and the shifted group. The elevated levels declined at CT16 in the control and at CT18 in the shifted group. Altogether, at P0-1, the profile of *c-fos* expression was not phase shifted in pups of mothers exposed to the shifting procedure at E20 compared with the profile of pups born to control mothers. The same hold true for *Avp* hnRNA profiles. At P0-1 (Fig. 4B), the 2-way ANOVA revealed a significant effect of time ($F = 22.1$, $p < 0.001$) and group ($F = 5.3$, $p < 0.05$), but not for the interaction. The daily profile of *Avp* expression in pups of mothers exposed to the shifting procedure at E20 was not phase shifted

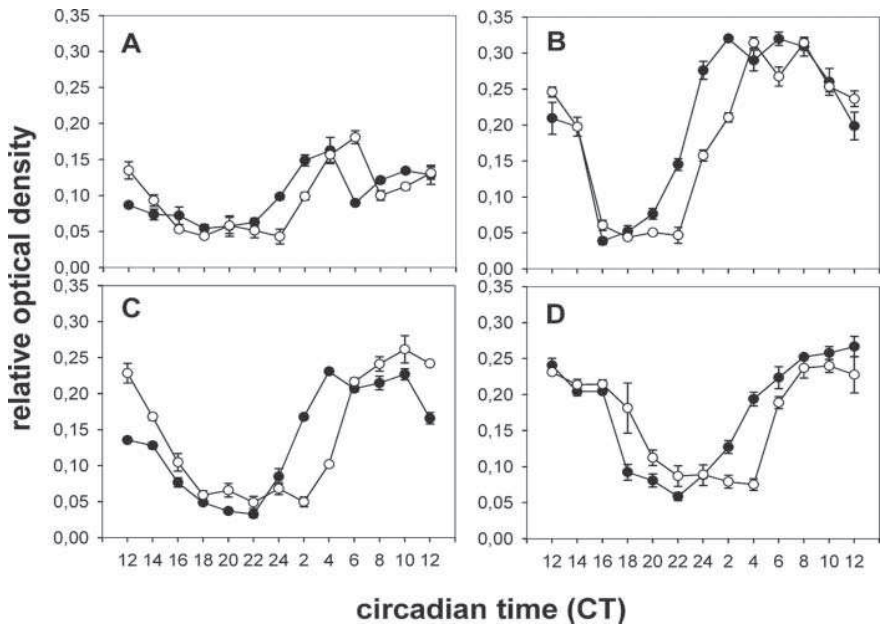

Figure 3. Effect of the shifting procedure on gene expression within the adult suprachiasmatic nucleus (SCN) clock. Daily profiles of *c-fos* (A), *Avp* (B), *Per1* (C), and *Per2* (D) mRNA were determined within the SCN of adult male rats. Control rats (full circles) were released into constant darkness and sampled 3 (A, B) and 5 (C, D) days later throughout the 24-h cycle starting at CT12. Group of rats exposed to the shifting procedure and released into darkness (open circles) were sampled 3 (A, B) and 5 (C, D) days after the treatment starting at CT12. For further details of experimental protocol, see Materials and Methods. Data represent mean values of 4 animals per time point and SEM.

relative to the profile of pups born to control mothers.

Regarding levels of *Per1* mRNA at P3 (Fig. 5A), the 2-way ANOVA revealed a significant effect of time ($F = 39.7$, $p < 0.001$). Although the effect of group was not significant, the highly significant interaction effect ($F = 6.3$, $p < 0.001$) suggested the presence of differences at specific time points between both groups. *Per1* mRNA levels at CT24, CT2, and CT4 were significantly higher ($p < 0.001$) and at CT8, CT10, and CT12 significantly lower ($p < 0.001$, 0.05, and 0.001, respectively) in controls compared with the shifted group. Similarly, at P6 (Fig. 5C), the 2-way ANOVA revealed a significant effect of time ($F = 24.1$, $p < 0.001$) though not of group for levels of *Per1* mRNA. However, the highly significant interaction effect ($F = 6.2$, $p < 0.001$) suggested that there may indeed be differences between the control and the shifted group. *Per1* mRNA levels were significantly higher at CT24 ($p < 0.05$), CT2, and CT4 ($p < 0.001$) and lower at CT8, CT10 ($p < 0.01$), and CT14 ($p < 0.001$) in the control group compared with the shifted group. Altogether, at P3 as well as at P6, the entire daily profile of *Per1* expression was phase delayed by about 2 h in pups born to mothers exposed to the shifting procedure at E20 relative to the profile of pups born to control mothers (correlation coefficient $R = 0.988$ and 0.920, respectively, $p < 0.001$).

For levels of *Per2* mRNA at P3 (Fig. 5B), the 2-way ANOVA revealed a significant effect of time ($F = 50.9$, $p < 0.001$) and of group ($F = 12.9$, $p < 0.001$) as well as a significant interaction effect ($F = 11.2$, $p < 0.001$). *Per2* mRNA levels at CT14 ($p < 0.001$), CT16, and CT18 ($p < 0.01$) were significantly lower and at CT24 and CT8 ($p < 0.001$) were significantly higher in controls than in the shifted group. Similarly for levels of *Per2* mRNA at P6 (Fig. 5D), the 2-way ANOVA revealed a significant effect of time ($F = 89.1$, $p < 0.001$). Although the effect of group was not significant, a highly significant interaction effect ($F = 8.5$, $p < 0.001$) again suggested the presence of differences at specific time points in the expression profiles for the control and the shifted group. *Per2* mRNA levels were significantly higher at CT2 and CT4 ($p < 0.001$) and lower at CT18 ($p < 0.001$) in controls compared with the shifted group. In summary, at P3 as well as at P6, the entire daily profile of *Per2* expression was phase delayed by about 2 h in pups born to mothers exposed to the shifting procedure at E20 relative to the profile of pups born to control mothers (correlation coefficient $R = 0.934$ and 0.950, respectively, $p < 0.001$).

The data indicate that the fetal SCN did not entrain in parallel with the maternal SCN, that is, within 3 days after the shifting procedure, but rather later during the postnatal period at P3, that is, within 5 days after the shift. A similar phase delay as that observed at P3 was also confirmed at P6.

Effect of the Maternal Shift at E18 on Profiles of *c-fos* and *Avp* Expression in the SCN at P0-1

To elucidate whether the prenatal SCN can be entrained by maternal cues, pregnant rats were

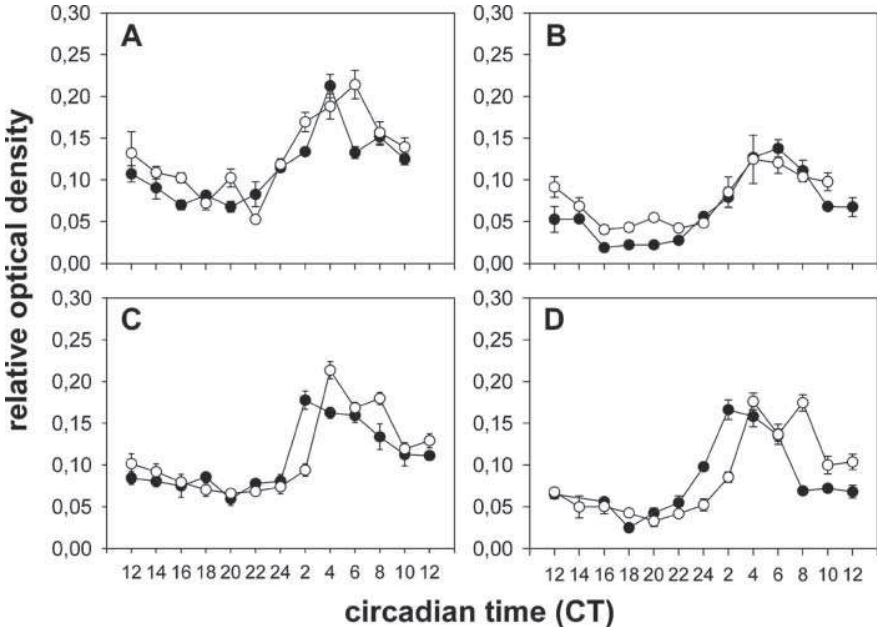

Figure 4. Effect of the shifting procedure on gene expression within the prenatal suprachiasmatic nucleus (SCN) clock. Daily profiles of *c-fos* mRNA (A, C) and *Avp* hnRNA (B, D) were determined within the SCN of pups at P0-1 born either to control mothers (full circles) or to those exposed to the shifting procedure (open circles) at gestational day 20 (A, B) or 18 (C, D). For further details of the experimental protocol, see Material and Methods. Data represent mean values of 4 (occasionally 3) animals per time point and SEM.

exposed to the shifting procedure at E18 rather than at E20, and profiles of *c-fos* and *Avp* gene expression were determined in the newborn pups at P0-1. This experimental design allowed the fetal SCN to be exposed to the shifting maternal entraining cues for 5 days instead of 3 days, that is, for the same time interval as the period between a shift at E20 and sampling of pups at P3 (see above). This arrangement permitted exclusively prenatal maternal cues to impinge on the pup's SCN.

For levels of *c-fos* mRNA at P0-1 (Fig. 4C), the 2-way ANOVA revealed a significant effect of time ($F = 47.6$, $p < 0.001$). The effect of group was not significant, but a highly significant interaction effect ($F = 8.0$, $p < 0.001$) implied differences at specific time points between the control and the shifted group. *c-fos* mRNA level at CT2 was significantly higher ($p < 0.001$) and at CT4 and CT8 lower ($p < 0.001$) in the control compared with the shifted group. The daily profile of *c-fos* expression in pups born to mothers exposed to the shifting procedure at E18 appeared to be phase delayed by about 2 h relative to the profile of pups born to control mothers (correlation coefficient $R = 0.963$, $p < 0.001$).

For levels of *Avp* hnRNA at P0-1 (Fig. 4D), the 2-way ANOVA revealed a significant effect of time ($F = 39.7$, $p < 0.001$). The effect of group was not significant, but the highly significant interaction effect ($F = 9.2$, $p < 0.001$) indicated the presence of differences at specific time points between the control and the shifted group. *Avp* hnRNA levels at CT24 and CT2 were significantly higher ($p < 0.01$ and $p < 0.001$, respectively) and at CT8, CT10, and CT12 lower ($p < 0.001$, $p < 0.05$, and $p < 0.01$, respectively) in the control compared with the shifted group. At P0-1, the entire daily profile in *Avp* expression in pups born to mothers exposed to the shifting procedure at E18 was phase delayed by about 2 h relative to the profile of pups born to control mothers (correlation coefficient $R = 0.920$, $p < 0.001$).

These data indicate that the fetal SCN did entrain within 5 days after exposure of pregnant rats to the shifting procedure at E18.

DISCUSSION

Our data demonstrate that exposure of pregnant rats to a 6-h delay in the dark period induced a significant phase delay in the profiles of *c-fos* and *Avp* expression within the newborn pup's SCN at P0-1 if the shifting procedure was performed at E18, but not at E20. The shifting procedure at E20 was, however, able to phase-shift the profile of *Per1* and *Per2* expression in pups at P3 and P6.

The efficiency of the procedure for phase-shifting the maternal SCN clock was proven by a noted phase delay of locomotor activity as well as of profiles of *c-fos*, *Avp*, *Per1*, and *Per2* gene expression within the SCN of adult rats. Locomotor activity recordings revealed that exposure of adult rats to the shifting procedure induced a significant phase delay within 3 days after shift. On the 3rd and 5th day after the shifting procedure, profiles of *c-fos* and *Avp*, and *Per1* and

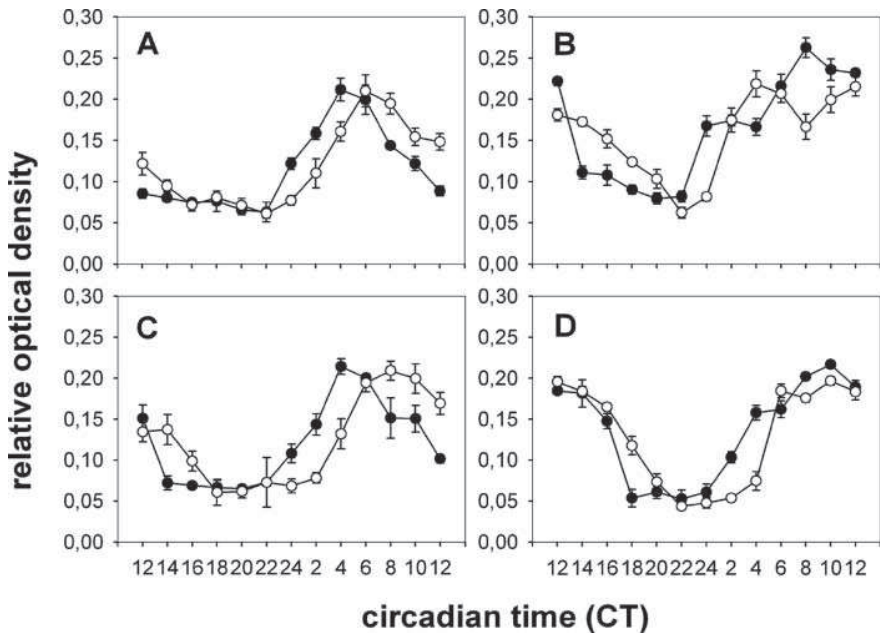

Figure 5. Effect of the shifting procedure on gene expression within the postnatal suprachiasmatic nucleus (SCN) clock. Daily profiles of *Per1* (A, C) and *Per2* (B, D) mRNA were determined within the SCN of rat pups at P3 (A, B) and P6 (C, D) born to control mothers (full circles) and those exposed to the shifting procedure at gestational day 20 (open circles). For further details of the experimental protocol, see Materials and Methods. Data represent mean values of 4 animals per time point and SEM.

Per2, gene expression, respectively, within the SCN of adult rats released into DD were significantly phase delayed compared with the profiles of control rats. Similarly, another study showed that profiles of *Per1*, *Per2*, and *Cry1* expression in the mouse SCN were phase delayed within 2 cycles after the mice were exposed to a 6-h delay of the LD cycle and kept in a new LD regimen (Reddy et al., 2002). The magnitude of phase delays was larger, however, in mice held in LD than in rats kept under DD conditions. Nevertheless, our data clearly demonstrate that after the shifting procedure and subsequent release of rats into DD, the adult and hence also the most likely maternal SCN was significantly phase delayed. The delay was clearly detectable on the 3rd day after the shift both at the locomotor activity as well as the gene expression profile levels.

In newborn rat pups at P0-1, significant circadian rhythms in *c-fos* and *Avp* expression were detected (this study; Kováčiková et al., 2006; Leard et al., 1994). Therefore, we used profiles of *c-fos* mRNA and *Avp* hnRNA as phase markers of circadian rhythmicity within the newborn SCN. At P3 and P6, we used *Per1* and *Per2* mRNA profiles as phase markers of the rhythmicity, as our recent studies have shown that those rhythms exhibit already significant amplitude at these developmental stages. In previous studies, maternal entrainment during fetal stages was studied by monitoring various overt rhythms postnatally, for example, the pineal arylalkylamine N-acetyltranferase in rats after P10 (Reppert and Schwartz, 1986b; Duncan et al., 1986), the running wheel activity and drinking behavior rhythm in rats and hamsters following weaning (Davis and Gorski, 1985a,1985b; Viswanathan et al., 1994; Weaver and Reppert, 1989; Bellavia et al., 2006), or the corticosterone rhythm after P28 (Honma et al., 1984). The general outcome of the studies was that the fetal SCN was entrained by maternal cues. However, in these reports, a relatively long time elapsed between manipulation of pregnant rats and the recording period, and, therefore, postnatal entraining cues might have also interfered. In the fetal rat SCN, a rhythm in metabolic activity detected by 2-deoxyglucose uptake was used to study maternal entrainment (Reppert and Schwartz, 1984, 1986a). Usually, 1 day time point and 1 night time point were determined and significance of difference between the 2 time points increased between E19 and E21 (Reppert and Schwartz, 1984). After complete surgical removal of the maternal SCN, the day-night difference was abolished (Reppert and Schwartz, 1986b). It was concluded that this resulted from a desynchronization of the rhythms between individual fetuses rather than to loss of the fetal SCN rhythmicity. The maternal SCN was thus recognized as an important component of maternal entrainment during fetal development.

In the current study, we examined the impact of a phase shift of an intact maternal SCN on the phase of the newborn rat SCN. Exposure of mothers to a 6-h delay of the dark period at E18 induced a significant phase delay in the rhythms of *c-fos* and *Avp* expression

in the SCN of newborn pups at P0-1. As pregnant rats were released into DD immediately after the manipulation and pups were born in darkness, the observed phase shift in both gene expression profiles was accomplished solely by nonphotic maternal cues during the fetal development. This phase delay was similar to the phase shift observed in adult rats. However, when the same shifting procedure was applied to pregnant rats at E20, profiles of *c-fos* and *Avp* expression at P0-1 were not phase shifted. This result could not be attributed to the possibility that the phase-shifting of the maternal SCN had not completed within 3 days (see above), nor to the possibility that the fetal SCN was not sensitive to the shift, because a significant delay in the *Per1* and *Per2* expression profiles was detected at P3 and at P6. Rather, it seems that the interval elapsing between the maternal manipulation and detection of the phase shift within the pup's SCN is important: 5 days were necessary for phase-shifting the pup's SCN clock by maternal cues, whether the interval between E18 and P0-1 or the interval between E20 and P3. In contrast, only 3 days were needed to significantly phase-shift the adult and hence also maternal SCN by photic cues. Our data thus support the hypothesis that the maternal SCN is necessary for entrainment of the fetal SCN clock. If entrainment of the fetal SCN were mediated independently of the maternal SCN, for example, via a direct effect of a cue upon the fetal SCN, the maternal and fetal SCN would shift at the same rate.

Our results show for the first time a maternal entrainment of rhythms in clock gene expression at such early developmental stages. In previous studies, only about 2-h phase shifts of *Per1* and *Per2* rhythms were demonstrated at P6 in the SCN of blinded pups, induced by nursing of the pups by foster mothers synchronized to a reverse LD cycle. Between P6 and P13, maternal cues were ineffective (Ohta et al., 2002). The ability of maternal cues to entrain the pup's molecular clockwork thus decreases during postnatal development. Maternal entrainment is gradually replaced by developing photic entrainment, which may be capable of overriding the maternal cues after P6 (Duncan et al., 1986).

The most intriguing question that still remains is what is the substrate that mediates the maternal entrainment of the fetal SCN clock. In the rat SCN, synchronized spontaneous rhythms in the SCN clock gene expression had only begun to develop and the rhythm in clock-controlled *Avp* gene expression was not detectable by late fetal stages (Kováčiková et al., 2006; Sládek et al., 2004). This might result from a lack of intercellular communication between individual SCN neurons at fetal stages when the rate of synaptogenesis was still very low. Indeed, the increase in amplitude of clock gene expression rhythms nicely paralleled synaptogenesis; the amplitude achieved the adult-like magnitude only at P10 when synaptogenesis was completed. The data suggest that only a small population of the SCN cells may be spontaneously rhythmic during late fetal stage. As synapses gradually maturate during early postnatal development, more and more SCN cells may become synchronized and rhythmic. Alternatively, a minority of the SCN cells may become rhythmic because they are selectively sensitive to the cyclically appearing maternal SCN-derived cues. These cues might, in turn, directly drive the activity of these cells during fetal stages. Later on, as synaptogenesis progresses, previously insensitive cells may also become rhythmic, allowing development of the autonomous SCN clock to proceed spontaneously. With the gradual development of the autonomous clock, the original mechanism that drove the rhythmicity might become redundant. The developmental decline in sensitivity of the SCN clock to maternal cues may favor the latter hypothesis. To achieve more insight into the underlying mechanisms, future studies should investigate the nature of the maternal entraining cues and the phenotype of the rhythmic fetal SCN cells.

ACKNOWLEDGMENTS

The authors thank Prof. Helena Illnerová for her heplful comments on the manuscript and Eva Suchanová and Jiri Sedlmajer for their excellent technical assistance. The authors' work is supported by the Grant Agency of the Czech Republic, Grant Nos. 309050350, 309080503, and 30908H079, by Research Project Nos. AV0Z50110509, LC554, and by the 6th Framework Project EUCLOCK No. 018741.

REFERENCES

Bellavia SL, Carpentieri AR, Vaque AM, Macchione AF, and Vermouth NT (2006) Pup circadian rhythm entrainment—Effect of maternal ganglionectomy or pinealectomy. Physiol Behav 89:342-349.

Burbach JP, Luckman SM, Murphy D, and Gainer H (2001) Gene regulation in the magnocellular hypothalamo-neurohypophysial system. Physiol Rev 81:1197-1267.

Davis FC and Gorski RA (1985a) Development of hamster circadian rhythms. I. Within-litter synchrony of mother

and pup activity rhythms at weaning. Biol Reprod 33:353-362.
Davis FC and Gorski RA (1985b) Development of hamster circadian rhythms: Prenatal entrainment of the pacemaker. J Biol Rhythms 1:77-89.
Duncan MJ, Banister MJ, and Reppert SM (1986) Developmental appearance of light-dark entrainment in the rat. Brain Res 369:326-330.
Fu L and Lee CC (2003) The circadian clock: Pacemaker and tumor suppressor. Nat Rev Cancer 3:350-361.
Honma S, Honma KI, Shirakawa T, and Hiroshige T (1984) Maternal phase setting of fetal circadian oscillation underlying the plasma corticosterone rhythm in rats. Endocrinology 114:1791-1796.
Iwasaki Y, Oiso Y, Saito H, and Majzoub JA (1997) Positive and negative regulation of the rat vasopressin gene promoter. Endocrinology 138:5266-5274.
Jud C and Albrecht U (2006) Circadian rhythms in murine pups develop in absence of a functional maternal circadian clock. J Biol Rhythms 21:149-154.
Klein DC, Moore RY, and Reppert SM, eds (1991) *Suprachiasmatic Nucleus: The Mind's Clock*. New York: Oxford University Press.
Ko CH and Takahashi JS (2006) Molecular components of the mammalian circadian clock. Hum Mol Genet 15(Spec No 2):R271-R277.
Kováčiková Z, Sládek M, Bendová Z, Illnerová H, and Sumová A (2006) Expression of clock and clock-driven genes in the rat suprachiasmatic nucleus during late fetal and early postnatal development. J Biol Rhythms 21:140-148.
Leard LE, Macdonald ES, Heller HC, and Kilduff TS (1994) Ontogeny of photic-induced c-fos mRNA expression in rat suprachiasmatic nuclei. Neuroreport 5:2683-2687.
Li X and Davis FC (2005) Developmental expression of clock genes in the Syrian hamster. Dev Brain Res 158:31-40.
Moore RY (1991) Development of the suprachiasmatic nucleus. In *Suprachiasmatic Nucleus: The Mind's Clock*, DC Klein, RY Moore, and SM Repperts, eds, pp 197-216, New York, Oxford University Press.
Ohta H, Honma S, Abe H, and Honma K (2002) Effects of nursing mothers on rPer1 and rPer2 circadian expressions in the neonatal rat suprachiasmatic nuclei vary with developmental stage. Eur J Neurosci 15:1953-1960.
Ohta H, Honma S, Abe H, and Honma K (2003) Periodic absence of nursing mothers phase-shifts circadian rhythms of clock genes in the suprachiasmatic nucleus of rat pups. Eur J Neurosci 17:1628-1634.
Pittendrigh CL (1981) Circadian systems: Entrainment. In *Handbook of Behavioral Neurology*, Vol. 4, J Aschoff, ed, pp 95-124, New York, Plenum.
Reddy AB, Field MD, Maywood ES, and Hastings MH (2002) Differential resynchronisation of circadian clock gene expression within the suprachiasmatic nuclei of mice subjected to experimental jet lag. J Neurosci 22:7326-7330.
Reppert SM and Schwartz WJ (1984) The suprachiasmatic nuclei of the fetal rat: Characterization of a functional circadian clock using 14C-labeled deoxyglucose. J Neurosci 4:1677-1682.
Reppert SM and Schwartz WJ (1986a) Maternal endocrine extirpations do not abolish maternal coordination of the fetal circadian clock. Endocrinology 119:1763-1767.
Reppert SM and Schwartz WJ (1986b) Maternal suprachiasmatic nuclei are necessary for maternal coordination of the developing circadian system. J Neurosci 6: 2724-2729.
Reppert SM and Uhl GR (1987) Vasopressin messenger ribonucleic acid in supraoptic and suprachiasmatic nuclei: Appearance and circadian regulation during development. Endocrinology 120:2483-2487.
Reppert SM and Weaver DR (2001) Molecular analysis of mammalian circadian rhythms. Annu Rev Physiol 63:647-676.
Shearman LP, Sriram S, Weaver DR, Maywood ES, Chaves I, Zheng B, Kume K, Lee CC, van der Horst GT, Hastings MH, et al. (2000) Interacting molecular loops in the mammalian circadian clock. Science 288:1013-1019.
Shibata S and Moore RY (1987) Development of neuronal activity in the rat suprachiasmatic nucleus. Brain Res 431:311-315.
Shimomura H, Moriya T, Sudo M, Wakamatsu H, Akiyama M, Miyake Y, and Shibata S (2001) Differential daily expression of Per1 and Per2 mRNA in the suprachiasmatic nucleus of fetal and early postnatal mice. Eur J Neurosci 13:687-693.
Sládek M, Sumová A, Kováčiková Z, Bendová Z, Laurinová K, and Illnerová H (2004) Insight into molecular core clock mechanism of embryonic and early postnatal rat suprachiasmatic nucleus. Proc Natl Acad Sci U S A 101:6231-6236.
Sumová A, Bendová Z, Sládek M, El-Hennamy R, Matějů K, Polidarová L, Sosniyenko S, and Illnerová H (2008) Circadian molecular clocks ticking along ontogenesis. Physiol Res, May 13 (Epub ahead of print).
Viswanathan N, Weaver DR, Reppert SM, and Davis FC (1994) Entrainment of the fetal hamster circadian pacemaker by prenatal injections of the dopamine agonist SKF 38393. J Neurosci 14:5393-5398.
Weaver DR and Reppert SM (1989) Periodic feeding of SCN-lesioned pregnant rats entrains the fetal biological clock. Dev Brain Res 46:291-296.
Weinert D (2005) Ontogenetic development of the mammalian circadian system. Chronobiol Int 22:179-205.

EJN fens European Journal of Neuroscience

European Journal of Neuroscience, Vol. 29, pp. 490–501, 2009 doi:10.1111/j.1460-9568.2009.06609.x

MOLECULAR AND DEVELOPMENTAL NEUROSCIENCE

Development of the light sensitivity of the clock genes *Period1* and *Period2*, and immediate-early gene *c-fos* within the rat suprachiasmatic nucleus

Kristýna Matějů, Zdena Bendová, Rehab El-Hennamy, Martin Sládek, Serhiy Sosniyenko and Alena Sumová
Institute of Physiology, v.v.i., Academy of Sciences of the Czech Republic, Prague, Czech Republic

Keywords: circadian clock, ontogenesis, photic entrainment

Abstract

The molecular mechanism underlying circadian rhythmicity within the suprachiasmatic nuclei (SCN) of the hypothalamus has two light-sensitive components, namely the clock genes *Per1* and *Per2*. Besides, light induces the immediate-early gene *c-fos*. In adult rats, expression of all three genes is induced by light administered during the subjective night but not subjective day. The aim of the present study was to ascertain when and where within the SCN the photic sensitivity of *Per1*, *Per2* and *c-fos* develops during early postnatal ontogenesis. The specific aim was to find out when the circadian clock starts to gate photic sensitivity. The effect of a light pulse administered during either the subjective day or the first or second part of the subjective night on gene expression within the rat SCN was determined at postnatal days (P) 1, 3, 5 and 10. *Per1*, *Per2* and *c-fos* mRNA levels were assessed 30 min, 1 and 2 h after the start of each light pulse by *in situ* hybridization histochemistry. Expression of *Per1* and *c-fos* was light responsive from P1, and the responses began to be gated by the circadian clock at P3 and P10, respectively. Expression of *Per2* was only slightly light responsive at P3, and the response was not fully gated until P5. These data demonstrate that the light sensitivity of the circadian clock develops gradually during postnatal ontogenesis before the circadian clock starts to control the response. The photoinduction of the clock gene *Per2* develops later than that of *Per1*.

Introduction

In a non-periodic environment, many behavioural, physiological and molecular events in mammals exhibit self-sustained rhythms with a period close to 24 h. These circadian rhythms are driven by a master circadian pacemaker that resides in the suprachiasmatic nuclei (SCN) of the hypothalamus (Ralph *et al.*, 1989; Klein *et al.*, 1991; LeSauter *et al.*, 1996). The SCN circadian rhythmicity is generated by a system of interconnected transcriptional–translational feedback loops composed of clock genes and their protein products (reviewed in Ko & Takahashi, 2006). Light entrains circadian rhythms to the period of the solar day, i.e. exactly 24 h, via resetting the phase of the circadian pacemaker (Daan & Pittendridgh, 1976). Exposure to light during the first part of the subjective night delays and during the second part advances the phase of circadian rhythms. During the subjective day, light does not affect the circadian phase. This gating of light sensitivity to the specific time of day represents a formal property of the circadian clock itself that enables the entrainment of the endogenous rhythms to a light–dark cycle (Klein *et al.*, 1991). The mechanism by which light entrains the circadian clock has not yet been fully elucidated. At a molecular level, the phase-shifting effect of light correlates with the induction of expression of the clock genes *Per1* and *Per2* within the SCN (Shigeyoshi *et al.*, 1997; Albrecht *et al.*, 2001). In the adult rat SCN, *Per1* expression is sensitive to light during the subjective night, when the level of the endogenously expressed *Per1* is low, but not during the subjective day, when the endogenous *Per1* expression is high (Shearman *et al.*, 1997). Expression of *Per2* appears to be sensitive to light only during the early subjective night when endogenous *Per2* mRNA levels decline (Yan *et al.*, 1999; Miyake *et al.*, 2000). Spontaneous *Per1* and *Per2* expression exhibit circadian rhythms mostly in the dorsomedial part of the SCN (dmSCN), the site of the self-sustained circadian rhythmicity. In contrast, photoinduction of *Per1* occurs within the ventrolateral part of the SCN (vlSCN; Yan & Okamura, 2002; Yan & Silver, 2004), where the retinohypothalamic tract (RHT) that conveys photic information from the retina terminates (Johnson *et al.*, 1988). Apart from the clock genes, the expression of the immediate-early gene *c-fos* within the vlSCN is induced by phase-shifting light pulses (Aronin *et al.*, 1990; Rusak *et al.*, 1990). Though *c-fos* does not participate in the core clockwork mechanism and its role in the photic entrainment pathway has not been proven, the SCN clock precisely gates its induction in the vlSCN so that it occurs only at the time when the intrinsic clock rhythmicity is reset by photic stimuli (Jelínková *et al.*, 2000). All of these data suggest that the vlSCN is responsible for the entrainment of the circadian clock by light.

The mammalian circadian system matures gradually during ontogenesis (for a review, see Weinert, 2005). In the rat, the prenatal period lasts about 22 days, and neurogenesis within the SCN is completed roughly 5 days before birth (Moore, 1991). Synaptogenesis within the SCN develops during the late prenatal and early postnatal periods,

Correspondence: Dr A. Sumová, as above.
E-mail: sumova@biomed.cas.cz

Received 12 August 2008, revised 20 November 2008, accepted 4 December 2008

increasing rapidly from postnatal day (P) 4 to P10 (Moore & Bernstein, 1989). The SCN begins to be innervated by the RHT at P1, and the connections reach their adult levels near P10 (Speh & Moore, 1993). Although the eyes open at about P15, light already induces the expression of *c-fos* within the SCN at P1 (Leard *et al.*, 1994). Light sensitivity develops further gradually between P3 and P10 (Bendová *et al.*, 2004). The spontaneous expression of the clock genes *Per1* and *Per2* is detectable within the rat SCN before birth, but the mRNA levels of these genes do not exhibit pronounced circadian rhythms (Sládek *et al.*, 2004). Low-amplitude circadian rhythms of *Per1* and *Per2* expression are detectable by P1 and P2, respectively (Kováčiková *et al.*, 2006). The rhythms then mature gradually during early postnatal ontogenesis with increases in their amplitudes (Sládek *et al.*, 2004).

While ontogenesis of the light-induced expression of *c-fos* has been studied in rats (Weaver & Reppert, 1995; Bendová *et al.*, 2004) as well as other species, it is not yet known when during ontogenesis light begins to induce *Per1* and *Per2* expression within the SCN. Therefore, the aim of this study was to elucidate when and where within the rat SCN the photic sensitivity of *Per1* and *Per2* develops during the early postnatal ontogenesis and compare it with development of *c-fos* photoinduction. The specific aim was to uncover when the circadian clock begins to gate the sensitivity to light and, therefore, when it likely begins to be entrained by photic cues.

Materials and methods

Animals

Male and female Wistar rats (BioTest s.r.o.; Konárovice, Czech Republic) were maintained under a light–dark regime with 12 h of light and 12 h of darkness per day (LD12 : 12) at a temperature of 23 ± 2°C with free access to the food and water. Light was provided by overhead 40-W fluorescent tubes, and illumination was between 50 and 200 lux, depending on the cage position. Animals were maintained at LD12 : 12 for at least 4 weeks before mating. The day of delivery was designated as P0.

All experiments were conducted under license no A5228-01 with the U.S. National Institutes of Health, and in accordance with Animal Protection Law of the Czech Republic (license no. 42084/2003-1020).

Experimental protocol

Female rats with their pups were released into constant darkness at the time of dark to light transition (designated as circadian time 0; CT0) on P1, P3, P5 or P10. During the first cycle in darkness, experimental groups of pups were exposed to a 30-min light pulse (700 lux) at either CT7 (i.e. during subjective day), CT15 (i.e. during the first part of subjective night) or CT21 (i.e. during the second part of subjective night); control groups were left untreated in darkness. Pups from both groups were subjected to maternal deprivation from the beginning of the light pulse in experimental animals until the time of decapitation and rapid tissue sampling at 30 min, 1 h and 2 h after the start of each light pulse. At each of these time points, four to eight animals from the light-pulsed group and four control animals were sampled. Whole heads (at P1, P3 and P5) or brains (at P10) were immediately frozen on dry ice and stored at −80°C.

Adult male Wistar rats were exposed to light pulses and sampled using the experimental schedule described above. Three (occasionally four) experimental and control animals at each time point were deeply anaesthetized by intraperitoneal injection of thiopental (Valeant Czech Pharma s.r.o., Praha, Czech Republic; 50 mg/kg) and decapitated. Brains were removed, immediately frozen on dry ice and stored at −80°C.

Whole heads or brains were sectioned into series of 12-μm-thick coronal slices in an alternating order throughout the rostral-caudal extent of the SCN. Levels of *rPer1*, *rPer2* and *c-fos* mRNA were assessed by *in situ* hybridization. To delineate the position of the dm-part within the developing SCN, expression of arginin–vasopressin (*rAVP*) hnRNA was detected in a few sections from control animals at P1, P3, P5 and P10 (see Dardente *et al.*, 2002; Hamada *et al.*, 2004). The position of the vl-part of the developing SCN was delineated according to the area of *c-fos* expression in sections from light-pulsed animals at P1, P3, P5 and P10.

In situ *hybridization histochemistry*

The cDNA fragments of rat *rPer1* (980 bp; corresponds to nucleotides 581–1561 of the sequence in GenBank accession no AB002108), rat *rPer2* (1512 bp; corresponds to nucleotides 369–1881 of the sequence in GenBank accession no NM031678), rat *c-fos* (1160 bp; corresponds to nucleotides 141–1300 of the sequence in GenBank accession no X06769) and rat *rAVP* (506 bp; corresponds to nucleotides 796–1302 of the intronic sequence in GenBank accession no. X01637) were used as templates for *in vitro* transcription of complementary RNA probes (T7, T3 or SP6 MAXIscript kit, Applied Biosystems/Ambion, Austin, TX, USA). The *rPer1* and *rPer2* fragment-containing vectors were generously donated by Professor H. Okamura (Kobe University School of Medicine, Japan). The rat *c-fos* fragment-containing vector (originally cloned by Dr Tom Curran from Children's Hospital of Philadelphia, PA, USA) was generously donated by Professor W. J. Schwartz (University of Massachusetts Medical School, Worcester, MA, USA). The whole cDNA was recloned into a pBluescript SK vector (Stratagene, La Jolla, CA, USA) in our laboratory. The *rAVP* fragment-containing vector was cloned in our laboratory (Kováčiková *et al.*, 2006). Probes were labelled by α-^{35}S-UTP (MP Biomedicals, Irvine, CA, USA) and purified using Chroma-Spin 100-DEPC H2O columns (Clontech Laboratories, Mountain View, USA). *In situ* hybridization was performed as described previously (Shearman *et al.*, 2000; Sládek *et al.*, 2004). Briefly, sections were hybridized for 21 h at 60°C. Following a post-hybridization wash, the sections were dehydrated in ethanol and dried. Finally, the slides were exposed to a BioMax MR film (Kodak) for 10 days (*rPer1*, *rPer2*), 12 days (*rAVP*) or 14 days (*c-fos*), and the film was developed in film processor Optimax (PROTEC GmbH, Oberstenfeld, Germany) using AdefoMix and AdefoFix solutions (ADEFO-CHEMIE GmbH, Dietzenbach, Germany). For each gene, sections of the SCN from pups of the same age were hybridized with the same probe and processed simultaneously under identical conditions.

Film autoradiographs of sections were analysed by an image analysis system ImagePro (Olympus, New Hyde Park, NY, USA) to detect the relative optical density (OD) of the specific hybridization signal in the SCN. In each animal, the mRNA level was quantified bilaterally at the mid-caudal SCN section containing the strongest hybridization signal. Each measurement was corrected for non-specific background by subtracting the OD values from neighbouring areas expected to be free of specific signal and thus serving as their own internal standard. The OD value for each animal was calculated as the mean of the left and right SCN relative OD values.

To differentiate spatial distribution of the mRNA signal within the SCN, slides from three light-pulsed and three control animals for each time point were dipped in autoradiographic emulsion LM-1 (Amersham Biosciences, Piscataway, NJ, USA). After 6 weeks of exposure, the slides were developed using the developer Fomatol LQN and fixer

FOMAFIX (FOMA, Hradec Králové, Czech Republic) and mounted for optical microscopy. Representative pictures of emulsion autoradiographs were taken using a digital Olympus DP70 camera (Olympus, New Hyde Park, NY, USA) connected to an Olympus Ax-70 microscope (Olympus). For delineating the position and shape of the SCN on brain sections from pups at P1, P3, P5 and P10, and for comparison with the signal area on the autoradiographic film and/or emulsion, parallel sections were counterstained with Cresyl violet. The intensity of the signal may depend on the thickness of the emulsion, which may vary slightly across the slides. Therefore, the results from emulsion autoradiography were used only for spatial resolution of the signal and not for quantification of the signal intensity.

Statistical analysis

Mean values of relative OD from control and experimental animals were compared at each time point using a *t*-test. Data were expressed as the percentage of the highest mean value ± SEM. For *Per1*, *Per2* and *c-fos* mRNA expression at P1, data from two independent experiments were converted into the percentage of the highest mean value, pooled and analysed with a *t*-test.

Results

Light sensitivity of Per1*,* Per2 *and* c-fos *expression within the SCN of rat pups and adult animals*

First, we investigated the effect of a 30-min light pulse delivered at CT7 (i.e. during the subjective day), CT15 or CT21 (i.e. during the first or second part of the subjective night) on the expression of the clock genes *Per1* and *Per2* and immediate-early gene *c-fos* within the SCN of both rat pups at P1, P3, P5 and P10 and adult animals. To reveal the dynamics of the photic response, the expression of each gene was detected 30 min, 1 h and 2 h after the beginning of the light

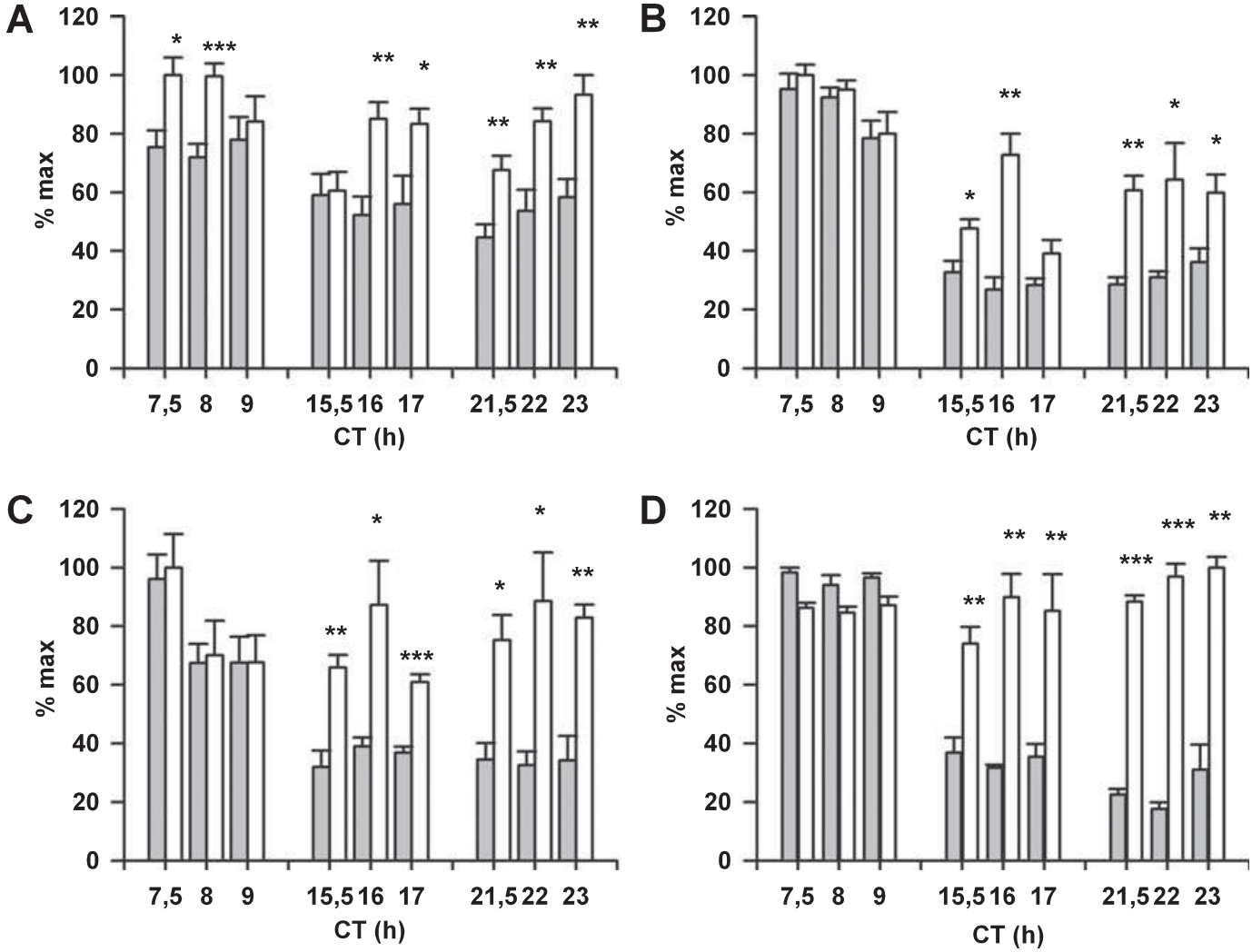

FIG. 1. Effect of light pulses on *Per1* mRNA within the SCN of rat pups at P1, 3, 5 and 10. Rat pups at (A) P1, (B) P3, (C) P5 and (D) P10 were released into constant darkness and exposed to a 30-min light pulse (700 lux) during the subjective day (CT7) or first (CT15) or second (CT21) part of the subjective night. Control pups were left in darkness. Levels of *Per1* mRNA within the SCN of control (dark columns) and light-pulsed (open columns) animals were assessed by *in situ* hybridization histochemistry. The mRNA levels were measured 30 min, 1 h and 2 h after the start of each light pulse (depicted by three couples of control-pulsed/dark-open columns for CT7, CT15 and CT21). The levels of mRNA were determined as the relative OD of the signal in the SCN region measured on autoradiographic film. Data were expressed as the percentage of the maximum OD value. Each column represents the mean of six to eight (at P1) or four (occasionally three; at P3, P5 and P10) animals ± SEM. *$P < 0.05$; **$P < 0.01$; ***$P < 0.001$ (*t*-test). Time is expressed as circadian time (CT), where CT12 corresponds to the time of the previous lights-off and CT24 corresponds to the time of the previous lights-on.

pulse and compared with expression in controls sampled in darkness at the corresponding CT.

At P1, the levels of *Per1* mRNA (Fig. 1A) increased significantly above the corresponding control levels following light pulses delivered at CT7 (CT7.5: $t_{11} = -2.97$, $P = 0.0127$; CT8: $t_{13} = -4.29$, $P = 0.0009$), CT15 (CT16: $t_{12} = -3.82$, $P = 0.0024$; CT17: $t_{12} = -2.47$, $P = 0.0294$) and CT21 (CT21.5: $t_{13} = -3.46$, $P = 0.0042$; CT22: $t_{14} = -3.61$, $P = 0.0028$; CT23: $t_{14} = -3.83$, $P = 0.0018$). At P3 (Fig. 1B), P5 (Fig. 1C) and P10 (Fig. 1D), *Per1* mRNA levels increased significantly above control levels following light pulses administered at CT15 and CT21, but not CT7, and the response occurred as early as 30 min after the beginning of each light pulse: the levels of *Per1* mRNA increased at P3 (CT15.5: $t_5 = -3.06$, $P = 0.0282$; CT16: $t_6 = -5.49$, $P = 0.0015$; CT21.5: $t_6 = -5.79$, $P = 0.0012$; CT22: $t_6 = -2.63$, $P = 0.0388$; CT23: $t_6 = -3.04$, $P = 0.0227$), P5 (CT15.5: $t_6 = -4.84$, $P = 0.0029$; CT16: $t_6 = -3.15$, $P = 0.0199$; CT17: $t_5 = -7.37$, $P = 0.0007$; CT21.5: $t_5 = -3.68$, $P = 0.0143$; CT22: $t_6 = -3.24$, $P = 0.0177$; CT23: $t_5 = -5.54$, $P = 0.0026$) and P10 (CT15.5: $t_4 = -4.83$, $P = 0.0084$; CT16: $t_4 = -7.29$, $P = 0.0019$; CT17: $t_6 = -3.77$, $P = 0.0092$; CT21.5: $t_6 = -22.27$, $P = 0.0001$; CT22: $t_6 = -16.23$, $P = 0.0001$; CT23: $t_5 = -6.55$, $P = 0.0012$).

For *Per2* mRNA levels at P1 (Fig. 2A), no statistical differences between the control groups and pups exposed to light pulses at CT7, CT15 and CT21 were detected. At P3 (Fig. 2B), *Per2* mRNA levels increased only 1 h ($t_6 = -3.32$, $P = 0.0161$) and 2 h ($t_6 = -5.05$, $P = 0.0023$) after the beginning of a light pulse administered at CT21, whereas the administration of light pulses at CT7 and CT15 did not increase significantly *Per2* mRNA levels. At P5 (Fig. 2C), *Per2* mRNA levels increased following light pulses administered at CT15 (CT16: $t_6 = -6.68$, $P = 0.0005$; CT17: $t_5 = -10.39$, $P = 0.0001$) and CT21 (CT22: $t_5 = -2.81$, $P = 0.0374$; CT23: $t_6 = -4.46$, $P = 0.0043$), but a low induction 2 h after the light pulse at CT7 was also detected ($t_6 = -3.05$, $P = 0.0224$). At P10 (Fig. 2D), levels of *Per2* mRNA

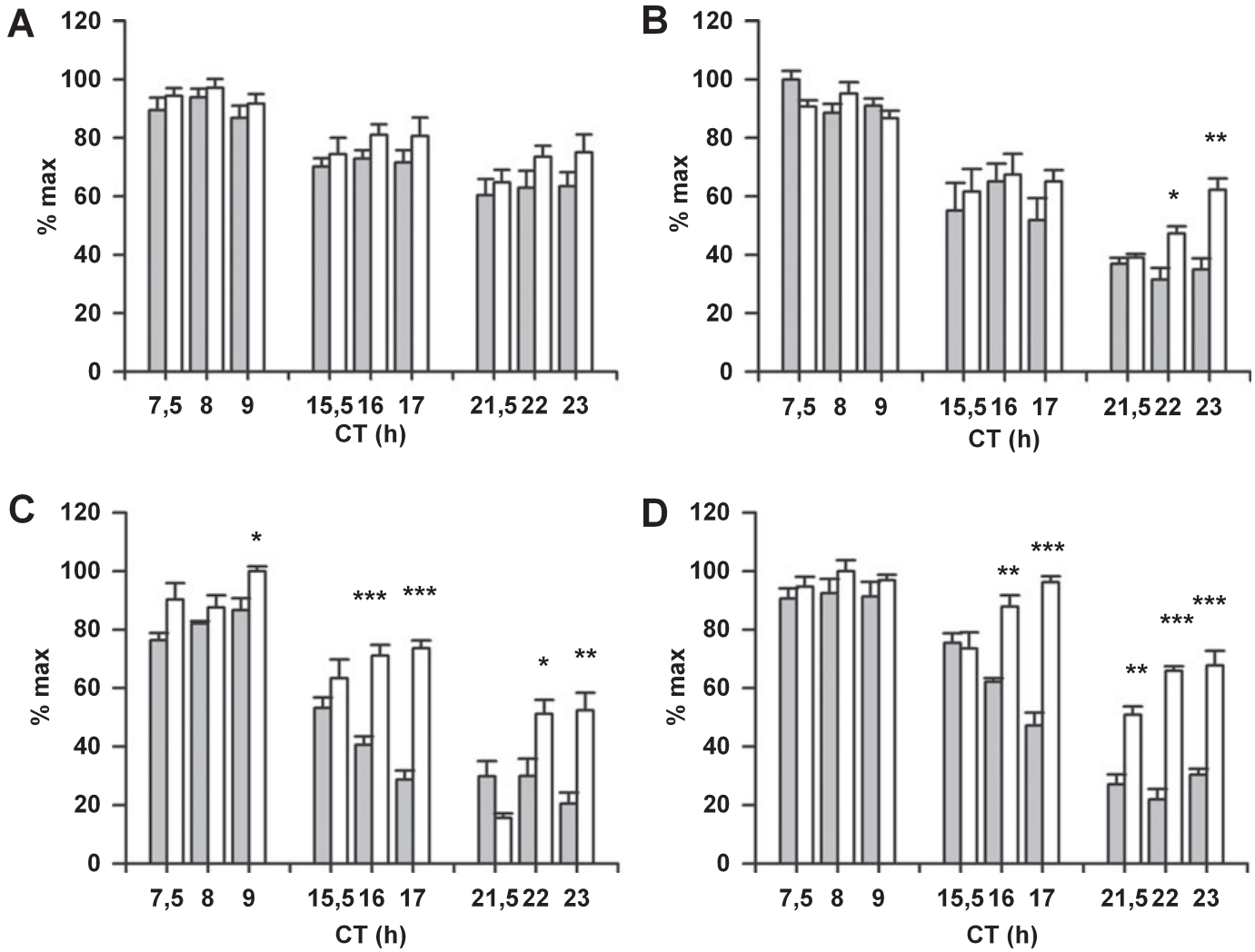

FIG. 2. Effect of light pulses on *Per2* mRNA within the SCN of rat pups at P1, 3, 5 and 10. Rat pups at (A) P1, (B) P3, (C) P5 and (D) P10 were released into constant darkness and exposed to a 30-min light pulse (700 lux) during the subjective day (CT7) or first (CT15) or second (CT21) part of the subjective night. Control pups were left in darkness. Levels of *Per2* mRNA within the SCN of control (dark columns) and light-pulsed (open columns) animals were assessed by *in situ* hybridization histochemistry. The mRNA levels were measured 30 min, 1 h and 2 h after the start of each light pulse (depicted by three couples of control-pulsed/dark-open columns for CT7, CT15 and CT21). The levels of mRNA were determined as the relative OD of the signal in the SCN region measured on autoradiographic film. Data were expressed as the percentage of the maximum OD value. Each column represents the mean of six to eight (at P1) or four (occasionally three; at P3, P5 and P10) animals ± SEM. *$P < 0.05$; **$P < 0.01$; ***$P < 0.001$ (*t*-test). Time is expressed as circadian time (CT), where CT12 corresponds to the time of the previous lights-off and CT24 corresponds to the time of the previous lights-on.

increased significantly above control levels following light pulses administered at CT15 (CT16: $t_4 = -6.33$, $P = 0.0032$; CT17: $t_5 = -11.21$, $P = 0.0001$) and CT21 (CT21.5: $t_6 = -5.42$, $P = 0.0016$; CT22: $t_6 = -11.33$, $P = 0.0001$; CT23: $t_5 = -7.83$, $P = 0.0005$), but not CT7.

Similarly to *Per1*, the levels of *c-fos* mRNA at P1 (Fig. 3A) increased significantly above the corresponding control levels following light pulses delivered at CT7 (CT7.5: $t_{13} = -3.09$, $P = 0.0087$; CT8: $t_{13} = -5.93$, $P = 0.0001$; CT9: $t_{13} = -2.89$, $P = 0.0126$), CT15 (CT15.5: $t_{14} = -11.87$, $P = 0.0001$; CT16: $t_{13} = -13.87$, $P = 0.0001$; CT17: $t_{12} = -5.07$, $P = 0.0003$) and CT21 (CT21.5: $t_{12} = -6.10$, $P = 0.0001$; CT22: $t_{12} = -6.91$, $P = 0.0001$; CT23: $t_{14} = -2.88$, $P = 0.0121$). At P3 (Fig. 3B), P5 (Fig. 3C) and P10 (Fig. 3D), *c-fos* mRNA levels increased significantly above control levels after the light pulses administered at CT15 and CT21, but not CT7: the levels of *c-fos* mRNA increased at P3 (CT15.5: $t_5 = -15.04$, $P = 0.0001$; CT16: $t_6 = -15.21$, $P = 0.0001$; CT17: $t_5 = -57.72$, $P = 0.0006$; CT21.5: $t_6 = -13.78$, $P = 0.00001$; CT22: $t_6 = -16.76$, $P = 0.0001$; CT23: $t_6 = -14.58$, $P = 0.0001$), P5 (CT15.5: $t_6 = -26.68$, $P = 0.0001$; CT16: $t_4 = -34.39$, $P = 0.0001$; CT17: $t_5 = -3.76$, $P = 0.01312$; CT21.5: $t_5 = -26.84$, $P = 0.0001$; CT22: $t_5 = -4.09$, $P = 0.0094$; CT23: $t_6 = -10.95$, $P = 0.0001$) and P10 (CT15.5: $t_5 = -18.48$, $P = 0.0001$; CT16: $t_5 = -10.08$, $P = 0.0002$; CT17: $t_5 = -5.99$, $P = 0.0019$; CT21.5: $t_6 = -16.61$, $P = 0.0001$; CT22: $t_6 = -24.09$, $P = 0.0001$; CT23: $t_5 = -6.33$, $P = 0.0015$). While *Per1* and *Per2* mRNA levels after the nighttime light pulses increased to levels roughly as high as endogenous daytime levels (with the exception of *Per2* photoinduction at CT21), *c-fos* mRNA levels remarkably exceeded the elevated daytime levels. From visual comparison between the developmental stages (Figs 1–3) it appears that the circadian clock starts to gate its photosensitivity gradually. The light-induced responses within the SCN at P1 were either not gated by

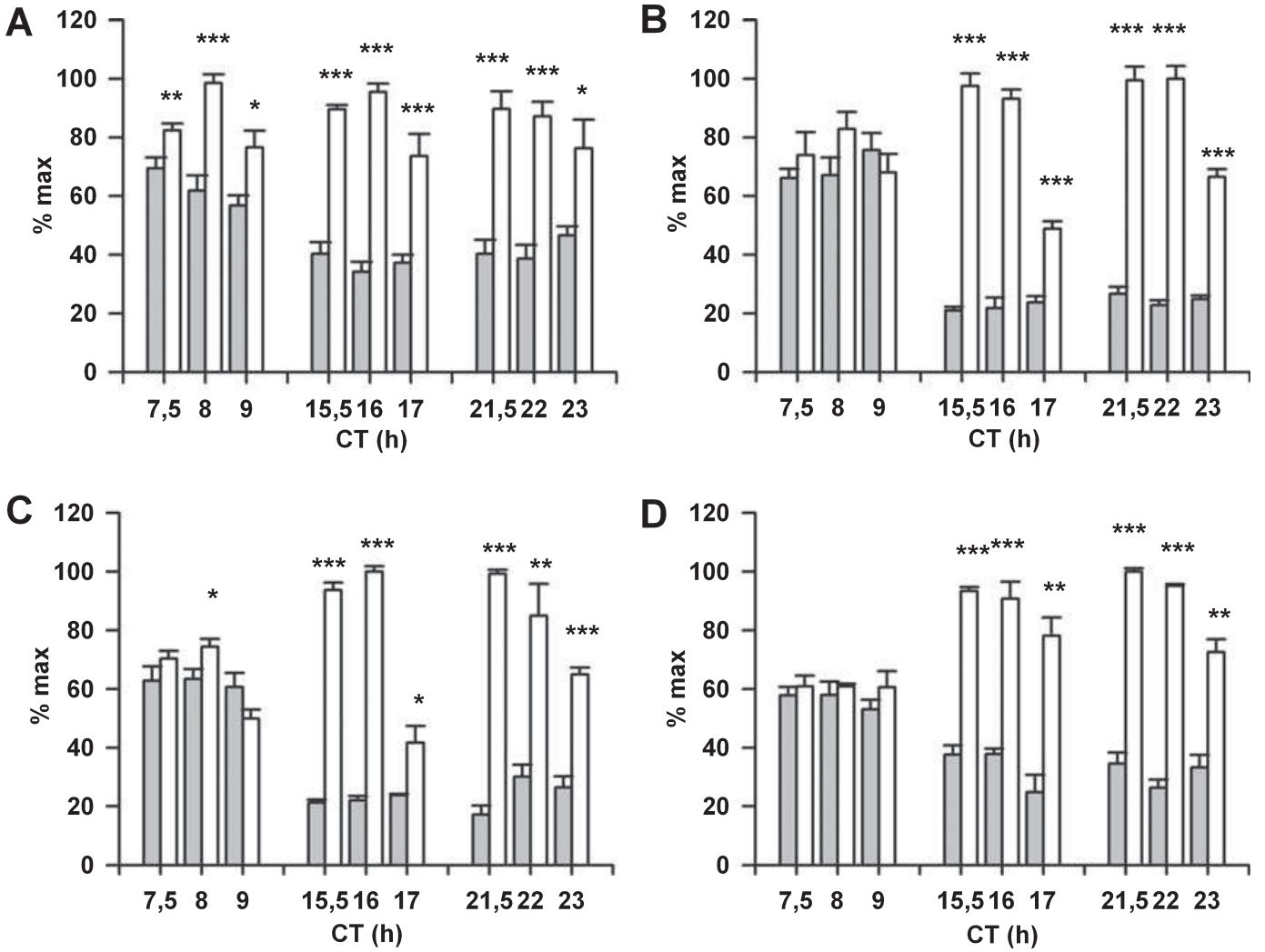

FIG. 3. Effect of light pulses on *c-fos* mRNA within the SCN of rat pups at P1, 3, 5 and 10. Rat pups at (A) P1, (B) P3, (C) P5 and (D) P10 were released into constant darkness and exposed to a 30-min light pulse (700 lux) during the subjective day (CT7) or first (CT15) or second (CT21) part of the subjective night. Control pups were left in darkness. Levels of *c-fos* mRNA within the SCN of control (dark columns) and light-pulsed (open columns) animals were assessed by *in situ* hybridization histochemistry. The mRNA levels were measured 30 min, 1 h and 2 h after the start of each light pulse (depicted by three couples of control-pulsed/dark-open columns for CT7, CT15 and CT21). The levels of mRNA were determined as the relative OD of the signal in the SCN region measured on autoradiographic film. Data were expressed as the percentage of the maximum OD value. Each column represents the mean of six to eight (at P1) or four (occasionally three; at P3, P5 and P10) animals ± SEM. *$P < 0.05$; **$P < 0.01$; ***$P < 0.001$ (*t*-test). Time is expressed as circadian time (CT), where CT12 corresponds to the time of the previous lights-off and CT24 corresponds to the time of the previous lights-on.

the circadian clock (*Per1* and *c-fos*) or were not yet significant (*Per2*). At P3, light induced *Per1* and *c-fos* expression only during subjective night but not during subjective day. Therefore, the response to photic stimuli seems to be already gated by the circadian clock. However, the expression of *Per2* was still only marginally sensitive to light at this developmental stage. At P5, the response of all examined genes to light pulses was restricted mostly to the subjective night; following the daytime light pulse, only marginal responses were detected. Hence, the circadian clock gates the photic response in gene expression at P5, but the gating mechanism may not yet be completely precise at this developmental stage. At P10, the response of gene expression to light pulses occurred only during the subjective night but not during the subjective day. Therefore, it was completely gated by the circadian clock.

For comparison with the above-mentioned data, the sensitivity of gene expression to photic stimuli was determined within the SCN of adult rats. Levels of *Per1* (Fig. 4A) and *c-fos* (Fig. 4C) mRNA were induced by a light pulse administered at CT15 and CT21, but not at CT7. For *Per1* mRNA, the levels increased significantly above the control levels at CT15.5 ($t_6 = -3.11$, $P = 0.0208$), CT16 ($t_4 = -3.25$, $P = 0.0314$), CT17 ($t_5 = -3.13$, $P = 0.0261$), CT21.5 ($t_4 = -4.79$, $P = 0.0087$) and CT22 ($t_4 = -3.08$, $P = 0.0367$). For *c-fos* mRNA, the levels increased significantly at CT15.5 ($t_6 = -10.40$, $P = 0.0001$), CT16 ($t_4 = -2.99$, $P = 0.0404$), CT17 ($t_4 = -4.71$, $P = 0.0092$), CT21.5 ($t_4 = -4.84$, $P = 0.0084$) and CT22 ($t_4 = -10.18$, $P = 0.0005$). Light-induced *Per1* mRNA levels corresponded roughly to high endogenous daytime levels, whereas photoinduced *c-fos* mRNA levels significantly exceeded the highest daytime levels. *Per2* expression (Fig. 4B) was induced significantly 2 h after the light pulse administered at CT15 (CT17: $t_3 = -5.37$, $P = 0.0126$), but it reached only control levels 1 h earlier. Slight *Per2* photoinduction was also suggested 30 min and 1 h after the light pulse at CT21, but the rise in *Per2* mRNA levels was not significant in comparison to control levels. Light pulse administered at CT7 did not affect significantly *Per2* mRNA levels. These data demonstrate that *Per1*, *Per2* and *c-fos* gene expression in the adult SCN are induced by light pulses administered during the subjective night but not subjective day. Therefore, the response to light is fully gated by the circadian clock. In our experiments, photoinduction of *Per1* differed from that of *Per2* not only in the timing but also in the magnitude of the response.

Spatial distribution of photic induction of Per1*,* Per2 *and* c-fos *expression within the SCN of the developing rat*

Further, we aimed to differentiate the spatial distribution of endogenously expressed and photoinduced *Per1*, *Per2* and *c-fos* mRNAs within the SCN during early ontogenesis. To accomplish this task, slides exposed to films to determine relative signal intensities were

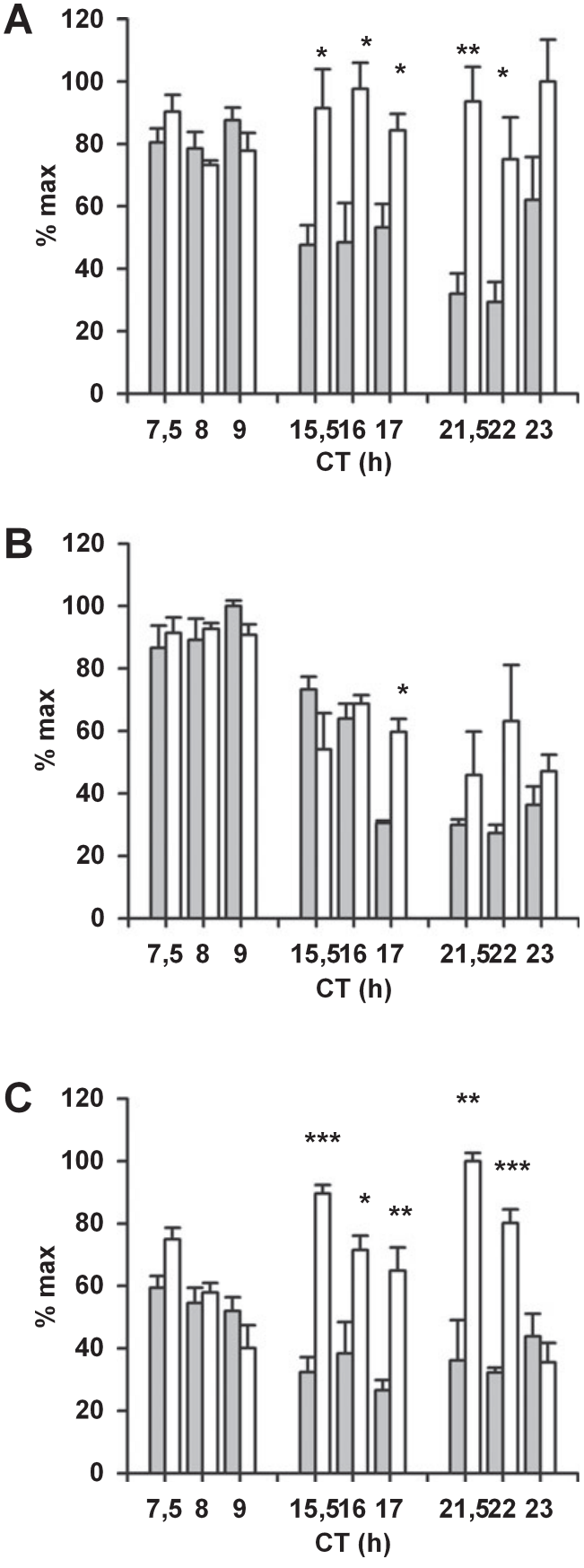

FIG. 4. Effect of light pulses on levels of *Per1*, *Per2* and *c-fos* mRNA within the SCN of adult rats. Adult male Wistar rats were released into constant darkness, and either left in darkness (controls; dark columns) or exposed to a 30-min light pulse during the subjective day (CT7) or first (CT15) or second (CT21) part of the subjective night, and sampled 30 min, 1 h and 2 h later (open columns). Levels of (A) *Per1*, (B) *Per2* and (C) *c-fos* within the SCN were assessed by *in situ* hybridization histochemistry. The levels of mRNA were determined as the relative OD of the signal in the SCN region measured on autoradiographic film. Data were converted to the percentage of the maximum OD value. Each column represents the mean of three (occasionally four or two) values ± SEM. *$P < 0.05$; **$P < 0.01$; ***$P < 0.001$ (*t*-test). For further details, see the legend of Fig. 1. CT, circadian time.

covered by an autoradiographic emulsion and developed 6 weeks later. To delineate the dmSCN region, the endogenous expression of *Avp* hnRNA was assessed on some slices from control pups. The vlSCN region was characterized as the area of *c-fos* photoinduction in pups at the same developmental stage. Emulsion autoradiography revealed that *Avp* hnRNA was detected at P1 in only a few cells and, therefore, the dmSCN region could not be delineated using this approach at such an early age (data not shown). At P3, P5 and P10, the *Avp* hnRNA signal was localized within the dmSCN and could thus be used for characterization of the dmSCN region at these developmental stages. Figure 5 depicts representative autoradiographs with *Avp* hnRNA and *c-fos* mRNA signal within the SCN at P3 and P10.

The distribution of endogenous *Per1* mRNA (Fig. 6, control) changed during development. At P1, the signal overlapped the entire area of the SCN. At P3, P5 and P10, spontaneous *Per1* expression prevailed primarily within the dmSCN. The administration of light pulses (Fig. 6, pulse) induced *Per1* mRNA mostly within the vlSCN. An exception to this trend occurred at P1 after a light pulse at CT7 (Fig. 6A), when *Per1* expression was induced within the whole SCN 30 min and 1 h after the light pulse. Light pulses administered during the subjective night (Fig. 6B and C) induced *Per1* mRNA levels within a thin layer at the ventral border of the SCN at P1, and the area of photoinduced signal expanded gradually with age. At P10, this area already resembled the adult vlSCN pattern.

The distribution of endogenously expressed *Per2* mRNA (Fig. 7, control) at P1, P3, P5 and P10 prevailed primarily within the dmSCN. Light pulse administered at CT7 (Fig. 7A) did not affect the intensity or distribution of the autoradiographic signals in comparison to controls at any of the studied developmental stages. Similarly, administration of a light pulse at CT15 (Fig. 7B) and CT21 (Fig. 7C) at P1 did not affect the intensity and distribution of the signal. At P3, the intensity of the signal after a light pulse at CT15 (Fig. 7B) did not change; however, it increased significantly in the vlSCN 1 and 2 h after a light pulse at CT21 (Fig. 7C). At P5 and P10, a light pulse administered at CT15 (Fig. 7B) induced *Per2* expression within the entire area of the SCN, while a pulse at CT21 (Fig. 7C) induced expression mostly within the vlSCN.

At P1, P3, P5 and P10, the endogenous expression of *c-fos* (Fig. 8A, control) was located exclusively within the dmSCN. The administration of a light pulse at CT7 (Fig. 8A, pulse) induced *c-fos* expression primarily within a thin layer at the ventral border of the SCN at P1, P3 and P5 and throughout the vlSCN at P10. At P10, the intensity of the signal following the pulse did not exceed the endogenous dmSCN signal. The signal intensity of the entire SCN was thus not increased, and photoinduction was consequently not recognized by film autoradiography (see Fig. 3). Following the administration of light pulses at CT15 (Fig. 8B, pulse) and CT21 (Fig. 8C, pulse), *c-fos* expression was induced mainly at the ventral border of SCN at P1, and the ventrolateral area spread in the dorsal direction between P3 and P10. Interestingly, at P1, both these nighttime light pulses induced *c-fos* expression within the dm-part of the SCN as well. This response weakened at P3 and disappeared thereafter. At all developmental stages, the intensity of the vlSCN signal after nighttime light pulses greatly exceeded that of the dmSCN. In addition, nighttime light pulses induced *c-fos* expression very rapidly, i.e. within 30 min, and light-induced levels declined markedly 2 h after the beginning of the light pulse.

Discussion

In this study, we demonstrate the temporal and spatial development of the photosensitivity of the canonical clock genes *Per1* and *Per2* and of immediate-early gene *c-fos* within the rat SCN during the early postnatal period. *Per1* and *c-fos* expression were sensitive to light pulses on the first postnatal day, whereas expression of *Per2* was sensitive only on the third. At P1, the expression of *Per1* and *c-fos* was

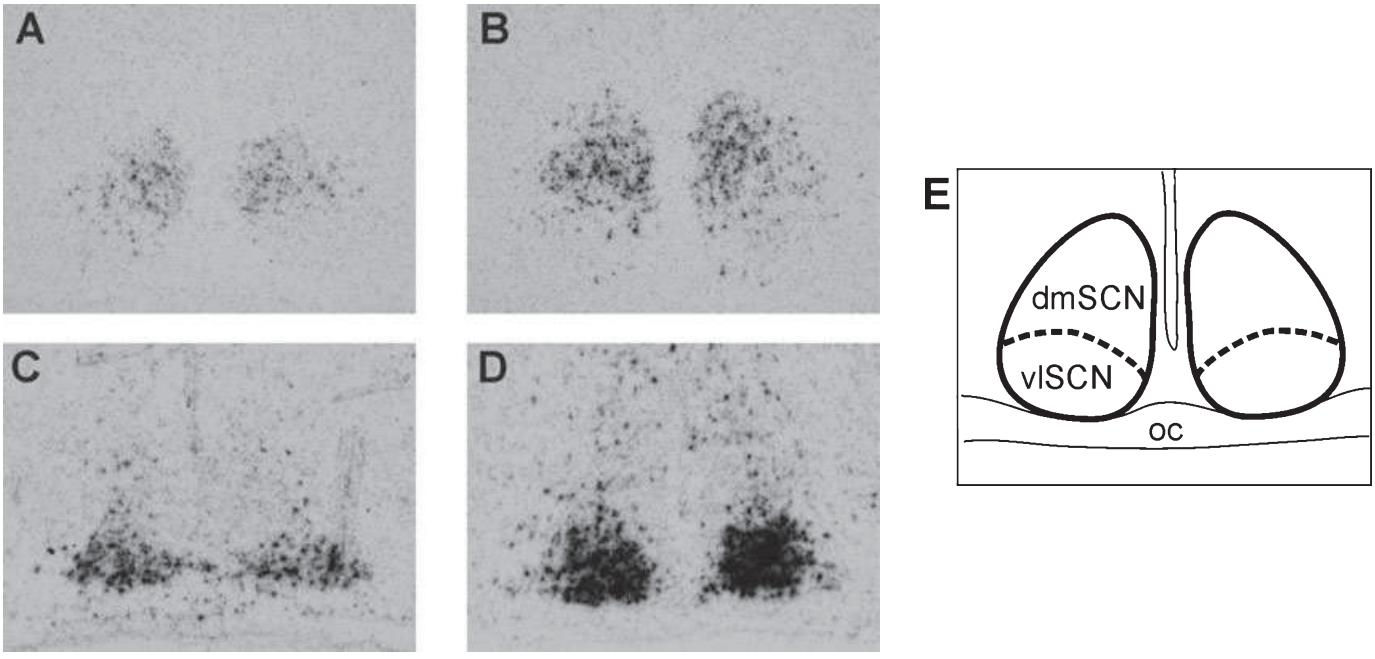

FIG. 5. Compartmentalization of the rat SCN during early postnatal ontogenesis. Representative emulsion autoradiographs delineate the distribution of cells exhibiting spontaneous *Avp* (A, B) and light-induced *c-fos* (C, D) expression within the SCN at P3 (A, C) and P10 (B, D). The images were used as templates to determine the areas of the dorsomedial (A, B) and ventrolateral (C, D) regions of the SCN at early developmental stages. The template is schematically summarized in (E). dmSCN, dorsomedial part of the suprachiasmatic nucleus; oc, optic chiasm; vlSCN, ventrolateral part of the suprachiasmatic nucleus.

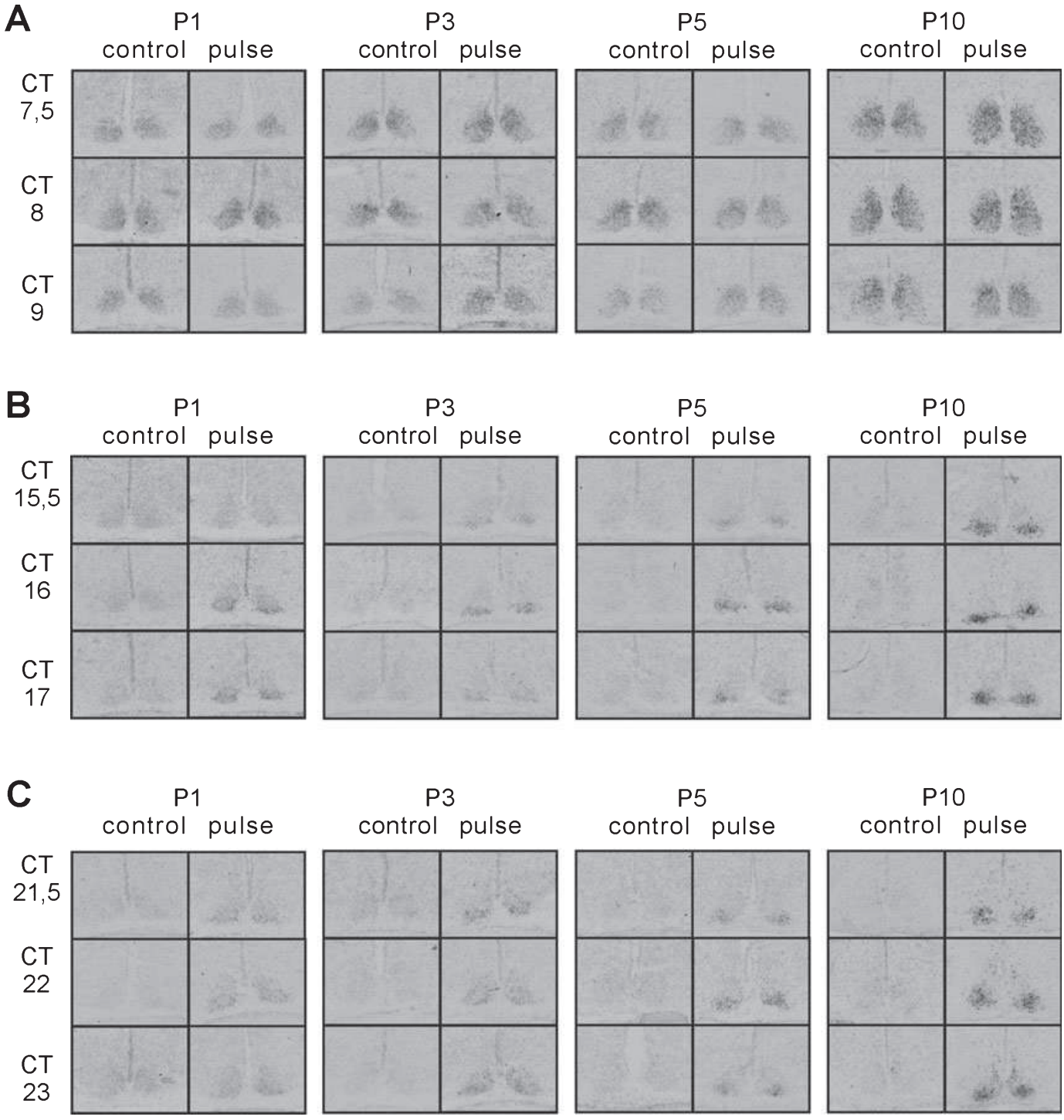

FIG. 6. Spatio-temporal distribution of *Per1* expression within the SCN of rat pups. Representative emulsion autoradiographs demonstrating the distribution of *Per1* expression in SCN sections of rat pups at P1, P3, P5 and P10. Pups were either kept in darkness (control) or exposed to a 30-min light pulse at (A) CT7, (B) CT15 or (C) CT21 (pulse), and sampled 30 min (CT7.5, CT15.5, CT21.5), 1 h (CT8, CT16, CT22) and 2 h (CT9, CT17, CT23) after the start of each light pulse. Note: the intensity of the signal on individual emulsion autoradiographs may not exactly reflect the relative mRNA levels (for details, see Materials and methods). CT, circadian time; P, postnatal day.

induced by light pulses delivered during either the nighttime or daytime. Apparently, the newborn pups lack the mechanism present in adult animals that restricts photic responses to the nighttime. The gating mechanism was present at P3, though it developed gradually further with age.

Our data, which demonstrate the photosensitivity of the rat SCN already during the first postnatal day, are in accordance with earlier reports on *c-fos* photoinduction at this developmental stage (Leard *et al.*, 1994). In the present study, light pulses at P1 affected not only *c-fos* expression as the neuronal activity marker but also the

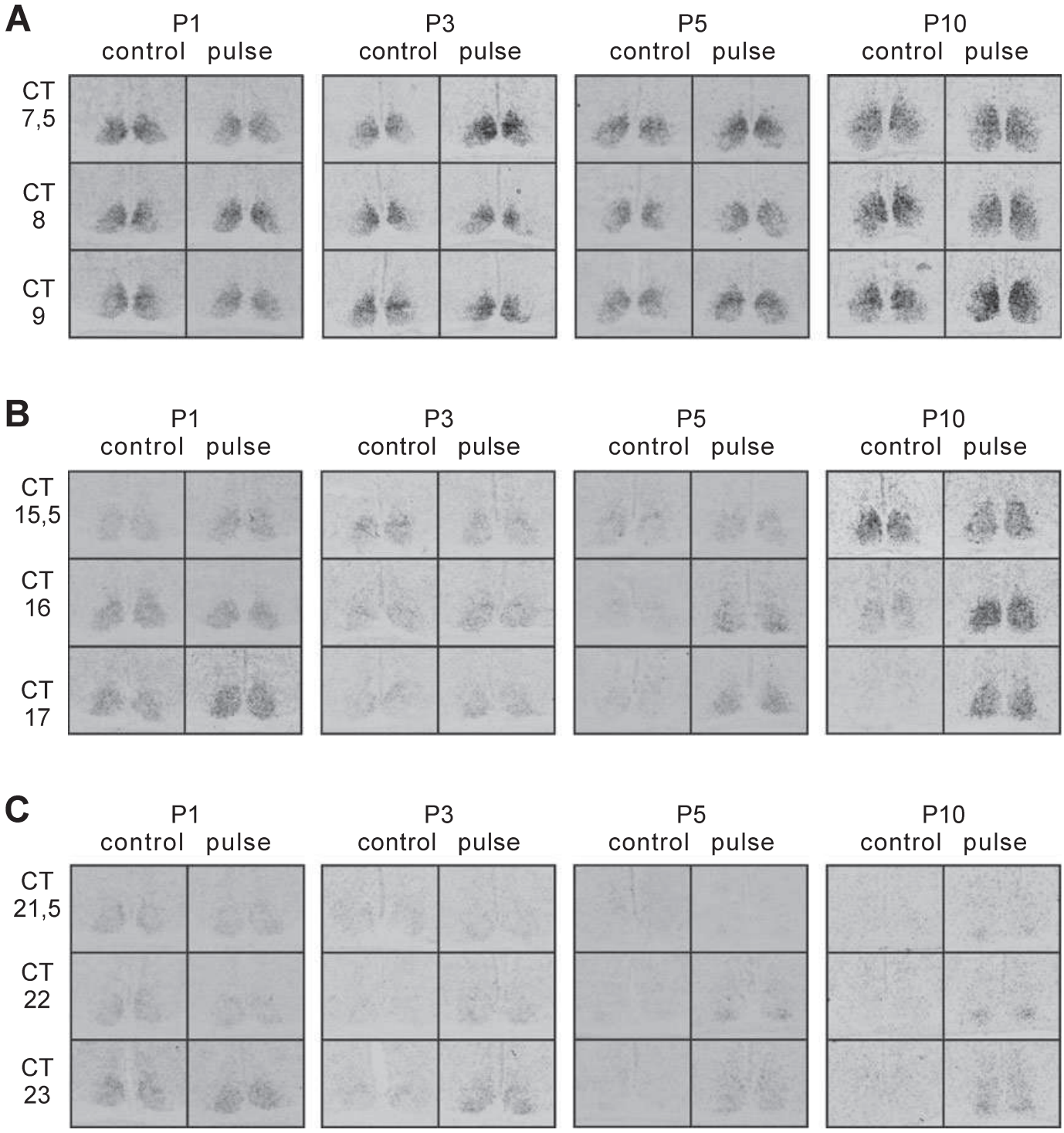

FIG. 7. Spatio-temporal distribution of *Per2* expression within the SCN of rat pups. Representative emulsion autoradiographs demonstrating the distribution of *Per2* expression in SCN sections of rat pups at P1, P3, P5 and P10. Pups were either kept in darkness (control) or exposed to a 30-min light pulse at (A) CT7, (B) CT15 or (C) CT21 (pulse), and sampled 30 min (CT7.5, CT15.5, CT21.5), 1 h (CT8, CT16, CT22) and 2 h (CT9, CT17, CT23) after the start of each light pulse. Note: the intensity of the signal on individual emulsion autoradiographs may not exactly reflect the relative mRNA levels (for details, see Materials and methods).

expression of the clock gene *Per1* mRNA. Apparently, photic information may reach the core clockwork components very early during the postnatal development. The RHT, which connects the retina with the SCN, reaches the vlSCN by P1 (Speh & Moore, 1993). The RHT contains filaments of intrinsically photoreceptive retinal ganglion cells expressing the non-visual photopigment melanopsin (Hattar *et al.*, 2002). Melanopsin-containing retinal ganglion cells are present within the retina at prenatal stages in mice and rats, and they may thus transmit information about external lighting conditions during the early postnatal period, i.e. well before the visual photopigments maturate and eyes open (Fahrenkrug *et al.*, 2004; Hannibal & Fahrenkrug, 2004; Sekaran *et al.*, 2005). These findings, together with

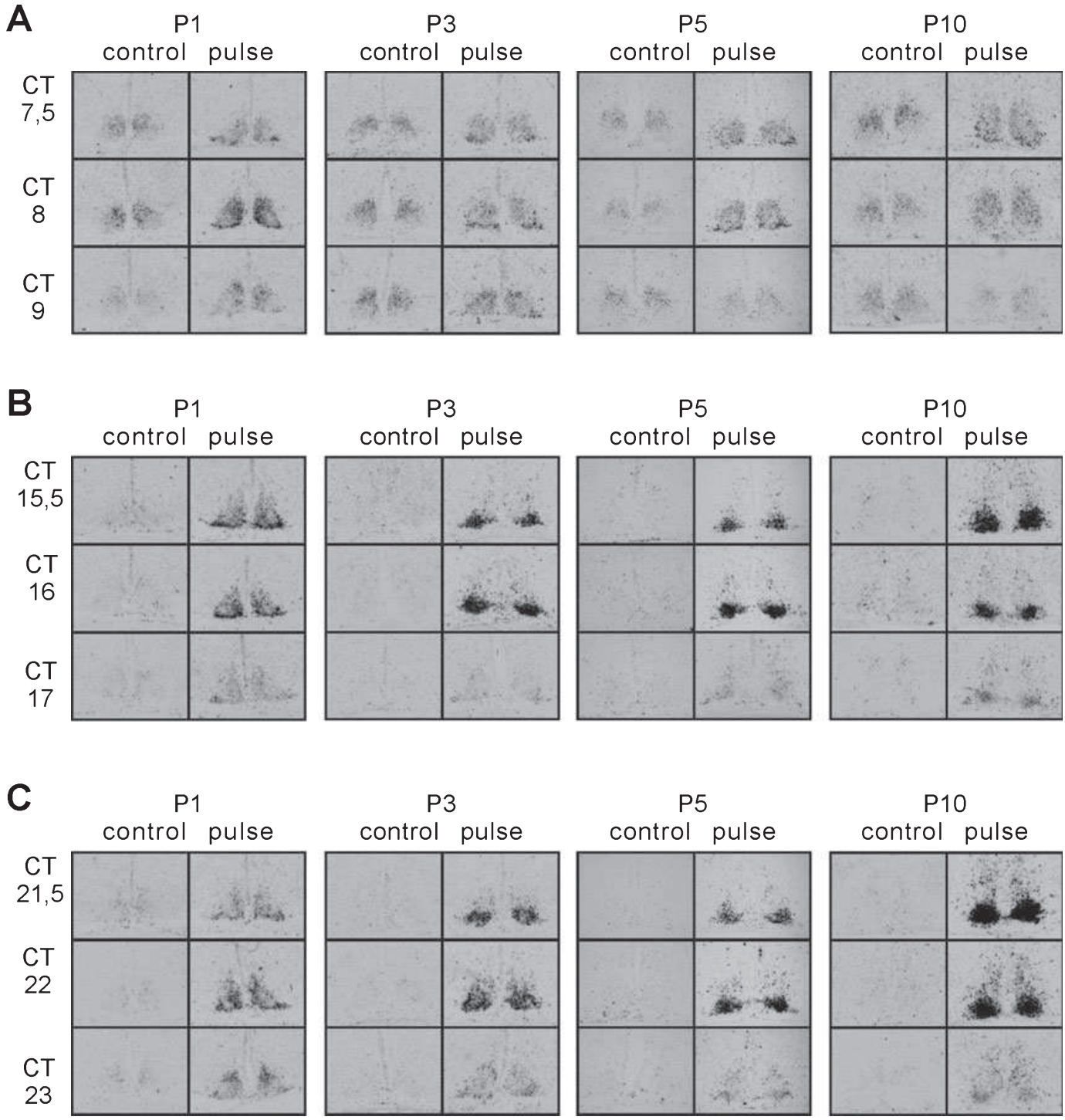

FIG. 8. Spatio-temporal distribution of *c-fos* expression within the SCN of rat pups. Representative emulsion autoradiographs demonstrating the distribution of *c-fos* expression in SCN sections of rat pups at P1, P3, P5 and P10. Pups were either kept in darkness (control) or exposed to a 30-min light pulse at (A) CT7, (B) CT15 or (C) CT21 (pulse), and sampled 30 min (CT7.5, CT15.5, CT21.5), 1 h (CT8, CT16, CT22) and 2 h (CT9, CT17, CT23) after the start of each light pulse. Note: the intensity of the signal on individual emulsion autoradiographs may not exactly reflect the relative mRNA levels (for details, see Materials and methods).

our current data, demonstrate that pathways conveying photic information to the circadian clock in the SCN are fully developed not only morphologically but also functionally at birth. Hence, the immature responses of the newborn rat SCN to photic stimulation during the daytime observed in this work are due to undeveloped functional properties of the circadian clock itself rather than non-functioning photic pathways.

In adult animals, the sensitivity of the circadian clock to light is restricted to the period of subjective night. In the rat SCN, the duration of the subjective night was correlated with either the interval in which light pulses induced high expression of *c-fos* within the vlSCN (Sumová & Illnerová, 1998) or the interval when endogenous expression of *c-fos* within the dmSCN was low (Sumová *et al.*, 1998). During this window, the SCN core clockwork permits the

photoinduction of the light-sensitive clock genes *Per1* and *Per2* from low nighttime levels. This is believed to be a crucial step in light's ability to reset the molecular core clockwork. In adult rats, *Per1* expression is light sensitive during the first and second part of subjective night, but *Per2* is supposed to be photoinduced only during the early subjective night (Yan *et al.*, 1999; Miyake *et al.*, 2000). In our study of adult rats, *Per2* expression was induced 2 h after the light pulse delivered at CT15, and also slightly (though not significantly) 1 and 2 h after the light pulse administered at CT21.

Our current data demonstrate that the gating mechanism was not present immediately after birth. At P1, light pulses induced the expression of *Per1* and *c-fos* during the daytime as well as during the nighttime. No *Per2* expression was induced at any time during this developmental stage. Interestingly, the spatial distribution of the signal induced by the daytime light pulse differed for *c-fos* and *Per1* expression. While *c-fos* expression was photoinduced primarily within a thin layer of the ventral part of the vlSCN, *Per1* expression was photoinduced throughout the entire SCN. The circadian control of *Per1* photoinduction resembled that of adult rats at P3, while that of *Per2* only at P5. At P3, P5 and P10, light pulse delivered during the second part of the night induced the expression of *Per2* within the same region as *Per1*, i.e. in the vlSCN. However, light pulse administered during the first part of the night induced the expression of *Per2* within the entire SCN region, but expression of *Per1* only in the vlSCN at P5 and P10, but not yet at P3. Therefore, it seems that the photoinduction of *Per2* differs from that of *Per1* not only in timing but also in spatial distribution, and may thus be controlled by different mechanisms since its beginning.

Interestingly, the response of the immediate-early gene *c-fos* to light pulses was more dramatic than the responses of the clock genes. Apparently, during early ontogenesis pathways mediating photic information may massively activate neuronal activity within the SCN. These pathways involve a clock-controlled step likely shared with that affecting *Per1* photoinduction. *c-fos* photoinduction was found to be gated at P3, when the signal intensity was measured on autoradiographic film from the whole SCN. A detailed examination of the spatial distribution of the *c-fos* photoinduction by emulsion autoradiography revealed that daytime light pulse induced *c-fos* expression at the ventral border of the vlSCN until P5, and a slight response in the entire vlSCN was detectable even at P10. While the photoinduction of *Per1* and *Per2* thus seemed to be restricted to the subjective night beginning at P3 and P5, respectively, the photoinduction of *c-fos* was not completely gated until P10. These data are in accordance with our previous findings on development of the circadian gate for the interval of *c-fos* protein photoinduction within the vlSCN (Bendová *et al.*, 2004). While light pulses induced *c-fos* immunoreactivity throughout the circadian cycle at P3, an interval of insensitivity to light pulses was detected at P10. Similarly, Weaver & Reppert (1995) reported the photic induction of *c-fos* expression during both day and night from P0 to P6.

The mechanism how the circadian clock in the SCN gates its response to photic stimuli has not yet been elucidated, though Ras-like G-protein Dexras1 has been recently recognized as a potential gatekeeper molecule (Cheng *et al.*, 2006). The gating is obviously property of photosensitive cells located in the vl-part of the SCN. Because the self-oscillating cells are mostly located in the dm-part, the inter-cellular rather than intra-cellular mechanisms are likely operating. The current model suggests that spontaneously oscillating cells impose their outputs upon the photosensitive cells, controlling thus the interval of their photosensitivity (Antle *et al.*, 2007). In accordance with this hypothesis, the absence of the gating mechanism during the early postnatal stage, as revealed in this study, might be due to a lack of functional synapses connecting the spontaneously oscillating cells with the photosensitive gate cells. In the rat SCN, synaptogenesis proceeds well into the postnatal stage and is completed at P10 (Weinert, 2005), i.e. just around the time when the gating mechanism develops. We further hypothesize that presence and degree of responses of *Per* genes expression to light might be conditional to the presence of a day/night variation in their endogenous expression. Although the experimental design of this study did not allow comparison of the amplitude of the rhythms, a gradual increase of the amplitude was demonstrated in our previous studies (Sládek *et al.*, 2004; Kováčiková *et al.*, 2006). The absence of the gating mechanism at P1 parallels the absence of significant circadian variations in clock gene expression within the SCN of newborn rats (Sládek *et al.*, 2004; Kováčiková *et al.*, 2006). Only very low-amplitude synchronized rhythms of *Per1* and *Per2* mRNA levels were detected at P1 and P2, respectively, and rhythms in the expression of other clock genes did not develop until P3. Apparently, the core clock mechanism may restrict the *Per1* and *Per2* photoinduction to subjective night only when synchronized circadian oscillations in their expression with low nighttime and high daytime levels have fully developed. It is plausible to speculate that these circumstances may facilitate the prevalence of the maternal influence on entrainment of the developing circadian clock over the photic influence during the first few postnatal days.

In conclusion, our data demonstrate that light affects the molecular core clock mechanism within the SCN immediately after birth. The photoinduction of the clock gene *Per2* develops later than that of *Per1*. The circadian clock begins to restrict *Per1* and *Per2* photoinduction to the subjective night during the first postnatal week, again earlier for *Per1* than for *Per2*. These data clearly demonstrate that the molecular circadian clock within the rodent SCN is not completely developed at the time of birth, but rather undergoes substantial postnatal maturation to function as a circadian clock in the whole complexity of the body demands. Only upon completing the development, the molecular core clockwork begins to be entrained by photic cues while maternal entrainment gradually loses importance.

Acknowledgements

We thank Eva Suchanová and Jiří Sedlmajer for their excellent technical assistance, Prof. Hitoshi Okamura for his generous gift of the plasmid templates used for the synthesis of *rPer1* and *rPer2* riboprobes, Prof. W.J. Schwartz for his generous gift of plasmid template for the synthesis of *c-fos* probe, and Prof. Helena Illnerová for her helpful comments on the manuscript. This work was supported by the Czech Science Foundation grants No. 309/08/0503 and 309/08/H079, Research Projects LC554 and AV0Z 50110509, and by 6th Framework Project EUCLOCK No. 018741.

Abbreviations

AVP, arginin-vasopressin; CT, circadian time, CT0 is the time of the previous lights-on, CT12 is the time of the previous lights-off; dmSCN, dorsomedial part of the suprachiasmatic nucleus of the hypothalamus; LD, light–dark regime; OD, optical density; P, postnatal day, the day of birth is P0; *Per1,* Period1; *Per2,* Period2; r, rat; RHT, retinohypothalamic tract; SCN, suprachiasmatic nuclei of the hypothalamus; vlSCN, ventrolateral part of the suprachiasmatic nucleus of the hypothalamus.

References

Albrecht, U., Zheng, B., Larkin, D., Sun, Z.S. & Lee, C.C. (2001) m*Per1* and m*Per2* are essential for normal resetting of the circadian clock. *J. Biol. Rhythms*, **16**, 100–104.

Antle, M.C., Foley, N.C., Foley, D.K. & Silver, R. (2007) Gates and oscillators II: zeitgebers and the network model of the brain clock. *J. Biol. Rhythms*, **22**, 14–25.

Aronin, N., Sagar, S.M., Sharp, F.R. & Schwartz, W.J. (1990) Light regulates expression of a Fos-related protein in rat suprachiasmatic nuclei. *Proc. Natl. Acad. Sci. U.S.A.*, **87**, 5959–5962.

Bendová, Z., Sumová, A. & Illnerová, H. (2004) Development of circadian rhythmicity and photoperiodic response in subdivisions of the rat suprachiasmatic nucleus. *Brain Res. Dev. Brain Res.*, **148**, 105–112.

Cheng, H.Y., Dziema, H., Papp, J., Mathur, D.P., Koletar, M., Ralph, M.R., Penninger, J.M. & Obrietan, K. (2006) The molecular gatekeeper Dexras1 sculpts the photic responsiveness of the mammalian circadian clock. *J. Neurosci.*, **26**, 12984–12995.

Daan, S. & Pittendridgh, C.S. (1976) A functional analysis of circadian pacemakers in nocturnal rodents II. The variability of phase response curves. *J. Comp. Physiol.*, **106**, 255–266.

Dardente, H., Poirel, V.J., Klosen, P., Pévet, P. & Masson- Pévet, M. (2002) *Per* and neuropeptide expression in the rat suprachiasmatic nuclei: compartmentalization and differential cellular induction by light. *Brain Res.*, **958**, 261–271.

Fahrenkrug, J., Nielsen, H.S. & Hannibal, J. (2004) Expression of melanopsin during development of the rat retina. *Neuroreport*, **15**, 781–784.

Hamada, T., Antle, M.C. & Silver, R. (2004) Temporal and spatial expression of canonical clock genes and clock-controlled genes in the suprachiasmatic nucleus. *Eur. J. Neurosci.*, **19**, 1741–1748.

Hannibal, J. & Fahrenkrug, J. (2004) Melanopsin containing retinal ganglion cells are light responsive from birth. *Neuroreport*, **15**, 2317–2320.

Hattar, S., Liao, H.W., Takao, M., Berson, D.M. & Yau, K.W. (2002) Melanopsin-containing retinal ganglion cells: architecture, projections, and intrinsic photosensitivity. *Science*, **295**, 1065–1070.

Jelínková, D., Illnerová, H. & Sumová, A. (2000) Gate for photic resetting of intrinsic rhythmicity of the rat suprachiasmatic nucleus under a long photoperiod. *Neurosci. Lett.*, **280**, 143–146.

Johnson, R.F., Morin, L.P. & Moore, R.Y. (1988) Retinohypothalamic projections in the hamster and rat demonstrated using cholera toxin. *Brain Res.*, **462**, 301–312.

Klein, D.C., Moore, R.Y. & Reppert, S.M. (1991) *Suprachiasmatic Nucleus: The Mind's Clock*. Oxford University Press, New York.

Ko, C.H. & Takahashi, J.S. (2006) Molecular components of the mammalian circadian clock. *Hum. Mol. Genet.*, **15**, R271–R277.

Kováčiková, Z., Sládek, M., Bendová, Z., Illnerová, H. & Sumová, A. (2006) Expression of clock and clock-driven genes in the rat suprachiasmatic nucleus during late fetal and early postnatal development. *J. Biol. Rhythms*, **21**, 140–148.

Leard, L.E., Macdonald, E.S., Heller, H.C. & Kilduff, T.S. (1994) Ontogeny of photic-induced *c-fos* mRNA expression in rat suprachiasmatic nuclei. *Neuroreport*, **5**, 2683–2687.

LeSauter, J., Lehman, M.N. & Silver, R. (1996) Restoration of circadian rhythmicity by transplants of the SCN "micropunches". *J. Biol. Rhythms*, **11**, 163–171.

Miyake, S., Sumi, Y., Yan, L., Takekida, S., Fukuyama, T., Ishida, Y., Yamaguchi, S., Yagita, K. & Okamura, H. (2000) Phase-dependent responses of *Per1* and *Per2* genes to a light-stimulus in the suprachiasmatic nucleus of the rat. *Neurosci. Lett.*, **294**, 41–44.

Moore, R.Y. (1991) Development of the suprachiasmatic nucleus. In Klein, D.C., Moore, R.Y. & Reppert, S.M. (Eds), *Suprachiasmatic Nucleus: The Mind's Clock*. Oxford University Press, New York, pp. 197–216.

Moore, R.Y. & Bernstein, M.E. (1989) Synaptogenesis in the rat suprachiasmatic nucleus demonstrated by electron microscopy and synapsin I immunoreactivity. *J. Neurosci.*, **9**, 2151–2162.

Ralph, M.R., Foster, R.G., Davis, F.C. & Menaker, M. (1989) Transplanted suprachiasmatic nucleus determines circadian period. *Science*, **247**, 975–978.

Rusak, B., Robertson, H.A., Wisden, W. & Hunt, S.P. (1990) Light pulses that shift rhythms induce gene expression in the suprachiasmatic nucleus. *Science*, **248**, 1237–1240.

Sekaran, S., Lupi, D., Jones, S.L., Sheely, C.J., Hattar, S., Yau, K.W., Lucas, R.J., Foster, R.G. & Hankins, M.W. (2005) Melanopsin-dependent photoreception provides earliest light detection in the mammalian retina. *Curr. Biol.*, **15**, 1099–1107.

Shearman, L.P., Zylka, M.J., Weaver, D.R., Kolakowski, L.F. Jr & Reppert, S.M. (1997) Two period genes: circadian expression and photic regulation in the suprachiasmatic nuclei. *Neuron*, **19**, 1261–1269.

Shearman, L.P., Jin, X., Lee, C., Reppert, S.M. & Weaver, D.R. (2000) Targeted disruption of the *mPer3* gene: subtle effects on circadian clock function. *Mol. Cell. Biol.*, **20**, 6269–6275.

Shigeyoshi, Y., Taguchi, K., Yamamoto, S., Takekida, S., Yan, L., Tei, H., Moriya, T., Shibata, S., Loros, J.J., Dunlap, J.C. & Okamura, H. (1997) Light-induced resetting of a mammalian circadian clock is associated with rapid induction of the m*Per1* transcript. *Cell*, **91**, 1043–1053.

Sládek, M., Sumová, A., Kováčiková, Z., Bendová, Z., Laurinová, K. & Illnerová, H. (2004) Insight into molecular core clock mechanism of embryonic and early postnatal rat suprachiasmatic nucleus. *Proc. Natl. Acad. Sci. U.S.A.*, **101**, 6231–6236.

Speh, J.C. & Moore, R.Y. (1993) Retinohypothalamic tract development in the hamster and rat. *Brain Res. Dev. Brain Res.*, **76**, 171–181.

Sumová, A. & Illnerová, H. (1998) Photic resetting of intrinsic rhythmicity of the rat suprachiasmatic nucleus under various photoperiods. *Am. J. Physiol.*, **274**, R857–R863.

Sumová, A., Trávníčková, Z., Mikkelsen, J.D. & Illnerová, H. (1998) Spontaneous rhythm in the dorsomedial part of the rat suprachiasmatic nucleus. *Brain Res.*, **801**, 254–258.

Weaver, D.R. & Reppert, S.M. (1995) Definition of the developmental transition from dopaminergic to photic regulation of *c-fos* gene expression in the rat suprachiasmatic nucleus. *Brain Res. Mol. Brain Res.*, **33**, 136–148.

Weinert, D. (2005) Ontogenetic development of the mammalian circadian system. *Chronobiol. Int.*, **22**, 179–205.

Yan, L. & Okamura, H. (2002) Gradients in the circadian expression of *Per1* and *Per2* genes in the rat suprachiasmatic nucleus. *Eur. J. Neurosci.*, **15**, 1153–1162.

Yan, L. & Silver, R. (2004) Resetting the brain clock: time course and localization of mPER1 and mPER2 protein expression in suprachiasmatic nuclei during phase shifts. *Eur. J. Neurosci.*, **19**, 1105–1109.

Yan, L., Takekida, S., Shigeyoshi, I. & Okamura, H. (1999) *Per1* and *Per2* gene expression in the rat suprachiasmatic nucleus: circadian profile and the compartment-specific response to light. *Neuroscience*, **94**, 141–150.

Physiol. Res. 57 (Suppl. 3): S139-S148, 2008

MINIREVIEW

Circadian Molecular Clocks Tick along Ontogenesis

A. SUMOVÁ, Z. BENDOVÁ, M. SLÁDEK, R. EL-HENNAMY, K. MATĚJŮ, L. POLIDAROVÁ, S. SOSNIYENKO, H. ILLNEROVÁ

Institute of Physiology, Academy of Sciences of the Czech Republic, v.v.i., Prague, Czech Republic

Received February 15, 2008
Accepted April 16, 2008
On-line May 13, 2008

Summary

The circadian system controls the timing of behavioral and physiological functions in most organisms studied. The review addresses the question of when and how the molecular clockwork underlying circadian oscillations within the central circadian clock in the suprachiasmatic nuclei of the hypothalamus (SCN) and the peripheral circadian clocks develops during ontogenesis. The current model of the molecular clockwork is summarized. The central SCN clock is viewed as a complex structure composed of a web of mutually synchronized individual oscillators. The importance of development of both the intracellular molecular clockwork as well as intercellular coupling for development of the formal properties of the circadian SCN clock is also highlighted. Recently, data has accumulated to demonstrate that synchronized molecular oscillations in the central and peripheral clocks develop gradually during ontogenesis and development extends into postnatal period. Synchronized molecular oscillations develop earlier in the SCN than in the peripheral clocks. A hypothesis is suggested that the immature clocks might be first driven by external entraining cues, and therefore, serve as "slave" oscillators. During ontogenesis, the clocks may gradually develop a complete set of molecular interlocked oscillations, i.e., the molecular clockwork, and become self-sustained clocks.

Key words

Circadian clock • Ontogenesis • Suprachiasmatic nucleus • Peripheral clock • Clock gene

Corresponding author

A. Sumová, Institute of Physiology, Academy of Sciences of the Czech Republic, Vídeňská 1083, 142 20 Praha 4, Czech Republic. E-mail: sumova@biomed.cas.cz

Introduction

The circadian system has evolved as an adaptation to cyclic changes in light and darkness due to the Earth's rotation that occurs within a period of solar day, i.e., 24 hours. It ensures the proper timing of vital processes in most organisms studied thus far. In mammals, the circadian system consists of a central clock in the brain and numerous peripheral clocks that are subordinate to the central clock. Via the molecular clockwork in cells, the clocks generate circadian rhythmicity, which controls bodily functions through rhythmic regulation of gene transcription. The rhythmicity is thus manifested at the behavioral as well as at the physiological levels. The mammalian central clock is strategically located in the suprachiasmatic nucleus (SCN) of the ventral hypothalamus just above the optic chiasm. It receives photic input from the retina, which synchronizes it with the 24-h day. The SCN is a paired organ, and each of the two nuclei is composed of about 10 000 mutually interconnected cells (for review see Moore *et al.* 2002, Lee *et al.* 2003). The peripheral clocks in mammals have lost their photosensitivity during evolution. They are synchronized with the 24-h day mostly via outputs from the central SCN clock, as well as by their local environment (Hastings *et al.* 2003, Yoo *et al.* 2004). The ontogenetic development of the mammalian circadian system has already been the subject of an extensive review (Weinert 2005). This mini-review mainly summarizes recent data that addresses the crucial question of when and how the mammalian circadian molecular clockwork develops during ontogenesis. Are the central and peripheral clocks functional at the time of

birth? Do they develop even earlier, i.e., during the fetal stage? Data has recently accumulated to suggest that, although mammalian circadian clocks are genetically equipped to generate rhythmicity well before birth, they undergo a gradual postnatal development in order to function adequately.

The molecular clock within a single cell

Cells in the mammalian body are equipped with a set of genes that are indispensable for circadian clock function. The principles of circadian rhythmicity generation have been partly ascertained at the molecular level and are similar for the central and peripheral clocks. The basic components of the clockwork are the clock genes that encode clock proteins. Malfunction or absence of the clock components render severe abnormalities in circadian rhythmicity (Bae *et al.* 2001, van der Horst *et al.* 1999, Zheng *et al.* 2001). The abnormalities may range from lengthening or shortening of the circadian period to complete arrhythmicity. A contemporary model of the molecular core clockwork presumes that rhythmical expression of clock genes and their proteins drives the circadian clock in a cell-autonomic fashion (for review see Fu and Lee 2003, Ko and Takahashi 2006, Reppert and Weaver 2001). In principle, clock proteins CLOCK and BMAL1 serve as transcriptional activators that switch on the transcription of genes that contain E-box response elements (CACGTG) in their promoters. Both of these proteins contain a basic helix-loop-helix DNA-binding domain and two PAS (Per-Arnt-Sim) protein interaction domains. E-boxes are present in the promoters of the clock genes *Per1,2* and *Cry1,2* and two orphan nuclear receptors *Rev-erbα* and *Rora*, as well as in the promoters of the clock-controlled genes, i.e., the genes that are not part of the core clockwork, but are controlled by it and thus transmit the rhythmical signal outside of the clock. After the CLOCK:BMAL1 heterodimer switches on transcription of *Per1,2*, *Cry1,2* clock genes, the proteins corresponding to these genes are formed with a clock protein-specific delay. The PER1,2 and CRY1,2 proteins accumulate in the cytoplasm and form homo- and heterodimers via their PAS domains. The dynamics of this checkpoint are controlled by post-translational modifications of the clock proteins, mainly by phosphorylation and subsequent proteasomal degradation. PER protein phosphorylation by CASEIN KINASE 1ε (CKIε) and CKIδ facilitates PER1 and PER2 ubiquitinylation and degradation and masks their nuclear localization signals. Consequently, the entry of the PER:CRY heterodimer into the nucleus is delayed (Lee *et al.* 2001, Lowrey *et al.* 2000, Akashi *et al.* 2002). This may be a crucial step for maintaining the circadian period of the molecular clock. After entering the nucleus, the PER:CRY heterodimers inhibit CLOCK:BMAL1 mediated transcription, most likely by mechanisms involving directed histone deacetylation and other chromatin modification (Etchegaray *et al.* 2003). Later on, PER:CRY repression is relieved by degradation of PERs and CRYs. The rhythmical transcription of the CLOCK:BMAL1 transcription activator complex is controlled via circadian oscillations in the transcription of clock gene *Bmal1*. REV-ERBα and RORA compete to bind to ROR-response elements in the *Bmal1* promoter, and repress or activate its transcription, respectively (Shearman *et al.* 2000, Preitner *et al.* 2002, Sato *et al.* 2004). These interlocked positive and negative transcriptional-translational feedback loops repeat with a circadian period and thus form the basis for a self-sustained circadian clock.

However, recent findings suggest that the core clockwork mechanism might be much more complex and the current model may represent only a part of the complete system. It is plausible that not only more genes, but even additonal mechanisms not considered in the current feedback loop model, may be involved. For example, miRNA, namely miR-219, has recently been implicated in the regulation of the central circadian clock (Cheng *et al.* 2007). miRNAs are small molecules that act as potent silencers of gene expression *via* translational repression of mRNA degradation. miR-219 is a target of the CLOCK:BMAL1 complex and exhibits robust circadian rhythms of expression as a clock-regulated gene. Moreover, *in vivo* knock-down of miR-219 lengthens the circadian period in a manner similar to a knock-out of the clock gene *Clock*. Translation control via miRNAs may, therefore, represent a novel regulatory level of the circadian clock. Another novel regulatory mechanism might be based on the finding that bZIP transcription factor *E4BP4* is a key negative component of the circadian clock (Ohno *et al.* 2007). Moreover, three recent reports confirmed the importance of targeted protein degradation as a key feature of the circadian clock (Siepka *et al.* 2007, Busino *et al.* 2007, Godinho *et al.* 2007). They revealed that the clock protein CRY is targeted for degradation by a member of F box family of ubiquitin E3 ligases, FBXL3. *Overtime* (Siepka *et al.* 2007) and *after hours* (Godinho *et al.* 2007) mutations

both lie in the region of FBXL3 that binds to CRY. Due to these mutations, binding of FBXL3 to CRY is disrupted, CRY degradation is prevented and the duration of its repressive function on clock gene activation is prolonged. Therefore, mice with a targeted mutation of FBXL3 have a longer circadian period than wild-type mice. Although the mechanisms of the degradation pathways have not been fully ascertained, targeted degradation is likely to control not only the rate at which clock protein complexes accumulate in the cytoplasm, but also the rate of their degradation.

Although the basic principles of the core clockwork seem to be conserved across the central and peripheral clocks, they might not be absolutely identical. In contrast to peripheral clocks, the central clock within the SCN is formed of a web of inter-connected cell-autonomous oscillators (see below). Recent data have demonstrated that the inter-cellular clock mechanisms may significantly contribute to the robustness of the clock system (Liu *et al.* 2007). The oscillator network interactions in the SCN can partly compensate for *Per1* or *Cry1* deficiency and preserve sustained rhythmicity in behavior and *in vitro* in the SCN slices of *Per1* or *Cry1* mutant mice. In contrast, *Per1* and *Cry1* genes are implicitly required for sustained rhythms in peripheral tissues, cells and dissociated SCN neurons (Liu *et al.* 2007). Therefore, a new model that is specific for the central SCN clock is needed to incorporate the ability of inter-cellular coupling among the SCN neurons to confer the robustness of molecular oscillations.

SCN clock: a single cell oscillator or a web of coupled oscillators?

To function properly as a master clock, the SCN must not only be able to generate circadian oscillations, but must also entrain the oscillations at single cell level to cyclically occurring cues and transmit the synchronized rhythmic information to the rest of the body. These tasks are highly dependent upon inter-neuronal coupling within the SCN. In the adult SCN, information regarding photic entraining cues is first processed by a set of neurons located in the retinorecipient zone of the SCN. In rodents, this zone is called the ventrolateral (VL) part or the core of the SCN. Thereafter, the information is sent *via* intra-SCN coupling pathways to the non-photosensitive cells located mostly within the dorsomedial (DM) part or the shell of the SCN (Yamaguchi *et al.* 2003, Yan and Okamura 2002, Yan and Silver 2004, Yan *et al.* 1999). Inter-cellular communication between clusters of SCN cells has recently been considered to be important for entrainment of the central clock to a change in day length, i.e., in the photoperiod (Inagaki *et al.* 2007, VanderLeest *et al.* 2007). The mechanism by which the coupling is accomplished is not well understood. Several mechanisms underlying the intercellular synchrony have been considered, namely electrical coupling (Aton and Herzog 2005) and coupling by neurotransmitters, such as vasoactive intestinal polypeptide (VIP) (Harmar *et al.* 2002, Aton *et al.* 2005, Maywood *et al.* 2006) and gamma aminobutyric acid (GABA) (Albus *et al.* 2005, Aton *et al.* 2006).

Recent findings support the idea that inter-cellular coupling is crucial not only for entrainment and transmission of the synchronized output signals out of the clock, but also for the time-keeping mechanism *per se*. In particular, the VIP signaling through the VIPR2 receptor has been shown not only to contribute to synchrony between cells, but also to help maintain a robust rhythmicity in individual SCN neurons. In $Vip^{-/-}$ and $Vipr2^{-/-}$ mice, the circadian firing rhythm was abolished in about half of all SCN neurons (Aton *et al.* 2005). Similarly, the rhythmicity was disrupted in cells within the SCN organotypic slices from $Vipr2^{-/-}$ mice carrying *Per1::luciferase* and *Per1::GFP* reporter transgenes as reporters of activity within the core circadian feedback loop (Maywood *et al.* 2006). Recently, it has been shown that coupling between single cell SCN oscillators may amplify and stabilize unstable component oscillators, and, therefore, establish a more reliable rhythmicity at the SCN and behavioral level (Liu *et al.* 2007, To *et al.* 2007). Thus, the coupling between individual rhythmic cells is likely to contribute the autonomous time-keeping mechanism and ensure stability of the central clock.

Development of the central SCN clock

From the data summarized above, it is obvious that the adult central clock is not only a simple sum of self-oscillating neurons, but is rather a well organized entity. The multi-level organization includes coupling between individual neurons as well as coupling between the defined subdivisions of the nucleus. Therefore, development of the central clock within the SCN obviously does not depend only on the presence of individual components of the molecular core clockwork and the ability of single cells to oscillate, but also on development of a hierarchical organization of the

nucleus. Only maturation of the complex clock enables the development of synchronized oscillatory signaling from the central clock to the rest of the body. In this context, data regarding the morphological development of the mammalian SCN might be highly relevant.

Morphologically, the rodent SCN develops gradually (Moore 1991). Gestational periods among different rodent species differ and therefore, for simplification, most of the further discussion relates to development of the rat SCN. In the rat, the prenatal period lasts about 22 days. Neurogenesis of the SCN begins on embryonic day (E) 14 and continues through E17 from a specialized zone of the ventral diencephalic germinal epithelium as a component of periventricular cell groups. Neurons of the VL SCN are generated at E15 - E16 and those of the DM SCN at E16 - E17. The neurogenesis is completed at E18, but the morphological maturation of the SCN neurons gradually proceeds until postnatal day (P) 10. Synaptogenesis in the SCN is a slower process; at E19, only very sparse synapses may be observed. It begins to progress only in the late prenatal and early postnatal periods, and then increases noticeably from P4 to P10 (Weinert 2005). Therefore, during the prenatal period, the SCN neurons are present but the multi-level inter-cellular coupling may not yet be functional. The coupling strengthens during the first postnatal week and, the rat SCN is fully developed to its full complexity only at P10.

Intrinsic rhythms in the SCN may appear as early as the late embryonic stage. A day-night variation in metabolic activity monitored by a 2-deoxyglucose uptake was detected in the fetal rat SCN from E19 through E21 (Reppert and Schwartz 1984), in the *Avp* mRNA level at E21 (Reppert and Uhl 1987) and in the firing rate of the SCN neurons at E22 (Shibata and Moore 1987). All these rhythms are supposed to be driven by the SCN clock in adults, and the rodent fetal clock has therefore been considered to be functionally developed well before birth. However, direct evidence that the above mentioned fetal SCN rhythms are indeed driven by the molecular core clockwork is lacking. Alternatively, the observed rhythmicity might arise from cyclically appearing maternal cues, which impinge on fetal SCN neurons and driving the oscillations in a "slave" oscillator-like fashion. Such maternal "zeitgebers" might trigger the rhythm in neuronal activity, as reflected in the rhythms in firing rate and metabolic activity, as well as in gene transcription, as is the case with the observed rhythm in *Avp* mRNA levels. It is relevant to note that transcription of *Avp* might be regulated not only by the clockwork via activation of the E-box sequence in its promoter (Jin *et al.* 1999), but also via activation of CRE (Iwasaki *et al.* 1997, Burbach *et al.* 2001) and AP1 (Burbach *et al.* 2001) elements by a non-clock-related mechanism. Moreover, recent data using detection of heteronuclear RNA as a nascent transcript, which is a more reliable marker of transcriptional rate than detection of mRNA, did not reveal any circadian rhythmicity in transcription of the *Avp* gene in the rat SCN at E20. However, the expression was rhythmic at P1 (Kováčiková *et al.* 2006).

A solution to the question of whether the central clock is functional before birth might come from studies on the development of the molecular core clockwork mechanism. According to the current model described above, the circadian rhythms in the levels of the clock gene transcripts and protein products are essential for the molecular timekeeping mechanism. Therefore, several groups of researchers have measured the daily profiles of clock gene expression in the rat SCN by *in situ* hybridization, but outcome of these studies was ambiguous. Ohta *et al.* reported high amplitude rhythms of *Per1* and *Per2* mRNA in the fetal rat SCN at E20 (Ohta *et al.* 2002, 2003). Other authors studied the daily profiles of *Per1*, *Per2*, *Cry1* and *Bmal1* mRNA at E19, i.e., at the embryonic day when the fetal rat SCN is already formed (Moore 1991) and the rhythm in metabolic activity present (Reppert and Schwartz 1984). However, none of the above-mentioned clock genes were expressed rhythmically at that embryonic stage (Sládek *et al.* 2004). Moreover, levels of clock gene proteins PER1, PER2 and CRY1 not only did not exhibit any circadian variation, but were in fact undetectable at E19 (Sládek *et al.* 2004). These data suggest that at this stage of fetal development, the SCN circadian clock might not be able to generate synchronized oscillations. The same authors performed a detailed developmental study and found that at E20, some of the rhythms were just about beginning to form, but the amplitude of rhythmicity was very low or did not reach a significant level (Kováčiková *et al.* 2006). Rhythms in clock gene expression developed gradually during the postnatal period, and adult-stage-like amplitudes were achieved only at P10 (Kováčiková *et al.* 2006) (Fig 1). Similarly, molecular oscillations equivalent to those observed in adults were not detected in the fetal hamster SCN (Li and Davis 2005). In mice, Shimomura *et al.* found a significant oscillation in *Per1* but not in *Per2* mRNA in the SCN at E17, and the amplitude of the oscillations increased progressively with

postnatal age (Shimomura *et al.* 2001).

Using this approach, it was possible to study the development of synchronized rhythmicity, but not the development of single cell rhythmicity. Low amplitude rhythms in clock gene expression might already be present in individual SCN neurons, but they may not yet be mutually synchronized due to insufficient synapses in the embryonic SCN (Moore 1991). The increase in the amplitude of the rhythms in clock gene expression correlated well with synaptogenesis within the SCN. Therefore, it is plausible that mutual synchronization of the SCN neurons due to developing synapses may account for the gradual rise in the amplitude of clock gene oscillations. Theoretically, development of the synapses might also be conditional for the oscillations. Daily profiles of clock gene expression in the rat SCN at E19 seem to support the idea of undeveloped molecular oscillations in individual neurons rather than the idea of fully developed but desynchronized oscillations, since levels of constitutively expressed *Per1*, *Cry1* and *Bmal1* genes at E19 corresponded either to the minimum or maximum, but not to the mean of their P3 values. Moreover, at E19, not only rhythms in clock gene mRNA levels, but also protein products PER1, PER2 and CRY1 were undetectable. In fact, no PER1, PER2 and CRY1immunoreactive cells were detected in the fetal SCN at any circadian time (Sládek *et al.* 2004). The absence of the basic components of the molecular core clockwork is rather in favor of the hypothesis that the mechanism enabling the rhythmic expression of clock genes may not yet be mature at E19. However, the possibility cannot be ruled out that only a very small proportion of the SCN cells is rhythmic during the fetal stage, and that the number of rhythmic cells increases due to development of synaptic communication between these rhythmic cells and the non-rhythmic ones. The methodological approach used in the above-mentioned studies would not detect a very low oscillating signal, which could potentially arise from a few SCN cells.

The use of newly introduced experimental tools, such as transgenic animals, will be necessary for addressing these issues in the future. In SCN slices explanted from transgenic animals, it is possible to detect rhythms in clock gene expression with a single cell resolution. However, even in the case of detection of a significant rhythm in clock gene expression at a single cell level during the fetal stage, the question still remains as to whether these rhythms are indeed reliable markers of a functional circadian clock. If so, individual cellular oscillators without any coupling must be able to drive synchronized rhythmicity. However, such characteristics have not been observed in *in vitro* cell lines that are devoid of inter-cellular coupling like the fetal clock. Without entraining cues, these cells are desynchronized or arrhythmic. As soon as the cultured cells are subjected to a "zeitgeber", e.g., to serum shock, the cells become synchronized and exhibit synchronized rhythmicity (Balsalobre *et al.* 1998). Therefore, the question of whether the fetal SCN cells are able to maintain oscillations, or whether the oscillations would soon be dampened in the isolated SCN may still remain. The possibility that other mechanisms besides the molecular clockwork might drive the SCN rhythmicity during late embryonic development should be considered. For example, maternal cues, such as dopamine or melatonin, might directly trigger the fetal SCN rhythm in metabolic activity (Davis and Mannion 1988, Weaver *et al.* 1995). Complete lesions of the maternal SCN at E7 disrupt rhythms in SCN glucose utilization in rat fetuses (Reppert and Schwartz 1986). This disruption might be due to desynchronization among the fetuses, but also might be due to the lack of a rhythmical input to the slave fetal clock. Strikingly, a periodic feeding cue delivered to SCN-lesioned pregnant rats is sufficient to entrain the fetal SCN clock (Weaver and Reppert 1989). The fetal clock is therefore sensitive to feeding cues in a way similar to adult peripheral clocks, but not the adult SCN clock. These observations suggest that multiple and more complex pathways mediate rhythmic information to the fetal SCN clock as compared to the adult SCN clock. They also indicate that formal properties of the fetal and of the postnatal SCN clock may differ. Therefore, the possibility cannot be excluded that during ontogenesis, the SCN clock develops spontaneously from a slave oscillator at the prenatal stage to a master clock at the postnatal stage.

More strikingly, the restructuring of the slave oscillator to the master clock may occur spontaneously without entraining cues driven by the maternal SCN. Surgical ablation of the maternal SCN did not prevent development of the clock during the postnatal period (Reppert and Schwartz 1986, Davis and Gorski 1988). Moreover, genetic ablation of functional central as well as peripheral maternal clocks did not prevent spontaneous development of the clocks, since heterozygous off-spring of m$Per1^{Brdm1}/Per2^{Brdm1}$ and $mPer2^{Brdm1}/Cry1^{-/-}$ double mutant arrhythmic females crossed with wild-type males developed circadian rhythm in locomotor activity.

However, within a litter, pups were less synchronized than pups born to wild-type controls (Jud and Albrecht 2006). Also, transplantation of fetal SCN tissue to arrhythmic SCN-lesioned animals leads to a recovery in the circadian rhythm of locomotor activity (Ralph *et al.* 1990). Therefore, development of the circadian clock appears to be genetically predetermined.

Peripheral clocks during ontogenesis

Studies on the development of peripheral clocks have only recently commenced after the finding that rhythms in clock gene expression are detectable in cells of the peripheral organs, and are therefore not unique to the central SCN clock (Abe *et al.* 2001, Balsalobre 2002, Schibler and Sassone-Corsi 2002). Two methodological approaches for these studies were used. In the first approach, daily profiles of clock gene expression within a peripheral tissue sampled throughout the circadian cycle were examined. In the rat heart, circadian rhythms in the expression of clock genes *Per1*, *Per2* and *Bmal1* and a clock-controlled gene *Dbp* were not detected by Northern blot analysis on P2 (Sakamoto *et al.* 2002). Expression of *Per1*, *Bmal1* and *Dbp* began to be rhythmic between P2 and P5, but expression of *Per2* did not exhibit any rhythmicity until P14. Similarly, in the rat liver, clock gene expression as determined by RT-PCR developed gradually during postnatal ontogenesis (Sládek *et al.* 2004) (Fig.1). At E20, only *Rev-erbα* mRNA exhibited a significant, high amplitude circadian oscillation, but the expression of *Per1*, *Per2*, *Cry1*, *Bmal1* and *Clock* mRNA did not. Even at P2, *Rev-erbα* was still the only gene expressed rhythmically with high amplitude. At P10 *Per1* mRNA and at P20 *Per2* and *Bmal1* also began to be expressed in a circadian way. Only as late as at P30, all of the studied clock genes were expressed rhythmically in an adult-like pattern (Sládek *et al.* 2004). Development of the molecular oscillations in the liver was therefore similar to that in the heart. Apparently, rhythms in synchronized clock gene expression develop earlier in the central SCN clock (see above) than in peripheral oscillators. The stable detection of the high-amplitude rhythm in *Rev-erbα* expression throughout ontogenesis rules out the possibility that the lack of rhythmicity in the early development is due to desynchronization of oscillating cells in the liver. Unlike the SCN clock cells, the peripheral oscillating cells are not mutually interconnected via synapses and are likely to be synchronized by rhythmic humoral or neuronal cues

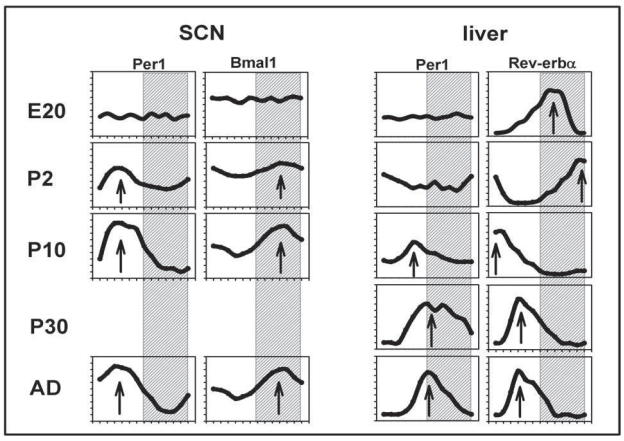

Fig. 1. Schematic drawings of development of the circadian clocks in the rat. Daily profiles of clock gene *Per1* and *Bmal1* mRNA in the SCN and *Per1* and *Rev-erbα* in the liver are depicted in 20-day-old embryos (E20), in pups at postnatal day 2 (P2), P10, P30 and in adult rats. X axis represents day time with the shaded area defining night hours. Y axis represents relative mRNA levels. Drawings are based on results published previously in Sládek *et al.* (2004), Kováčiková *et al.* (2006) and Sládek *et al.* (2007).

impinging upon individual cells. The significant rhythm in *Rev-erbα* expression in the absence of rhythms in other clock genes during ontogenesis may give us clues regarding the mechanism that underlies peripheral clock development. During an early developmental stage, rhythmic expression of *Rev-erbα* might be triggered by mechanisms other than E-box mediated induction. Apart from the E-box, the *Rev-erbα* promoter contains other response elements that may be responsible for switching on/off gene transcription, namely Rev-DR2/RORE, DBPE/D-box etc. (Adelmant *et al.* 1996, Raspe *et al.* 2002, Yamamoto *et al.* 2004). The rhythmically appearing mediators may activate transcription of *Rev-erbα* by stimulation of some of these elements independently of the core clockwork. Moreover, it is tempting to speculate that the rhythmic expression of *Rev-erbα* might trigger the newly appearing rhythms in clock gene expression, since a constant phase relationship between rhythms in the expression of *Rev-erbα* and other clock genes is maintained during different developmental stages (Sládek *et al.* 2004) (Fig.1). Therefore, theoretically, a peripheral clock may function as a slave oscillator during early ontogenesis, and may only later, with the development of clock gene oscillations, become a self-autonomous clock.

Importantly, phases of the rhythms in clock gene expression in the liver (Sládek *et al.* 2007) as well as in the heart (Sakamoto *et al.* 2002) change during development. The acrophase of these rhythms shifts in a coordinated

manner so that the expressions of individual clock genes keep stable phase relationships throughout development (Fig.1). Feeding regimes accompanied by behavioral activity may account for these phase changes. Mothers feed their pups mostly during the daytime; therefore, during the period of maternal breast feeding, pups are diurnal rather than nocturnal in their food consumption (Weinert 2005). The nocturnal feeding pattern develops during the weaning period, but it is preceded by a period when pups still suckle some maternal milk during the daytime and consume solid food during the nighttime. These changes in feeding behavior appear to be mirrored in changing phases of the rhythms in clock gene expression.

Recently, another approach was used for studying the ontogenesis of oscillations in clock gene expression (Saxena *et al.* 2007). *In vivo* rhythms in bioluminiscence were monitored *in utero* in the fetuses of transgenic rats carrying *Per1::luciferase* transgene throughout the whole gestational period (Saxena *et al.* 2007). The bioluminiscence increased dramatically at E10 and continued to increase progressively until birth. Diurnal fluctuations in *Per1* expression in the whole body were already suggested prior to birth. From this study, it is not apparent which parts of the fetal body might account for the whole-fetal bioluminiscence recorded *in vivo* or for the suggested day-night differences observed. It is possible that some peripheral clocks may start to exhibit circadian rhythms in *Per1* expression before birth. Tissue-specific differences in the development of molecular oscillations in peripheral clocks are suggested.

Conclusions

The data summarized in this mini-review cannot definitively answer the question of exactly when the central and peripheral clocks develop during the mammalian ontogenesis. Depending on the methods used, different results have been produced; therefore, more studies are still needed. However, most results support the hypothesis that synchronized oscillations in clock gene expression develop gradually during ontogenesis, and development extends well into the postnatal period. It is feasible that the ability to function as a self-sustained clock may develop gradually, and that the immature clock may function first as a "slave" oscillator. Only later, with the development of a complete set of molecular oscillations, may it become a self-sustaining clock. Such development occurs earlier in the central SCN clock than in peripheral clocks.

Conflict of Interest

There is no conflict of interest.

Acknowledgements

The authors are supported by the Grant Agency of the Czech Republic, grant No. 309080503; Grant Agency of the Academy of Sciences of the Czech Republic, grant No. IAA500110605; by Research Projects AV0Z 50110509, and LC554; and by the 6th Framework Project EUCLOCK 018741.

References

ABE H, HONMA S, NAMIHIRA M, MASUBUCHI S, IKEDA M, EBIHARA S, HONMA K: Clock gene expressions in the suprachiasmatic nucleus and other areas of the brain during rhythm splitting in CS mice. *Mol Brain Res* **87**: 92-99, 2001.

ADELMANT G, BEGUE A, STEHELIN D, LAUDET V: A functional Rev-erb alpha responsive element located in the human Rev-erb alpha promoter mediates a repressing activity. *Proc Natl Acad Sci USA* **93**: 3553-3558, 1996.

AKASHI M, TSUCHIYA Y, YOSHINO T, NISHIDA E: Control of intracellular dynamics of mammalian period proteins by casein kinase I epsilon (CKI epsilon) and CKI delta in cultured cells. *Mol Cell Biol* **22**: 1693-1703, 2002.

ALBUS H, VANSTEENSEL MJ, MICHEL S, BLOCK GD, MEIJER JH: A GABAergic mechanism is necessary for coupling dissociable ventral and dorsal regional oscillators within the circadian clock. *Curr Biol* **15**: 886-893, 2005.

ATON SJ, COLWELL CS, HARMAR AJ, WASCHEK J, HERZOG ED: Vasoactive intestinal polypeptide mediates circadian rhythmicity and synchrony in mammalian clock neurons. *Nat Neurosci* **8**: 476-483, 2005.

ATON SJ, HERZOG ED: Come together, right … now: synchronization of rhythms in a mammalian circadian clock. *Neuron* **48**: 531-534, 2005.

ATON SJ, HUETTNER JE, STRAUME M, HERZOG ED: GABA and $G_{i/o}$ differentially control circadian rhythms and synchrony in clock neurons. *Proc Natl Acad Sci USA* **103**: 19188-19193, 2006.

BAE K, JIN X, MAYWOOD ES, HASTINGS MH, REPPERT SM, WEAVER DR: Differential functions of mPer1, mPer2, and mPer3 in the SCN circadian clock. *Neuron* **30**: 525-536, 2001.

BALSALOBRE A: Clock genes in mammalian peripheral tissues. *Cell Tissue Res* **309**: 193-199, 2002.

BALSALOBRE A, DAMIOLA F, SCHIBLER U: A serum shock induces circadian gene expression in mammalian tissue culture cells. *Cell* **93**: 929-937, 1998.

BURBACH JP, LUCKMAN SM, MURPHY D, GAINER H: Gene regulation in the magnocellular hypothalamo-neurohypophysial system. *Physiol Rev* **81**: 1197-1267, 2001.

BUSINO L, BASSERMANN F, MAIOLICA A, LEE C, NOLAN PM, GODINHO SI, DRAETTA GF, PAGANO M: SCFFbxl3 controls the oscillation of the circadian clock by directing the degradation of cryptochrome proteins. *Science* **316**: 900-904, 2007.

DAVIS FC, GORSKI RA: Development of hamster circadian rhythms: role of the maternal suprachiasmatic nucleus. *J Comp Physiol A* **162**: 601-610, 1988.

DAVIS FC, MANNION J: Entrainment of hamster pup circadian rhythms by prenatal melatonin injections to the mother. *Am J Physiol* **255**: R439-R448, 1988.

ETCHEGARAY JP, LEE C, WADE PA, REPPERT SM: Rhythmic histone acetylation underlies transcription in the mammalian circadian clock. *Nature* **421**: 177-182, 2003.

FU L, LEE CC: The circadian clock: pacemaker and tumour suppressor. *Nature Rev Cancer* **3**: 350-361, 2003.

GODINHO SI, MAYWOOD ES, SHAW L, TUCCI V, BARNARD AR, BUSINO L, PAGANO M, KENDALL R, QUWAILID MM, ROMERO MR, O'NEILL J, CHESHAM JE, BROOKER D, LALANNE Z, HASTINGS MH, NOLAN PM: The after-hours mutant reveals a role for Fbxl3 in determining mammalian circadian period. *Science* **316**: 897-900, 2007.

HARMAR AJ, MARSTON HM, SHEN S, SPRATT C, WEST KM, SHEWARD WJ, MORRISON CF, DORIN JR, PIGGINS HD, REUBI JC, KELLY JS, MAYWOOD ES, HASTINGS MH: The $VPAC_2$ receptor is essential for circadian function in the mouse suprachiasmatic nuclei. *Cell* **109**: 497-508, 2002.

HASTINGS MH, REDDY AB, MAYWOOD ES: A clockwork web: circadian timing in brain and periphery, in health and disease. *Nat Rev Neurosci* **4**: 649-661, 2003.

CHENG HY, PAPP JW, VARLAMOVA O, DZIEMA H, RUSSELL B, CURFMAN JP, NAKAZAWA T, SHIMIZU K, OKAMURA H, IMPEY S, OBRIETAN K: microRNA modulation of circadian-clock period and entrainment. *Neuron* **54**: 813-829, 2007.

INAGAKI N, HONMA S, ONO D, TANAHASHI Y, HONMA K: Separate oscillating cell groups in mouse suprachiasmatic nucleus couple photoperiodically to the onset and end of daily activity. *Proc Natl Acad Sci USA* **104**: 7664-7669, 2007.

IWASAKI Y, OISO Y, SAITO H, MAJZOUB JA: Positive and negative regulation of the rat vasopressin gene promoter. *Endocrinology* **138**: 5266-5274, 1997.

JIN X, SHEARMAN LP, WEAVER DR, ZYLKA MJ, DE VRIES GJ, REPPERT SM: A molecular mechanism regulating rhythmic output from the suprachiasmatic circadian clock. *Cell* **96**: 57-68, 1999.

JUD C, ALBRECHT U: Circadian rhythms in murine pups develop in absence of a functional maternal circadian clock. *J Biol Rhythms* **21**: 149-154, 2006.

KO CH, TAKAHASHI JS: Molecular components of the mammalian circadian clock. *Hum Mol Genet* **15** (Spec No 2): R271-277, 2006.

KOVÁČIKOVÁ Z, SLÁDEK M, BENDOVÁ Z, ILLNEROVÁ H, SUMOVÁ A: Expression of clock and clock-driven genes in the rat suprachiasmatic nucleus during late fetal and early postnatal development. *J Biol Rhythms* **21**: 140-148, 2006.

LEE C, ETCHEGARAY JP, CAGAMPANG FR, LOUDON AS, REPPERT SM: Posttranslational mechanisms regulate the mammalian circadian clock. *Cell* **107**: 855-867, 2001.

LEE HS, BILLINGS HJ, LEHMAN MN: The suprachiasmatic nucleus: a clock of multiple components. *J Biol Rhythms* **18**: 435-449, 2003.

LI X, DAVIS FC: Developmental expression of clock genes in the Syrian hamster. *Dev Brain Res* **158**: 31-40, 2005.

LIU AC, WELSH DK, KO CH, TRAN HG, ZHANG EE, PRIEST AA, BUHR ED, SINGER O, MEEKER K, VERMA IM, DOYLE FJ, 3RD, TAKAHASHI JS, KAY SA: Intercellular coupling confers robustness against mutations in the SCN circadian clock network. *Cell* **129**: 605-616, 2007.

LOWREY PL, SHIMOMURA K, ANTOCH MP, YAMAZAKI S, ZEMENIDES PD, RALPH MR, MENAKER M, TAKAHASHI JS: Positional syntenic cloning and functional characterization of the mammalian circadian mutation tau. *Science* **288**: 483-492, 2000.

MAYWOOD ES, REDDY AB, WONG GK, O'NEILL JS, O'BRIEN JA, MCMAHON DG, HARMAR AJ, OKAMURA H, HASTINGS MH: Synchronization and maintenance of timekeeping in suprachiasmatic circadian clock cells by neuropeptidergic signaling. *Curr Biol* **16**: 599-605, 2006.

MOORE RY: Development of the suprachiasmatic nucleus. In: *Suprachiasmatic Nucleus: The mind's Clock*. DC KLEIN, RY MOORE, SM REPPERT (eds), Oxford University Press, New York, 1991, pp 197-216.

MOORE RY, SPEH JC, LEAK RK: Suprachiasmatic nucleus organization. *Cell Tissue Res* **309**: 89-98, 2002.

OHNO T, ONISHI Y, ISHIDA N: The negative transcription factor E4BP4 is associated with circadian clock protein PERIOD2. *Biochem Biophys Res Commun* **354**: 1010-1015, 2007.

OHTA H, HONMA S, ABE H, HONMA K: Effects of nursing mothers on rPer1 and rPer2 circadian expressions in the neonatal rat suprachiasmatic nuclei vary with developmental stage. *Eur J Neurosci* **15**: 1953-1960, 2002.

OHTA H, HONMA S, ABE H, HONMA K: Periodic absence of nursing mothers phase-shifts circadian rhythms of clock genes in the suprachiasmatic nucleus of rat pups. *Eur J Neurosci* **17**: 1628-1634, 2003.

PREITNER N, DAMIOLA F, LOPEZ-MOLINA L, ZAKANY J, DUBOULE D, ALBRECHT U, SCHIBLER U: The orphan nuclear receptor REV-ERB alpha controls circadian transcription within the positive limb of the mammalian circadian oscillator. *Cell* **110**: 251-260, 2002.

RALPH MR, FOSTER RG, DAVIS FC, MENAKER M: Transplanted suprachiasmatic nucleus determines circadian period. *Science* **247**: 975-978, 1990.

RASPE E, MAUTINO G, DUVAL C, FONTAINE C, DUEZ H, BARBIER O, MONTE D, FRUCHART J, FRUCHART JC, STAELS B: Transcriptional regulation of human Rev-erb alpha gene expression by the orphan nuclear receptor retinoic acid-related orphan receptor alpha. *J Biol Chem* **277**: 49275-49281, 2002.

REPPERT SM, SCHWARTZ WJ: Maternal suprachiasmatic nuclei are necessary for maternal coordination of the developing circadian system. *J Neurosci* **6**: 2724-2729, 1986.

REPPERT SM, SCHWARTZ WJ: The suprachiasmatic nuclei of the fetal rat: characterization of a functional circadian clock using ^{14}C-labeled deoxyglucose. *J Neurosci* **4**: 1677-1682, 1984.

REPPERT SM, UHL GR: Vasopressin messenger ribonucleic acid in supraoptic and suprachiasmatic nuclei: Appearance and circadian regulation during development. *Endocrinology* **120**: 2483-2487, 1987.

REPPERT SM, WEAVER DR: Molecular analysis of mammalian circadian rhythms. *Annu Rev Physiol* **63**: 647-676, 2001.

SAKAMOTO K, OISHI K, NAGASE T, MIYAZAKI K, ISHIDA N: Circadian expression of clock genes during ontogeny in the rat heart. *Neuroreport* **13**: 1239-1242, 2002.

SATO TK, PANDA S, MIRAGLIA LJ, REYES TM, RUDIC RD, MCNAMARA P, NAIK KA, FITZGERALD GA, KAY SA, HOGENESCH JB: A functional genomics strategy reveals Rora as a component of the mammalian circadian clock. *Neuron* **43**: 527-537, 2004.

SAXENA MT, ATON SJ, HILDEBOLT C, PRIOR JL, ABRAHAM U, PIWNICA-WORMS D, HERZOG ED: Bioluminescence imaging of period1 gene expression in utero. *Mol Imaging* **6**: 68-72, 2007.

SHEARMAN LP, SRIRAM S, WEAVER DR, MAYWOOD ES, CHAVES I, ZHENG B, KUME K, LEE CC, VAN DER HORST GT, HASTINGS MH, REPPERT SM: Interacting molecular loops in the mammalian circadian clock. *Science* **288**: 1013-1019, 2000.

SHIBATA S, MOORE RY: Development of neuronal activity in the rat suprachiasmatic nucleus. *Brain Res* **431**: 311-315, 1987.

SHIMOMURA H, MORIYA T, SUDO M, WAKAMATSU H, AKIYAMA M, MIYAKE Y, SHIBATA S: Differential daily expression of Per1 and Per2 mRNA in the suprachiasmatic nucleus of fetal and early postnatal mice. *Eur J Neurosci* **13**: 687-693, 2001.

SCHIBLER U, SASSONE-CORSI P: A web of circadian pacemakers. *Cell* **111**: 919-922, 2002.

SIEPKA SM, YOO SH, PARK J, SONG W, KUMAR V, HU Y, LEE C, TAKAHASHI JS: Circadian mutant Overtime reveals F-box protein FBXL3 regulation of cryptochrome and period gene expression. *Cell* **129**: 1011-1023, 2007.

SLÁDEK M, JINDRÁKOVÁ Z, BENDOVÁ Z, SUMOVÁ A: Postnatal ontogenesis of the circadian clock within the rat liver. *Am J Physiol* **292**: R1224-R1229, 2007.

SLÁDEK M, SUMOVÁ A, KOVÁČIKOVÁ Z, BENDOVÁ Z, LAURINOVÁ K, ILLNEROVÁ H: Insight into molecular core clock mechanism of embryonic and early postnatal rat suprachiasmatic nucleus. *Proc Natl Acad Sci USA* **101**: 6231-6236, 2004.

TO TL, HENSON MA, HERZOG ED, DOYLE FJ, 3RD: A molecular model for intercellular synchronization in the mammalian circadian clock. *Biophys J* **92**: 3792-3803, 2007.

VAN DER HORST GT, MUIJTJENS M, KOBAYASHI K, TAKANO R, KANNO S, TAKAO M, DE WIT J, VERKERK A, EKER AP, VAN LEENEN D, BUIJS R, BOOTSMA D, HOEIJMAKERS JH, YASUI A: Mammalian Cry1 and Cry2 are essential for maintenance of circadian rhythms. *Nature* **398**: 627-630, 1999.

VANDERLEEST HT, HOUBEN T, MICHEL S, DEBOER T, ALBUS H, VANSTEENSEL MJ, BLOCK GD, MEIJER JH: Seasonal encoding by the circadian pacemaker of the SCN. *Curr Biol* **17**: 468-473, 2007.

WEAVER DR, REPPERT SM: Periodic feeding of SCN-lesioned pregnant rats entrains the fetal biological clock. *Dev Brain Res* **46**: 291-296, 1989.

WEAVER DR, ROCA AL, REPPERT SM: c-fos and jun-B mRNAs are transiently expressed in fetal rodent suprachiasmatic nucleus following dopaminergic stimulation. *Dev Brain Res* **85**: 293-297, 1995.

WEINERT D: Ontogenetic development of the mammalian circadian system. *Chronobiol Int* **22**: 179-205, 2005.

YAMAGUCHI S, ISEJIMA H, MATSUO T, OKURA R, YAGITA K, KOBAYASHI M, OKAMURA H: Synchronization of cellular clocks in the suprachiasmatic nucleus. *Science* **302**: 1408-1412, 2003.

YAMAMOTO T, NAKAHATA Y, SOMA H, AKASHI M, MAMINE T, TAKUMI T: Transcriptional oscillation of canonical clock genes in mouse peripheral tissues. *BMC Mol Biol* **5**: 18, 2004.

YAN L, OKAMURA H: Gradients in the circadian expression of Per1 and Per2 genes in the rat suprachiasmatic nucleus. *Eur J Neurosci* **15**: 1153-1162, 2002.

YAN L, SILVER R: Resetting the brain clock: Time course and localization of mPER1 and mPER2 protein expression in suprachiasmatic nuclei during phase shifts. *Eur J Neurosci* **19**: 1105-1109, 2004.

YAN L, TAKEKIDA S, SHIGEYOSHI Y, OKAMURA H: Per1 and Per2 gene expression in the rat suprachiasmatic nucleus: circadian profile and the compartment-specific response to light. *Neuroscience* **94**: 141-150, 1999.

YOO SH, YAMAZAKI S, LOWREY PL, SHIMOMURA K, KO CH, BUHR ED, SIEPKA SM, HONG HK, OH WJ, YOO OJ, MENAKER M, TAKAHASHI JS: PERIOD2:LUCIFERASE real-time reporting of circadian dynamics reveals persistent circadian oscillations in mouse peripheral tissues. *Proc Natl Acad Sci USA* **101**: 5339-5346, 2004.

ZHENG B, ALBRECHT U, KAASIK K, SAGE M, LU W, VAISHNAV S, LI Q, SUN ZS, EICHELE G, BRADLEY A, LEE CC: Nonredundant roles of the mPer1 and mPer2 genes in the mammalian circadian clock. *Cell* **105**: 683-694, 2001.